



UNIVERSIDADE DE LISBOA
INSTITUTO SUPERIOR TÉCNICO

**A phenylboronate chromatography based approach as an effective
alternative for the downstream processing of biomolecules**

Sara Alexandra da Silva Lourenço Rosa

Supervisor: Doctor Ana Margarida Nunes da Mata Pires de Azevedo

Co-Supervisor: Doctor Cláudia Alexandra Martins Lobato da Silva

Thesis approved in public session to obtain the PhD Degree in
Biotechnology and Biosciences

Jury final classification: Pass with Distinction and Honour

UNIVERSIDADE DE LISBOA
INSTITUTO SUPERIOR TÉCNICO

**A phenylboronate chromatography based approach as an effective
alternative for the downstream processing of biomolecules**

Sara Alexandra da Silva Lourenço Rosa

Supervisor: Doctor Ana Margarida Nunes da Mata Pires de Azevedo

Co-Supervisor: Doctor Cláudia Alexandra Martins Lobato da Silva

Thesis approved in public session to obtain the PhD Degree in
Biotechnology and Biosciences

Jury final classification: Pass with Distinction and Honour

Jury

Chairperson: Doctor Duarte Miguel de França Teixeira dos Prazeres, Instituto Superior Técnico, Universidade de Lisboa

Members of the Committee:

Doctor Maria Raquel Múrias dos Santos Aires Barros, Instituto Superior Técnico, Universidade de Lisboa

Doctor Duarte Miguel de França Teixeira dos Prazeres, Instituto Superior Técnico, Universidade de Lisboa

Doctor Ana Cristina Mendes Dias Cabral, Faculdade de Ciências, Universidade da Beira Interior

Doctor Ana Margarida Nunes da Mata Pires de Azevedo, Instituto Superior Técnico, Universidade de Lisboa

Doctor Ana Gabriela Gonçalves Neves Gomes, Escola Superior de Tecnologia do Barreiro – Instituto Politécnico de Setúbal

Funding Institution

FCT - Fundação para a Ciência e Tecnologia

A ti, que me fizeste acreditar que seria possível.

Resumo

O potencial terapêutico dos anticorpos monoclonais (mAbs) tem vindo a crescer significativamente a nível mundial. Actualmente, existem mais de 70 produtos em uso clínico para o tratamento de diversas doenças contudo, o acesso geral da população a estes continua a ser impedido pelos altos preços praticados. Como uma elevada parcela dos custos está associada ao processo de fabrico, ao desenvolverem-se processos mais eficientes, poder-se-á conseguir que um maior número de doentes usufrua do potencial terapêutico dos mAbs.

Esta tese tem como principal objectivo o desenvolvimento de um processo de purificação de mAbs baseado na cromatografia de fenilboronato que constitua uma alternativa à dispendiosa captura por proteína A habitualmente utilizada. Inicialmente foram investigados os fenómenos envolvidos na adsorção de um mAb específico para a interleucina-8 humana ao ligando sintético *m*-aminofenilboronato. A combinação do uso da calorimetria de fluxo com ensaios cromatográficos permitiu compreender o comportamento multimodal do ligando assim como que a sua tolerância ao sal pode ser aumentada manipulando as condições cromatográficas. O ligando foi depois avaliado para a captura directa do mAb proveniente de sobrenadantes de culturas celulares. O desenvolvimento de um passo intermédio e a optimização da eluição foram essenciais para alcançar bons parâmetros de desempenho, reproduzíveis em todas as escalas testadas (0.4-40 mL de resina). O processo desenvolvido proporciona recuperações de 97.7%, purezas de 82.6% e remoções de DNA genómico superiores a 96%.

Nesta tese foi, também, possível demonstrar que o *m*-aminofenilboronato pode ser usado para a captura e eluição selectiva de diferentes tipos de proteínas – glicoproteínas, com diferentes pontos isoeléctricos e proteínas acídicas/neutras, glicosiladas ou não – pelo uso de competidores como o Tris e o citrato, respectivamente.

Os resultados obtidos pretendem contribuir para a adoção da cromatografia de fenilboronato para a captura ou polimento de mAbs ou até para a separação de isoformas, por métodos analíticos.

Palavras-chave: Processamento a jusante, Purificação de proteínas, Cromatografia de fenilboronato, Anticorpos monoclonais, Proteínas glicosiladas e não glicosiladas

Abstract

The potential of therapeutic monoclonal antibodies (mAbs) has increased significantly, with more than 70 products in clinical use worldwide for the treatment of different diseases. The access of the general population to mAbs is unfortunately barred by high-selling prices. If mAbs were cheaper, a larger number of individuals would benefit from their therapeutic potential. Since a significant fraction of the costs is attributed to the manufacturing, one way to achieve this is to develop more efficient processes.

This thesis aims to develop a purification process based on phenylboronate chromatography as an alternative to the costly protein A capture step currently used in the purification train of mAbs. To achieve this goal, the phenomena underlying the adsorption of an anti-human IL-8 (anti-IL8) mAb onto an *m*-aminophenylboronic acid synthetic ligand was thoroughly investigated. The combination of on-line flow microcalorimetry and chromatographic assays allowed to understand the multimodal behaviour of the ligand and that its salt tolerance can be enhanced by manipulating the chromatographic conditions. The ligand was then challenged for the direct capture of anti-IL8 mAb from cell culture supernatants. The development of a washing step and the optimization of the elution step were crucial to the achievement of good performance parameters reproducible at every scale tested (0.4 to 40 cm³ resin volume). This process yields recoveries of 97.7%, purities of 82.6% and gDNA removals higher than 96%.

It was also possible to demonstrate that this ligand can be useful for the capture and effective separation of a wide range of proteins from glycoproteins, differing in overall charge, to acidic/neutral proteins (glycosylated or not), by the use of displacers as Tris and citrate, respectively.

The results obtained are expected to contribute towards the adoption of such chromatographic process either for mAb capture or polishing steps or for analytical purposes, envisaging isoforms separations.

Keywords: Downstream processing, Protein purification, Phenylboronate chromatography, Monoclonal antibodies, Glycosylated and non-glycosylated proteins

Acknowledgments

Gostaria de começar por agradecer ao Professor Joaquim Sampaio Cabral e à Professora Raquel Aires-Barros por me terem apoiado na candidatura à bolsa de doutoramento e por me terem dado a oportunidade de desenvolver o meu trabalho nos seus grupos, no agora Stem Cell Engineering Research Group e no Bioseparation Engineering Laboratory, respectivamente. Gostaria, ainda de agradecer à Professora Raquel Aires-Barros por todas as oportunidades que me proporcionou a nível científico, industrial e até de discussão de pedagogia.

Um muito obrigada à Professora Ana Azevedo e à Professora Cláudia Lobato da Silva por terem aceite embarcar neste desafio comigo. Obrigada por tudo o que me ensinaram a nível científico e, principalmente, por confiarem no meu trabalho e capacidade de resolução de problemas.

Durante estes anos, tive ainda a oportunidade de trabalhar com Professora Ana Cristina Cabral, na Faculdade de Ciências da Saúde da Universidade da Beira Interior. Queria deixar aqui expresso o meu agradecimento pela maneira como me recebeu e integrou no seu grupo e, claro, por todos os ensinamentos que me passou. A sua disponibilidade, interesse e horas de discussão foram essenciais para o desenvolvimento de parte desta tese. Aproveito ainda para agradecer ao João Cardoso, Gregory Dutra e ao João Duarte por todo o apoio no laboratório, troca de ideias e companheirismo que me proporcionaram ao longo da minha estadia na Covilhã.

Não podia deixar de agradecer a todos os colegas e professores com que me cruzei no iBB – Institute for Biotechnology and Biosciences. A minha estadia por cá já vai longa. Durante este percurso tive o privilégio de conhecer profissionais dedicados e colegas que gostam de trabalhar em equipa e que são deveras apaixonados pela ciência. Só não os vou enumerar, pois certamente iria esquecer-me de alguém. Contudo, quero que saibam que muitos foram os exemplos que me levaram a trilhar este caminho. Aliás houve mesmo alguns que acreditaram, até mais do que eu, que este seria o passo mais indicado a seguir. Obrigada por todos os momentos que me proporcionaram e sobretudo por me fazerem ver que é preciso, mais do que fazer, perceber o que se faz e saber transmitir. Porque sem transmissão de conhecimento e discussão do mesmo, tornamo-nos obsoletos e incapazes de progredir.

Aos meus colegas Rimenys Carvalho e Alexandra Wagner do Bioseparation Engineering Laboratory, o meu obrigada. Obrigada ao Rimenys pela análise crítica e construtiva de resultados e obrigada à Alexandra Wagner por ter abraçado um projecto tão intenso como o que abraçou a meu lado. Obrigada pela companhia aos jantares e pela partilha de músicas que nos faziam sentir velhas mas nada emo. Obrigada ainda à Maria João Jacinto pelo seu companheirismo e preocupação e à Cláudia Alves e à Ana Rita Silva pela partilha de conhecimento. Obrigada a todas pelos convívios durante estes anos. Foram essenciais.

Aos meus colegas e amigos, fundadores e participantes activos dos Santos B., muito muito obrigada. Antes de mais, obrigada por terem sido colegas tão interessantes, trabalhadores e respeitadores. Convosco aprendi a maioria das coisas que sei sobre células estaminais. Embora nunca tivesse trabalhado com esse tipo de células, a discussão de ideias e/ou protocolos era recorrente e

bastante motivante. Obrigada por me terem proporcionado um ambiente de trabalho para o qual queria sempre voltar. Por fim e mais importante, claro está, queria agradecer o companheirismo de todos ao longo destes anos. Foram anos de ouro! O que eu gosto de reunir esta malta! Todos foram especiais nestes últimos 4 anos mas terei de destacar algumas pessoas. Obrigada ao Diogo Pinto por todo o apoio que me tem dado nestes últimos 2 anos. Já falámos sobre isto! Não foi algo espectacular mas foste e és um grande apoio. Obrigada também à Joana Serra por estar sempre lá quando eu preciso. Obrigada à Marta Costa pelas mensagens cirúrgicas e obrigada à Márcia Mata por me fazer sentir parte da sua família. Ah espera... Fazemos mesmo! Sacavém! Gosto muito de vocês!

Obrigada à Andreia Matos e à Beatriz Monteiro pela amizade partilhada. Obrigada ainda à Rita Costa e à Carla Moura por me terem incluindo em momentos tão bonitos da vossa vida.

Falta agradecer às amigas mais recentes que fiz na minha estadia pela Covilhã. Há quem saiba que “ia para lá trabalhar e não fazer amigas” mas não foi o que aconteceu. Conheci pessoas genuinamente boas. Comecei por dividir casa com uma pessoa maravilhosa, a Alexandra Fante. Alexandra, tenho cada vez mais saudades dos nossos serões acompanhados do chá quentinho. Foram momentos de troca de experiências, de ideias, de conhecimento sobre culturas e religiões de que eu tenho a maior saudade. Um muito obrigada por, ainda hoje, fazeres de maninha mais velha. És um exemplo de luta e perseverança que levarei sempre comigo. Queria ainda deixar um muito obrigada à Filipa Pires, à Filipa Ferreira e à Rita Machado. Obrigada por me terem integrado, obrigada pelas noites no North Walls, pelas passeatas (especialmente aquela por Seia), pelas guardidas, mas sobretudo, por terem estado presentes naquele momento e por estarem também agora. Posso não ter demonstrado, mas valeu muito, muito mesmo.

As amigas de sempre também não podem ser esquecidas. Quero aqui deixar um obrigada, do fundo do coração, à minha amiga de sempre, a Vanessa Jorge. Já lá vão 25 anos desde que nos conhecemos e, se às vezes, não dá jeito nenhum que me conheças tão bem, outras é tudo. A vida meteu-se, mas nunca nos separámos. É para a vida! Obrigada por teres estado presente, por me dares na cabeça mas sobretudo por zelares por mim. Obrigada à Susana (agora do Couto) e à Rita Silva por tudo o que fizeram, especialmente nestes últimos 2 anos. As fases menos boas afastam muitas pessoas mas tendem a fortalecer o que é real e importante. Obrigada pelos jantares, cafés, conversas. Obrigada também à Ana Mateus. Embora um pouco afastadas pelas responsabilidades da vida, sei e sinto que estás sempre a torcer por mim.

Finalmente, por quem eu faço tudo... A minha família. Antes de tudo, quero deixar um obrigada do tamanho do mundo ao meu pai. Se houve alguém que acreditou, foi ele. Se houve alguém que mostrou entusiasmo, foi ele. E acima de tudo, se houve alguém que percebia o que isto poderia exigir e estava disposto a dar, também foi ele. Ao contrário de muitos, o que mais queria era ver-me feliz, nem que para isso eu tivesse de voar. Não te ter ao meu lado dificulta, mas sabes? Tenho os teus ensinamentos guardados. Sabes aqueles que trocávamos em silêncio? Esses mesmo! E vou sempre levá-los comigo nesta vida. Um dia colocá-los-ei em prática, e voarei...

Um obrigada também especial à minha mãe, a quem devo a capacidade de persistir e não desistir, por mais difícil que algo seja. Estes 4 anos foram especialmente difíceis para nós mas temos de acreditar que a bonança, pelo menos, passará por aqui.

Um obrigada muito especial às minhas sobrinhas Filipa e Mafalda. Elas ainda não percebem bem mas significam muito para mim e os seus abraços e sorrisos deixam-me muito feliz e até com algum sentimento de dever cumprido. Um beijinho grande para a minha sobrinha Ana Rita e para o mais recente membro, o Afonso. Digam o que disserem... Amor de tia é muito muito especial, e eu adoro os meus sobrinhos.

Index

Resumo	VII
Abstract.....	IX
Acknowledgments	XI
Index	XV
List of Figures	XXI
List of Tables	XXXIII
List of Abbreviations	XXXV
Thesis Scope and Outline	1
<i>Chapter I - General Introduction</i>	3
I.1. Protein therapeutics overview	5
I.1.1. Introduction to therapeutic monoclonal antibodies	6
I.1.1.1. Evolution of monoclonal antibodies	8
I.2. Manufacturing platforms: an overview of the advances and bottlenecks.....	9
I.3. Trends in non-chromatographic methods.....	13
I.3.1. High performance tangential flow filtration (HPTFF)	13
I.3.2. Flocculation / Precipitation.....	14
I.3.3. Crystallization	15
I.3.4. Liquid-liquid extraction	16
I.4. Trends in chromatographic methods.....	17
I.4.1. Chromatographic bed format.....	18
I.4.1.1. Fluidized bed	18
I.4.1.2. Fixed-bed.....	19
I.4.2. Stationary phase design	22
I.4.2.1. Diffusive and perfusive beads	22
I.4.2.2. Adsorptive microfiltration membranes	23
I.4.2.3. Monoliths	24
I.4.2.4. Fibres.....	25
I.4.3. Chromatographic processes.....	26
I.4.3.1. Size-exclusion chromatography (SEC).....	26
I.4.3.2. Hydrophobic interaction chromatography (HIC)	26
I.4.3.3. Anion-exchange (AEX) chromatography	26
I.4.3.4. Cation-exchange (CEX) chromatography.....	27
I.4.3.5. Immobilized metal affinity chromatography (IMAC).....	28
I.4.3.6. Multimodal chromatography (MMC)	28
I.4.3.6.1. Metal coordination multimodal ligands.....	29
I.4.3.6.2. Hydrogen bond-enhanced anion-exchangers.....	29
I.4.3.6.3. Hydrophobic charge induction chromatography (HCIC)	30
I.4.3.7. Affinity chromatography	30

I.4.3.7.1.	Protein A	30
I.4.3.7.2.	Synthetic biomimetic ligands.....	33
I.4.3.7.3.	Phenylboronic acid.....	34
I.5.	Methods for biomolecules adsorption elucidation	35
I.5.1.	Thermodynamics of biomolecules adsorption in chromatography	37
I.5.1.1.	Van't Hoff plot analysis	38
I.5.1.2.	Calorimetry techniques.....	39
I.5.1.2.1.	Isothermal titration calorimetry (ITC)	39
I.5.1.2.2.	Flow microcalorimetry (FMC).....	42
I.5.1.2.3.	Differential scanning calorimetry (DSC).....	43
I.6.	References	45
<i>Chapter II - Thermodynamic evaluation of the mechanisms underlying the adsorption of monoclonal antibodies in phenylboronate chromatography: The influence of different mobile phase modulators ..</i>		
59		
II.1.	Background	61
II.2.	Material and Methods	62
II.2.1.	Chemicals	62
II.2.2.	Production, purification, concentration and diafiltration of anti-IL8 mAb	62
II.2.3.	Flow Microcalorimetry (FMC) assays.....	63
II.2.3.1.	Evaluation of the adsorption of anti-IL8 mAb.....	64
II.2.3.2.	Thermodynamic profiling of cis-diol interactions using D-sorbitol.....	64
II.2.4.	Structural characterization of anti-IL8 mAb.....	64
II.2.4.1.	Circular Dichroism.....	65
II.2.4.2.	Fluorescence measurements.....	65
II.2.4.3.	Dynamic light scattering	65
II.2.5.	Contribution of matrix and resin components to the adsorption of anti-IL8: interaction studies	65
II.2.6.	Anti-IL8 quantification	66
II.2.7.	Total protein quantification.....	67
II.3.	Results and Discussion	67
II.3.1.	Evaluation of the adsorption of anti-IL8 mAb in the absence of added salt and in presence of NaCl.....	68
II.3.1.1.	Flow Microcalorimetry (FMC) studies	68
II.3.1.1.1.	FMC studies in the absence of added salt.....	71
II.3.1.1.2.	FMC studies in the presence of NaCl	72
II.3.1.1.3.	Thermodynamic profiling of cis-diol interactions using D-sorbitol.....	73
II.3.1.2.	Contribution of matrix and resin components to the adsorption of anti-IL8 mAb: interaction studies.....	75
II.3.1.2.1.	Evaluation of aromatic interactions	75
II.3.1.2.2.	Evaluation of hydrogen bonding and van der Waals interactions.....	76

II.3.1.2.3. Evaluation of ionic interactions: salt tolerance studies	77
II.3.2. Evaluation of the adsorption of anti-IL8 mAb in presence of different mobile phase modulators	78
II.3.2.1. Flow Microcalorimetry (FMC) studies	79
II.3.2.2. Adsorption studies in presence of a Lewis base - <i>NaF</i>	82
II.3.2.3. Adsorption studies in presence of a chaotropic salt - <i>MgCl₂</i>	84
II.3.2.4. Adsorption studies in presence of a kosmotropic salt - <i>(NH₄)₂SO₄</i>	85
II.4. Conclusions	87
II.5. References	88
II.6. Supplementary Material.....	92
II.S1. Structural characterization of anti-IL8 mAb in the absence of added salt and in presence of NaCl.....	92
II.S2. Structural characterization of anti-IL8 mAb studies in presence of different mobile phase modulators	93
 <i>Chapter III - Phenylboronic acid chromatography as a rapid, reproducible and easy scalable multimodal process for the capture of monoclonal antibodies</i>	
III.1. Background	97
III.2. Materials and Methods	98
III.2.1. Chemicals	98
III.2.2. IgG production.....	98
III.2.2.1. Anti-human interleukin-8 monoclonal antibodies	98
III.2.2.2. Anti-human recombinant hepatitis C virus subtype 1b monoclonal antibodies	99
III.2.3. Monoclonal antibodies purification.....	100
III.2.3.1. Phenylboronic acid chromatography	100
III.2.3.1.1. Development and optimization of wash and elution steps.....	100
III.2.3.1.2. Scale-up process optimization	100
III.2.3.1.2.1. Superficial velocities studies	100
III.2.3.1.2.2. Loading studies	101
III.2.3.1.3. Process scale-up	101
III.2.3.2. Protein A chromatography	101
III.2.3.3. CPG and phenyl-Sepharose chromatography	102
III.2.4. IgG quantification	102
III.2.5. Total protein quantification	102
III.2.6. Protein gel electrophoresis	102
III.2.7. Host cell proteins quantification	103
III.2.8. CHO genomic DNA quantification.....	103
III.2.9. IgG characterization	103
III.2.9.1. Isoelectric focusing	103
III.2.9.2. High performance size-exclusion chromatography.....	103
III.2.9.3. Competitive enzyme linked immunosorbent assay.....	103

III.3. Results and Discussion	104
III.3.1. Development and optimization of wash and elution steps.....	104
III.3.1.1. Dynamic binding capacity evaluation.....	104
III.3.1.2. Optimization studies.....	104
III.3.1.2.1. Adsorption step	104
III.3.1.2.2. Washing step studies.....	105
III.3.1.2.3. Elution step studies	107
III.3.1.3. Matrix and resin interactions	109
III.3.1.4. Phenylboronic acid vs protein A	110
III.3.1.4.1. IgG characterization.....	110
III.3.1.5. Proof of concept.....	112
III.3.1.5.1. Anti-IL8 mAbs from serum-free cell cultures.....	112
III.3.1.5.2. Anti-recombinant HCV subtype 1b mAbs from serum-free cell cultures	112
III.3.2. Scale-up process optimization	115
III.3.2.1. Dynamic binding capacity studies.....	115
III.3.2.2. Superficial velocity studies.....	116
III.3.2.3. Loading studies	118
III.3.2.4. Reproducibility performance	119
III.3.2.5. Process scale-up	120
III.4. Conclusions.....	122
III.5. References	123
III.6. Supplementary Material	126
<i>Chapter IV - Exploring the selectivity of phenylboronate chromatography towards glycosylated and non-glycosylated proteins: proof of concept.....</i>	<i>129</i>
IV.1. Background.....	131
IV.2. Materials and Methods.....	132
IV.2.1. Chemicals	132
IV.2.2. Biologics	132
IV.2.3. Phenylboronate chromatography: development and optimization of elution steps...	133
IV.2.3.1. Displacer gradients.....	133
IV.2.3.1.1. Displacer selection	135
IV.2.3.1.2. Linear gradients optimization	135
IV.2.3.1.3. Step gradients: Proof of concept	135
IV.2.3.2. pH gradients	136
IV.2.4. Protein gel electrophoresis	137
IV.3. Results and Discussion.....	137
IV.3.1. Displacer gradient studies	138
IV.3.1.1. Displacer gradient studies for the separation of glycosylated proteins	138
IV.3.1.2. Displacer gradient studies for the separation of acidic to neutral proteins.....	144
IV.3.2. pH gradient studies.....	149

IV.3.2.1. pH gradient studies for the separation of glycosylated proteins.....	150
IV.3.2.2. pH gradient studies for the separation of acidic to neutral proteins	152
IV.4. Conclusions.....	155
IV.5. References.....	156
IV.6. Supplementary Material	158
IV.S1 Characterization of the commercial proteins used by SDS-PAGE	158
IV.S2 Displacer studies for glycoproteins using a P6XL resin	158
IV.S3 Displacer studies for acid/neutral proteins using a P6XL resin.....	161
<i>Chapter V - General Conclusions and Future Perspectives</i>	163
V.1. References.....	169

List of Figures

Figure I.1 Distribution of FDA-approved therapeutic proteins (2011-2016) by drug class [4].	5
Figure I.2 Immunoglobulin (Ig) molecule. All immunoglobulin monomers are composed of two identical light (L) chains and two identical heavy (H) chains. Light chains are composed of one constant domain (CL) and one variable domain (VL), whereas heavy chains are composed of three constant domains (CH1, CH2 and CH3) and one variable domain (VH). The heavy chains are covalently linked at the hinge region and the light chains are covalently linked to the heavy chain by disulphide bonds. The variable domains of both the heavy and light chains compose the antigen-binding of the molecule (Fab), termed Fv. Within the variable domains there are three loops designated complementary-determining regions (CDRs) 1, 2, and 3, which confer the highest diversity and define the specificity of antibody binding. The Fc portion is glycosylated and contains the sites for interaction with effector molecules.[17]	6
Figure I.3 Monoclonal antibody types and nomenclature. Therapeutic mAbs can be murine (suffix: -omab), chimeric (suffix: -ximab), humanized (suffix: e.g. –zumab) or human (suffix: e.g. –umab) and are named accordingly. [16]	8
Figure I.4 Evolution of mammalian cell culture media. [48]	11
Figure I.5 Platform approach employed in the downstream processing of mAbs at industrial scale (AEX: Anion-exchange chromatography; CEX: Cation-exchange chromatography; HIC: Hydrophobic interaction chromatography; SEC: Size exclusion chromatography). [22]	12
Figure I.6 HPTFF schematics for separation of mAbs and host cell proteins. In this case, CHO host cell proteins (CHOP). [68]	13
Figure I.7 Outline of the flocculation mechanism for cationic flocculants. Negatively charged particles such as cells, cell debris, nucleic acids, and host cell proteins bind to the positively charged polymers, leaving the protein of interest in solution. [74]	14
Figure I.8 Expanded adsorption chromatography principle.[112]	18
Figure I.9 Schematics of two different chromatographic systems: (A) 4-column simulated moving bed (SMB) chromatography and (B) Rotating annular chromatography. [139]	21
Figure I.10 (A) Comparison of liquid flow through the axial (A.1) and radial (A.2) columns. (B) CRIO-MD 62: side view and upper view.[144]	21
Figure I.11 Types of chromatographic beads. (A) Non-porous, (B) Porous (dead-end porous), (C) MesoPorous (perfusion beads) and (D) solid core beads.	22
Figure I.12 Transports mechanisms in a perfusive bead and monoliths. (A) Perfusive bead, (B) Monolith.	244
Figure I.13 Chemical structures of ligands used for immunoglobulin isolation and purification. (A) Dipeptide motif present in native SpA, (B) Artificial protein A (ApA) and (C) Ligand 22/8. (B) and (C) are triazine-based ligands.[223]	33
Figure I.14 Schematic of the interaction between phenylboronic acids and cis-diol containing compounds. 1 and 2 – PBA trigonal and tetrahedral conformations, respectively. 3 and 4 - illustration of the esterification bond between cis-diol containing compounds and the trigonal and tetrahedral conformation of PBA ligands, respectively. [202]	35

Figure I.15 (A) Principle of SPR instrument and (B) typical SPR sensorgram showing the steps of an analytical cycle. [253]	36
Figure I.16 Schematic drawing of an isothermal titration calorimeter. The guest molecule is stepwise inserted via syringe into the sample cell which contains the receptor or ligand. [278]	40
Figure I.17 Illustrative ITC data example. (A) Control experiments performed with chromatographic particles titrated against buffer (1) and the biomolecule (2), and the biomolecule against only buffer (3). (B) ITC experiments with two different types of ligands titrated against the biomolecule in buffer system. The data were corrected against the dilution experiments. [278].....	41
Figure I.18 Schematics of a flow microcalorimeter system and its components. [286].....	43
Figure I.19 Representative DSC thermogram of a monoclonal antibody, with CH2, Fab, and CH3 domains identified. The dashed red lines are the deconvoluted peaks of each domain transition, with the three melting temperatures (TMs) indicated. [288]	44
Figure II.1 Chemical structure and characteristics of the buffers used in anti-IL8 mAb adsorption studies onto a phenylboronate chromatographic agarose-based support..	67
Figure II.2 PeakFit de-convolution of thermograms obtained for the anti-human IL-8 mAb (5 mg/mL) adsorption onto P6XL resin at different pH values, in the absence and in the presence of 150 mM NaCl. Injection loop: 100 μ L. Mobile phase flow-rate: 1.5 mL/h. (A) 20 mM HEPES, pH 7.5, (B) 20 mM HEPES, 150 mM NaCl, pH 7.5, (C) 20 mM EPPS, pH 8.5, (D) 20 mM EPPS, 150 mM NaCl, pH 8.5, (E) 20 mM CHES, pH 9.0, (F) 20 mM CHES, 150 mM NaCl, pH 9.0, (G) 20 mM CHES, pH 9.5, (H) 20 mM CHES, 150 mM NaCl, pH 9.5, (I) 20 mM CHES, pH 10, (J) 20 mM CHES, 150 mM NaCl, pH 10. Curves presented are for total peak fit (black line) and peaks resulting from de-convolution (endothermic peaks – blue dotted lines, exothermic peaks – red and green dotted lines). Vertical dashed lines represent the time where the protein-containing plug of solution is replaced with protein-free mobile phase.....	70
Figure II.3 PeakFit de-convolution of thermograms obtained for 20 mM (3.64 mg/mL) D-sorbitol adsorption onto P6XL resin at different pHs, in absence and in presence of 150 mM NaCl. Injection loop: 100 μ L. Mobile phase flow-rate: 1.5 mL/h. (A) 20 mM HEPES, pH 7.5, (B) 20 mM HEPES, 150 mM NaCl, pH 7.5, (C) 20 mM EPPS, pH 8.5, (D) 20 mM EPPS, 150 mM NaCl, pH 8.5, (E) 20 mM CHES, pH 9.0, (F) 20 mM CHES, 150 mM NaCl, pH 9.0. Curves showed are for total peak fit (black line) and peaks resulting from de-convolution (endothermic peaks – blue dotted lines, exothermic peaks – red and green dotted lines). Vertical dashed lines represent the time where the protein-containing plug of solution is replaced with protein-free mobile phase.....	74
Figure II.4 Contribution of the phenyl group to the interaction between <i>m</i> -APBA agarose-based supports and the anti-IL8 mAb. Studies were performed under different pH and salt concentrations using a phenyl-Sepharose 6 FF resin. (A) Schematics of boronic acid (top) and boronate anion (bottom) structures. The ligand group under study is highlighted. (B) Recovery yields of purified anti-IL8 mAb in flow-through (■) and elution (■) fractions. Results are displayed as mean \pm STDV	76
Figure II.5 Contribution of the bare resin to the interaction between <i>m</i> -APBA agarose-based supports and the anti-IL8 mAb. Studies were performed under different pH and salt concentrations using a Sepharose 6 FF resin. (A) Schematics of boronic acid (top) and boronate anion (bottom) structures. The	

ligand group under study is highlighted. (B) Recovery yields of purified anti-IL8 mAb in flow-through (■) and elution (■) fractions. Results are displayed as mean ± STDV.....77

Figure II.6 Evaluation of the contribution of the negative charge present in the ligand (C) to the interaction between *m*-APBA agarose-based supports and the anti-IL8 mAb. Studies were performed under different pH and salt concentrations using an Aminophenylboronate P6XL resin. (A) Schematics of boronic acid (top) and boronate anion (bottom) structures. The ligand groups under study are highlighted. (B) Recovery yields of purified anti-IL8 mAb in flow-through and elution fractions. Buffers composition at pH 7.5 (■), pH 8.5 (■) and 9.0 (■) was 20 mM HEPES, 20 mM EPPS and 20 mM CHES, respectively. Results are displayed as mean ± STDV.....77

Figure II.7 PeakFit de-convolution of thermograms obtained for the anti-IL8 mAb (5 mg/mL) adsorption onto P6XL resin at different pH values (pH 7.5, 8.5 and 9.0) and salt types (NaF, MgCl₂ and (NH₄)₂SO₄). Injection loop: 100 µL. Mobile phase flow-rate: 1.5 mL/h. (A) 20 mM HEPES, 150 mM NaF, pH 7.5, (B) 20 mM EPPS, 150 mM NaF, pH 8.5, (C) 20 mM CHES, 150 mM NaF, pH 9.0, (D) 20 mM HEPES, 50 mM MgCl₂, pH 7.5, (E) 20 mM EPPS, 50 mM MgCl₂, pH 8.5, (F) 20 mM CHES, 50 mM MgCl₂, pH 9.0, (G) 20 mM HEPES, 50 mM (NH₄)₂SO₄, pH 7.5, (H) 20 mM EPPS, 50 mM (NH₄)₂SO₄, pH 8.5 and (I) 20 mM CHES, 50 mM (NH₄)₂SO₄, pH 9.0. Curves represented are for total peak fit (black line) and peaks resulting from de-convolution (endothermic peaks – blue dotted lines and exothermic peaks – red and green dotted lines). Vertical dashed lines represent the time at which the protein-containing plug of solution is replaced with protein-free mobile phase.....81

Figure II.8 Schematics on the influence of the pH (A) and the presence of the mobile phase modulators NaF (B), MgCl₂ (C) and (NH₄)₂SO₄ (D) on the *m*-APBA ligand conformation.....83

Figure II.9 Evaluation of the boronate anion contribution for ionic interactions between the aminophenylboronate P6XL resin and anti-IL8 mAb at pH 9.0 using different salts – NaF, 150 mM (■), (NH₄)₂SO₄, 50 mM (■) and MgCl₂, 50 mM (■). Recovery yields of purified anti-IL8 in elution (lighter colors) and stripping fractions (darker colors) using boronate chromatography. Adsorption and elution studies were performed with buffers containing 20 mM CHES, pH 9.0. Column stripping was accomplished with 1.5 M Tris-HCl, pH 8.5. Results are displayed as mean ± STDV.....85

Figure II.S1.1. Anti-IL8 mAb far UV circular dichroism spectra at different pH and salt concentrations – 0 (solid lines) and 150 mM NaCl (dashed lines). Buffers concentration used was 5 mM for all conditions tested.....92

Figure II.S1.2. Fluorescence spectra of (A) Tyrosine at an excitation wavelength of 280 nm and (B) Tryptophan at an excitation wavelength of 296 nm at different pH and salt concentrations – 0 (solid lines) and 150 mM NaCl (dashed lines). Buffers concentration used was 5 mM for all conditions tested. $\lambda(\max)$ obtained were similar for all the conditions in both analysis - $\lambda(280\text{ nm})= 349.74 \pm 1.08$ and $\lambda(296\text{ nm})= 348.96 \pm 1.25$ 92

Figure II.S1.3 Size analysis of anti-IL8 mAb at the different working pH and salt concentrations – 0 (dark grey) and 150 mM NaCl (light grey) by dynamic light scattering. Buffer systems used were composed by HEPES for pH 7.5, EPPS for pH 8.5 and CHES for the pH values of 9.0, 9.5 and 10, at a concentration of 20 mM. Results are presented as mean of the hydrodynamic diameter ± STDV. Results are

represented considering the number of particles in solution. The dashed line corresponds to the anti-IL8 mAb pl (≥ 9.3).....93

Figure II.S2.1 Anti-IL8 mAb far UV circular dichroism spectra at different pH - 7.5 (full lines), 8.5 (dashed lines) and 9.0 (dotted lines) - and salts – NaF, 150 mM (black lines), MgCl₂, 50 mM (blue lines) and (NH₄)₂SO₄, 50 mM (green lines). Buffer systems used were composed by HEPES for pH 7.5, EPPS for pH 8.5 and CHES for pH 9.0 at a concentration of 5 mM.....93

Figure II.S2.2 Fluorescence spectra of (A) Tyrosine at an excitation wavelength of 280 nm and (B) Tryptophan at an excitation wavelength of 296 nm at different pH values - 7.5 (full lines), 8.5 (dashed lines) and 9.0 (dotted lines) - and salts – NaF, 150 mM (black lines), MgCl₂, 50 mM (blue lines) and (NH₄)₂SO₄, 50 mM (green lines). Buffer systems used were composed by HEPES for pH 7.5, EPPS for pH 8.5 and CHES for pH 9.0 at a concentration of 5 mM. $\lambda(\text{max})$ obtained were similar for all the conditions in both analysis - $\lambda(280 \text{ nm}) = 351.48 \pm 1.14$ and $\lambda(296 \text{ nm}) = 349.36 \pm 1.32$ 94

Figure II.S2.3 Size analysis of anti-IL8 mAb at the different working pH - 7.5 (■), 8.5 (▣) and 9.0 (▢) - and salts – NaF (150 mM), MgCl₂ (50 mM) and (NH₄)₂SO₄ (50 mM) performed by dynamic light scattering. Buffer systems used were composed by HEPES for pH 7.5, EPPS for pH 8.5 and CHES for the pH value of 9.0, at a concentration of 20 mM. Results are presented as mean of the hydrodynamic diameter \pm STDV. Results are represented considering the number of particles in solution.....94

Figure III.1 Coomassie Blue stained SDS-PAGE of fractions collected during IgG purification from a clarified serum-containing CHO DP-12 cell supernatant by PBA chromatography using different wash buffers: (A) 100 mM D-sorbitol, 10 mM Tris-HCl, pH 7.5 and (B) 150 mM NaCl, 10 mM Tris-HCl, pH 7.5. In both runs the adsorption buffer was 20 mM HEPES, 150 mM NaCl, pH 7.5 and the elution buffer, 1.5 M Tris-HCl, pH 7.5. Lanes ID: 1: Precision Plus Protein™ Dual Color Standards (from top to bottom: 200, 150, 100, 75, 50, 37, 25 and 20 kDa); 2: feed sample of CHO DP-12 supernatant; 3: flow-through fraction; 4: wash fraction; 5: elution fraction. Position of IgG heavy (H) (50 kDa) and light (L) (25 kDa) chains are indicated in the right side of the gel. The concentration of IgG in lane 5A and 5B was 52 mg/dm³ and 86 mg/dm³, respectively.....106

Figure III.2 (A) Chromatographic profile of IgG purification by PBA chromatography from a clarified serum-containing CHO DP-12 cell supernatant, using as adsorption buffer 20 mM HEPES, 150 mM NaCl, pH 7.5, wash buffer 100 mM D-sorbitol, 10 mM Tris-HCl, pH 7.5 and as elution buffer 0.5 M D-sorbitol, 150 mM NaCl, 10 mM Tris, pH 7.5. Absorbance at 280 nm (mAU) – black line, conductivity (mS/cm) – dashed black line, FT: Flow-through; W: Wash; E: Elution. (B) Coomassie Blue stained SDS-PAGE of fractions collected during IgG purification from clarified CHO DP-12 cell supernatant by PBA chromatography using the same buffers as in (A). Lanes ID: 1: Precision Plus Protein™ Dual Color Standards (from top to bottom: 200, 150, 100, 75, 50, 37, 25, 20, and 10 kDa); 2: feed sample of CHO DP-12 supernatant; 3: flow-through fraction; 4: wash fraction; 5: elution fraction. Position of IgG heavy (H) (50 kDa) and light (L) (25 kDa) chains are indicated in the right side of the gel. The concentration of IgG in lane 5B was 41 mg/dm³.....109

Figure III.3 Silver stained IEF gel of the fractions collected after the purifications of IgG from serum-containing CHO DP-12 cell culture supernatants by (A) Protein A affinity chromatography and (B) PBA chromatography using as elution buffer 0.5 M D-sorbitol, 150 mM NaCl in 10 mM Tris-HCl, pH 7.5 (S)

or 1.5 M Tris-HCl, pH 7.5 (T). Lanes ID: 1: pI broad standards (from bottom to top: Amylglucosidase - 3.50 pI (Native); Methyl red (dye) - 3.75 (pI Native); Trypsin inhibitor - 4.55 (pI Native); b-Lactoglobulin A - 5.20 (pI Native); Carbonic anhydrase B (bovine) - 5.85 (pI Native); Carbonic anhydrase B (human) - 6.55 (pI Native); Myoglobin, acidic band - 6.85 (pI Native); Myoglobin, basic band - 7.35 (pI Native); Lentil lectin, acidic - 8.15 (pI Native); Lentil lectin, middle - 8.45 (pI Native); Lentil lectin, basic - 8.65 (pI Native) and Trypsinogen - 9.30 (pI Native)); 2: feed sample of CHO DP-12 supernatant; 3: elution fraction from Protein A purification; 3S: elution fraction from PBA chromatography (0.5 M D-sorbitol, 150 mM NaCl in 10 mM Tris-HCl, pH 7.5); 3T: elution fraction from PBA chromatography (1.5 M Tris-HCl, pH 7.5).....110

Figure III.4 Activity of purified anti-IL8 monoclonal antibodies from clarified serum-containing CHO DP-12 cell culture supernatants determined by competitive ELISA. (A) Elution fraction from protein A chromatography; (B) Elution fraction from PBA chromatography using as elution buffer 1.5 M Tris-HCl, all at pH 7.5; C – Elution fraction from PBA chromatography using as elution buffer 0.5 M D-sorbitol, 150 mM NaCl in 10 mM Tris-HCl, all at pH 7.5. Results are displayed as mean ± STDV.....111

Figure III.5 Coomassie Blue stained SDS-PAGE of fractions collected during the purification by PBA chromatography of (A) anti-IL8 mAb from clarified serum-free media CHO DP-12 cell culture supernatants and (B) anti-HCV mAb from clarified serum-free CHOEBNALT85 cell culture supernatants, using as adsorption buffer 20 mM HEPES with 150 mM NaCl at pH 7.5, as wash buffer 100 mM D-sorbitol in 10 mM Tris-HCl at pH 7.5 and as elution buffer 0.5 M D-sorbitol with 150 mM NaCl in 10 mM Tris-HCl at pH 7.5. Lanes ID: 1: Precision Plus Protein™ Dual Color Standards (from top to bottom: 250, 150, 100, 75, 50, 37, 25, 20, 15 and 10 kDa); 2: feed sample of serum-free CHO supernatants; 3: flow-through fraction; 4: wash fraction; 5: elution fraction. Position of IgG heavy (H) (50 kDa) and light (L) (25 kDa) chains are indicated in the right side of the gel. The concentration of IgG in lane 5A and 5B was 66 mg/dm³ and 117 mg/dm³, respectively.....113

Figure III.6 Silver stained IEF gel of the fractions collected during the purifications of the anti-HCV mAb by (A) Protein A affinity chromatography and (B) PBA chromatography (wash buffer: 100 mM D-sorbitol in 10 mM Tris-HCl at pH 7.5). Lanes ID: 1: pI broad standards (from bottom to top: Amylglucosidase - 3.50 pI (Native); Methyl red (dye) - 3.75 (pI Native); Trypsin inhibitor - 4.55 (pI Native); b-Lactoglobulin A - 5.20 (pI Native); Carbonic anhydrase B (bovine) - 5.85 (pI Native); Carbonic anhydrase B (human) - 6.55 (pI Native); Myoglobin, acidic band - 6.85 (pI Native); Myoglobin, basic band - 7.35 (pI Native); Lentil lectin, acidic - 8.15 (pI Native); Lentil lectin, middle - 8.45 (pI Native); Lentil lectin, basic - 8.65 (pI Native) and Trypsinogen - 9.30 (pI Native)); 2: feed sample of CHOEBNALT85 supernatant; 3: wash fraction; 4: elution fraction.....114

Figure III.7 Effect of residence time in the dynamic binding capacity of PBA resin. (A) Frontal analysis for a residence time of 2 minutes and a pure IgG feedstock of 1 g/dm³. Absorbance at 280 nm (—). (B) Schematic of the breakthrough curves for the different residence times tested – 0.4 (—), 0.8 (—), 2 (—) and 4 minutes (—) – using an IgG feedstock of 1 g/dm³. (C) Dynamic (■) and Total (■) binding capacities for the different residence times tested. (D) Relation between the calculated DBC and the slope of the respective breakthrough curves, displayed in (B). Results are displayed as mean ± STDV.....116

Figure III.8 Silver stained SDS-PAGE of fractions collected during IgG purification from clarified serum-free CHO DP-12 cell culture supernatants, by PBA chromatography. IgG concentration on the feedstock was of 74 mg/dm³. (A) Superficial velocity study using 5.1 cm³/min in adsorption, wash and elution steps. (B) Superficial velocities study using 5.1, 15.3 and 25.5 cm³/min in adsorption, wash and elution steps, respectively. Lanes ID: 1: Precision Plus Protein™ Dual Color Standards (from top to bottom: 250, 200, 150, 100, 75, 50, 37, 25, 15, and 10 kDa); 2: feed sample of CHO DP-12 supernatant; 3: flow-through fraction; 4: wash fraction; 5: elution fraction. Position of IgG heavy (H) (50 kDa) and light (L) (25 kDa) chains are indicated in the right side of the gel.....117

Figure III.9 Effect of different loading volumes in the (A) chromatographic profile: 2 cm³ (—), 5 cm³ (—) and 10 cm³ (—); and in the (B) performance parameters, namely recovery yield (■), protein purity (■), protein removal (■) and gDNA removal (■) of IgG purification from clarified serum-free CHO DP-12 cell culture supernatants, by PBA chromatography. IgG concentration on the feedstock was 58 mg/dm³. Results are displayed as mean ± STDV (except for gDNA removal: ± standard error). Protein purity was assessed by the ratio between IgG and total protein concentration. Protein and gDNA removal were determined by the difference between the total amount of molecules in the feedstock and in the elution pools divided by the same amount of molecules on the feedstock.....118

Figure III.10 Run-to run reproducibility demonstrated by chromatographic profiles of IgG capture from different clarified serum-free CHO DP-12 cell culture supernatants using PBA ligands. Each individual run took 8.7 minutes. IgG concentration in the different runs were: (I and II) 65 mg/dm³; 73.9 mg/dm³ (III and IV) and 58.3 mg/dm³ (V). I and II are duplicates as III and IV.....119

Figure III.11 (A) Chromatographic profiles at different scales: 4 cm³ (—), 16 cm³ (—) and 40 cm³ (—) and (B) performance parameters: recovery yield (■), protein purity (■), protein removal (■), HCP removal (■) and gDNA removal (■) obtained for the IgG capture from clarified serum-free CHO DP-12 cell culture supernatants by PBA chromatography. IgG concentration on the feedstock was 57.8 ± 0.3 mg/dm³. Results are displayed as mean ± STDV (except for gDNA removal: ± standard error). Protein purity was assessed by the ratio between IgG and protein concentration. Protein, HCP and gDNA removal were determined by the difference between the total amount of molecules in the feedstock and in the elution pools divided by the same total amount of molecules on the feedstock.....121

Figure III.S1 Analytical chromatogram from SEC-HPLC analysis of the purified IgG fractions from 2.5% serum-containing CHO DP-12 cell culture supernatants. (A) Protein A chromatography. Adsorption buffer: 10 mM PBS, pH 7.4; elution buffer: 100 mM glycine-HCl, pH 2. (B) PBA chromatography: Adsorption buffer: 20 mM HEPES, 150 mM NaCl, pH 7.5; wash buffer: 100 mM D-sorbitol in 10 mM Tris-HCl, pH 7.5; elution buffer: 0.5 M D-sorbitol and 150 mM NaCl in 10 mM Tris-HCl, pH 7.5. (C) PBA chromatography: Adsorption buffer: 20 mM HEPES, 150 mM NaCl, pH 7.5; wash buffer: 100 mM D-sorbitol in 10 mM Tris-HCl, pH 7.5; elution buffer: 1.5 M Tris-HCl, pH 7.5.....126

Figure III.S2 Analytical chromatogram from SEC-HPLC analysis of the purified IgG fractions from serum-free CHO DP-12 cell culture supernatants. (A) Protein A chromatography. Adsorption buffer: 10 mM PBS, pH 7.4; elution buffer: 100 mM glycine-HCl, pH 2. (B) PBA chromatography: Adsorption buffer: 20 mM HEPES, 150 mM NaCl, pH 7.5; wash buffer: 100 mM D-sorbitol in 10 mM Tris-HCl, pH 7.5; elution buffer: 0.5 M D-sorbitol and 150 mM NaCl in 10 mM Tris-HCl, pH 7.5.....127

Figure III.S3 Analytical chromatogram from SEC-HPLC analysis of the purified IgG fractions from serum-free CHOEBNALT85 cell culture supernatants. (A) Protein A chromatography. Adsorption buffer: 10 mM PBS, pH 7.4; elution buffer: 100 mM glycine-HCl, pH 2. (B) PBA chromatography: Adsorption buffer: 20 mM HEPES, 150 mM NaCl, pH 7.5; wash buffer: 100 mM D-sorbitol in 10 mM Tris-HCl, pH 7.5; elution buffer: 0.5 M D-sorbitol and 150 mM NaCl in 10 mM Tris-HCl, pH 7.5..... 128

Figure IV.1 Mobile phase modulators concentration required to promote complete elution of the different glycoproteins under study. Studies were performed using a ProSep®-PB resin. Adsorption of glycoproteins was performed using 20 mM CHES, 300 mM NaCl, pH 9.0. Results are based on the mobile phase concentration present in the elution buffer at which was obtained the maximum peak height. Acidic invertase (■), acidic amyloglucosidase (■), neutral cellulase (■) and basic RNase B (□). Results are displayed as average ± STDV.....140

Figure IV.2 (A) Chromatograms obtained using a ProSep®-PB resin for the separation of an artificial mixture containing 1 mg/mL of each glycoprotein under study prepared in the adsorption buffer 20 mM CHES, 300 mM NaCl at pH 9.0. Five different gradient slopes were performed considering an elution buffer containing 0.5 M Tris as displacer agent (a-e). The gradients were performed under the rates of (a) 5 % Tris/min, (b) 2.5 % Tris/min, (c), 1.25 % Tris/min, (d) 0.75 % Tris/min and (e) 0.6 % Tris/min giving rise to five distinct chromatograms – C1 to C5, respectively. The times at which the system was imposed to start to pump 100% (v/v) of the elution buffer are marked with a yellow arrow. C5 presents five peaks denominated as flow-through (FT), peak 1 (P1), peak 2 (P2), peak 3 (P3) and peak 4 (P4), from left to right. (B) Coomassie Blue stained SDS-PAGE of the fractions collected during glycoproteins separation by PB chromatography using a ProSep®-PB resin and an elution gradient strategy accomplished by the use of 0.5 M Tris as displacer agent at a rate of 0.6% Tris/min. Lanes ID: 1: Precision Plus Protein™ Dual Color Standards (from top to bottom: 250, 200, 150, 100, 75, 50, 37, 25, 20 and 10 kDa); 2: artificial mixture containing 5 µg of each glycoprotein under study; 3: flow-through (FT) fraction; 4: P1; 5: P2; 6: P3; 7: P4.....141

Figure IV.3 (A) Chromatograms obtained using a ProSep®-PB resin for the separation of an artificial mixture containing 1 mg/mL of each glycoprotein under study prepared in the adsorption buffer 20 mM CHES, 300 mM NaCl at pH 9.0. The elution process was performed using a series of step gradients – 2.0%, 4.5%, 8.5%, 15% and 100% (v/v). The elution buffer used was obtained by addition of 0.5 M Tris to the adsorption buffer. The chromatogram presents six peaks denominated as flow-through (FT), peak 1 (P1), peak 2 (P2), peak 3 (P3), peak 4 (P4) and peak 5 (P5), from left to right. (B) Coomassie Blue stained SDS-PAGE of the fractions collected during glycoproteins separation by PB chromatography using a ProSep®-PB resin and an elution strategy accomplished by the use of a series of step gradients – 2%, 4.5%, 8.5%, 15% and 100% (v/v). Lanes ID: 1: Precision Plus Protein™ Dual Color Standards (from top to bottom: 250, 200, 150, 100, 75, 50, 37, 25, 20 and 10 kDa); 2: artificial mixture containing 5 µg of each glycoprotein under study; 3: flow-through (FT) fraction; 4: P1; 5: P2; 6: P3; 7: P4; 8: P5...142

Figure IV.4 (A) Chromatograms obtained using a ProSep®-PB resin for the separation of an artificial mixture containing 2.5 mg/mL of each glycoprotein under study prepared in the adsorption buffer 20 mM CHES, 300 mM NaCl at pH 9.0. The elution process was performed using a linear gradient performed at a rate of 0.6% Tris/min. The elution buffer used was obtained by addition of 0.5 M Tris to the

adsorption buffer. The chromatogram presents five peaks denominated as flow-through (FT), peak 1 (P1), peak 2 (P2), peak 3 (P3) and peak 4 (P4), from left to right. (B) Coomassie Blue stained SDS-PAGE of the fractions collected during glycoproteins separation by PB chromatography using a ProSep®-PB resin and an elution gradient strategy accomplished by the use of 0.5 M Tris as displacer agent at a rate of 0.6% Tris/min. Lanes ID: 1: artificial mixture containing 5 µg of each glycoprotein under study; 2: flow-through (FT) fraction; 3: Precision Plus Protein™ Dual Color Standards (from top to bottom: 250, 200, 150, 100, 75, 50, 37, 25, 20 and 10 kDa); 4: P1; 5: P2; 6: P3; 7: P4.....143

Figure IV.5 (A) Chromatograms obtained using a ProSep®-PB resin for the separation of an artificial mixture containing 2.5 mg/mL of each glycoprotein under study prepared in the adsorption buffer 20 mM CHES, 300 mM NaCl at pH 9.0. The elution process was performed using a series of step gradients – 2%, 4.5%, 8.5%, 15% and 100% (v/v). The elution buffer used was obtained by addition of 0.5 M Tris to the adsorption buffer. The chromatogram presents six peaks denominated as flow-through (FT), peak 1 (P1), peak 2 (P2), peak 3 (P3), peak 4 (P4) and peak 5 (P5), from left to right. (B) Coomassie Blue stained SDS-PAGE of the fractions collected during glycoproteins separation by PB chromatography using a ProSep®-PB resin and an elution strategy accomplished by the use of a series of step gradients – 2%, 4.5%, 8.5%, 15% and 100% (v/v). Lanes ID: 1: artificial mixture containing 5 µg of each glycoprotein under study; 2: flow-through (FT) fraction; 3: P1; 4: Precision Plus Protein™ Dual Color Standards (from top to bottom: 250, 200, 150, 100, 75, 50, 37, 25, 20 and 10 kDa); 5: P2; 6: P3; 7: P4; 8: P5.....143

Figure IV.6 Sodium citrate concentration required to promote complete elution of the different acidic/neutral proteins under study. Studies were performed using a ProSep®-PB resin. Adsorption of acidic/neutral proteins was performed using 50 mM acetate, pH 5.0. Results are based on the sodium citrate concentration on the elution buffer at which was obtained the maximum peak height. Results are displayed as average ± STDV.....145

Figure IV.7 (A) Chromatograms obtained using a ProSep®-PB resin for the separation of an artificial mixture containing 1 mg/mL of each acidic/neutral protein under study prepared in the adsorption buffer 50 mM citrate at pH 5.0. Four different gradient slopes were applied considering an elution buffer containing 0.5 M citrate as displacer agent (a-d). The gradients were performed under the rates of (a) 5 % citrate/min, (b) 2.5 % citrate/min, (c), 1.25 % citrate/min and (d) 0.75 % citrate/min giving rise to four distinct chromatograms – C1 to C4, respectively. Immediately after the elution, the column regeneration was conducted using 1.5 M Tris-HCl, pH 8.5. C4 presents five peaks denominated as flow-through (FT), peak 1 (P1), peak 2 (P2), peak 3 (P3) and peak 4 (P4), from left to right. (B) Coomassie Blue stained SDS-PAGE of the fractions collected during acidic/neutral proteins separation by PB chromatography using a ProSep®-PB resin and an elution gradient strategy accomplished by the use of 0.5 M citrate as displacer agent at a rate of 0.75% citrate/min. Lanes ID: 1: Precision Plus Protein™ Dual Color Standards (from top to bottom: 250, 200, 150, 100, 75, 50, 37, 25, 20 and 10 kDa); 2: artificial mixture containing 5 µg of each acidic/neutral protein under study; 3: flow-through (FT) fraction; 4: P1; 5: P2; 6: P3; 7: P4.....146

Figure IV.8 (A) Chromatograms obtained using a ProSep®-PB resin for the separation of an artificial mixture containing 1 mg/mL of each acidic/neutral protein under study prepared in the adsorption buffer

50 mM citrate at pH 5.0. The elution process was performed using a series of step gradients – 1.5%, 4%, and 15% (v/v). The elution buffer used was obtained by addition of 0.5 M citrate to the adsorption buffer. The chromatogram presents five peaks denominated as flow-through (FT), peak 1 (P1), peak 2 (P2), peak 3 (P3) and peak 4 (P4), from left to right. The time at which the system was imposed to start to pump 100% (v/v) of the regeneration buffer – 1.5 M Tris-HCl, pH 8.5 – is marked with a yellow arrow. (B) Coomassie Blue stained SDS-PAGE of the fractions collected during acidic/neutral proteins separation by PB chromatography using a ProSep®-PB resin and an elution strategy accomplished by the use of a series of step gradients – 1.5%, 4%, and 15% (v/v). Lanes ID: 1: Precision Plus Protein™ Dual Color Standards (from top to bottom: 250, 200, 150, 100, 75, 50, 37, 25, 20 and 10 kDa); 2: artificial mixture containing 5 µg of each acidic/neutral protein under study; 3: flow-through (FT) fraction; 4: P1; 5: P2; 6: P3; 7: P4.....147

Figure IV.9 (A) Chromatogram obtained using a ProSep®-PB resin for the separation of an artificial mixture containing 2.5 mg/mL of each acidic/neutral protein under study prepared in the adsorption buffer 50 mM citrate at pH 5.0. The elution process was performed using a linear gradient performed at a rate of 0.75% citrate/min. The elution buffer used was obtained by addition of 0.5 M citrate to the adsorption buffer. Immediately after the elution, the column regeneration was conducted using 1.5 M Tris-HCl, pH 8.5. The chromatogram presents five peaks denominated as flow-through (FT), peak 1 (P1), peak 2 (P2), peak 3 (P3) and peak 4 (P4), from left to right. (B) Coomassie Blue stained SDS-PAGE of the fractions collected during acidic/neutral proteins separation by PB chromatography using a ProSep®-PB resin and an elution gradient strategy accomplished by the use of 0.5 M citrate as displacer agent at a rate of 0.75% citrate/min. Lanes ID: 1: artificial mixture containing 5 µg of each cidic/neutral protein under study); 2: flow-through (FT) fraction; 3: P1; 4: P2; 5: Precision Plus Protein™ Dual Color Standards (from top to bottom: 250, 200, 150, 100, 75, 50, 37, 25, 20 and 10 kDa; 6: P3; 7: P4.....148

Figure IV.10 (A) Chromatogram obtained using a ProSep®-PB resin for the separation of an artificial mixture containing 2.5 mg/mL of each acidic/neutral protein under study prepared in the adsorption buffer 50 mM citrate at pH 5.0. The elution process was performed using a series of step gradients – 1.5%, 4%, and 15% (v/v). The elution buffer used was obtained by addition of 0.5 M citrate to the adsorption buffer. The chromatogram presents five peaks denominated as flow-through (FT), peak 1 (P1), peak 2 (P2), peak 3 (P3), and peak 4 (P4), from left to right. The time at which the system was imposed to start to pump 100% (v/v) of the regeneration buffer – 1.5 M Tris-HCl, pH 8.5 – is marked with a yellow arrow. (B) Coomassie Blue stained SDS-PAGE of the fractions collected during acidic/neutral proteins separation by PB chromatography using a ProSep®-PB resin and an elution strategy accomplished by the use of a series of step gradients – 1.5%, 4%, and 15% (v/v). Lanes ID: 1: artificial mixture containing 5 µg of each acidic/neutral protein under study; 2: Precision Plus Protein™ Dual Color Standards (from top to bottom: 250, 200, 150, 100, 75, 50, 37, 25, 20 and 10 kDa); 3: flow-through (FT) fraction; 4: P1; 5: P2; 6: P3; 7: P4.....148

Figure IV.11 pH gradient curves obtained for the elution of glycosylated proteins from (A) ProSep®-PB and (B) P6XL matrices. pH gradients were performed using BGly buffer formulation, based on Kröner *et al.* (2013) [24]. Column regeneration was achieved using 1.5 M Tris-HCl, pH 8.5. 1 mg/mL of each

glycosylated protein - amyloglucosidase (red circle), cellulase (green square), RNase B (yellow triangle) and invertase (orange diamond) - were separately loaded in each column. The elution points represented, correspond to the maximum peak height obtained.....150

Figure IV.12 Percentage of each glycoprotein recovered from (A) ProSep®-PB and (B) P6XL matrices during the employed elution pH gradient (■) or at the regeneration step (▣). pH gradients were performed using BGly buffer formulation, based on Kröner *et al.* (2013) [24]. Column regeneration was achieved using 1.5 M Tris-HCl, pH 8.5. 1 mg/mL of each glycosylated protein - amyloglucosidase (AMY), cellulase (CEL), RNase B (RB) and invertase (INV) - were separately loaded in each column. Results correspond to the ratio between the areas of the peaks obtained during the elution peak gradient and regeneration step and the total peak area of the chromatogram. Results are displayed as average ± STDV.....151

Figure IV.13 pH gradient curves obtained for the elution of acidic/neutral proteins from ProSep®-PB (A and B) and P6XL matrices (C and D). pH gradients were performed using two different buffer formulations – BAN1 (A and C) and BAN2 (B and D) - based on Kröner *et al.* (2013) [24]. Column regeneration was achieved using 1.5 M Tris-HCl, pH 8.5. 1 mg/mL of each acidic/neutral protein - amyloglucosidase (red and orange circles), cellulase (green square), pepsin (dark and light blue triangles) - were separately loaded in each column. The elution points represented, correspond to the maximum peak height obtained.....153

Figure IV.14 Percentage of each acidic/neutral protein recovered from ProSep®-PB (A and B) and P6XL matrices (C and D) during the employed elution pH gradient (■ and ▣) or at the regeneration step (▣). pH gradients were performed using the buffer formulations BAN1 and BAN2, based on Kröner *et al.* (2013) work [24]. Column regeneration was achieved using 1.5 M Tris-HCl, pH 8.5. 1 mg/mL of each glycosylated protein - amyloglucosidase (AMY), cellulase (CEL) and pepsin (PEP) - were separately loaded in each column. Results correspond to the ratio between the areas of the peaks obtained during the elution peak gradient and regeneration step and the total peak area of the chromatogram. Results are displayed as average ± STDV.154

Figure IV.S1 Coomassie Blue stained SDS-PAGE of the commercial proteins constituents of the protein library under study. Lanes ID: 1: Precision Plus Protein™ Dual Color Standards (from top to bottom: 250, 200, 150, 100, 75, 50, 37, 25, 20 and 10 kDa); 2: Invertase (glycosylated and acidic protein), 3: Amyloglucosidase (glycosylated and acidic protein), 4: Pepsin (non-glycosylated and acidic protein), 5: Cellulase (glycosylated and acidic/neutral protein), 6: RNase B (glycosylated and basic protein). The mass of protein in lanes 2 to 6 is 5 µg.....158

Figure IV.S2.1 (A) Chromatogram obtained using a P6XL resin for the separation of an artificial mixture containing 2.5 mg/mL of each glycoprotein under study, prepared in the adsorption buffer 20 mM CHES, 300 mM NaCl at pH 9.0. The elution process was performed using a linear gradient performed at a rate of 0.6% Tris/min. The elution buffer used was obtained by addition of 0.5 M Tris to the adsorption buffer. The chromatogram presents five peaks denominated as flow-through (FT), peak 1 (P1), peak 2 (P2), peak 3 (P3) and peak 4 (P4), from left to right. The time at which the system was imposed to start to pump 100% (v/v) of the regeneration buffer – 1.5 M Tris-HCl, pH 8.5 – is marked with a yellow arrow. (B) Coomassie Blue stained SDS-PAGE of the fractions collected during glycoproteins separation by

PB chromatography using a P6XL resin and an elution gradient strategy accomplished by the use of 0.5 M Tris as displacer agent at a rate of 0.6% Tris/min. Lanes ID: 1: artificial mixture containing 5 µg of each glycoprotein under study; 2: flow-through (FT) fraction; 3: P1; 4: Precision Plus Protein™ Dual Color Standards (from top to bottom: 250, 200, 150, 100, 75, 50, 37, 25, 20 and 10 kDa); 5: P2; 6: P3; 7: P4.....159

Figure IV.S2.2 (A) Chromatogram obtained using a P6XL resin for the separation of an artificial mixture containing 2.5 mg/mL of each glycoprotein under study, prepared in the adsorption buffer 20 mM CHES, 300 mM NaCl at pH 9.0. The elution process was performed using a series of step gradients – 2%, 4.5%, 8.5%, 15% and 100% (v/v). The elution buffer used was obtained by addition of 0.5 M Tris to the adsorption buffer. The chromatogram presents six peaks denominated as flow-through (FT), peak 1 (P1), peak 2 (P2), peak 3 (P3), peak 4 (P4) and peak 5 (P5) from left to right. The time at which the system was imposed to start to pump 100% (v/v) of the regeneration buffer – 1.5 M Tris-HCl, pH 8.5 – is marked with a yellow arrow. (B) Coomassie Blue stained SDS-PAGE of the fractions collected during glycoproteins separation by PB chromatography using a P6XL resin and an elution strategy accomplished by the use of a series of step gradients – 2%, 4.5%, 8.5%, 15% and 100% (v/v). Lanes ID: 1: Precision Plus Protein™ Dual Color Standards (from top to bottom: 250, 200, 150, 100, 75, 50, 37, 25, 20 and 10 kDa); 2: artificial mixture containing 5 µg of each glycoprotein under study; 3: flow-through (FT) fraction; 4: P1; 5: P2; 6: P3; 7: P4; 8: P5.....160

Figure IV.S3.1 (A) Chromatogram obtained using a P6XL resin for the separation of an artificial mixture containing 2.5 mg/mL of each acidic/neutral protein under study prepared in the adsorption buffer 50 mM citrate at pH 5.0. The elution process was performed using a linear gradient performed at a rate of 0.75% citrate/min. The elution buffer used was obtained by addition of 0.5 M citrate to the adsorption buffer. Immediately after the elution, column regeneration was conducted using 1.5 M Tris-HCl, pH 8.5. The chromatogram presents 3 peaks denominated as flow-through (FT), peak 1 (P1) and peak 2 (P2), from left to right. (B) Coomassie Blue stained SDS-PAGE of the fractions collected during acidic/neutral proteins separation by PB chromatography using a P6XL resin and an elution gradient strategy accomplished by the use of 0.5 M citrate as displacer agent at a rate of 0.75% citrate/min. Lanes ID: 1: artificial mixture containing 5 µg of each cidic/neutral protein under study); 2: Precision Plus Protein™ Dual Color Standards (from top to bottom: 250, 200, 150, 100, 75, 50, 37, 25, 20 and 10 kDa); 3: flow-through (FT) fraction; 4: P1; 5: P2.....161

Figure IV.S3.2 (A) Chromatogram obtained using a P6XL resin for the separation of an artificial mixture containing 2.5 mg/mL of each acidic/neutral protein under study prepared in the adsorption buffer 50 mM citrate at pH 5.0. The elution process was performed using a series of step gradients – 1.5%, 4%, and 15% (v/v). The elution buffer used was obtained by addition of 0.5 M citrate to the adsorption buffer. The chromatogram presents five peaks denominated as flow-through (FT), peak 1 (P1), peak 2 (P2), peak 3 (P3), and peak 4 (P4), from left to right. The time at which the system was imposed to start to pump 100% (v/v) of the regeneration buffer – 1.5 M Tris-HCl, pH 8.5 – is marked with a yellow arrow. (B) Coomassie Blue stained SDS-PAGE of the fractions collected during acidic/neutral proteins separation by PB chromatography using a P6XL resin and an elution strategy accomplished by the use of a series of step gradients – 1.5%, 4%, and 15% (v/v). Lanes ID: 1: artificial mixture containing 5 µg

of each acidic/neutral protein under study; 2: flow-through (FT) fraction; 3: P1; 4: Precision Plus Protein™ Dual Color Standards (from top to bottom: 250, 200, 150, 100, 75, 50, 37, 25, 20 and 10 kDa); 5: P2; 6: P3; 7: P4.....162

List of Tables

Table I.1 Different antibodies classes and their characteristics concerning function, structure and availability on serum. [20].....	7
Table II.1 Heat of adsorption for the anti-human IL-8 mAb onto P6XL resin considering a sample loop, adsorbent volumes and a protein loading of 100 μ L, 171 μ L and 5 mg/mL, respectively. All experiments were performed under a flow-rate of 1.5 mL/h. The amount of mAb in the flow-through (not binding to the column) is given as percentage of the total mass of mAb loaded into the column. ΔH^I , ΔH^{II} and ΔH^{III} were determined by integration of the individual peaks obtained from the de-convolution of thermograms using PeakFit software (Figure II.2). Results are displayed as mean \pm STDV. I and FT stand for ionic strength and flow-through, respectively. RSD stands for relative standard deviation. n.a. – not applicable.	69
Table II.2 Heat of adsorption for D-sorbitol onto P6XL resin considering a sample loop, adsorbent volumes and a loading of 100 μ L, 171 μ L and 20 mM (3.64 mg/mL), respectively. All experiments were performed under a flow-rate of 1.5 mL/h. ΔH^I , ΔH^{II} and ΔH^{III} were determined from the de-convoluted thermograms by PeakFit software (Figure II.3). Results are displayed as mean \pm STDV. I and RSD stand for ionic strength and relative standard deviation, respectively.....	73
Table II.3 Heat of adsorption for the anti-human IL-8 mAb onto P6XL resin considering a sample loop, adsorbent volumes and a protein loading of 100 μ L, 171 μ L and 5 mg/mL, respectively. All experiments were performed under a flow-rate of 1.5 mL/h and at a constant ionic strength of 0.15 M. No flow-through was observed in all the conditions tested. ΔH^I , ΔH^{II} and ΔH^{III} were determined by integration of the individual peaks obtained from the de-convolution of thermograms using PeakFit software (Figure II.7). Results are displayed as mean \pm STDV. RSD stands for relative standard deviation.....	80
Table III.1. Performance parameters (recovery yield, protein purity and purification factor - PF) of IgG purification from a clarified serum-containing CHO DP-12 cell supernatant by PBA chromatography using 20 mM HEPES, 150 mM NaCl as adsorption buffer, different wash buffers and step elution with 1.5 M Tris-HCl. All buffers are at pH 7.5. Results are displayed as mean \pm STDV. W: wash buffer, E: elution buffer.....	107
Table III.2. Performance parameters (recovery yield, protein purity and purification factor - PF) of IgG purification from a clarified serum-containing CHO DP-12 cell supernatant by PBA chromatography using 20 mM HEPES, 150 mM NaCl as adsorption buffer, 100 mM D-sorbitol in 10 mM Tris-HCl as wash buffer and different elution buffers. All buffers are at pH 7.5. Results are displayed as mean \pm STDV. W: wash buffer, E: elution buffer.....	110
Table III.3 Performance parameters of IgG purification from a clarified serum-containing CHO DP-12 cell supernatant by CPG and phenyl-Sepharose chromatography. All the buffers used were at pH 7.5. Results are displayed as mean \pm STDV. A: adsorption buffer; W: wash buffer; E: elution buffer.....	111
Table III.4 Performance parameters regarding the purification by PBA chromatography of anti-IL-8 and anti-HCV mAbs produced in serum-free media. All buffers are at pH 7.5. Results are displayed as mean \pm STDV. A: adsorption buffer; W: wash buffer; E: elution buffer.....	114
Table III.5 Effect of superficial velocity in the performance parameters (recovery yield, protein purity and protein removal) of IgG purification from clarified CHO DP-12 cell supernatants by PBA chromatography	

at a scale of 0.4 cm³. IgG concentration in the feedstock was 74 mg/dm³. Results are displayed as mean ± STDV.....119

Table IV.1 Summary table of the most important characteristics of proteins to the current study. A glimpse about the function of each protein is also present. PDB ID stands for Protein Data Bank Identity. MW and pI stand for molecular weight and isoelectric point, respectively. ^a Product specifications provided by the supplier.....5

Table IV.2 Buffer systems used to obtained linear pH gradients for the separation of glycoproteins (BGly) and acidic/neutral proteins (BAN1 and BAN2).....8

List of Abbreviations

(NH ₄) ₂ SO ₄	Ammonium sulfate
ADAs	Anti-drug antibodies
ADCs	Antibody-drug conjugates
AEX	Anionic exchange
AIDS	Acquired immunodeficiency syndrome
Ala	Alanine
AMY	Amyloglucosidase
ApA	Artificial protein A
Asn	Asparagine
ATCC	American Type Culture Collection
ATPE	Aqueous two-phase extraction
ATPS	Aqueous two-phase system
ATR-FTIR	Attenuated total reflection Fourier transform IR
B-cells	B lymphocytes
BSA	Bovine serum albumin
CAGR	Compound Annual Growth Rate
CD	Circular dichroism
CD34	Cluster of differentiation 34
CDRs	Complementary-determining regions
CEA	Carcinoembryonic antigen
CEL	Cellulase
CEX	Cationic exchange
CHES	2-(cyclohexylamino)ethanesulfonic acid
CHO	Chinese Hamster Ovary
CHOP	Chinese Hamster Ovary proteins
CIP	Cleaning-in-place
CV	Column volume
DBC	Dynamic binding capacity
d _H	Hydrodynamic diameter
DHFR	Dihydrofolate reductase
DLS	Dynamic light scattering
DMAE	Dimethylamino ethyl anion exchange ligand
DMEM	Dulbecco's modified Eagle's medium
DNA	Deoxyribonucleic acid
DSC	Differential scanning calorimetry
DSP	Downstream processing
DTT	Dithiothreitol
DVB	Divinylbenzene
<i>E. coli</i>	<i>Escherichia coli</i>
<i>e.g.</i>	<i>exempli gratia</i> or for example
EBA	Expanded bed adsorption
EMA	European Medicines Agency
EOPO	Ethylene oxide propylene oxide
EPO	Erythropoietin
EPPS	4-(2-hydroxyethyl)-1-piperazinepropanesulfonic acid
Fab	Fragment antigen binding
FBS	Fetal bovine serum

FBS UL	Fetal bovine serum Ultra low IgG
Fc	Fragment crystallizable
FDA	Food and Drug Administration
FMC	Flow microcalorimetry
Fv	Fragment variable
gDNA	genomic DNA
GHT	Glycine, Hypoxanthine and Thymidine
Gln	Glutamine
Gly	Glycine
GS	Glutamine synthetase
HA	Hydroxyapatite
HCIC	Hydrophobic charge induction chromatography
HCP	Host cell protein
HCV	Hepatitis C virus
HEPES	4-(2-hydroxyethyl)-1-piperazineethanesulfonic acid
HGMF	High gradient magnetic fishing
hHSCs	human Hematopoietic stem cells
HIC	Hydrophobic interaction chromatography
His	Histidine
HPLC	High performance liquid chromatography
HPTFF	High performance tangential flow filtration
i.d.	internal diameter
<i>i.e.</i>	<i>id est</i> or in other words
IDA	Iminodiacetic acid
IEF	Isoelectric focusing
Ig	Immunoglobulin
IL	Interleukin
IMAC	Immobilized metal affinity chromatography
INV	Invertase
IR	Infrared radiation
ITC	Isothermal titration calorimetry
mAb	Monoclonal antibody
<i>m</i> -APBA	<i>m</i> -aminophenylboronic acid
MCSGP	Multicolumn countercurrent solvent gradient purification
MgCl ₂	Magnesium chloride
MMC	Multimodal chromatography
MSX	Methionine sulfoximine
MTX	Methotrexate
MW	Molecular weight
NaCl	Sodium chloride
NaF	Sodium fluoride
NCBI	National Center for Biotechnology Information
NMR	Nuclear magnetic resonance
PB	Phenyl boronate
PBA	Phenylboronic acid
PBS	Phosphate buffered saline
pDADMAC	polydiallyldimethylammonium
PEG	Polyethylene glycol
PEI	Polyethyleneimine

PEP	Pepsin
<i>per se</i>	by itself
Phe	Phenylalanine
pI	Isoelectric point
Q	Quaternary amino ethyl ligand
rAAV	Recombinant adeno-associated virus
RB or RNase B	Ribonuclease B
rDNA	Recombinant DNA
SAXS	Small-angle X-ray scattering
SDS-PAGE	Sodium dodecyl sulphate polyacrylamide gel electrophoresis
SEC	Size exclusion chromatography
SMAE	Diethylamino ethyl anion exchange ligand
SMB	Simulated moving bed
SmP	Smart polymer or partially benzylated poly(allylamine) salt-tolerant cationic polymer
SpA	Staphylococcal protein A
SPR	Surface plasmon resonance
STDV	Standard deviation
T	Temperature
Thr	Threonine
TMAE	Trimethylammonium ethyl anion exchange ligand
Tris	Tris(hydroxymethyl)aminomethane or 2-Amino-2-hydroxymethyl-propane-1,3-diol
TRPA	Thermo-responsive protein A
TNF	tumor necrosis factor
Tyr	Tyrosine
Val	Valine
WPC	Weak partitioning chromatography
xMRV	Xenotropic murine leukemia virus-related virus
ZFNs	Zinc finger nucleases
ΔG	Gibbs free energy
ΔH	Enthalpy
ΔH_{ads}	Enthalpy of adsorption or net heat of adsorption
ΔS	Entropy
MS	Mass spectrometry
ELISA	Enzyme-linked immunosorbent assay
RU	Response unit
pKa	Acid dissociation constant

Thesis Scope and Outline

The present thesis was developed in the framework of the Biotechnology and Biosciences PhD program of Instituto Superior Técnico (IST) (Lisbon, Portugal) and was performed in the context of the PureMAb project (PTDC/QEQPRS/0286/2014) funded by FCT - Fundação para a Ciência e Tecnologia. The experimental work was mainly carried out at Institute for Biotechnology and Bioengineering, IST (Lisbon, Portugal) in a close collaboration with the Professor Cristina Dias-Cabral group located at the Health Sciences Research Centre hosted at Faculdade de Ciências da Saúde, Universidade da Beira Interior (Covilhã, Portugal). This collaboration was essential to proceed with the flow microcalorimetry studies carried out.

The main goal of this thesis was to develop a cost-effective process based on the multimodal phenylboronic acid chromatography as an alternative to the well-established protein A capture step used in the purification train of monoclonal antibodies (mAbs) with the ultimate goal of reducing the cost of mAb-based products and, consequently fostering the accessibility of these biomolecules to the general population.

This thesis has been divided into five chapters. Chapter I provides a literature review where the production platform currently used to manufacture mAbs is described with particular detail in the downstream processing. The current trends to intensify and integrate the whole process are also described. Furthermore, some of the techniques currently used to study ligand-protein molecular interactions and protein conformational changes will be presented.

In Chapter II, on-line flow microcalorimetry (FMC) studies were performed in order to try to disclose the phenomena underlying the adsorption of an anti-IL8 mAb onto an *m*-aminophenylboronic acid (*m*-APBA) ligand, in the absence and in the presence of different mobile phase modulators. The measurements of instantaneous heat energy transfers accomplished using the FMC technique gave insights about the contribution of specific and non-specific interactions to the adsorptive process under different pH values and in the absence and presence of salts such as NaCl, NaF, MgCl₂ and (NH₄)₂SO₄. The combination of FMC and chromatographic assays revealed to be essential to understand (i) the multimodal behaviour of the *m*-APBA ligand at the different conditions studied and that (ii) salt tolerance of the bond established between ligand and mAb can be enhanced by manipulating the chromatographic conditions. Indeed, higher salt tolerance of the bond was observed at pH values above ligand's pKa in the presence of NaF and (NH₄)₂SO₄ due to their ability to diminish electrostatic interactions between ligand and biomolecule, when compared to the commonly used NaCl. Also, it could be concluded that specific *cis*-diol interactions are predominant at pH values below the pKa of ligand, contrarily to what has been reported.

Chapter III describes the successful development and optimization of a process using the multimodal *m*-APBA ligand for the direct capture anti-IL8 mAb from real Chinese Hamster Ovary (CHO) cell culture supernatants. Firstly, the study was focused on the development of a washing step and in the optimization of the elution step using a serum-containing supernatant with anti-IL8 mAbs. The best recoveries - 99% - and purifications – protein purity of 81% and a purification factor of 16 (out of a maximum of 20) - were achieved using 100 mM D-sorbitol in 10 mM Tris-HCl as washing buffer and 0.5

M D-sorbitol with 150 mM NaCl in 10 mM Tris-HCl as elution buffer. Results comparable to the ones obtained using protein A chromatography that revealed a recovery of 99%, 87% of protein purity and 29 (out of a maximum of 33) of purification factor. Consequently, and since the industrial upstream process setting is engaging the use of serum-free cultures, the *m*-APBA ligand was used for the purification of two different mAbs (both IgG1) – an anti-IL8 mAb and an anti-HCV mAb – from serum-free CHO cell cultures with higher protein purities being achieved (94.9 -100%) at the elution fraction. At last, the feasibility of scaling-up PBA chromatography for the purification of anti-IL8 mAbs from clarified serum-free CHO cell cultures was addressed. Here, column performance optimization regarding superficial velocity was extremely important to accomplish a faster process not neglecting the good performance parameters already achieved at every scale tested (0.4 to 40 cm³ resin volume). The 100-fold scale-up was successfully achieved with a recovery yield of 97.7%, a protein purity of 82.6% and a gDNA removal higher than 96%.

The work developed and presented in both Chapter II and III was of major importance in order to demonstrate the potential of the multimodal phenylboronic acid chromatography for the capture of monoclonal antibodies.

Then, in Chapter IV, the multimodal behaviour of *m*-APBA potential was further exploited in order to understand if phenylboronic acid chromatography can be used as a useful tool for the capture and effective separation of a wider range of proteins from glycoproteins, differing in overall charge, to acidic/neutral proteins (glycosylated or not). From previous studies, it was known that the different proteins studied adsorb to the *m*-APBA ligand and that, depending on the adsorption conditions, different types of interaction between proteins and ligand would be involved in the adsorptive and, consequently, in the elution process. Understanding which of the interactions play a major role in the adsorptive process was determinant to develop effective elution strategies for (i) glycoproteins, comprising a broad range of isoelectric points and (ii) acidic/neutral proteins, including glycosylated and non-glycosylated proteins, by the use of displacers as Tris and citrate, respectively.

The thesis ends with Chapter V, where the main results obtained are summarised and analysed and future perspectives are discussed. Overall, the results obtained are expected to contribute towards the adoption of phenyl boronate chromatographic process either for (i) mAb capture and/or polishing steps or as a pre-chromatographic step for a longer life-time of the costly protein A or for (ii) analytical purposes, envisaging the separation of protein isoforms.

Chapter I - General Introduction

Abstract: In this chapter, the relevance of protein therapeutics as monoclonal antibodies (mAbs) to the biopharmaceutical market is addressed and the evolution of these molecules throughout the last decades as well as the unique features responsible for their successful implementation in the treatment of cancer, autoimmune and inflammatory disorders, are described. Special emphasis will be given to the manufacturing process of mAbs describing the major developments achieved at upstream processing and the challenges that downstream processing has been suffering. Accordingly, the technology trends that have been arising in antibody purification will be described and discussed. Firstly, the trends in non-chromatographic methods that aim to reduce or even replace chromatographic operations in the purification pipeline will be addressed. These new approaches based on an *ABC-Anything But Chromatography* strategy have been rising, and turning into feasible alternatives to overcome chromatography limitations such as high resin cost, diffusion and capacity constraints, and at the same time, to cope with high titres and volumes produced at upstream. Nevertheless, chromatography continues to be widely used and subjected to continuous advances in order to meet future industrial needs. Chromatographic methods will be also covered along this chapter. Trends in the bed formats and stationary phase configurations of the fixed bed media will be presented, with the most recent advances in size exclusion (SEC), anion-exchange (AEC), cation-exchange (CEX), hydrophobic interaction (HIC), immobilized metal affinity (IMAC), multimodal (MMC) and affinity chromatography being described. In the last section of this chapter, the type of techniques currently used to study ligand-protein molecular interactions and protein conformational changes during the adsorptive process of biomolecules onto a chromatographic bead will be presented. Calorimetry and non-calorimetry methods will be discussed in order to present some of the available methods that can contribute for a broader biomolecules adsorption elucidation, with a special focus towards the mAbs case.

Keywords: Protein therapeutics, Monoclonal antibodies, Downstream processing, Purification trends, Methods for biomolecules adsorption elucidation

I.1. Protein therapeutics overview

The protein therapeutics field has grown significantly since the introduction of the first human insulin, obtained by recombinant DNA (rDNA) technology and marketed under the tradename Humulin® R (rapid) and N (NPH, intermediate-acting), in 1982 [1, 2]. Currently, the protein therapeutics market counts with a large variety of biomolecule types (Figure I.1) that have shown to be highly effective and to serve as modernized treatment for rare and chronic diseases by offering a custom-made treatment approach. The goal of such therapies is to support a specifically targeted therapeutic process by compensating the deficiency of an essential protein. Human insulin for diabetes, erythropoietin (EPO) for anemia and chronic renal failure, interferon-beta and gamma for cancer, Interleukin-2 (IL-2) for AIDS, Prourokinase for heart attacks, tissue plasminogen activator (enzyme) for strokes, factors VIII and IX for haemophilia A and B, respectively, and different kinds of monoclonal antibodies (mAbs) for diagnosis and treatment of different types of cancer, are just a few examples of how these biomolecules are powerful and diverse in terms of application treatments [3].

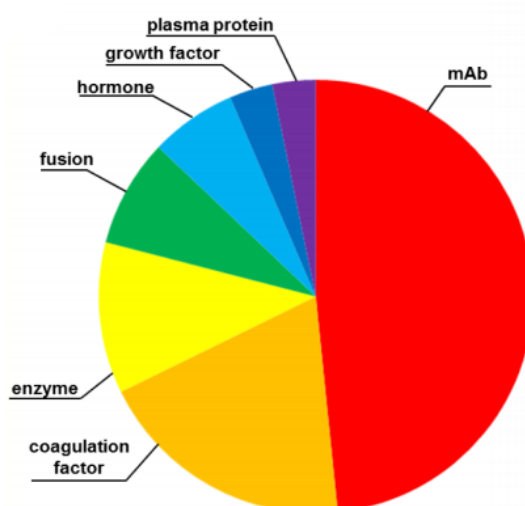


Figure I.1 Distribution of FDA-approved therapeutic proteins (2011-2016) by drug class [4].

The global protein therapeutics market was valued at \$140 billion in 2016, and is projected to reach \$217 billion by 2023, growing at a CAGR of 6.5% from 2017 to 2023 [5]. This growth rate is expected to be bolstered by advances in protein engineering strategies aiming to the enhancement of particular functional attributes while maintaining product safety and efficacy [6]. Engineering proteins enable modifications towards maximization of the clinical potential of the protein-based product. For example, a protein with additional glycosylation sites or changes in its glycosylation pattern can improve the protein's receptor-binding properties and overall effector function [7, 8]. On the other hand, strategies as the addition of signalling peptides or the generation of antibody-drug conjugates (ADCs) [9] could be employed to target drugs with the aim of limiting toxicity and increasing drug efficacy. Also, derivatization approaches have been explored with Fc-fusion [10, 11], albumin-fusion [12], and PEGylation [13], being reported to be used to extend drug's circulating half-life.

According to the National Center for Biotechnology Information (NCBI) data of 2017, the U.S. Food and Drug Administration (FDA) approved over 140 recombinant therapeutic proteins for human use with several hundred currently under development [6]. The majority of these proteins are recombinant mAbs. Therapeutic monoclonal antibody (mAb) products are the major class of biopharmaceutical products with 76 mAbs already approved by regulatory agencies (FDA, EMA) for the treatment of different diseases, including cancer, autoimmune and inflammatory disorders [14] and worldwide sales expected to reach \$125 billion by 2020 [15].

I.1.1. Introduction to therapeutic monoclonal antibodies

Antibodies are large (~150 kDa) glycoproteins belonging to the immunoglobulin (Ig) superfamily that are secreted by B cells in order to identify and neutralize foreign organisms or antigens [16].

Mammalian antibodies are typically made up of four polypeptide chains: two identical heavy chains (H) and two identical light chains (L), arranged in a Y-shaped conformation (Figure I.2). The antibody variable regions (V; Figure I.2), which are the sections that make up the tips of the Y's arms, vary greatly from one antibody to another, creating a pocket uniquely shaped to enfold a specific antigen. On the other hand, the constant regions (C; Figure I.2) constitute the stem of the Y and serves to link the antibody to other participants in the immune system. This region is identical in all antibodies of the same class.

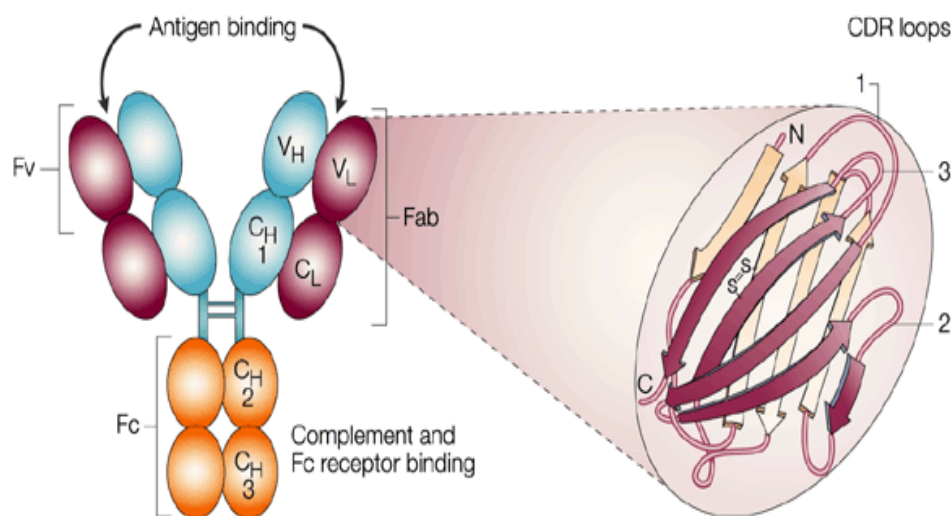
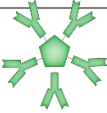


Figure I.2 Immunoglobulin (Ig) molecule. All immunoglobulin monomers are composed of two identical light (L) chains and two identical heavy (H) chains. Light chains are composed of one constant domain (CL) and one variable domain (VL), whereas heavy chains are composed of three constant domains (CH1, CH2 and CH3) and one variable domain (VH). The heavy chains are covalently linked at the hinge region and the light chains are covalently linked to the heavy chain by disulphide bonds. The variable domains of both the heavy and light chains compose the antigen-binding of the molecule (Fab), termed Fv. Within the variable domains there are three loops designated complementary-determining regions (CDRs) 1, 2, and 3, which confer the highest diversity and define the specificity of antibody binding. The Fc portion is glycosylated and contains the sites for interaction with effector molecules.[17]

The five classes of antibodies in humans and other placental mammals differ in their heavy chain sequences, with heavy chain types μ , δ , γ , ϵ and α found in IgM, IgD, IgG, IgE, and IgA antibodies, respectively (Table I.1). Each heavy chain can pair with one of two types of light chain, called λ or κ . The IgM class can also exist as a pentamer, with a resultant 10 heavy and 10 light chains held together by interconnected disulfide bonds in the Fc region and by a J chain (a joining chain with around 20 kDa), while IgA can occur in a form called secretory IgA, where an additional J chain stabilizes the dimerization of two antibodies, to give a total of four heavy and four light chains [18] (Table I.1).

The majority of antibodies found in the serum belong to the IgG class, and most structural information has been derived for this class of antibody [19]. An intact IgG molecule has two heavy chains (≈ 55 kDa each) and two light chains (≈ 24 kDa each) that fold into three large domains: two Fab fragments (one light and the N-terminal half of a heavy chain) and one Fc fragment (two C-terminal heavy chain halves). Fab and Fc are abbreviations for fragment-antibody binding and fragment-crystallizable [18].

Table I.1 Different antibodies classes and their characteristics concerning function, structure and availability on serum. [20]

Name	Function	Molecular structure	Location	%Serum	
IgA	Plays an important role in mucosal surfaces, such as lungs and gastrointestinal tract.		Monomer (160 kDa)	External secretions	5
	Prevents colonization by pathogens. Also found in saliva, tears, sweat and breast milk.		Dimer (390 kDa)		
IgD	Acts as an antigen receptor on B cells. Involved in the activation of basophils and mast cells to produce antimicrobial factors.		Monomer (175 kDa)	B-cells surface	<1
IgE	Helps in the protection against parasites. Binds to mast cells or basophils in response to allergic reactions.		Monomer (190 kDa)	Serum, Mast cells surface or basophils	<1
IgG	Plays a crucial role in protecting against invasion of bacteria and viruses. The only antibodies capable of pass through the placenta to give immunity to the fetus.		Monomer (150 kDa)	Serum, intracellular fluids	85
IgM	First antibody produced in an immune response. Protects against bacterial and fungal infections.		Pentamer (950 kDa)	Serum	5-10

I.1.1.1. Evolution of monoclonal antibodies

Whilst the immune response to an antigen or organism is usually polyclonal in nature, in 1975 Kohler and Milstein were the first to describe the *in vitro* production of murine mAbs from hybridomas [21]. While polyclonal antibodies identify several epitopes, mAbs only recognize one epitope on the surface of the antigen. Hybridoma technology development was the first important step towards the development of human mAbs as therapeutic agents. In a first step, a mouse is immunized with the target antigen. The spleen is removed and antibody-producing cells (B-cells) are isolated. B-cells are then fused with myeloma cells and the resulting hybrid cells are named hybridoma cells. This fusion is very important because it links the specific production of mAbs with a faster and immortal process of growth. The next step consists on screening hybridomas for the target antibody production. Positive clones are then selected and expanded *ex vivo* [21].

In the late 1980s, murine mAbs (suffix: -omab; Figure I.3) were in clinical development; however, they had significant drawbacks. Murine mAbs were often associated with allergic reactions, and the induction of anti-drug antibodies (ADAs). Nonetheless, in 1986, Orthoclone OKT3® (Muromonab- CD3), produced in hybridoma cell lines, became the first mAb approved by the FDA. At the same time, *E. coli* was being used as host for the production of recombinant pharmaceuticals with Eli Lilly obtaining approval for recombinant human insulin in 1982, as previously mentioned [1]. Later, in 1988, it was also reported the expression of an antibody fragment in *E. coli* [22].

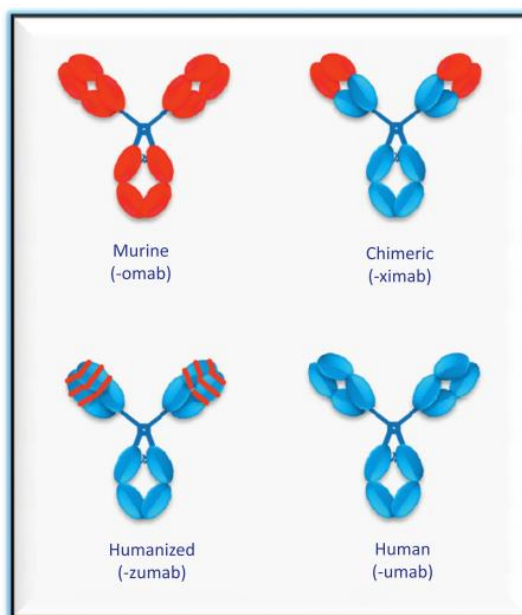


Figure I.3 Monoclonal antibody types and nomenclature. Therapeutic mAbs can be murine (suffix: -omab), chimeric (suffix: -ximab), humanized (suffix: e.g. -zumab) or human (suffix: e.g. -umab) and are named accordingly. [16]

Genetic engineering made possible to design and produce less immunogenic products such as chimeric ("-ximab") and humanized ("-zumab") mAbs [23]. Chimeric mAbs have around one-third of murine sequence and two-thirds of human sequences, with a human constant region (Figure I.3). This configuration results in a lower immunogenicity compared to murine mAbs. The first chimeric mAb to

reach the market was ReoPro® (Abciximab), produced in its chimeric form and then cleaved to the corresponding Fab molecule. Rituxan® (Rituximab) was the first complete chimeric mAb to reach the market [24].

The production of high-affinity murine mAbs against human antigens became a routine process in the mid 1990s, which in this decade was achieved through the humanization of mice. Surface amino acids for human and murine variable region heavy (VH) and light (VL) chains are conserved with 98% fidelity across species [25]. Therefore, only a few amino acids needed to be changed by resurfacing to convert a murine Fv surface to a human one. In this way, a human sequence that retains its full antibody binding capacity is obtained (Figure I.3). The first humanized mAb to reach the market was Zenapax® (Daclixumab), licensed by Roche and prescribed for transplant rejection.

State-of-the-art genetic engineering today focuses on producing fully human mAbs ("-umab"), which have the advantage of having practically negligible secondary effects on the host (Figure I.3). Fully human mAbs can be produced using human Ig transgenic mice or phage display libraries. Humira® (Adalimumab) was the first fully human mAb to be approved by the FDA. It is a TNF inhibitor obtained from a phage display library. Other examples include Simponi® (Golimumab), which is prescribed for inflammatory diseases and Stelera® (Ustekinumab), prescribed for psoriasis.

I.2. Manufacturing platforms: an overview of the advances and bottlenecks

The combination of an ever-growing patient population with the relatively low potency of mAbs has led to the demand for large quantities of pharmaceutical-grade mAbs [26]. In order to meet the requirements, mammalian cell lines have become the dominant antibody expression system, with Chinese Hamster Ovary (CHO) cells being the main choice [27, 28]. The continuous discoveries in molecular biology, genetics and protein engineering [29-31], combined with new advances in medium and feed development, higher cell culture productivities and antibody titres over 10 g/L were achieved with CHO expression systems [32].

The ability to identify high productivity clones has been streamlined through the use of different selection systems. Antibiotic selection has been used for some years, but the requirement to maintain cells in antibiotics is costly and requires removal of the antibiotic from the production media during downstream steps. Consequently, the use of gene amplification systems as the dihydrofolate reductase (DHFR) using methotrexate (MTX) resistance and more recently, glutamine synthetase (GS) using methionine sulfoxamine (MSX) resistance, have become the preferred methods by industry [33, 34].

The DHFR enzyme catalyses the conversion of folate to tetrahydrofolate, a precursor necessary for the *de novo* synthesis of purines, pyrimidines, and glycine [35]. If the expression of DHFR is reduced through chemical or genetic means, cells will die unless they are either cultured in media supplemented with glycine, hypoxanthine, and thymidine or have an alternative DHFR exogenously expressed. For the selection of highly productive CHO cells using the DHFR/MTX system, cells are commonly transformed with recombinant DNA (rDNA) consisting of the gene of interest closely linked to the gene for DHFR. When undergoing gene amplification, cells are cultured in increasingly higher levels of MTX, drug which is an analogue to folate. MTX will then bind to DHFR, inhibiting the production of tetrahydrofolate. Those

CHO cells that have increased copies of the DHFR gene, and therefore higher levels of the enzyme, will survive and be selected [36].

The GS/MSX system operates in a similar basis to the DHFR/MTX system. The GS enzyme catalyses the production of glutamine from glutamate and ammonia. Here if GS content decrease, cells will not be able to survive unless glutamine is present in the media or have an alternative GS exogenously expressed. In this case, cells are previously transfected using plasmids containing the gene of interest and the GS gene. During gene amplification, cells are then subjected to increasing concentrations of MSX, a compound that will bind to the GS enzyme preventing the production of glutamine. The surviving cells will be then selected since they are the ones comprising the cassette stably integrated into the genome which will confer an expression of the protein of interest (e.g. a monoclonal antibody) proportional to the high amounts of GS expressed, responsible for cell viability at the described conditions [36].

Furthermore, gene amplification systems using MTX or MSX are often performed using a number of amplification steps to increase copy number and expression levels of clones, which has led to some concerns over the long-term stability of the final producer clone. Together with the increased downstream processing burden, null cell lines are a preferable technology for using selection through DHFR or GS. Using null cells for the DHFR gene, such as CHO DG44 cells, there is no need to add MTX to the media [37]. The selection of the high producing cells is achieved by using a GHT- minus medium [38]. Those expressing insufficient DHFR, and by extension a low level of monoclonal antibody, will be unable to survive. In the case of null cells for the GS gene, as CHO K1, its selection is accomplished by placing cells into media that lacks glutamine [39]. These null cells have been engineered using different gene editing technologies as (i) recombinant adeno-associated virus (rAAV) technology, used by Horizon Discovery, (ii) meganucleases, used by Lonza and (iii) Zinc Fingers (ZFNs) used by Sigma-Aldrich [40-42].

As expression technologies have developed, focus on increasing titre has mainly been achieved through process development (e.g., batch, fed-batch, perfusion, etc.) and medium optimization.

CHO cell cultures used for the production of mAbs are commonly adapted suspension cultures. The ability of CHO cells to grow in suspension cultures decrease (i) the waste produced since no culture flasks or roller bottles have to be used and (ii) the clarification burden by eliminating the need to use structures as microcarriers to maintain adherent cultures in stirred-tank bioreactors. Considering all these developments, CHO cell cultures are typically carried out using stirred-tank bioreactors operating under fed-batch or perfusion modes [43]. Fed-batch still dominates the CHO cell culture in the biopharmaceutical sector due to practical factors including: (i) good lot consistency, (ii) easy implementation, (iii) lower risk of contamination and (iv) small footprint, compared to perfusion mode [44]. However, a considerable number of mAbs are being produced using perfusion/continuous systems, such as ReoPro® (abciximab) and the blockbuster mAb Remicade® (infliximab).

Moreover, in order to increase mAbs titre, as well as to reduce batch-to-batch variability and to ensure that the product is not contaminated with any adventitious agent that can be in the serum, CHO cells are currently being grown in serum-free media. The fetal bovine serum (FBS) components, e.g. growth factors, hormone, vitamins, lipids, etc, essential to ensure proper cell growth, especially in

adherent cell cultures, are now being substituted for products of non-animal origin such as recombinant albumin produced in *Saccharomyces cerevisiae*, recombinant insulin produced either in *E. coli* or *S. cerevisiae*, protein hydrolysates derived from microorganisms (yeast derived proteins) or plants (soy or rapeseed), among others [45]. The goal is to reach chemically defined animal-free media formulations (Figure I.4) that could increase batch-to-batch consistency and protein therapeutics titres at the same time that the downstream complexity is reduced and the fluctuating costs are stopped [46, 47].

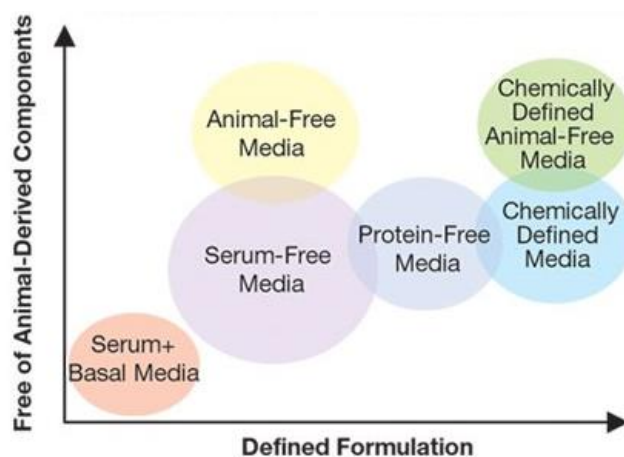


Figure I.4 Evolution of mammalian cell culture media. [48]

However, despite all accomplishments obtained at upstream process, the general access to these biopharmaceuticals is still barred by high selling prices with downstream processing (DSP) being considered the bottleneck in the manufacturing of mAbs.

Due to the conserved domains of mAbs (Figure I.2), a general purification process based on a common sequence of unit operations is currently employed by many companies [49]. The established downstream processing of mAbs follows a platform-based approach that encompasses a protein A affinity chromatography capture step and two polishing steps to ensure a high clearance of impurities as host cell proteins, DNA, viruses, aggregates and low molecular clipped species (Figure I.5) [49, 50]. Protein A chromatography exploits the specific interaction between the Fc region of the antibodies and the immobilized protein A, a cell wall associated protein exposed on the surface of the Gram-positive bacterium *Staphylococcus aureus* [51]. Given its high selectivity for antibodies, purities greater than 98% are typically achieved in a single step from a clarified complex cell culture medium [52]. However, despite being highly stable, reliable, and reproducible, protein A capture step is considered to be a productivity bottleneck and especially expensive, representing more than 70% of the total downstream process [53] and up to 25% of the total mAbs manufacturing process [54, 55]. Coupled with the high costs associated, it present other drawbacks as ligand leaching, instability at high pH and the formation of product aggregates under low pH standard elution conditions [56]. Therefore, the design of novel and cost-effective operations and their implementation in the current industrial technological apparatus constitutes a pressing need.

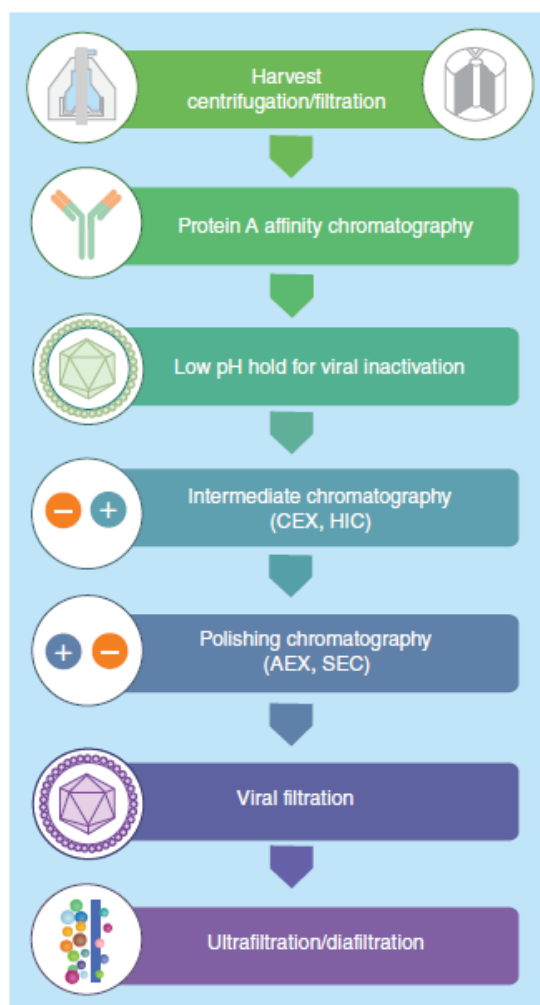


Figure I.5 Platform approach employed in the downstream processing of mAbs at industrial scale (AEX: Anion-exchange chromatography; CEX: Cation-exchange chromatography; HIC: Hydrophobic interaction chromatography; SEC: Size exclusion chromatography). [22]

Another driving-force for innovation on the DSP of mAbs-based products is the emergence of biosimilars, also known as “follow-on pharmaceuticals” in the US and Japan. These terms arise from the loss of patent protection by many first generation products in the last few years, enabling the entry of competing manufacturers. Importantly, the need for a competitive advantage may drive innovation beyond cheaper and faster ways to achieve current levels of purification and extend to quality improvements in the antibody products themselves. [57, 58]

Alternatives to the current DSP methodology used in recovery and purification of mAbs range from non-chromatographic techniques, like tangential flow filtration, aqueous two-phase extraction, high gradient magnetic fishing, precipitation or crystallization [53, 59-63], to novel affinity-based separations that have emerged from the development of synthetic ligands including biomimetic peptides obtained by combinatorial libraries and artificial ligands generated by *de novo* process designs [64, 65].

I.3. Trends in non-chromatographic methods

Non-chromatographic methods have been more and more considered as valuable alternatives to some of the chromatographic steps. Several promising methodologies have been described in the literature, including, high performance tangential flow filtration, affinity precipitation, crystallization and liquid–liquid extraction (e.g. aqueous two-phase partitioning). These alternative technologies, and in particular aqueous two-phase partitioning, aim at high throughput and seek to avoid problems associated with most chromatographic supports, such as high cost, limited capacity and diffusional limitations.

I.3.1. High performance tangential flow filtration (HPTFF)

HPTFF is an emerging technology that can combine protein purification, concentration and formulation in a single step. This technique is based on electrostatic interactions between proteins and charged ultrafiltration membranes with a large molecular weight cut off ($\approx 100\text{--}300$ kDa) membrane, compare with the $10\text{--}30$ kDa used with neutral membranes for ultrafiltration/diafiltration (UF/DF) [66–69]. In this way, HPTFF performance is governed by membrane properties, such as pore size and surface charge-density and process parameters, such as filtrate flow-rate, number of diafiltration volumes, load pH and ionic strength [68].

Although this kind of membranes could be exploited as an ion exchange adsorber, here the antibody selectivity is mediated by ion exclusion (Figure I.6). Protein impurities are separated by exploiting differences in their size as well as charge [66, 67, 70, 71].

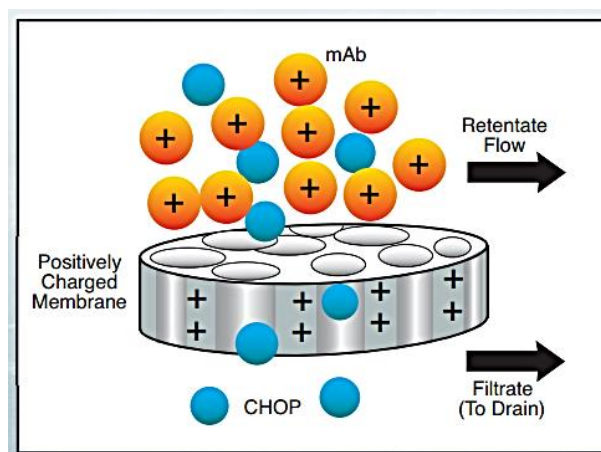


Figure I.6 HPTFF schematics for separation of mAbs and host cell proteins (CHOP). [68]

In the case presented in Figure I.6, a positively charged ultrafiltration membrane rejects positively charged proteins such as mAbs, despite them being small enough to pass through the pores. This permits their selective retention and concentration while weakly alkaline, neutral, and weakly acidic impurities pass through the membrane. However, strongly acidic contaminants pose an apparent challenge. At conductivity values low enough to repel IgG, positively charged surfaces can bind negatively charged molecules such as DNA. If present at high concentration, DNA binding could reduce the charge potential on the membrane surface sufficiently to reduce the intensity of antibody exclusion

[71]. This means that consistently effective use of HPTF as a capture method could require a sample-conditioning step to remove DNA. Another limitation concerns variability among antibodies since only the most alkaline mAbs will be excluded to the greatest degree.

I.3.2. Flocculation / Precipitation

Processes employing flocculants and precipitants have been a topic of interest for almost 30 years now [72, 73]. These processes not only purify the target product as may offer further economic benefit of significant volume reduction in cases where the precipitated product is readily soluble at high concentrations in another buffer system [74]. In order to get higher clearance, these procedures are usually followed by depth filtration [57, 74].

Singh and co-workers [74] recently reviewed the use of different precipitants and flocculants as alternative technologies for clarification. Among them, it can be found several precipitants, as cationic, anionic and mixed mode flocculants. IgG recoveries ranging from >80% to >90% followed by impressive impurity reductions have been reported. A polyallylamine precipitation-based multistep purification process achieved overall purity and recovery roughly equivalent to protein A-based process [75].

The most promising results came from the use of flocculants as polydiallyldimethylammonium (pDADMAC; cation flocculation) [75-77] and modified benzyl poly(allylamine) (mixed-mode flocculation) [78-80]. For the first, the mode of action is based on electrostatic interactions and hydrogen bonding (Figure I.7). The second also accounts with hydrophobic effects to increase selectivity towards non-IgG impurities such as host cell proteins, DNA and whole cells and cell debris.

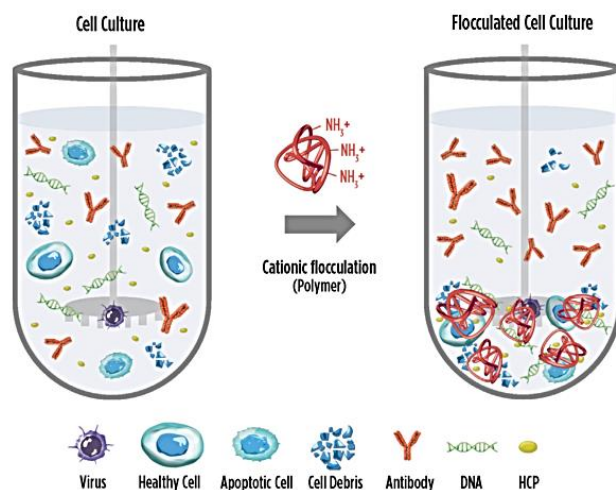


Figure I.7 Outline of the flocculation mechanism for cationic flocculants. Negatively charged particles such as cells, cell debris, nucleic acids, and host cell proteins bind to the positively charged polymers, leaving the protein of interest in solution. [74]

Despite the impressive results achieved, these methodologies still need to demonstrate effective clearance to an acceptable residual level in the final drug substance to ensure safety of the drug product. McNerney *et al.* have recently ranked four flocculants based on their hemolytic and toxic behaviour: polyethylene amine (PEI) > chitosan > pDADMAC > DEAE dextran [81]. In general, polymer toxicity correlates directly with an increase in molecular weight, charge density, and hydrophobicity and a decrease in order of amines (primary > quaternary) [74].

Nevertheless, recent developments point out pDADMAC and SmP (EMD Millipore, Bedford, MA) such as biopharmaceutical grade flocculants since they present reduced levels of low molecular weight polymer, < 0.1% monomer and < 10 CFU/mL microbial count. These features will result in low variability and help to meet GMP requirements [74]. Chitosan [82] and coagulation reagents as calcium chloride and potassium phosphate [83] have also been studied to avoid potential issues related to polymer or residual monomer toxicity and the need of their removal through subsequent purification steps.

Finally, several other factors such as (i) scalability, (ii) impact on product quality attributes such as mAb charged variants and clipped species, (iii) effects on resin's lifetime used in the capture step of mAbs, especially protein A, (iv) step yield and (v) HCP removal should be assessed for successful implementation and scale-up.

I.3.3. Crystallization

The interest in crystallization from a purification point of view increased due to the low costs associated, the ability to cope with high volumes, and with high concentrations of the target molecule. Therefore, crystallization has the ability to integrate protein purification, stabilization and concentration in one single step what is of real importance for the application in the downstream processing of biopharmaceuticals [63].

Crystallization is mostly applied in protein structure analysis and is already used as a cost effective and scalable purification procedure for small molecules such as insulin. Insulin is a small and extremely stable peptide able to refold easily into its native structure even after exposure to organic solvents. It is crystallized late in the purification sequence where most of the impurities have already been removed [63]. Additional benefits of protein crystallization from a formulation perspective are the higher stability of crystalline proteins in comparison to protein solutions, making crystalline formulations an attractive alternative with potentially longer shelf life, and the possibility to control delivery of a protein by making use of crystal dissolution kinetics [84].

However, the application of crystallization in antibody purification is limited due to product size and heterogeneity due to their different glycosylation patterns [85]. Zang and colleagues first demonstrated the feasibility of having a crystallization step in the downstream process of mAbs at a μL scale [86]. In this study, IgG4 crude extract was purified by protein A chromatography and dialyzed to 20 mM Tris buffer pH 7.0 before the crystallization step. As precipitant solution, 5% (w/v) PEG 8000, 0.2 M $\text{Ca}(\text{OAc})_2$, 0.1 M imidazole at pH 7.0 was used and crystals were obtained after 5 days at room temperature. After mAb IgG4 solubilization, the final solution presented very high of protein purity (90%) with a recovery yield of 31.3%. Following, Smejkal and collaborators were able to crystallize an IgG1 in 1 h using 5 mM histidine/acetate buffer, 10 mM NaCl, pH 6.8 at 4 °C. Here, a scale-up from μL to L in batch conditions was successfully accomplished, with a final protein purity and recovery yield of 96.9% and 90%, respectively [87]. The results obtained were similar to those obtained with protein A chromatography with crystallization presenting a reduce cost (in two orders of magnitude) and a higher capacity towards IgG (2.5 fold) [63].

1.3.4. Liquid-liquid extraction

Aqueous two-phase extraction (ATPE) has been widely studied for the purification of biopharmaceuticals such as mAbs since protein A affinity capture step began to reveal productivity limitations. ATPE rely on systems capable of creating two separate phases in solution. These systems are formed spontaneously by mixing two different polymers (e.g., PEG, dextran, ethylene oxide propylene oxide co-polymer [EOPO], polyacrylates), or a polymer and a kosmotropic salt (e.g., phosphate, sulphate, citrate), above a certain concentration [88]. The composition of these systems (70-90% of water) turns ATPE into a very biocompatible technique, which at the same time supports protein structure stability conferred by the polymers and some salts used [88].

Partition of biomolecules depends on intrinsic and extrinsic parameters, which should be considered for optimization purposes. Intrinsic parameters are related to the size, electrochemical properties, surface hydrophobicity and conformation of the target biomolecule. Extrinsic parameters to have into consideration are the type of aqueous two-phase system (ATPS) used. The molecular weight and concentration of phase forming compounds, ionic strength, pH, temperature and the presence of additives such as affinity ligands, among other, have to be thoroughly analysed [89].

The use of PEG-salt systems was already exploited for the extraction of IgG. In early studies, PEG-phosphate systems were applied to the extraction of antibodies showing good partition coefficients when higher concentrations of a neutral salt, such as NaCl, were added [90, 91]. However, the phosphate streams were known to have a strong impact on the environment [53]. Alternatives were then pursued and the biodegradable salt citrate was chosen. Overall yields greater than 95% and a final protein purities ranging 74 to 95% were achieved having as feedstock hybridoma [92] and CHO cell supernatants [93], with IgG being recovered in the citrate-rich phase. To further increase purity, hydrophobic interaction chromatography and size-exclusion chromatography were used as polishing steps for the removal of excess salt and IgG aggregates [94]. The strategies used in PEG-salt systems to enhance the partition of antibodies to the PEG-rich phase, whenever this is required to achieve a selective purification, include the use of PEG molecules with low molecular weights or of increasing salt concentrations [53].

The feasibility of operation in continuous mode is another important feature that characterize ATPE especially when continuous manufacturing of mAbs is been seek and presented as the future [95]. A continuous ATPS process incorporating three different steps (extraction, back-extraction, and washing) was set up and validated in a pump mixer-settler battery. This ATPS process allowed the recovery of IgG from a CHO cell supernatant with a global recovery yield of 80%, a HPLC purity of 97% and protein purity of more than 99%. A PER.C6 cell supernatant was also processed with a total recovered yield of 100%, a final total purity of 97% and an HCP purity of 95% [96]. The economic viability of this ATPS process has been evaluated and compared with the currently established platform based on protein A chromatography [97].

In ATPS composed of two structurally different polymers, such as PEG and dextran, most proteins (including antibodies) partition preferentially to the more hydrophilic, dextran-rich phase. Hence, to enhance the affinity of antibodies towards the PEG-rich phase, PEG molecules have been modified with a wide range of ligand molecules. This strategy is not feasible in polymer-salt systems because of the

high concentration of salt, which masks any affinity or electrostatic interaction between the ligand and biomolecule [53]. Reports describing affinity extraction using protein A [98], iminodiacetate with different metal chelators [99], dye [100] and hydrophobic [101-104] ligands were described. Although these modifications increase partition efficiency, they impose the requirement for a dissociation step to remove the ligand-bearing polymer from the antibody. Nevertheless, more affordable and efficient affinity tags are breaking into ATPS. For example, the use of the dual tag ligand LYTAG was successfully established using affinity driven extraction towards PEG-rich phase [105, 106]. The integration of such separation with quaternary amine matrices allowed (i) a more efficient process with higher recovery yield and purity of the final product (95% yield and 91.4% purity vs. 89% yield with 42% purity [106]); (ii) the recovery of the LYTAG-Z dual ligand with high purity; (iii) the recovery of the final mAb-product in a mild solution and, consequently with the removal of the ATPS phase-forming compounds [105].

Further advances in ATPS can arrive from the use of non-conventional phase-forming components, such as ionic-liquids, surfactants and stimuli-responsive polymers, including temperature-, pH- and photo-responsive polymers.

The key advantage that keep ATPS as a viable alternative to traditional techniques is the possibility of handling solid-containing feedstock, and consequently, its application in the early stages of the purification, thereby integrating the clarification and capture of mAb in a single unit operation [88]. Nonetheless, it must be noted that system composition can be affected by the presence of a fermentation broth [88]. Zijlstra and collaborators [107, 108] were the first to developed an extractive fermentation using ATPSs, in which animal cells (hybridoma and CHO cells) were grown in the bottom phase and an IgG2a was recovered in the top phase [109]. This extractive fermentation was performed in a polymer–polymer system composed of dextran and PEG. Also using PEG-dextran system with and without added NaCl, revealed cell clearances of 100% at different conditions for hybridoma cell cultures as reported by Silva and colleagues [94] and Campos-Pinto *et al.* [106]. These kind of polymer-polymer systems similarly performed remarkably when used for the isolation of human hematopoietic stem/progenitor cells (hHSCs) from umbilical cord blood [110]. In the later, an immunoaffinity ligand – a monoclonal antibody against the CD34 antigen marker (anti-CD34) - was introduced into the two-phase system with the purpose of obtaining the specific partition [110]. Considering the therapeutic potential of hHSCs (*i.e.* bone marrow transplantation) and the high purity that the same have to present, costs associated with the use of an immunoaffinity ligand are not seen as a limitation.

I.4. Trends in chromatographic methods

Despite all the alternatives based on the ABC (Anything But Chromatography) strategy, chromatography continues to be widely used and subjected to continuous advances with the goal of meeting future industrial needs. In this section, current trends in bed formats and stationary phase configurations will be covered. Also, most recent advances in size exclusion (SEC), anion-exchange (AEC), cation-exchange (CEX), hydrophobic interaction (HIC) immobilized metal affinity (IMAC), multimodal (MMC) and affinity chromatography will be reviewed.

I.4.1. Chromatographic bed format

I.4.1.1. Fluidized bed

Currently, the two most promising adsorptive techniques based in fluidized beds are expanded bed adsorption (EBA) and high gradient magnetic fishing (HGMF) [111]. Both methodologies involve the use of adsorbent particles dispersed in a liquid medium and could be used for direct product recovery from crude feedstocks. One version relies on expanded bed chromatography. The simplest example is batch chromatography, with industry preference involving highly engineered up-flow columns that maintain the particles in an evenly dispersed state throughout equilibration, sample application, and washing. Once the unclarified feedstock is introduced within the column of the fluidized adsorbent, cells and cell debris pass unhindered through the interstitial voids created in the expanded bed and ultimately escape through the top of the column. The target adsorption onto the chromatographic media takes place in this stage. Elution, cleaning, and sanitization can be performed in packed bed mode or otherwise in the expanded bed mode at reduced superficial velocity [4, 5], with the first approach more commonly used (Figure I.8).

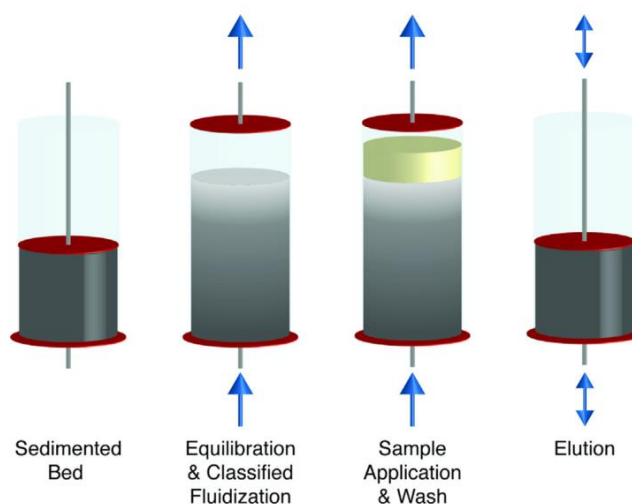


Figure I.8 Expanded adsorption chromatography principle.[112]

The particles are engineered to embody a narrow range of densities. When they are dispersed upwards by the flowing buffer, denser particles tend to stratify towards the bottom of the bed, and less denser particles towards the top. Stable stratification permits the formation of theoretical chromatographic plates that enable fair gradient fractionation of complex samples. Therefore, fluidized beds operation is considerably more complex than traditional packed beds. Nonetheless, they offer the valuable feature of integrating clarification and pre-capture of proteins in a single step since it has the ability to selective capture, for example, mAbs and mAb products, while cells and debris pass between the dispersed chromatography particles [88]. The economical and practical benefits of this shortcut have been discussed, but technical limitations in first generation materials stopped a broader implementation. One of the problems resided in the fact that the density of the chromatography particles was partially overlapped with the density of cells and debris that were intended to pass through. In this way, the

chromatographic media was virtually impossible to clean with frit fouling being common [113]. These problems aside, general cost-effectiveness issues include higher equipment and media costs, plus higher buffer consumption than packed beds.

Second generation systems have overcome the physical limitations [88]. A rotating arm at the inlet port achieves effective flow distribution without requiring a frit. Cellulose-coated tungsten carbide particles increase the density differential between cells and chromatography particles, and allow faster flow rates that achieve more efficient flow of debris through the system [114, 115].

EBA chromatography's higher process and energy efficiency as compared to conventional techniques [116] has led to several applications ranging from the purification of therapeutic and commercial proteins from bacterial [117, 118] and mammalian [119] expression systems. Besides ion-exchange systems and protein A based affinity interactions, multimodal ligands are gaining more and more interest with studies demonstrating the ability to purify polyclonal human IgG from plasma with 80% purity and 93% recovery [120].

The use of magnetic particles represents another branch of the fluidized bed lineage. High gradient magnetic fishing (HGFM) is based on batch adsorption of the product followed by a recovery process of the product-loaded adsorbent using high gradient magnetic separation [121]. In contrast to chromatographic resins, magnetic adsorbents are generally micron-sized and non-porous, and thus combine a high surface to volume ratio with reduced fouling tendency. Comparative studies between these techniques indicate that HGFM expresses a faster (4 to 8-fold) and more robust processing (uncoupling of product capture and separation from the feedstock), whereas EBA shows the advantage of higher resolution and probably lower buffer consumption (multistage column procedure) [122].

Initial applications have evaluated immobilized protein A [123, 124], achieving purity and recovery similar to conventional and fluidized bed applications, but requiring less time. Thiophilic magnetic microspheres were also used to extract IgG from a variety of feed streams, including cell-containing culture media and whole blood [125]. The authors highlighted purity and recovery similar to protein A, with IgG binding capacity up to about 30 mg/mL of particles in solution. Applications using phenylalanine and imidazole as ligands were also studied with IgG binding capacities ranging 780 to 843 mg/g of particles with 150 and 158 nm, respectively [126, 127]. Borlido and colleagues were able to selectively capture mAbs from a CHO supernatant using silica magnetic particle functionalized with phenylboronic acid with an overall yield of 86% while removing 88% of CHO host cell proteins and more than 97% of CHO genomic DNA [128].

1.4.1.2. Fixed-bed

Fixed-bed applications continue to dominate the chromatography field, whether conducted with membranes, monoliths, or porous particles packed in columns. Most applications are run with a single bed under axial flow. Bed dimensions can be increased if greater capacity is required, but chromatographic media and buffer costs increase proportionally. Cycling can increase capacity without increasing media costs. However, it could multiply buffer costs and process time. Simulated moving bed (SMB) chromatography can provide continuous (cyclic) operation for the separation of binary mixtures

by differential chromatography, for example, for removal of product variants or oligomers [129]. SMB systems use multiple packed columns with periodic switching of the feed, mobile phase, and recovery ports in a fashion that simulates countercurrent flow (but without any motion of the solid phase). A typical 4-column configuration is shown in Figure I.9A. At the start of the process, the feed (a binary mixture of product and impurity) is loaded to Column 1 in the upper right hand corner. Both components migrate through the column, with the more weakly bound species (in this case the product) recovered through the port at the column exit. Additional mobile phase is added between Columns 2 and 3, with the more strongly bound component being recovered from Column 3. When the product has migrated much of the way through Column 1, the location of the feed, mobile phase, and recovery ports are rotated clockwise (in the same direction as the flow) to simulate the countercurrent movement of the solid phase. This type of continuous operation is only possible if the loading time is greater than the regeneration time. SMB operates cyclically, with the concentration of recovered product decaying from its maximum value at the start of each cycle to its minimum right before switching.

SMB chromatography has been successfully implemented in large-scale manufacturing for the separation of enantiomers [130], fructo-oligosaccharides [131], and lysine [132], among others. Several SMB systems have also been developed for protein purification, including the Semba Octave Chromatography System and Tarpon Biosystems BioSMB. Bisschops and co-workers [133] showed an SMB model that required 90% less protein A media and 37% less buffer than required by a traditional process. In experimental comparisons at the 5 mL column scale, SMB throughput was double the traditional format, buffer consumption was 27% less, and host cell protein reduction was improved by 15%. In other works, 3-column SMB formats for IgG capture by cation-exchange chromatography, for high-resolution cation-exchange separation of antibody charge-variants [134, 135], and for 2-step IgG purification procedures of cation-exchange capture followed by polishing on a mixed mode column [136] were evaluated.

Nevertheless, commercial applications have been limited due to concerns about system complexity and potential issues with the large number of switching valves. Zobel and colleagues [137] have recently described a single-column SMB system with six containers and two pumps to collect and distribute the feed, product, and impurities. Also, Shinkazh and co-workers [138] developed a novel physical format that merges the principles of SMB with fluidized bed chromatography. They pumped slurried porous particle media through a series of static mixers and tangential flow membrane modules. Purification, recovery, and reduction of buffer volumes were similar to fixed bed SMB systems.

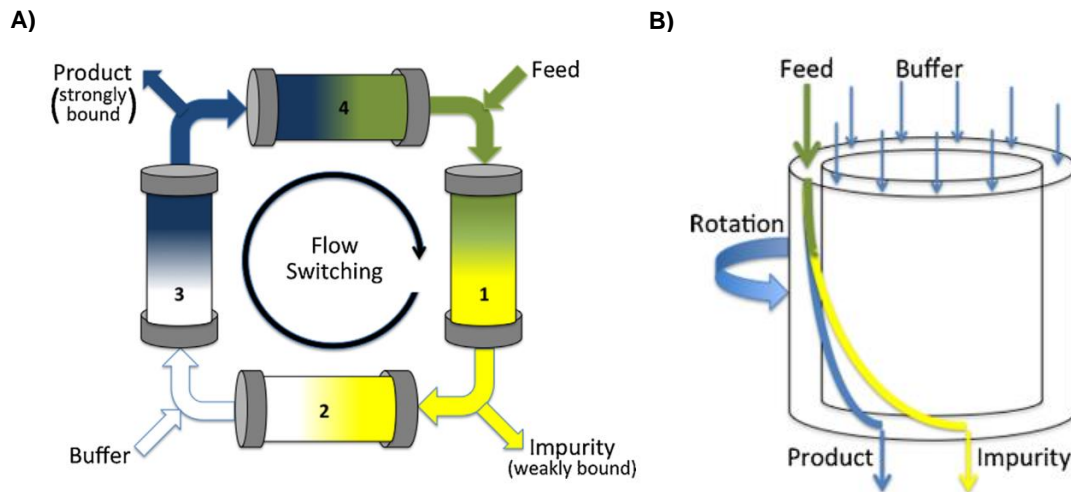


Figure I.9 Schematics of two different chromatographic systems: (A) 4-column simulated moving bed (SMB) chromatography and (B) Rotating annular chromatography. [139]

In contrast to SMB, annular chromatography provides truly continuous purification using a rotating column [140]. The feed is introduced at a fixed location in the annular space between two rotating concentric cylinders (Figure I.9B) with the product being recovered at fixed outlet ports at the bottom. Annular chromatography has been used for removal of protein aggregates from an intravenous (serum) immunoglobulin preparation by size exclusion [141] and for the continuous purification of recombinant Factor VIII produced in a perfusion bioreactor using a weak anion-exchange resin [142], among others.

The bigger challenges of this type of chromatography remain in obtaining a uniform column packing and flow distribution. Therefore, the technology has not yet been implemented for large-scale protein purification.

Radial flow chromatography has many similarities to annular chromatography except that the flow in the annular bed is in the radial direction, moving from the outer radius to the inner collection area (Figure I.10) [143]. Flow from the inner to outer cylinder is also possible. The feed, wash buffer, and elution buffer are introduced at different fixed angular positions, with the product (and impurities) collected at different angular positions [143]. Continuous operation can be achieved by rotating the annulus past the fixed positions of the feed and buffer inlets and product collection ports [143].

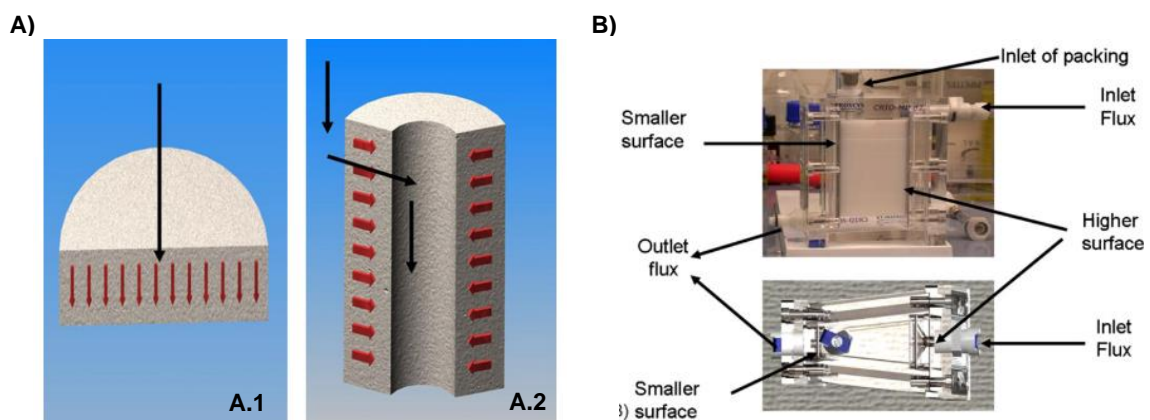


Figure I.10 (A) Comparison of liquid flow through the axial (A.1) and radial (A.2) columns. (B) CRIO-MD 62: side view and upper view.[144]

Radial flow chromatography systems have short bed heights, allowing operation at relatively low pressure drops. In addition, the radial configuration provides high cross-sectional area that can more easily accommodate high feed flow rates than conventional columns [144]. Although a number of companies provide radial flow chromatography systems for batch operations, e.g., Sepragen (Hayward, CA) and Proxcys (Nieuw-Amsterdam, Netherlands), there do not appear to be any commercial-scale continuous (rotating) radial flow chromatography systems available for bioprocessing applications. Nevertheless, batch radial chromatography using protein A for the purification of mAbs revealed to reduce processing times without compromising recovery, when comparing with axial chromatography [145]. This reduction in time consumption is due to the lower pressure drops obtained at every step of the process at bench and pilot scales, which turns possible to increase working flow-rates at all process steps [145]. Recently, batch radial chromatography using large beads with immobilized metal affinity (IMAC) ligands (Ni, in this case) was also used for the direct capture of His-tagged carcinoembryonic antigen (CEA) from a CHO unclarified feed, without detrimental effects on cell viability (96%). Recoveries of 71% and host cell proteases and DNA concentrations of ≈ 8 U/mL and $2 \mu\text{g}/\mu\text{L}$ were respectively reached [146].

I.4.2. Stationary phase design

I.4.2.1. Diffusive and perfusive beads

In conventional liquid chromatography (diffusion chromatography) (Figure I.11), molecules move to the outer surface of the stationary phase particles by convection, which constitutes a rapid step. Nevertheless, the transport of molecules through a stationary phase of porous particles occurs by molecular diffusion, which constitutes a very slow process, especially in the case of polypeptides and proteins that present high molecular weights and low diffusion coefficients. As a consequence, a significant loss in resolution could occur, since molecules still in the convective stream or bound to the outside of the particles could elute before those diffusing to the inner of the particle. Furthermore, binding capacity could also decrease, since part of the sample may pass through the column before all of the binding sites deep within the particles were occupied [147]. Nevertheless, diffusive beads still offer the highest IgG-accessible surface areas and dynamic binding capacities of all fixed-bed stationary phases [57].

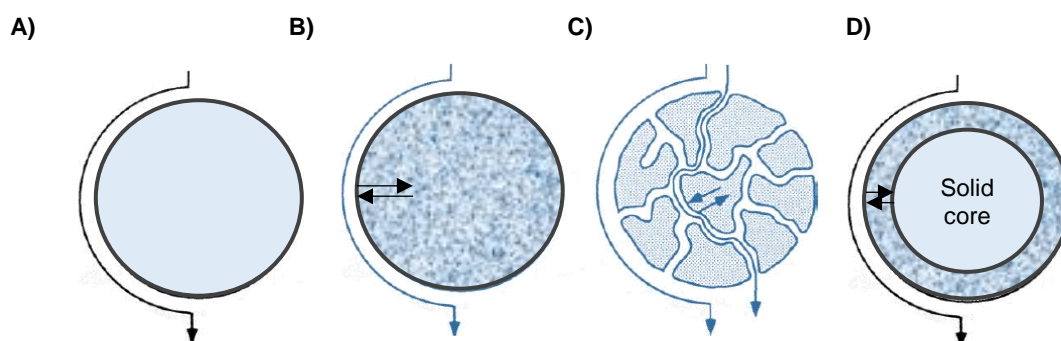


Figure I.11 Types of chromatographic beads. (A) Non-porous, (B) Porous (dead-end porous), (C) MesoPorous (perfusion beads) and (D) solid core beads.

In perfusion chromatography, stationary phase particles used are designed to enable a better access of molecules to the inner of these through two classes of pores: throughpores (6000–8000 Å), which cross the stationary phase particle from side to side and allow the transport of molecules into the interior of the particle by convective flow and diffusive pores (800–1500 Å), interconnecting the throughpores network and enabling the transport by diffusion (Figure I.11). In this way, molecules travel by convection through the column to the stationary phase particle, such as in conventional chromatography. Since there, molecules cross the stationary phase particles by means of a combination of convective and diffusive transport, thus, accelerating the transport of molecules through the particle [147]. Another strategy to overcome the limitations of diffusive beads is to use solid-core beads containing a thin porous layer in the surface.

Appropriate media for perfusion chromatography must possess outstanding chemical and mechanical stability. Although suitable media could consist of alumina, silica or even hydroxyapatite, most frequently, the matrix of perfusion media is constituted by highly crosslinked polystyrene–divinylbenzene. Their absolute capacities are generally lower than the highest capacity diffusive particles, and they are still burdened with eddy dispersion and turbulent shear in the void [57].

1.4.2.2. Adsorptive microfiltration membranes

Membrane adsorbers have a purpose similar to packed chromatography columns, but in the format of conventional filtration modules. Membrane chromatography uses microporous membranes, usually in multiple layers that contain functional ligands attached to the internal pore surface throughout the membrane structure.

The benefit of membrane chromatography over conventional bead chromatography is the elimination of diffusive pores. For membrane chromatography, binding sites are located along the flowthrough pores rather than inside long diffusive pores [148]. Accordingly, mass transfer of biomolecules to binding sites depends mainly on convection instead of diffusion and, consequently, binding capacities in membrane chromatography are largely independent of flow-rate.

Membranes used for chromatography consist of a polymeric substrate to which a functional ligand is chemically coupled. The polymer substrate is composed of multilayers of polyethersulfone, polyvinylidene fluoride or regenerated cellulose membrane. The most widely used functional ligands are the same as those used in traditional chromatography, including ion exchange, affinity, reverse-phase, hydrophobic interaction and anionic multimodal ligands [149, 150].

Among the adsorptive membranes commercially available, the Q membrane adsorber has attracted a lot of industry interest, especially in mAb purification processes [148, 151, 152]. Q membranes commercially available include Intercept™ (Millipore), Sartobind® (Sartorius) and Mustang® (Pall). Q membranes are normally exploited as polishing steps in flowthrough mode to remove trace amounts of impurities. The cation-exchanger Mustang® S from Pall is already capable to support IgG binding capacities of 60 mg/mL [150]. Recently available commercial anionic multimodal membrane such as ChromaSorb (Millipore) improves impurity binding capacity or impurity removal function at a higher loading conductivity range and broadens anionic membrane operation conditions [150].

Besides membranes being a considerable alternative to chromatographic beads, they present some limitations such as (i) irregular flow distribution, (ii) non-identical membrane size distribution, (iii) uneven membrane thickness, (iii) low binding capacities [70] and (iv) high dilution of the eluted fractions [151], that varies with the modulus under use. Nevertheless, improved binding capacities and flow distribution have been achieved by optimizing pore size, membrane chemistry, membrane thickness or the number of membrane layers and employment of tentacle ligands (as the one used in beads, *e.g.* Fractogel® technology from Millipore)[149].

I.4.2.3. **Monoliths**

Monoliths are fixed chromatography beds cast as a single unit, characterized by a network of large highly interconnected channels (Figure I.12) [153]. They offer the uniform flow distribution of packed particle beds and the convective mass transport efficiency of membranes. This translates into consistent capacity and high-resolution fractionation regardless of solute size, buffer viscosity, or flow-rate [154]. These structures are commonly composed by silica, polymethacrylate, polyacrylamide, or even cellulose that are being commercialized by companies as BIA Separations, Bio-Rad, Sepragen, Merck and Isco [155].

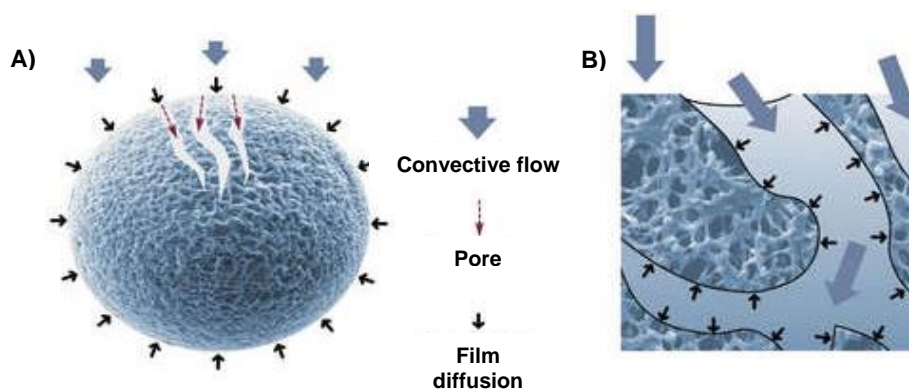


Figure I.12 Transports mechanisms in a perfusive bead and monoliths. (A) Perfusive bead, (B) Monolith.

Monoliths easily accommodate flow-rates of 10 bed volumes per minute without loss of performance. A valuable corollary of independence from flow rate is that dynamic binding capacity is largely liberated from the residence time requirements that burden porous particles exhibit. It also eliminates eddy dispersion, which is a major impediment to high-resolution fractionation in bead-based columns. The lack of eddy dispersion effect and diffusive mass transfer limitations allows monoliths to achieve high-resolution fractionation with short beds, which combined with a high porosity further enables low operating pressures at high flow rates. At large-scale, monoliths short beds are maintained by employing a radial-flow format.

The current marketed monoliths for industrial applications have average 2 μm channels, optimized for purification of large solutes as monoclonal antibodies, DNA plasmids and virus particles. Barroso and colleagues [156] reviewed the monolithic materials used for antibody purification. From there it can be found that monolithic materials are wide spread and new and more sustainable materials are arising, *e.g.* the chitosan derivatives [157, 158]. The type of ligand used range from affinity to multimodal being

the ionic exchange ligands the most used as polishing step in a mAb purification platform. Monoliths have intrinsic features that make them ideal for polishing situations. Monoliths, comparing to membranes, have a higher degree of pore diffusion which facilitates the binding of smaller impurities and, in comparison with resin-based columns, hold larger pores providing an adequate binding capacity for large biomolecules [151].

Very high recoveries (<90%) and purities (<94%) have been achieved using different affinity ligands immobilized in a plethora of different materials [156]. Dynamic binding capacities from 20 to 150 mg IgG/g monolith were described being the best result provided by using a chitosan-PVA material with a protein A mimetic ligand immobilized [157].

Ultramacroporous monoliths have been synthesized with channel sizes of 10–200 μm [159, 160] with the aim of turning monoliths in another option for bypassing clarification of cell culture supernatants. An ultra-macroporous protein A monolith achieved 88 mg IgG/g [159]. One with a histidyl chelating ligand bounded more than 100 mg polyclonal IgG/g from serum [160].

1.4.2.4. *Fibres*

In the recent years, only a few limited studies can be found on the activation of membrane fabrics by surface grafting as an alternative to cotton fabric for bioseparations. However, despite the effort the throughput and dynamic binding capacities of those remain low with values ranging lower to equal parameters than those obtained with commercial bead packed columns [161-164].

Recently, a consortium established between ChiPro GmbH, the Jacobs University in Bremen and the University of Buenos Aires came out with a technology based on non-woven materials, gPore, for the application in the recovery and purification of various molecules, e.g. recombinant proteins and monoclonal antibodies.

This composite fiber (gPore) was synthesized by a specific method using chitosan [165] and presented characteristics that turn it in a chromatography media candidate. The composite fibres give rise to irreversible open compact structures with internally grafted homogeneous hydrogel, where reactive groups could be directly introduced to perform ion exchange or affinity ligand immobilization to the fibre surface, and thus reducing diffusion limitations as the process fluid is transported across the fibre. The presence of this hydrogel provides mechanical and chemical stability to the medium and also exhibits high swelling ratio, particularly good flow and adsorption properties can be ascertained [166].

The characterization of this type of fibres was already published elsewhere [166-168]. In these cases, the fibre was synthesized by gamma irradiation what created a grafted material. These materials were further immobilized with a strong cation-exchanger - SP [166] and a strong anion-exchanger - Q [168]. Results were promising for both ligands. However, gPore Q presented the best results with dynamic bonding capacities (DBC) surpassing the one obtained for a traditional bead system Q Sepharose FF [168].

Composite fibres also offer promising prospects in developing single use disposable bioseparation devices in process scale operations due to low production cost and relative inexpensiveness of cotton fabric materials. The integration of this kind of chromatographic media in the process platform established for the downstream processing of monoclonal antibodies was tested. Preliminary results

showed that exits room for improvements in order to increment the DBC towards IgG [105]. Notwithstanding, gPore revealed to be a good alternative to use in integrated platforms where polymers are used, e.g. aqueous-two-phase systems, since these devices present lower pressure drop when compared to traditional agarose beads.

I.4.3. Chromatographic processes

I.4.3.1. *Size-exclusion chromatography (SEC)*

SEC is not usually used in the manufacturing process of mAbs since it presents low productivity [26]. Nonetheless, it remains an extremely important part of IgM purification, at lab scale, and for the analysis of IgG and IgM and the removal of their aggregates.

During SEC analysis is essential to evaluate if the mobile phase in use affects retention and recovery of the target proteins. Salts may suppress undesirable electrostatic interactions between the protein and resin, but they also may enhance hydrophobic interactions due to the high concentrations used. The occurrence of such interactions could lead to an underestimation of IgG aggregates present and/or contamination of IgG monomer fractions since aggregate flow is retarded by the non-specific interactions mentioned. Arginine, in the other hand, showed to be able to affect multiple modes of protein-resin interaction [169]. However, it is important to ensure that mobile phase changes that enhance chromatographic performance do not alter the aggregation state of the protein.

I.4.3.2. *Hydrophobic interaction chromatography (HIC)*

The most frequent application of HIC has been for aggregate removal. Some examples have been reported on porous particle media [56], others on membrane adsorbers [170-172] with both essentially operating in flowthrough mode. HIC is also effective for removal of DNA and host protein contaminants [173], but applications tend to be restricted because of the high salt concentrations at which antibodies elute. However, it has already published that purification of mAbs by HIC under no-salt conditions is possible [174]. A very hydrophobic resin is selected as the stationary phase and the pH of the mobile phase is modulated to achieve the required selectivity. Playing with the effect of the working pH on mAbs polarity and overall surface hydrophobicity, it can be possible to obtain the mAb in the flowthrough fractions with impurities such as aggregates and host cell proteins bound to the column. [174]

I.4.3.3. *Anion-exchange (AEX) chromatography*

AEX chromatography uses positively charged groups (weakly basic such as diethylamino ethyl – SEAE or dimethylamino ethyl – DMAE; or strongly basic such as quaternary amino ethyl – Q or trimethylammonium ethyl – TMAE) immobilized to the resin. It is powerful tool to remove process-related impurities such as host-cell proteins, DNA, endotoxins and leached protein and product-related impurities such as dimers/aggregates, endogenous retrovirus and adventitious viruses such as parvovirus and pseudorabies virus [175, 176].

Applications in flowthrough mode can be a better choice to remove impurities, however, for acidic to neutral antibodies, as the majority of the humanized IgG4, bind and elute mode can be used to remove process-related and product related impurities from the product [49].

Flowthrough operations are commonly conducted on membrane exchangers due to their higher throughput without compromising DNA or virus removal and for being frequently used as disposables [177, 178]. Nevertheless, the majority of applications are still conducted on porous particles because they offer higher capacity for protein contaminants with host cell protein removal usually being the limiting factor [57].

Displacement mode applications represent an extension beyond weak partitioning chromatography (WPC). In the latter, the process is run isocratically and in a bind-and-elute mode, taking the advantage of the fact that impurities to be removed are more acidic than the product [49]. The objective of WPC implementation is to achieve a two chromatography recovery process comprising protein A and AEX for different mAbs [179]. Challenges in WPC reside on the less efficient removal of high molecular weight species compared to recovery processes employing a third chromatographic step such as cation-exchange (CEX); and, on the pH and counterion conditions that cannot be the same to all products [49].

In displacement mode, mAbs are loaded continuously under conditions that promote a weakly bind of the product. On other hand, sample components that interact strongly with the exchanger accumulate and displace weakly retained antibody from the chromatography support. IgG recoveries greater than 99% were achieved with this methodology [180] that can be improved by being applied in monoliths since they have been demonstrated to produce sharp solute boundaries in displacement applications [181].

1.4.3.4. Cation-exchange (CEX) chromatography

CEX chromatography uses resins modified with negatively charged functional groups. They can be strong acidic ligands such as sulfopropyl, sulfoethyl and sulfoisobutyl groups or weak acidic ligand as a carboxyl group with the maximum binding capacity attained can be as high as >100 mg/mL of resin volume [57]. Considering this, CEX chromatography has been applied for purification processes for many mAbs with pI values ranging from neutral to basic (most humanized IgG1 and IgG2 subclasses) [49]. The most negatively charged process related impurities such as DNA, host cell proteins, leached protein A and endotoxin are removed in the flowthrough and wash fractions, with the removal depending on the loading density [49].

Application of cell supernatants typically requires that conductivity and pH be reduced to achieve good binding capacity. In order to achieve these optimal conditions, strategies as (i) diafiltration to equilibrate filtered supernatants [182], (ii) PEG precipitation followed by resuspension in the target buffer [172] or in-line dilution through the chromatography pumps [183] can be applied.

CEX can also provide separation power to reduce antibody variants from the target antibody product such as deaminated products, oxidized species and N-terminal truncated forms, as well as high molecular weight species [49]. Aggregates removal is also accomplished by CEX chromatography using salt or pH linear gradient elution. Salt gradient elution is the most used [184] however, higher pH encourages more effective elimination of host cell proteins in all cases [185].

The dynamic binding capacity of the antibodies was shown to be significantly reduced at low conductivities and low pH due to strong antibody binding that reduces the surface charge potential on the exchanger [71]. Moreover, pH control has emerged as an unexpected challenge for CEX applications [186, 187]. Positively charged hydrogen ions condense opposite negatively charged cation-exchange ligands during equilibration. Sodium ions have a higher affinity for the exchange groups than hydrogen ions, so when salt is introduced, for example upon sample loading or elution, it displaces hydrogen ions into the mobile phase, causing pH to drop. Response is more intense with weak cation-exchangers than strong ones however, it is important to note that some strong cation-exchangers have significant concentrations of carboxyl groups on their polymer backbones that can turn them susceptible to the same problems correspondent to weak cation-exchangers [186, 187].

1.4.3.5. *Immobilized metal affinity chromatography (IMAC)*

IMAC is chemically more complex because of (i) the diversity of adsorbents that may be used to immobilize the metal ion, (ii) the diversity of metals ions that may be employed to mediate selectivity, and (iii) the diversity of elution methods that may be applied [57]. IgG binding is dominated by a highly conserved histidyl cluster at the junction of the second and third constant domains of the heavy chain (Figure I.2) [188].

Many combinations of adsorbent-metal-elution method permit IgG to be purified to greater than 90% in a single step, but capacities are frequently less than 10 mg/mL. Most applications are conducted on supports substituted with iminodiacetic acid (IDA) and loaded with nickel or copper [189, 190]. Use of cobalt, zinc, and iron are less frequent. Prasana and Vijayalakshmi reported IgG binding capacities of 14–16 mg/mL for either polyclonal or monoclonal IgG on copper-loaded IDA monoliths at flow rates up to 9 bed volumes per minute [189]. Capacity with nickel was barely half that. Alternative metal adsorbents are occasionally used, such as nitriloacetic acid [191], aspartic acid [192], or Tris(2-aminoethyl)amine [193]. Other group, instead of immobilizing a chelating ligand to an inert support, they used a histidyl methacrylate derivative to synthesize chelating groups directly into the polymer backbone [159, 194] which showed to improve IgG capacity over IDA-based supports.

Despite IMAC's potential as an inexpensive alternative to biological affinity it is important to note that ligand leakage could be a serious problem and that polynucleotides, endotoxin, [195] and virus [196], have all been shown to bind various immobilized metals. Nonetheless, IMAC has also been used to selectively bind antibody fragments while endotoxin was removed by washing with a surfactant [197].

1.4.3.6. *Multimodal chromatography (MMC)*

Multimodal chromatography (MMC) exploits multiple types of interaction between the stationary phase and the mobile phase, in which the different solutes are present. The binding modes that are more frequently employed in multimodal ligands comprise ion exchange, hydrogen bonding and hydrophobic interaction groups [198], although others may be included for specific purposes, and the strength of each individual interaction can be manipulated accordingly.

Selectivities and specificities that differ from those of traditional ligands gives MMC the versatility needed to deal with challenging purification problems. However, considering secondary interactions as

metal coordination, π – π bonding, hydrogen bonding, and van der Waals forces that can be promoted with the ligand, and all the factors that govern the different selectivities, the optimization of conditions to be employed may be a complex process, in which several studies are required.

Despite these variations, multimodal ligands can be grouped by their dominant functionalities into three subsets that produce characteristic results with mAbs: those that augment anion-exchange with hydrogen bonding; metal coordination with electrostatic interactions, and those that augment hydrophobic charged induction interactions.

1.4.3.6.1. Metal coordination multimodal ligands

Hydroxyapatite (HA) chromatography is definitely the classic of MMC, with studies in protein purification dating back from the 1950s [199]. Hydroxyapatite chromatography is a technique that contains ceramic crystals of hydroxylated calcium phosphate – $\text{Ca}_{10}(\text{PO}_4)_6(\text{OH})_2$ – in the stationary phase. The presence of those crystals confers two types of binding sites: positively charged calcium groups that interact mainly through metal coordination; and negatively charged phosphate groups that act as cation-exchangers [50]. Calcium residues are capable of participating in metal coordination bonds with protein polycarboxyl domains or phosphate residues on nucleotides, endotoxins, and lipid envelope viruses [200].

HA has continued to be explored as a step in the purification of different recombinant proteins, particularly mAbs [200]. HA can be employed as a polishing step in mAbs purification, since it has demonstrated to be effective in removing aggregates [201] or other impurities [202], as well as host cell impurities and leached protein A [203]. The characteristic calcium coordination is largely unaffected by conductivity, endowing HA with a high degree of NaCl tolerance at low phosphate concentrations [204].

Murakami *et al.* [205] explored the use of HA modified with polyethyleneimine (PEI) and found that it increased retention of nucleotides and acidic proteins. PEI is believed to bind to HA phosphate and replace its native cation-exchange ability with a PEI-mediated anion-exchange functionality that works cooperatively with calcium coordination. Since calcium coordination is little affected by conductivity, this creates another class of salt-tolerant anion-exchangers. IgG binding via calcium coordination can be weakened or suspended by the presence of modest phosphate concentrations.

The multimodal potential of HA chromatography can also be explored by changing the immobilized metal ion [206].

1.4.3.6.2. Hydrogen bond-enhanced anion-exchangers

Ligands of this class are commonly called salt-tolerant anion-exchangers. Their ability to bind virus and DNA at moderate salt concentrations makes them strong candidates to replace traditional anion-exchangers as the preferred final polishing media in IgG purification. A polishing step that, with this kind of ligand, dispenses dilutions of buffer exchanges offers great advantages. An example of these types of ligands is *N*-benzyl-*N*-methyl ethanolamine, commercial name Capto Adhere (GE Healthcare), that already demonstrate to be efficient in terms of aggregates, host cell protein (HCP) and leached protein A removal [136, 207]. In batch processes, yields of around 80% and final HCP and aggregates concentrations of 14.5 ppm and 2.6% were obtained [207]. Better results were achieved when the

feedstock was an elution pool from continuous chromatography using protein A as ligand. Purities higher than 99.7% were achieved with HCP concentrations not exceeding 3 ppm [136]. The continuous process used was a multicolumn countercurrent solvent gradient (MCSGP) purification.

With a similar ligand, Bresolin and co-workers [208] obtained purities of 90-95% when purifying IgG from human serum. They immobilized Tris(2-aminoethyl)amine on agarose beads, producing a twin ethylamino ligand in order to use it for a low conductivity flowthrough purification of IgG.

1.4.3.6.3. Hydrophobic charge induction chromatography (HCIC)

Hydrophobic charge induction chromatography (HCIC) is based on the pH-dependent behaviour of ligands that ionize at low pH [209]. This technique employs heterocyclic ligands at high densities (typically a pyridyl ring) from which pend for instance an alkylthiol, alkylamine or hydroxylalkyl nucleophilic group so that adsorption can occur via hydrophobic interactions without the need for high concentrations of lyotropic salts [210]. To overcome the problem of harsh elution conditions, which are typically used with very hydrophobic resins, desorption in HCIC is facilitated by lowering the pH to produce charge repulsion between the ionizable ligand and the bound protein [209].

One of the most known and used member of the heterocyclic compounds family is the mercaptoethyl-pyridine (MEP HyperCel™, Pall Corporation), a cellulose-based media with 4-mercaptoethyl pyridine as the functional group. MEP exhibits a binding mechanism that includes a mild hydrophobic effect, an electrostatic group effect caused by the charge on the heterocyclic ring and also a thiophilic effect provided by the sulphur group [211].

Due to the high cost of protein A resins and their somewhat lower resistance to extreme conditions, HCIC resin has been suggested as a potential alternative to protein A resins for the initial capture and purification of mAbs. Salt-independent antibody binding and successful elution at a higher pH range than what is possible with protein A chromatography has been demonstrated [212, 213] however, one critical drawback of HCIC is that it has stronger non-specific binding and can be less efficient than protein A chromatography in reducing impurities such as host cell proteins. Nevertheless, in combination with other orthogonal purification steps that can provide sufficient removal of residual impurities, such as ion exchange chromatography, precipitation and crystallization, could have a prominent role in antibody purification process development in the future.

1.4.3.7. Affinity chromatography

Affinity separation is the most selective type of chromatography used in biotechnology. It separates proteins on the basis of a reversible interaction between a protein and a specific ligand covalently coupled to a chromatography matrix.

After successful harvesting, protein A affinity chromatography is the first step of choice for most industrial processes [214, 215].

1.4.3.7.1. Protein A

Protein A affinity chromatography is a well-known process in the pharmaceutical industry because of its high binding affinity to antibodies and the purity levels that can be obtained with it. This type of

chromatography uses a native or a recombinant protein ligand obtained from *Staphylococcus aureus* or *E. coli*, respectively. The native protein A is a polypeptide found anchored in the wall of *S. aureus* with a molecular weight (MW) of 54 kDa. Typically, the recombinant protein A used for IgG purification, produced as a secreted extracellular protein in *E. coli*, has been engineered to have the cell wall domain deleted. Therefore, its MW is reduced to around 42 kDa [215]. Regardless of its source, protein A binds to IgG at its Fc region, specifically at the junction between CH2 and CH3 (Figure 1.2) [216], characterized as being a hydrophobic region. The binding and specificity of the binding towards IgG is accomplished through the five homologous domains (E, D, A, B and C) that protein A contains [217]. The IgG-protein A binding mechanism consists on hydrophobic effects related to specific hydrogen bonds that are established as a function of pH. At alkaline pH, histidyl residues on the binding site of IgG–protein A remain uncharged. This contributes to bonding involving hydrophobic effects comprising van der Waals and electrostatic interactions. At low pH, these histidyl residues become charged and mutually repellent [215], thereby providing a mean for easy detachment of the IgG from protein A. Low pH elution usually takes place at pH values between 2 and 3.

A major issue in large-scale antibody purification is based on the harsh conditions required to achieve pyrogen removal and antiseptic management to low resin fouling [218]. For this purpose, sodium hydroxide in concentrations up to 0.5 M is the most commonly used cleaning agent. However, most proteins are sensitive to alkaline solutions. Therefore, repeated binding-elution cycles and continuous cleaning and sanitization will result in protein A three-dimensional tertiary structure modifications and in a consequent change in affinity towards IgG binding domain [218]. In order to improve the stability of protein A resins, staphylococcal protein A variants have been engineered. One example is the Z domain, a mutated analogue of B domain [219]. The Z domain contains two amino acid substitutions relatively to the B domain that confers a higher stability. The change of the Ala residue at position 1 by a Val was essential to furnish a non-palindromic restriction site [219] and the substitution of Gly by Ala, at position 29, prevented the presence of the dipeptide Asn-Gly, which has been reported to be the most sensitive amino acid sequence to alkaline conditions [220]. Consequently, the Z domain is not susceptible to protease degradation and has greater alkaline stability, thus allowing harsh elution or CIP conditions. Additional site-directed mutagenesis studies of Z domain have allowed the development of novel versions with additional improved characteristics. On one hand, the tolerance to alkaline conditions was further increased by the exchange of Phe30 for Ala or Asn23 for a Thr [221]. This improvement avoided deamination processes, which causes protein instability at alkaline pH value [218]. On the other hand, new protein A variants capable of allowing antibody elution at milder conditions were obtained. For instance, the double-mutation variant PAZ02 (Gln11His and Asn11His) exhibited higher pH sensitivity, enabling elution under milder conditions while maintaining affinity, thermal stability and alkaline tolerance [222].

Other examples of protein A ligands modifications comprises the so-called “Thermal Responsive Protein A” (TRPA) and PEGylation of protein A ligands [218, 223]. In order to achieve TRPAs, mutations are made in the core structure of protein A aiming to reduce its thermal instability. The goal is to obtain a protein A mutant with native structure at 2-10 °C, which unfolds at 40 °C. This phenomenon allows the IgG binding at low temperatures and its elution at higher temperature. After elution, TRPA will be able

to refold as a decrease in temperature occur. The refolded proteins will be able to participate again in the adsorption of antibodies. This strategy allows for the entire process to occur at neutral pH diminishing the protein A leakage promoted by the acidic conditions commonly used at the elution step of such biomolecules.[223] On the other hand, PEGylation has been applied as a mean to improve mostly the protein A ligand performance by reducing the non-specific binding of culture media components. In the work developed by González-Valdez *et al.* [224] it is possible to observe that indeed, ligand PEGylation improved the selectivity towards antibodies with the mass of media-associated contaminants being reduced by a factor of ≥ 2 and an increase of 15% in the IgG recovery on elution being observed. However, more studies and developments have to be conducted in this area since DBC was reduced due to a decrease in IgG pore diffusion and slower IgG association kinetics for the PEGylated ligands were obtained.

Overall, the re-engineering of random coil sequences of protein A ligands that eliminate the most vulnerable residues to proteolysis and alkaline hydrolysis led to the achievement of new recombinant protein A variants presenting several operational advantages such as: conformational stability; wide working pH range (2.0–11.0); compatibility with the use of reducing agents, such as urea or guanidinium hydrochloride; possibility of cleaning with reducing agents due to its lack of cysteine residues; and possibility of achieving potentially high recovery (>95%) and high purities (around 99%, in some cases) [28]. The dynamic binding capacity (DBC) for protein A resins can be as high as 50 g of IgG per mL of resin at industrial scale (from 100 to 1,000 kg) [225]. For instance, the Toyopearl® AF-rProtein A HC-650F from Tosoh Biosciences presents a DBC for IgG higher than 65 g/L at 5 min residence time and 10% breakthrough [218]. Features achieved by the use of a recombinant and alkaline stable protein A hexameric ligand with multiple coupling sites.

Although the purity of the eluted recovered pool is usually higher than 95%, other compounds, such as nucleic acids, HCP, leached protein A, and IgG aggregates, are still present in concentrations that need to be further reduced through polishing operations, most commonly by ionic exchange chromatography. Examples of mobile phases used for elution are: 0.1 M glycine-HCl pH 2.0, 20 mM HCl, 0.1 M sodium citrate pH 2.5, and 1 M propionic acid. The use of arginine and NaCl in the adsorption of mAbs as in intermediate washing steps and elution steps, have been also exploited. When used in the adsorption buffer, arginine was reported to enhanced virus removal and even inactivation [226]. Indeed, it was described that the use of L-arginine disrupt the interaction between the xenotropic murine leukemia virus (XMRV) and the mAb during the load or on the MabSelect™ SuRe™ column [227]. Since, in this case, the virus interacted with the resin backbone and the protein A ligand, and it was co-eluted with the mAb, the use of arginine was of great importance virus removal. In intermediate washing steps, the use of arginine could reduce the amount of host-cell proteins (HCPs) non-specifically bonded towards protein A resins, decreasing the amount of HCPs co-eluted with the mAb during the elution step [228]. Finally, its use in the elution buffer demonstrated to favour recovery of non-aggregated IgG [226, 229].

The main industrial manufacturers of protein A resins are GE Healthcare, with agarose-based matrices and Millipore®, with glass or silica-based backbones. Applied Biosystems® has their market more turned for analytical chromatography using organic polymer-based matrices as polystyrene-

divinylbenzene. However, other companies as Tosoh Biosciences, JSR Life Sciences and Kaneka have been revealing new products with matrices of polymethacrylate, methacrylic acid polymers and cellulose, respectively, that present some advantageous features in comparison to the agarose-based matrices, for example in terms of flow-rates of operation [218].

1.4.3.7.2. Synthetic biomimetic ligands

Despite protein A improvements, problems associated with its susceptibility to hydrolysis by chemicals and to proteolytic enzymes commonly present in animal plasma or other biologicals fluids still need to be overcome. Therefore, a new class of synthetic ligands with affinity towards the Fc region of antibodies has been developed. These synthetic ligands are obtained either by screening chemical combinatorial libraries based on nonpeptide backbones or by rationally designing small functional mimetics of natural Ig-binding proteins [230]. The latter approach relies on *de novo* design of compounds able to mimic the molecular interaction that occurs between the staphylococcal protein A (SpA) and antibodies. Through the analysis of the native molecular interaction it was concluded that the dipeptide motif Phe132-Tyr133 present on SpA is essential to the specific bond that occurs between the ligand and antibodies (Figure I.13A) [231]. Therefore, and since triazine rings allow the attachment of natural or artificial amino acid side-chain residues, these compounds have been used as scaffolds [232]. The first synthetic low-molecular weight affinity ligand, the artificial protein A (ApA) ligand was composed by the Phe and Tyr residues coupled to a triazine scaffold such as 1,3,5-trichloro-sym-triazine conferring to it the hydrophobic properties of the core exposed on a helical twist of the B domain of SpA (Figure I.13B) [231]. Based on the ApA structure, further developments were achieved by combinatorial synthesis, allowing the development of a library of 88 IgG-binding ligands coupled to an agarose solid phase. One particular ligand, the 22/8 ligand, composed by two aromatic amines (3-aminophenol and 4-amino-1-naphthol) linked to a triazine scaffold, stood out by the impressive features that presented (Figure I.13B) [232]. The 22/8 ligand demonstrated high bonding affinity ($K_a = 1.4 \times 10^5 \text{ M}$), high stability and a broad-range specificity [232].

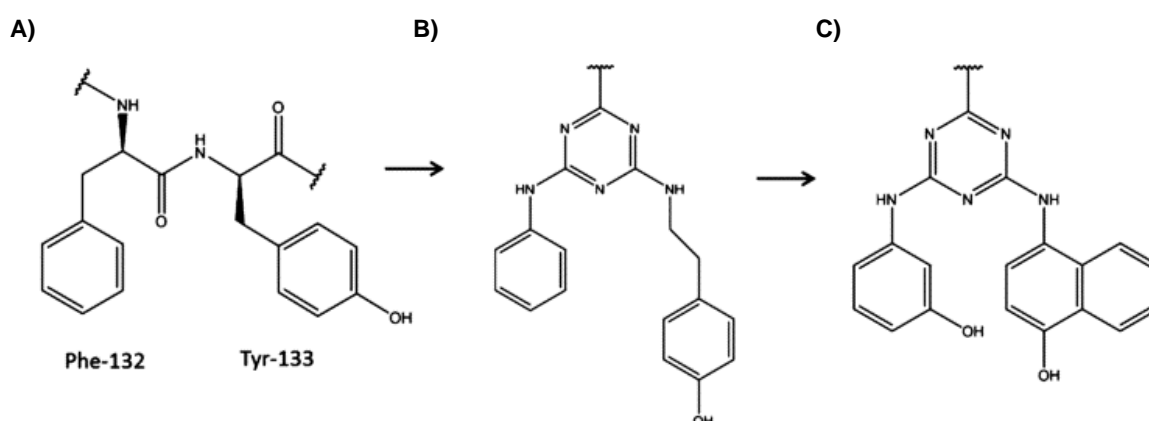


Figure I.13 Chemical structures of ligands used for immunoglobulin isolation and purification. (A) Dipeptide motif present in native SpA, (B) Artificial protein A (ApA) and (C) Ligand 22/8. (B) and (C) are triazine-based ligands.[223]

Besides the well-defined triazine scaffold, ligands based on products product of Ugi reactions have been developed for purification of IgG as other glycoproteins. The Ugi scaffold presents advantages over a common affinity matrix since it is formed directly within the matrix reducing the number of steps, the time and the reagents consumption needed for the production of the matrix [223]. For instance, an aldehyde-functionalized Sepharose™ solid support can constitute one component (aldehyde, or in other cases a ketone) in the four-component reaction, while the other three components (a primary/secondary amine, a carboxylic acid and an isonitrile-group-containing, as isocyanide) are varied in a combinatorial fashion to generate a tri-substituted Ugi scaffold. Thus, these scaffolds can adopt different degrees of rigidity by the possibility to develop branched, cyclized or even 3D affinity ligands [233]. This structural flexibility will be highly important in order to achieve an even more real mimicry to the native dipeptide bond established between native affinity ligands and antibodies [233]. To date, only one mimetic of the Fc-bonding domain has been develop based on Ugi reactions, the A2C1111 ligand [234]. This ligand particularly mimics the Fc-bonding domain of protein G with the advantage of being used in the purification of all mammalian immunoglobulins, including camelid IgGs with a K_d of 4.78 μM [234].

Since synthetic ligands represented cheap, scalable, and stable versions of ligands for affinity chromatography, a major number of novel synthetic ligands have been developed with some being already commercialized (e.g. MAbSorbent A1P and A2P from Prometic Life Sciences).

Taking advantage of the features of Ugi scaffolds, Lowe and co-workers have been studying the possibility of increasing the affinity towards the glycosylation site of glycoproteins, other than antibodies [235, 236]. For that purpose, boronic acid groups added to the Ugi scaffold structures turned out to be essential for glycoprotein binding [235]. Further studies have been carried out and demonstrated the possibility to identify high performance Ugi scaffold that bind specifically to the *cis*-diol groups of carbohydrates at physiological pH using Wulff-type boronic acids such as benzoboroxoles [236].

1.4.3.7.3. Phenylboronic acid

Boronate affinity chromatography has been rising as an alternative to protein A capture step. Phenylboronic acid (PBA) is the most commonly used in this type of chromatography as it contributes for the specific capture and effective enrichment of a large diversity of target *cis*-diol-containing molecules, such as carbohydrates, glycoproteins, RNA, nucleotides and nucleic acids [128, 237-240]. The described affinity relies on the boronate ligand ability to form a pair of covalent bonds with molecules containing *cis*-diols *via* a reversible esterification reaction [241]. Antibodies are glycoproteins bearing an N-linked glycosylation site at the Asn²⁹⁷ of CH2 domain of the Fc region of each heavy chain (Figure I.2) with oligosaccharides composed by 1,2- *cis*-diol saccharides as fucose, mannose and galactose typically found in these sites [242-244].

In acidic to neutral environments, boronic acids adopt a trigonal planar form which can be reverted to a tetrahedral boronate anion upon hydroxylation in alkaline conditions. Both the acid and its conjugate base can bind to diol compounds (Figure I.14) [245]. However, since the equilibrium constant for the tetrahedral (K_{tet}) is usually higher than that of the trigonal form (K_{trig}), complexes are less stable in acidic conditions [246, 247].

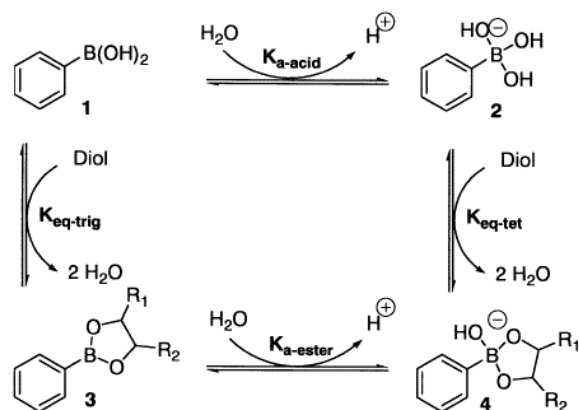


Figure I.14 Schematic of the interaction between phenylboronic acids and *cis*-diol containing compounds. 1 and 2 – PBA trigonal and tetrahedral conformations, respectively. 3 and 4 - illustration of the esterification bond between *cis*-diol containing compounds and the trigonal and tetrahedral conformation of PBA ligands, respectively. [202]

Additionally, ligands as PBA could present a more complex character with affinity being induced by non-specific interactions related to its intrinsic structure. For example, PBA are aromatic ligands and are thus able to establish hydrophobic and π - π interactions. Secondary ionic interactions between boronates and diols are also possible through coulombic attraction or repulsion effects, turning PBA in a weak cation-exchanger [248, 249]. Hydrogen bonding and charge transfer interactions are other types of interactions that can also occur. The latter is more prone to take place in acidic conditions, since in the trigonal uncharged form, the boron atom has an empty orbital and can thus serve as an electron receptor for a coordination interaction, enabling Lewis acid-base interactions to occur with negatively charged carboxylated (aspartate and glutamate) or unprotonated amino groups (asparagine and glutamine) present in the protein structure [238, 250].

Considering all the different interactions that PBA is able to trigger depending on the pH, ionic strength and target molecule properties, PBA should be described as a multimodal ligand and not simply as an affinity ligand towards *cis*-diol containing molecules. Recovery yields and purities achieved for mAbs are comparable to those obtained with protein A chromatography however, using milder elution conditions [237, 251]. PBA presents a lower DBC (22 mAb g/L resin), however being 12 times cheaper than protein A, larger column volumes can be used without compromising the cost-effectiveness of the process [252]. PBA is also competitive in the sense that it has a lifespan of around 400 cycles, a value 2 to 4 times higher than that of protein A [252]. The challenge therefore relies on understanding and consequently predict the adsorption behaviour of proteins, including mAbs, onto PBA chromatographic matrices. This knowledge combined with the already known economic advantages [252] could led industry to adopt such chromatographic process as a reliable alternative to protein A-based capture step.

I.5. Methods for biomolecules adsorption elucidation

The effective application of strategies aiming at the development of ligands and resins with improved performance can only be successful if the phenomena that occur during the adsorption

process of biomolecules are known and disclosed. For example, protein adsorption onto a surface is a complex process controlled by a series of sub processes with synergistic and antagonistic effects, where several types of driving forces are involved. The understanding of the protein adsorption phenomena, particularly at the molecular level, is crucial for the development of new and more cost-effective ligands and chromatographic supports. The knowledge retrieved will be of great importance to optimize adsorption conditions in order to achieve high resin capacities, affinity constants and product quality. Thus, it is also essential to characterize ligand-protein as protein-protein interactions that could occur at linear and overloaded conditions.

Surface plasmon resonance (SPR) is one of the most used techniques to study molecular interactions. SPR is a detection method that makes possible to measure interactions in real-time with high sensitivity and without the need of labels. SPR detects refractive index changes close to the surface and, since all biomolecules have refractive properties, no labelling is required. Furthermore, the accumulation of 1 pg/mm^2 gives a change of 1 response unit (RU), facilitating real-time measurements as a basis for acquiring kinetic data related to the adsorption process. The kinetic data is retrieved by the relation that exists between rate constants (time dependent) and equilibrium constants (time independent).

SPR occurs on the surface of a chip that is usually a polymer with functional groups with a gold layer beneath it (Figure I.15A). For the analyses to occur, two molecules are required: a ligand (an interaction reagent immobilized on the surface) and an analyte (an interaction reagent flowed over the surface). The mass changes during the analyte binding and dissociation at various concentrations are measured during time with sensorgrams of RU vs time being obtained (Figure I.15B).

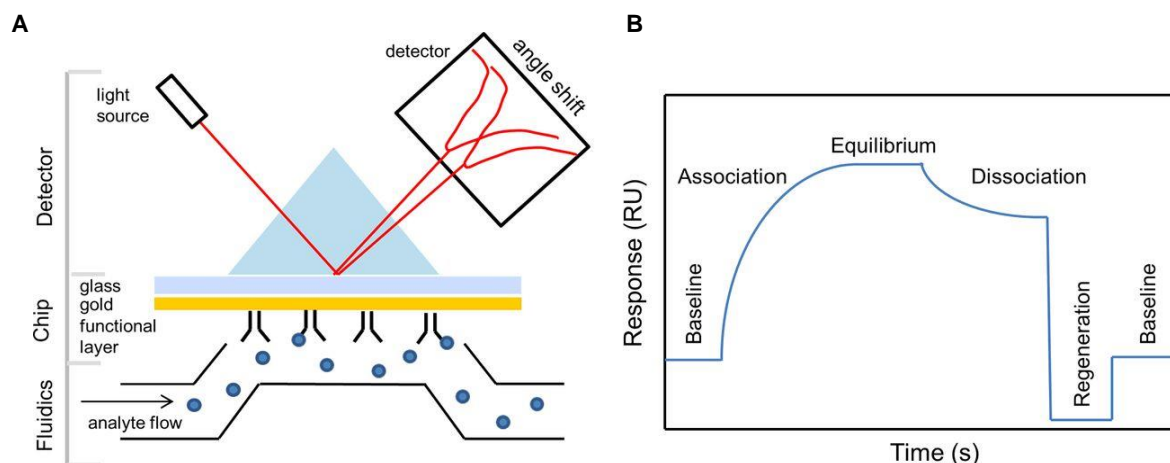


Figure I.15 (A) Principle of SPR instrument and (B) typical SPR sensorgram showing the steps of an analytical cycle. [253]

From sensorgrams acquired at different analyte concentrations, it is possible to get rates and/or equilibrium constants of adsorption and desorption of the analytes by fitting curves to mathematical models. The RU values withdrawn from the steady-state of each sensorgram give rise to a binding isotherm from which the equilibrium dissociation constant (K_d) can be determined. With the K_d calculated

it is possible to obtain the affinity constant of the bond established between the ligand and the analyte and, consequently some thermodynamic parameters as ΔG (see *Equation 2*) can also be obtained.

Among the advantages already cited, SPR presents low sample consumption, reusability of the ligand and most importantly, can be used as a high-throughput system for screening a multitude of analytes and ligands. Accordingly, this technique has been applied to diverse studies including: (i) the evaluation of the interaction of antibodies and multimodal ligands [254], (ii) the glycosylation fingerprinting of glycosylated proteins using lectins as ligands [255, 256] and (iii) the impact of IgG modifications on its interaction with Fc receptors and *vice-versa* [257].

Equipments as Biacore, ForteBio Octets, Bionavis and ProteOn systems are commercially available to perform SPR measurements.

Conventional isotherm models are a good starting point, however they cannot completely characterize the complex phenomena underneath adsorption mechanisms of biomolecules in liquid chromatography since they do not consider non-ideal effects associated with the adsorption of large biomolecules and/or in overloaded conditions [258]. Thermodynamic parameters related to adsorption of biomolecules onto chromatographic supports have been accessed by performing batch equilibrium experiments or by analysing chromatographic data through the Van't Hoff analysis [259, 260]. More recently, calorimetric measurements have been used showing to be more reliable and capable to distinguish isolated events related to the adsorption mechanism of different biomolecules onto chromatographic supports, both in linear and non-linear conditions [261-264].

1.5.1. Thermodynamics of biomolecules adsorption in chromatography

For an accurate interpretation of results, it is important to have into consideration thermodynamic concepts and the processes that can contribute to enthalpy and entropy changes during protein adsorption. The possibility of a protein to be reversibly adsorbed (at constant pressure and temperature) is determined by the change in standard Gibbs free energy (ΔG°) of the system (*Equation 1*).

$$\Delta G^\circ = \Delta H^\circ - T\Delta S^\circ$$

Equation 1

Where ΔH° and ΔS° are the standard enthalpy and entropy changes, respectively. Exothermic events ($\Delta H^\circ < 0$) result in heat released by the system, while endothermic events ($\Delta H^\circ > 0$) leads to the absorption of heat.

For a spontaneous process, such as protein adsorbing to a chromatographic support, ΔG° must be negative. In this way, the adsorption process is enthalpically driven when a negative net heat ($\Delta H^\circ < 0$) is observed. Affinity and pseudo-affinity chromatography types are examples of this case. On the other hand, when the adsorption process results in an overall increase of enthalpy ($\Delta H^\circ > 0$), the entropic effects are considered to be the driving force. In an entropically driven process, the binding strength of the protein towards the sorbent is generally expected to be enhanced by increases in temperature, as often occurs in the case of hydrophobic interaction (HIC) [265] and ion-exchange (IEX) chromatography [260, 266].

The equilibrium binding affinity constant (K) can be related to the standard Gibbs free energy (ΔG°) change for a specific protein-solid phase as described in *Equation 2*.

$$\Delta G^\circ = -RT \ln K$$

Equation 2

where R is the gas constant ($8.314462 \text{ J K}^{-1} \text{ mol}^{-1}$) and T is the absolute temperature in Kelvin.

From *Equations 1* and *2*, it is possible to conclude that the binding affinity constant (K) is related with ΔG° and, consequently, the enthalpy and entropy events involved in protein adsorption process. Therefore, the binding affinity of a protein can be evaluated and better understood in terms of energetic events involved in the binding process.

1.5.1.1. Van't Hoff plot analysis

Van't Hoff plots using linear and nonlinear regressions have been widely employed to obtain thermodynamic parameters from retention chromatographic data [265, 267-270]. While a linear Van't Hoff plot (obtained by *Equations 1* and *2*) is associated with a zero heat capacity (ΔC_p°) process, a nonlinear plot is a result of positive or negative values of ΔC_p° . Horváth and co-workers [267], using Kirchhoff's relations, derived the logarithmic equation that compensates for nonlinear Van't Hoff plots when ΔC_p° is a negligible function of temperature. However, temperature invariant heat capacity change has been shown to be a crude assumption [265]. Because of this, the same authors [267] proposed *Equation 3* that corrects for the variation of ΔC_p° with temperature.

$$\ln k' = a + \frac{b}{T} + \frac{c}{T^2} + \ln \varphi$$

Equation 3

In this equation k' is the retention factor, T is the temperature in Kelvin, φ is the phase ratio and a , b and c are parameters obtained by least squares fitting. k' and φ are obtained according to *Equations 4* and *5*.

$$k' = \frac{t_r - t_0}{t_0}$$

Equation 4

where t_r is the solute retention time and t_0 the hold-up time (obtained with an inert tracer).

$$\varphi = \frac{V - t_0 \bar{V}}{t_0 \bar{V}}$$

Equation 5

where V is the column volume and \bar{V} the volumetric flow-rate.

From Equation 3, changes in standard-state enthalpy, entropy and heat capacity can be obtained respectively from Equations 6 to 8.

$$\Delta H^\circ = -R \left(b + \frac{2c}{T} \right)$$

Equation 6

$$\Delta S^\circ = R \left(a - \frac{c}{T^2} \right)$$

Equation 7

$$\Delta C_p^\circ = \frac{2Rc}{T^2}$$

Equation 8

Nevertheless, appreciable differences between the calorimetric enthalpy values, obtained experimentally, and the Van't Hoff enthalpies have been reported in other studies [265, 268-272]. These data illustrate the limitations of Van't Hoff method when assessing thermodynamic quantities. Van't Hoff analysis is based on the assumption that a reversible equilibrium exists between the bound and the free protein [271], which is not always true. Also, the Van't Hoff analysis is limited to the linear region of the isotherm, and effects present at higher surface coverage cannot be quantified. For example, the influence of protein loading on thermodynamic parameters cannot be evaluated by this analysis [271].

1.5.1.2. Calorimetry techniques

Biomolecules adsorption and desorption processes have small, but measurable related thermal signals. Thus, through direct adsorption enthalpy measurements, calorimetry can provide valuable understanding of the adsorption mechanisms onto chromatographic media [263-265].

1.5.1.2.1. Isothermal titration calorimetry (ITC)

In recent years, calorimetric methods have gradually become a more and more powerful technique for label-free indication and quantification of binding events [273]. In contrast to label based methods (e.g. nuclear magnetic resonance), isothermal titration calorimetry (ITC) offers the major advantage of simple sample preparation combined with a fast calorimetric response and thermal equilibration [274, 275].

Furthermore, the major advantage of this technique is that the entire set of thermodynamic parameters, *i.e.* enthalpy ΔH , the free energy ΔG , entropy ΔS , the association constant K and the stoichiometry of the interaction n can be quantified by a single experiment [276]. This feature makes ITC truly important for the understanding of biological processes based on different kinds of interactions, including (i) protein–protein, (ii) protein–peptide, (iii) protein–drug, (iv) DNA–drug, (v) protein–DNA (vi) protein–carbohydrate interactions [277, 278] and more recently (vii) biomolecule-solid phase interactions in chromatography [262, 279-281]. In this way, ITC data can provide crucial information in

order to improve and design new systems capable of predict thermodynamic parameters for biomolecular processes what will fasten, for example drug screening and development [277].

An ITC equipment operates under batch mode and consists of a sample cell, in which the host is placed and a guest molecule is injected *via* a syringe (Figure I.16). The power change, which depends on the interaction between the host and the guest, is compared with a reference cell which only contains the solvent.

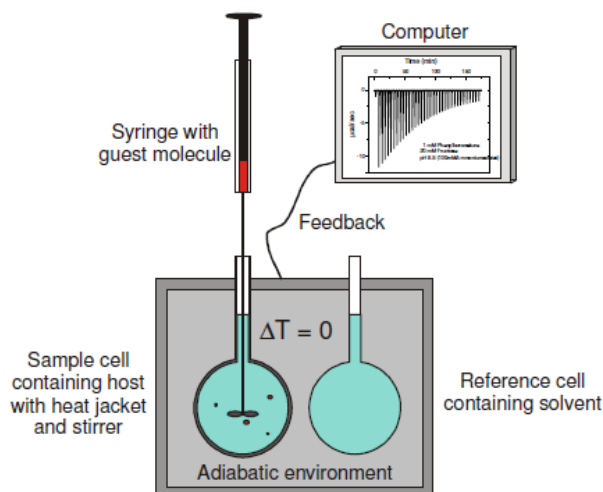


Figure I.16 Schematic drawing of an isothermal titration calorimeter. The guest molecule is stepwise inserted *via* syringe into the sample cell which contains the receptor or ligand. [278]

Using a feedback mode, the temperature of the sample cell is either increased or decreased to maintain a temperature difference of zero between the sample and the reference cell [282]. The primary analytical signal is therefore the power q , which is proportional to the concentration of the ligand ΔL in i^{th} each step combined with the volume of the sample cell v and the binding enthalpy ΔH for this reaction (Equation 9).

$$q_i = v \cdot \Delta H \cdot \Delta L_i$$

Equation 9

The heat for each injection can then be calculated by integration of the peaks obtained from a diagram of q versus time (Figure I.17B). The data processing will be performed by the software, which will present a Wiseman isotherm, fitted to the raw data, in a diagram of ΔH [kcal/mol of injectant] vs molar ratio. Enthalpy of adsorption is directly obtained from the Wiseman isotherm as the stoichiometry of binding n that is the molar ratio at the inflection point of the binding isotherm. The association constant K is model dependent and is extracted from the slope at the inflection point of the binding isotherm. ΔG and ΔS can be obtained by the use of Equation 2 and 1, respectively.

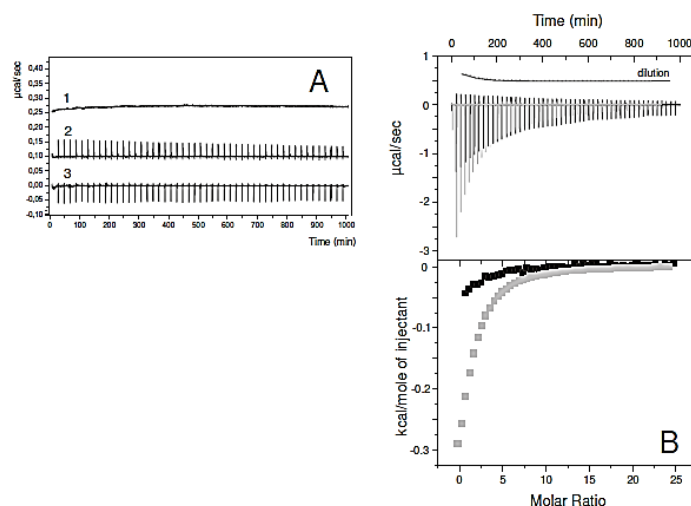


Figure I.17 Illustrative ITC data example. (A) Control experiments performed with chromatographic particles titrated against buffer (1) and the biomolecule (2), and the biomolecule against only buffer (3). (B) ITC experiments with two different types of ligands titrated against the biomolecule in buffer system. The data were corrected against the dilution experiments. [278]

From an ITC experiment an additive signal is obtained which is composed of many types of actions (Figure I.17). Most obviously, a contribution comes from the interaction under investigation. Apart from that, the heat observed during ITC titration results can also have contributions from:

- Dilution effects: heat released/adsorbed when the ligand is titrated into de buffer;
- Background heats due to buffer mixing. To avoid them, buffers with the same pH, salt concentration, etc. should be used in the cell and in the syringe;
- Heats of ionization of various buffers.

Therefore, crucial for the experimental design are the reference measurements in order to determine the different contributions that commonly occur when injecting the molecule under study into the buffer without receptors or ligands (Figure I.17).

Nevertheless, ITC based studies present some limitations as regards its use for the understanding adsorption mechanism in chromatography. An ITC cell does not replicate accurately the dynamics of a chromatographic process nor does it allows the observation of distinct events during adsorption period. Also, biomolecule rearrangements after interaction and desorption processes cannot be observed nor thermodynamically studied and consequently ITC cannot be applied to the study biomolecules interactions at overloaded conditions.

In order to overcome such disadvantages Flow microcalorimetry (FMC) is used. With this technique, it has been achieved the evidence of exothermic and endothermic peaks at different times during the complex phenomena of protein adsorption what can lead us to disclose the isolated events involved [261, 263, 264].

1.5.1.2.2. Flow microcalorimetry (FMC)

Flow microcalorimetry (FMC), just like ITC, seeks to measure enthalpy changes during interaction between two molecules at a constant temperature. However, in this case, measurements are done under a specific flow-rate.

A flow microcalorimeter has the ability to simulate a packed-bed chromatographic system at micro-scale. It allows a direct, dynamic and precise measurement of the heat signal, since the signal is measured within the column during the adsorption and desorption processes of a biomolecule that flows through a small column packed with the adsorbent of interest. Thus, the whole profile can give an overview on the kinetics of process adsorption and desorption. By integrating the obtained values, energy change can be determined and associated to mass transfer phenomena involved in the whole interaction process as for the isolated events occurring, by data de-convolution [268, 272, 283]. These characteristics allied to the fact that FMC does not interfere with the thermodynamic and kinetic adsorption equilibrium, turn it into the only experimental technique to date, that can be used for *in-situ* studies of molecular adsorption interactions during chromatography, allowing a better understanding of the driving forces, mechanisms and kinetics involved.

Flow microcalorimetric methods allow the measurement of the heat flow during the interaction occurring in any type of chromatography with several studies already reported for hydrophobic interaction [283], ion exchange [260, 263, 284] and metal affinity chromatography [285], under linear or overloaded conditions [263, 264, 269], and with different biomolecules such as proteins [260, 263, 285] and more recently pDNA [264].

The commonly used flow microcalorimeter, Microscal FMC 4 Vi (Microscal Limited, London, UK) (Figure I.18), was constructed to be operated in the heat conduction mode, contrarily to ITC operation mode. The equipment possesses a 171 μL cell located internally that is interfaced with two highly sensitive thermistors capable of detecting small power changes (in the order of 10^{-7} W [280]) produced during the protein adsorption process. The heat evolution during the process is indicated by changes in potential (imbalance in the thermistor bridge in which the two thermistors measure power changes in the cell), with no power compensation present. Thus, when an exothermic reaction occurs, the calorimeter will sense an increase in energy and a positive signal will appear in the thermogram. The opposite is observed for an endothermic reaction.

Energy changes are converted to heats of adsorption using an experimentally determined calibration factor [261]. The calibration is performed in order to evaluate the energetic pulse propagation under the resin equilibrated, with the chosen buffer system, in flow mode. For this, several electrical pulses are imposed for determined periods of time, which result in characteristic calibration peaks. Posteriorly, those are used to determine the relation between peak areas and its corresponding energy, allowing the conversion of power changes assessed by the thermistors in heats of adsorption. The calibration factor obtained is a result of the data treatment performed using CALDOS 4 software (Microscal, Limited, UK).

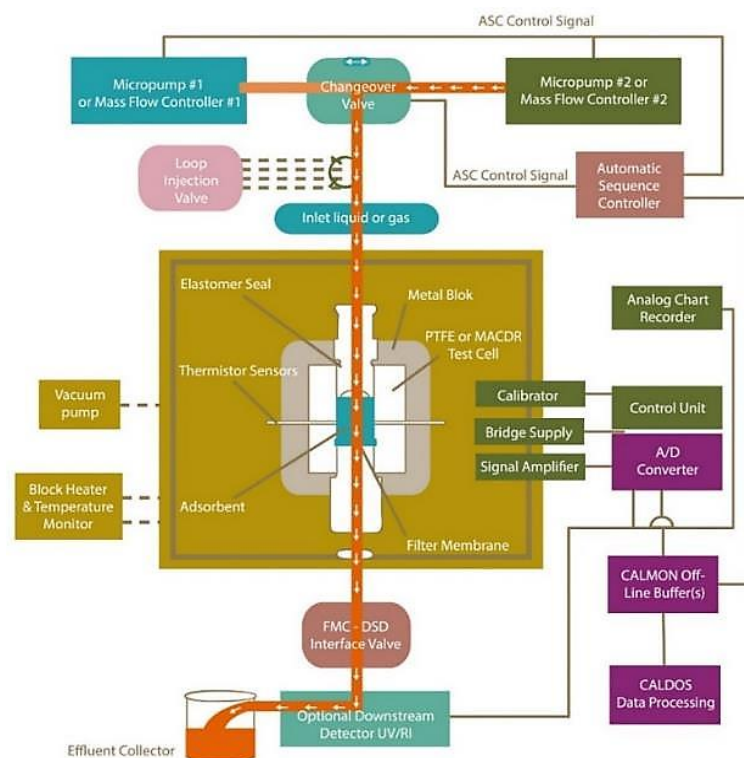


Figure I.18 Schematics of a flow microcalorimeter system and its components. [286]

1.5.1.2.3. Differential scanning calorimetry (DSC)

Differential scanning calorimetry (DSC) presents similarities towards ITC, regarding the equipment operation mode, however, the data retrieved is related to the folded and unfolded states of biomolecules. It is possible to reliably retrieve the transition midpoint between folded and unfolded protein state (melting temperature - T_m). At T_m , the concentration of the unfolded and folded species is equal. This parameter describes the susceptibility of the protein to thermal denaturation, *i.e.* the higher the T_m is, the more stable is the protein.

DSC provides other useful parameters that can be used to characterize protein stability, including the unfolding enthalpy (ΔH), which is measured by the area under the curves represented in Figure I.19. DSC also determines:

- the T_{onset} , temperature at which starts the unfolding transition (usually 5 to 10 °C lower than the T_m);
- the ΔC_p , heat capacity change of unfolding;
- the $T_{1/2}$, width at peak half height. This parameter is indicative of the broadness of the transition, with typical values of 1-15°C, which is correlated with protein packing. A broader transition corresponds to a less compact protein and *vice-versa*.

Since the equipment works in a power compensation mode and protein unfolding is an endothermic event, a positive peak will appear (Figure I.19). Protein unfolding is an endothermic event [287] since energy input is needed to break the secondary non-covalent bonds that keep the protein folded.

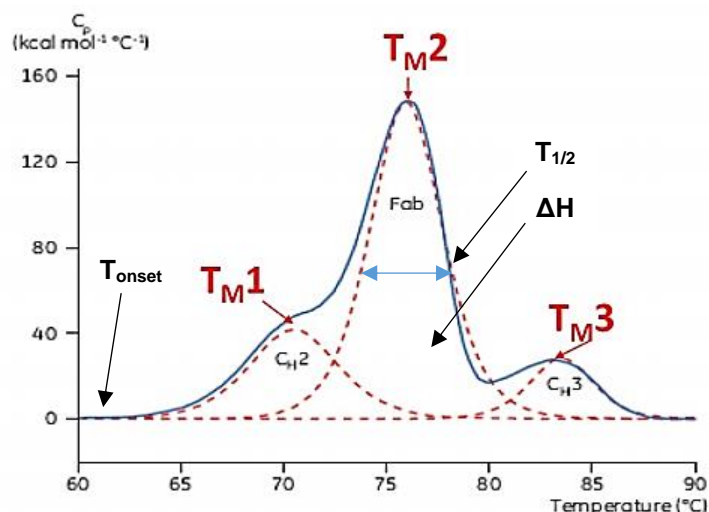


Figure I.19 Representative DSC thermogram of a monoclonal antibody, with CH2, Fab, and CH3 domains identified. The dashed red lines are the deconvoluted peaks of each domain transition, with the three melting temperatures (TMs) indicated. [288]

Also, in DSC, it is of high importance to perform a blank run. In this case, the blank run will be performed in the reference cell simultaneously and at the same conditions that the measurement of protein stability is being accomplished. The parameters that have to be chosen in order to carry out an experiment include (i) the number of runs, (ii) the scan rate and (iii) the temperature interval desired. The recorded signal will be transformed into heat capacity (C_p) as function of temperature by the software. The results can be then normalized in function of the number of moles present in the measuring cell. Previously to the deconvolution of the thermogram to obtain the correct T_m and to the integration of the thermogram to obtain ΔH , a baseline is created and subtracted. C_p is pressure dependent as described in *Equation 10* but under adiabatic conditions, the integration of the results can be done as in *Equation 11*.

$$C_p = \left(\frac{\partial \Delta H}{\partial T} \right)_p$$

Equation 10

$$\int_{T_1}^{T_2} C_p dT = \int_{T_1}^{T_2} \partial \Delta H$$

Equation 11

The application of this technique to chromatography studies turns possible to understand if conformational changes of a protein is occurring upon adsorption and if those are transient or not. For example, Beyer *et al.* [289] could conclude that the conformational changes occurring in an antibody upon adsorption to HIC media are directly proportional to the hydrophobicity of the stationary phase and that upon elution, the protein returns to its original conformation. On the other hand, Krepper *et al.* [290] employed DSC to analyse the eluted mAb from protein A affinity resins. Slight variations in the unfolding temperatures were observed but it was confirmed by circular dichroism (CD) that structural changes in

IgG are fully reversible. Moreover, in this study DSC measurements showed that the antibody undergoes structural changes during the adsorption and that those are dependent on the chromatographic material used. In both cases, the conformational changes were addressed by differences in the T_m of the proteins upon adsorption or desorption.

Comparing adsorption behaviour towards different types of stationary phases and other factors such as temperature and salt concentration can facilitate finding the optimal setup for a chromatographic process before fine-tuning other running conditions. The further insight about what happens to a molecule during the adsorption process to different kinds of surfaces can be also used for accurately modelling the type of interaction(s) in question in order to make predictions about chromatographic behaviour.

The use of DSC and ITC has been implemented as an alternative to attenuated total reflectance Fourier transform infrared (ATR FT-IR). Contrarily to DSC, ATR FT-IR measurements are heavily dependent on the optical characteristics of the stationary phase particles. While good results could be achieved for Sepharose-based materials [291], polymetacrylate particles, as the ones used by Beyer *et al.* [289], could not be analysed at all due to a lack of translucency and high background signals. Nevertheless, this non-calorimetric method was successfully used by Ueberbacher *et al.* [291] to identify *in situ* structural changes that occur in proteins upon adsorption to hydrophobic agarose-based media. The infrared spectra of the loading sample is compared to the samples that are undergoing adsorption. Knowing the absorption maximum for the secondary structures of antibodies, it is possible to understand if their conformation has changed. Complementary studies, as CD and ELISAs, are then necessary to understand if the changes that antibodies experienced are irreversible or not and if this implies a reduction in its biological activity.

I.6. References

- [1] FDA okays marketing of human insulin, Chemical & Engineering News Archive, 60 (1982) 5.
- [2] C.C. Quianzon, I. Cheikh, History of insulin, J Community Hosp Intern Med Perspect, 2 (2012) 1-3.
- [3] W.W.-F. Leung, Introduction, in: W.W.-F. Leung (Ed.) Centrifugal Separations in Biotechnology, Academic Press, Oxford, 2007, pp. 1-17.
- [4] H.A.D. Lagassé, A. Alexaki, V.L. Simhadri, N.H. Katagiri, W. Jankowski, Z.E. Sauna, C. Kimchi-Sarfaty, Recent advances in (therapeutic protein) drug development, F1000Res, 6 (2017) 113-113.
- [5] O. Sumant, S. Shaikh, Protein Therapeutics Market Report, in <https://www.alliedmarketresearch.com/protein-therapeutics-market>, Allied Market Research, March 27, 2019.
- [6] Recombinant Therapeutic Antibodies and Proteins Market, by Drug Class, by Application, and by Region - Size, Share, trends, and Forecast to 2026, in Coherent Market Insights, <https://www.coherentmarketinsights.com/market-insight/recombinant-therapeutic-antibodies-and-proteins-market-1981>, March 27, 2019, July, 2018.
- [7] R. Jefferis, Glycosylation as a strategy to improve antibody-based therapeutics, Nat Rev Drug Discov, 8 (2009) 226-234.
- [8] A.R. Costa, M.E. Rodrigues, M. Henriques, R. Oliveira, J. Azeredo, Glycosylation: impact, control and improvement during therapeutic protein production, Crit Rev Biotechnol, 34 (2014) 281-299.
- [9] G. Casi, D. Neri, Antibody-drug conjugates: basic concepts, examples and future perspectives, J Control Release, 161 (2012) 422-428.
- [10] T. Rath, K. Baker, J.A. Dumont, R.T. Peters, H. Jiang, S.W. Qiao, W.I. Lencer, G.F. Pierce, R.S. Blumberg, Fc-fusion proteins and FcRn: structural insights for longer-lasting and more effective therapeutics, Crit Rev Biotechnol, 35 (2015) 235-254.

- [11] D. Levin, B. Golding, S.E. Strome, Z.E. Sauna, Fc fusion as a platform technology: potential for modulating immunogenicity, *Trends Biotechnol*, 33 (2015) 27-34.
- [12] J.T. Andersen, R. Pehrson, V. Tolmachev, M.B. Daba, L. Abrahmsen, C. Ekblad, Extending half-life by indirect targeting of the neonatal Fc receptor (FcRn) using a minimal albumin binding domain, *J Biol Chem*, 286 (2011) 5234-5241.
- [13] P.L. Turecek, M.J. Bossard, F. Schoetens, I.A. Ivens, PEGylation of Biopharmaceuticals: A Review of Chemistry and Nonclinical Safety Information of Approved Drugs, *J Pharm Sci*, 105 (2016) 460-475.
- [14] A.C.T.I.P.- Monoclonal Antibodies Approved by the EMA and FDA for Therapeutic Use (status 2017), in <http://www.actip.org/products/monoclonal-antibodies-approved-by-the-ema-and-fda-for-therapeutic-use/>, 2017.
- [15] D.M. Ecker, S.D. Jones, H.L. Levine, The therapeutic monoclonal antibody market, *mAbs*, 7 (2015) 9-14.
- [16] N.A. Buss, S.J. Henderson, M. McFarlane, J.M. Shenton, L. de Haan, Monoclonal antibody therapeutics: history and future, *Curr Opin Pharmacol*, 12 (2012) 615-622.
- [17] O.H. Brekke, I. Sandlie, Therapeutic antibodies for human diseases at the dawn of the twenty-first century, *Nat Rev Drug Discov*, 2 (2003) 52-62.
- [18] Z. An, *Therapeutic Monoclonal Antibodies: From Bench to Clinic*, John Wiley & Sons, 2011.
- [19] S.J. Kim, Y. Park, H.J. Hong, Antibody engineering for the development of therapeutic antibodies, *Mol Cells*, 20 (2005) 17-29.
- [20] E.V. Capela, M.R. Aires-Barros, M.G. Freire, A.M. Azevedo, Monoclonal Antibodies – Addressing the Challenges on the Manufacturing Processing of an Advanced Class of Therapeutic Agents, in: Attar-Rahman (Ed.) *Frontiers in Clinical Drug Research - Anti-Infectives*, Bentham Science, 2017, pp. 142-203.
- [21] G. Köhler, C. Milstein, Continuous cultures of fused cells secreting antibody of predefined specificity, *Nature*, 256 (1975) 495.
- [22] M. Better, C.P. Chang, R.R. Robinson, A.H. Horwitz, Escherichia coli secretion of an active chimeric antibody fragment, *Science*, 240 (1988) 1041-1043.
- [23] J.M. Reichert, Monoclonal antibodies as innovative therapeutics, *Curr Pharm Biotechnol*, 9 (2008) 423-430.
- [24] P.A. Marichal-Gallardo, M.M. Alvarez, State-of-the-art in downstream processing of monoclonal antibodies: process trends in design and validation, *Biotechnol Prog*, 28 (2012) 899-916.
- [25] M.A. Roguska, J.T. Pedersen, C.A. Keddy, A.H. Henry, S.J. Searle, J.M. Lambert, V.S. Goldmacher, W.A. Blattler, A.R. Rees, B.C. Guild, Humanization of murine monoclonal antibodies through variable domain resurfacing, *Proc Natl Acad Sci USA*, 91 (1994) 969-973.
- [26] S. Aldington, J. Bonnerjea, Scale-up of monoclonal antibody purification processes, *J Chromatogr B*, 848 (2007) 64-78.
- [27] L. Chu, D.K. Robinson, Industrial choices for protein production by large-scale cell culture, *Curr Opin Biotech*, 12 (2001) 180-187.
- [28] J. Curling, The development of antibody purification technologies, in: U. Gottschalk (Ed.) *Process Scale Purification of Antibodies*, Wiley, New Jersey, 2009, pp. 25-52.
- [29] J. Zhu, Mammalian cell protein expression for biopharmaceutical production, *Biotechnol Adv*, 30 (2012) 1158-1170.
- [30] M. Butler, A. Meneses-Acosta, Recent advances in technology supporting biopharmaceutical production from mammalian cells, *Appl Microbiol Biotechnol*, 96 (2012) 885-894.
- [31] F. Li, N. Vijayasankaran, A. Shen, R. Kiss, A. Amanullah, Cell culture processes for monoclonal antibody production, *mAbs*, 2 (2010) 466-477.
- [32] B. Kelley, G.B. G., A. Lee, Downstream processing of monoclonal antibodies: current practices and future opportunities in: U. Gottschalk (Ed.) *Process Scale Purification of Antibodies*, Wiley, New York, 2009, pp. 1–23.
- [33] R.J. Kaufman, P.A. Sharp, Amplification and expression of sequences cotransfected with a modular dihydrofolate reductase complementary dna gene, *J Mol Biol*, 159 (1982) 601-621.
- [34] C.R. Bebbington, G. Renner, S. Thomson, D. King, D. Abrams, G.T. Yarranton, High-Level Expression of a Recombinant Antibody from Myeloma Cells Using a Glutamine Synthetase Gene as an Amplifiable Selectable Marker, *Bio/Technology*, 10 (1992) 169-175.
- [35] B.I. Schweitzer, A.P. Dicker, J.R. Bertino, Dihydrofolate reductase as a therapeutic target, *FASEB J*, 4 (1990) 2441-2452.
- [36] T. Lai, Y. Yang, S.K. Ng, Advances in Mammalian cell line development technologies for recombinant protein production, *Pharmaceuticals (Basel)*, 6 (2013) 579-603.
- [37] Z. Hu, D. Guo, S.S.M. Yip, D. Zhan, S. Misaghi, J.C. Joly, B.R. Snedecor, A.Y. Shen, Chinese hamster ovary K1 host cell enables stable cell line development for antibody molecules which are difficult

- to express in DUXB11-derived dihydrofolate reductase deficient host cell, *Biotechnol Progr*, 29 (2013) 980-985.
- [38] D.L. Hacker, M. De Jesus, F.M. Wurm, 25 years of recombinant proteins from reactor-grown cells — Where do we go from here?, *Biotechnol Adv*, 27 (2009) 1023-1027.
- [39] S.M. Noh, S. Shin, G.M. Lee, Comprehensive characterization of glutamine synthetase-mediated selection for the establishment of recombinant CHO cells producing monoclonal antibodies, *Sci Rep-UK*, 8 (2018) 5361.
- [40] M. Kohli, C. Rago, C. Lengauer, K.W. Kinzler, B. Vogelstein, Facile methods for generating human somatic cell gene knockouts using recombinant adeno-associated viruses, *Nucleic acids Res*, 32 (2004) e3.
- [41] J.P. Cabaniols, C. Ouvry, V. Lamamy, I. Fery, M.L. Craplet, N. Moulharat, S.P. Guenin, S. Bedut, O. Nosjean, G. Ferry, S. Devavry, C. Jacquemarcq, C. Lebuhotel, L. Mathis, C. Delenda, J.A. Boutin, P. Duchateau, F. Coge, F. Paques, Meganuclease-driven targeted integration in CHO-K1 cells for the fast generation of HTS-compatible cell-based assays, *J Biomol Screen*, 15 (2010) 956-967.
- [42] Y. Santiago, E. Chan, P.Q. Liu, S. Orlando, L. Zhang, F.D. Urnov, M.C. Holmes, D. Guschin, A. Waite, J.C. Miller, E.J. Rebar, P.D. Gregory, A. Klug, T.N. Collingwood, Targeted gene knockout in mammalian cells by using engineered zinc-finger nucleases, *P Natl Acad Sci USA*, 105 (2008) 5809-5814.
- [43] R. Kunert, D. Reinhart, Advances in recombinant antibody manufacturing, *Appl Microbiol Biotechnol*, 100 (2016) 3451-3461.
- [44] W.G. Whitford, Fed-Batch Mammalian Cell Culture in Bioproduction, *BioProcess Int*, *BioProcess Technical* (2006) 30-40.
- [45] S. Grosvenor, The Role of Media Development in Process Optimization: An Historical Perspective, *BioPharm Int*, Supplement (2008).
- [46] F. Lu, P.C. Toh, I. Burnett, F. Li, T. Hudson, A. Amanullah, J. Li, Automated dynamic fed-batch process and media optimization for high productivity cell culture process development, *Biotechnol Bioeng*, 110 (2013) 191-205.
- [47] S. Kuwae, I. Miyakawa, T. Doi, Development of a chemically defined platform fed-batch culture media for monoclonal antibody-producing CHO cell lines with optimized choline content, *Cytotechnology*, 70 (2018) 939-948.
- [48] G. Hodge, Media Development for Mammalian Cell Culture, *BioPharm International*, 18 (2005).
- [49] H.F. Liu, J. Ma, C. Winter, R. Bayer, Recovery and purification process development for monoclonal antibody production, *mAbs*, 2 (2010) 480-499.
- [50] I.F. Pinto, M.R. Aires-Barros, A.M. Azevedo, Multimodal chromatography: debottlenecking the downstream processing of monoclonal antibodies, *Pharm Bioprocess*, 3 (2015) 263-279.
- [51] S. Hober, K. Nord, M. Linhult, Protein A chromatography for antibody purification, *J Chromatogr B*, 848 (2007) 40-47.
- [52] A.A. Shukla, J. Thömmes, Recent advances in large-scale production of monoclonal antibodies and related proteins, *Trends Biotechnol*, 28 (2010) 253-261.
- [53] A.M. Azevedo, P.A. Rosa, I.F. Ferreira, M.R. Aires-Barros, Chromatography-free recovery of biopharmaceuticals through aqueous two-phase processing, *Trends Biotechnol*, 27 (2009) 240-247.
- [54] M.D. Costioli, C. Guillemot-Potelle, C. Mitchell-Logean, H. Broly, Cost of Goods Modeling and Quality by Design for Developing Cost-Effective Processes, *BioPharm Int*, 23 (2010).
- [55] M.A. Hashim, K.H. Chu, Modeling the performance of protein-A affinity columns using asymptotic solutions, *Sepr Purif Technol*, 68 (2009) 279-282.
- [56] A.A. Shukla, B. Hubbard, T. Tressel, S. Guhan, D. Low, Downstream processing of monoclonal antibodies -Application of platform approaches, *J Chromatogr B*, 848 (2007) 28-39.
- [57] P. Gagnon, Technology trends in antibody purification, *J Chromatogr A*, 1221 (2012) 57-70.
- [58] B.S. Sekhon, V. Saluja, *Biosimilars: an overview*, Dove Medical Press Ltd., (2011) 1-11.
- [59] C. Boi, Membrane adsorbers as purification tools for monoclonal antibody purification, *J Chromatogr B*, 848 (2007) 19-27.
- [60] J. Thömmes, M. Etzel, Alternatives to Chromatographic Separations, *Biotechnol Progr*, 23 (2007) 42-45.
- [61] V.L. Dhadge, A. Hussain, A.M. Azevedo, R. Aires-Barros, A.C.A. Roque, Boronic acid-modified magnetic materials for antibody purification, *J Roy Soc Interface*, 11 (2014).
- [62] R.D. Sheth, M. Jin, B.V. Bhut, Z. Li, W. Chen, S.M. Cramer, Affinity precipitation of a monoclonal antibody from an industrial harvest feedstock using an ELP-Z stimuli responsive biopolymer, *Biotechnol Bioeng*, 111 (2014) 1595-1603.
- [63] R. dos Santos, A.L. Carvalho, A.C.A. Roque, Renaissance of protein crystallization and precipitation in biopharmaceuticals purification, *Biotechnol Adv*, 35 (2017) 41-50.

- [64] Y. Liu, Y. Lu, Z. Liu, Restricted access boronate affinity porous monolith as a protein A mimetic for the specific capture of immunoglobulin G, *Chem Sci*, 3 (2012) 1467-1471.
- [65] A.C.A. Roque, C.R. Lowe, M.Á. Taipa, Antibodies and Genetically Engineered Related Molecules: Production and Purification, *Biotechnol Progr*, 20 (2004) 639-654.
- [66] R.D. Van Reis, Charged filtration membranes and uses therefor, in: Google Patents, 2006.
- [67] R. van Reis, J.M. Brake, J. Charkoudian, D.B. Burns, A.L. Zydney, High-performance tangential flow filtration using charged membranes, *J Membrane Sci*, 159 (1999) 133-142.
- [68] A. Mehta, M.L. Tse, J. Fogle, A. Len, R. Shrestha, N. Fontes, B. Lebreton, B. Wolk, R.v. Reis, Purifying therapeutic monoclonal antibodies, *Chem Eng Prog*, 104 (2008) S14.
- [69] R. van Reis, A. Zydney, Bioprocess membrane technology, *J Membrane Sci*, 297 (2007) 16-50.
- [70] J.X. Zhou, T. Tressel, Basic Concepts in Q Membrane Chromatography for Large-Scale Antibody Production, *Biotechnol Progr*, 22 (2006) 341-349.
- [71] C. Harinarayan, J. Mueller, A. Ljunglöf, R. Fahrner, J. Van Alstine, R. van Reis, An exclusion mechanism in ion exchange chromatography, *Biotechnol Bioeng*, 95 (2006) 775-787.
- [72] J.G. Aunins, D.I.C. Wang, Induced flocculation of animal cells in suspension culture, *Biotechnol Bioeng*, 34 (1989) 629-638.
- [73] D.E. Salt, S. Hay, O.R.T. Thomas, M. Hoare, P. Dunnill, Selective flocculation of cellular contaminants from soluble proteins using polyethyleneimine: A study of several organisms and polymer molecular weights, *Enzyme Microb Tech*, 17 (1995) 107-113.
- [74] N. Singh, A. Arunkumar, S. Chollangi, Z.G. Tan, M. Borys, Z.J. Li, Clarification technologies for monoclonal antibody manufacturing processes: Current state and future perspectives, *Biotechnol Bioeng*, 113 (2016) 698-716.
- [75] J. Ma, H. Hoang, T. Myint, T. Peram, R. Fahrner, J.H. Chou, Using precipitation by polyamines as an alternative to chromatographic separation in antibody purification processes, *J Chromatogr B*, 878 (2010) 798-806.
- [76] S. Tomic, L. Besnard, B. Fürst, R. Reithmeier, R. Wichmann, P. Schelling, C. Hakemeyer, Complete clarification solution for processing high density cell culture harvests, *Sep Purif Technol*, 141 (2015) 269-275.
- [77] T. McNerney, A. Thomas, A. Senczuk, K. Petty, X. Zhao, R. Piper, J. Carvalho, M. Hammond, S. Sawant, J. Bussiere, PDADMAC flocculation of Chinese hamster ovary cells: Enabling a centrifuge-less harvest process for monoclonal antibodies, *mAbs*, 7 (2015) 413-427.
- [78] F. Capito, J. Bauer, A. Rapp, C. Schröter, H. Kolmar, B. Stanislawski, Feasibility study of semi-selective protein precipitation with salt-tolerant copolymers for industrial purification of therapeutic antibodies, *Biotechnol Bioeng*, 110 (2013) 2915-2927.
- [79] F. Capito, R. Skudas, B. Stanislawski, H. Kolmar, Polyelectrolyte–protein interaction at low ionic strength: required chain flexibility depending on protein average charge, *Colloid Polym Sci*, 291 (2013) 1759-1769.
- [80] Y. Kang, J. Hamzik, M. Felo, B. Qi, J. Lee, S. Ng, G. Liebisch, B. Shanehsaz, N. Singh, K. Persaud, D.L. Ludwig, P. Balderes, Development of a novel and efficient cell culture flocculation process using a stimulus responsive polymer to streamline antibody purification processes, *Biotechnol Bioeng*, 110 (2013) 2928-2937.
- [81] T.M. McNerney, K. Petty, A.C. Thomas, X. Zhao, Flocculation method, in Google Patents, 2016.
- [82] F. Riske, J. Schroeder, J. Belliveau, X. Kang, J. Kutzko, M.K. Menon, The use of chitosan as a flocculant in mammalian cell culture dramatically improves clarification throughput without adversely impacting monoclonal antibody recovery, *J Biotechnol*, 128 (2007) 813-823.
- [83] N. Hammerschmidt, B. Hintersteiner, N. Lingg, A. Jungbauer, Continuous precipitation of IgG from CHO cell culture supernatant in a tubular reactor, *BiotechnolJ*, 10 (2015) 1196-1205.
- [84] S.K. Basu, C.P. Govardhan, C.W. Jung, A.L. Margolin, Protein crystals for the delivery of biopharmaceuticals, *Expert Opin Biol Th*, 4 (2004) 301-317.
- [85] D. Low, R. O'Leary, N.S. Pujar, Future of antibody purification, *J Chromatogr B*, 848 (2007) 48-63.
- [86] Y. Zang, B. Kammerer, M. Eisenkolb, K. Lohr, H. Kiefer, Towards Protein Crystallization as a Process Step in Downstream Processing of Therapeutic Antibodies: Screening and Optimization at Microbatch Scale, *PLOS ONE*, 6 (2011) e25282.
- [87] B. Smejkal, N.J. Agrawal, B. Helk, H. Schulz, M. Giffard, M. Mechelke, F. Ortner, P. Heckmeier, B.L. Trout, D. Hekmat, Fast and scalable purification of a therapeutic full-length antibody based on process crystallization, *Biotechnol Bioeng*, 110 (2013) 2452-2461.
- [88] R.N. D'Souza, A.M. Azevedo, M.R. Aires Barros, N.L. Krajnc, P. Kramberger, M.L. Carbajal, M. Grasselli, R. Meyer, M. Fernandez Lahore, Emerging technologies for the integration and intensification of downstream bioprocesses, *Pharm Bioprocess*, 1 (2013) 423-440.
- [89] P. Albertsson, *Partition of Cell Particles and Macromolecules*, (3rd edition), Wiley, New York, 1986.

- [90] P.A.J. Rosa, A.M. Azevedo, M.R. Aires-Barros, Application of central composite design to the optimisation of aqueous two-phase extraction of human antibodies, *J Chromatogr A*, 1141 (2007) 50-60.
- [91] A.M. Azevedo, P.A.J. Rosa, I.F. Ferreira, M.R. Aires-Barros, Optimisation of aqueous two-phase extraction of human antibodies, *J Biotechnol*, 132 (2007) 209-217.
- [92] A.M. Azevedo, A.G. Gomes, P.A.J. Rosa, I.F. Ferreira, A.M.M.O. Pisco, M.R. Aires-Barros, Partitioning of human antibodies in polyethylene glycol–sodium citrate aqueous two-phase systems, *Sep Purif Technol*, 65 (2009) 14-21.
- [93] A.M. Azevedo, P.A.J. Rosa, I.F. Ferreira, M.R. Aires-Barros, Integrated process for the purification of antibodies combining aqueous two-phase extraction, hydrophobic interaction chromatography and size-exclusion chromatography, *J Chromatogr A*, 1213 (2008) 154-161.
- [94] M.F.F. Silva, A. Fernandes-Platzgummer, M.R. Aires-Barros, A.M. Azevedo, Integrated purification of monoclonal antibodies directly from cell culture medium with aqueous two-phase systems, *Sep Purif Technol*, 132 (2014) 330-335.
- [95] A. Jungbauer, Continuous downstream processing of biopharmaceuticals, *Trends Biotechnol*, 31 (2013) 479-492.
- [96] P.A. Rosa, A.M. Azevedo, S. Sommerfeld, M. Mutter, W. Backer, M.R. Aires-Barros, Continuous purification of antibodies from cell culture supernatant with aqueous two-phase systems: from concept to process, *Biotechnol J*, 8 (2013) 352-362.
- [97] P.A. Rosa, A.M. Azevedo, S. Sommerfeld, W. Backer, M.R. Aires-Barros, Aqueous two-phase extraction as a platform in the biomanufacturing industry: economical and environmental sustainability, *Biotechnol Adv*, 29 (2011) 559-567.
- [98] B.A. Andrews, D.M. Head, P. Dunthorne, J.A. Asenjo, PEG activation and ligand binding for the affinity partitioning of proteins in aqueous two-phase systems, *Biotechnol Tech*, 4 (1990) 49-54.
- [99] G. Birkenmeier, M.A. Vijayalakshmi, T. Stigbrand, G. Kopperschläger, Immobilized metal ion affinity partitioning, a method combining metal–protein interaction and partitioning of proteins in aqueous two-phase systems, *J Chromatogr A*, 539 (1991) 267-277.
- [100] G.M. Zijlstra, M.J.F. Michielsen, C.D. de Gooijer, L.A. van der Pol, J. Tramper, IgG and hybridoma partitioning in aqueous two-phase systems containing a dye-ligand, *Bioseparation*, 7 (1998) 117-126.
- [101] P.A.J. Rosa, A.M. Azevedo, I.F. Ferreira, S. Sommerfeld, W. Bäcker, M.R. Aires-Barros, Downstream processing of antibodies: Single-stage versus multi-stage aqueous two-phase extraction, *J Chromatogr A*, 1216 (2009) 8741-8749.
- [102] A.M. Azevedo, P.A.J. Rosa, I.F. Ferreira, A.M.M.O. Pisco, J. de Vries, R. Korporaal, T.J. Visser, M.R. Aires-Barros, Affinity-enhanced purification of human antibodies by aqueous two-phase extraction, *Sep Purif Technol*, 65 (2009) 31-39.
- [103] I.F. Ferreira, A.M. Azevedo, P.A.J. Rosa, M.R. Aires-Barros, Purification of human immunoglobulin G by thermoseparating aqueous two-phase systems, *J Chromatogr A*, 1195 (2008) 94-100.
- [104] P.A.J. Rosa, A.M. Azevedo, I.F. Ferreira, J. de Vries, R. Korporaal, H.J. Verhoef, T.J. Visser, M.R. Aires-Barros, Affinity partitioning of human antibodies in aqueous two-phase systems, *J Chromatogr A*, 1162 (2007) 103-113.
- [105] I. Campos-Pinto, E.V. Capela, A.R. Silva-Santos, M.A. Rodríguez, P.R. Gavara, M. Fernandez-Lahore, M.R. Aires-Barros, A.M. Azevedo, LYTAG-driven purification strategies for monoclonal antibodies using quaternary amine ligands as affinity matrices, *J Chem Technol Biotechnol*, 93 (2018) 1966–1974.
- [106] I. Campos-Pinto, E. Espitia-Saloma, S.A.S.L. Rosa, M. Rito-Palomares, O. Aguilar, M. Arévalo-Rodríguez, M.R. Aires-Barros, A.M. Azevedo, Integration of cell harvest with affinity-enhanced purification of monoclonal antibodies using aqueous two-phase systems with a dual tag ligand, *Sep Purif Technol*, 173 (2017) 129-134.
- [107] G.M. Zijlstra, M.J. Michielsen, C.D. de Gooijer, L.A. van der Pol, J. Tramper, Separation of hybridoma cells from their IgG product using aqueous two-phase systems, *Bioseparation*, 6 (1996) 201-210.
- [108] G.M. Zijlstra, M.J.F. Michielsen, C.D. de Gooijer, L.A. van der Pol, J. Tramper, Hybridoma and CHO Cell Partitioning in Aqueous Two-Phase Systems, *Biotechnology Progr*, 12 (1996) 363-370.
- [109] G.M. Zijlstra, C.D. de Gooijer, J. Tramper, Extractive bioconversions in aqueous two-phase systems, *Curr Opin Biotechnol*, 9 (1998) 171-176.
- [110] A.F. Sousa, P.Z. Andrade, R.M. Pirzgalska, T.M. Galhoz, A.M. Azevedo, C.L. da Silva, M. Raquel Aires-Barros, J.M.S. Cabral, A novel method for human hematopoietic stem/progenitor cell isolation from umbilical cord blood based on immunoaffinity aqueous two-phase partitioning, *Biotechnol Lett*, 33 (2011) 2373-2377.
- [111] K. Schügerl, J. Hubbuch, Integrated bioprocesses, *Curr Opin Microbiol*, 8 (2005) 294-300.

- [112] P.B. Kakarla, R.N. Dsouza, U. Toots, M. Fernández-Lahore, Interactions of Chinese Hamster Ovary (CHO) cell cultures with second generation expanded bed adsorbents, *Sep Purif Technol*, 144 (2015) 23-30.
- [113] A. Shukla, J. Kandula, Harvest and Recovery of Monoclonal Antibodies: Cell Removal and Clarification, in: U. Gottschalk (Ed.) *Process Scale Purification of Antibodies*, J. Wiley and Sons, 2009.
- [114] A. Arpanaei, A. Heeboll-Nielsen, J.J. Hubbuch, O.R. Thomas, T.J. Hobley, Critical evaluation and comparison of fluid distribution systems for industrial scale expanded bed adsorption chromatography columns, *J Chromatogr A*, 1198-1199 (2008) 131-139.
- [115] H.-F. Xia, D.-Q. Lin, S.-J. Yao, Chromatographic performance of macroporous cellulose–tungsten carbide composite beads as anion-exchanger for expanded bed adsorption at high fluid velocity, *J Chromatogr A*, 1195 (2008) 60-66.
- [116] P. Hu, M. Liu, J. Zhao, H. Zhang, Y. Wang, M. Zhang, Integrated Expanded-Bed Ion Exchange Chromatography as a Tool for Direct Recovery of Shikimic Acid from *Illicium verum*, *Solvent Extr Ion Exc*, 32 (2014) 316-332.
- [117] X. Xu, J. Hirpara, K. Epting, M. Jin, S. Ghose, S. Rieble, Z.J. Li, Clarification and capture of high-concentration refold pools for *E. coli*-based therapeutics using expanded bed adsorption chromatography, *Biotechnol Progr*, 30 (2014) 113-123.
- [118] C. Cabanne, A.M. Noubhani, A. Hocquellet, F. Dole, W. Dieryck, X. Santarelli, Purification and on-column refolding of EGFP overexpressed as inclusion bodies in *Escherichia coli* with expanded bed anion exchange chromatography, *J Chromatogr B*, 818 (2005) 23-27.
- [119] Y. Gonzalez, N. Ibarra, H. Gomez, M. Gonzalez, L. Dorta, S. Padilla, R. Valdes, Expanded bed adsorption processing of mammalian cell culture fluid: comparison with packed bed affinity chromatography, *J Chromatogr B*, 784 (2003) 183-187.
- [120] A. Lihme, M.B. Hansen, I.V. Andersen, T. Burnouf, A novel core fractionation process of human plasma by expanded bed adsorption chromatography, *Anal Biochem*, 399 (2010) 102-109.
- [121] J.J. Hubbuch, O.R. Thomas, High-gradient magnetic affinity separation of trypsin from porcine pancreatin, *Biotechnol Bioeng*, 79 (2002) 301-313.
- [122] J.J. Hubbuch, D.B. Matthiesen, T.J. Hobley, O.R. Thomas, High gradient magnetic separation versus expanded bed adsorption: a first principle comparison, *Bioseparation*, 10 (2001) 99-112.
- [123] K. Holschuh, A. Schwämmle, Preparative purification of antibodies with protein A—an alternative to conventional chromatography, *J Magn Magn Mater*, 293 (2005) 345-348.
- [124] Y. Cao, W. Tian, S. Gao, Y. Yu, W. Yang, G. Bai, Immobilization Staphylococcal Protein A on Magnetic Cellulose Microspheres for IgG Affinity Purification, *Artif Cells Blood Substit Biotechnol*, 35 (2007) 467-480.
- [125] C.C. Dawes, P.J. Jewess, D.A. Murray, Thiophilic paramagnetic particles as a batch separation medium for the purification of antibodies from various source materials, *Anal Biochem*, 338 (2005) 186-191.
- [126] D. Turkmen, A. Denizli, N. Ozturk, S. Akgol, A. Elkak, Phenylalanine containing hydrophobic nanospheres for antibody purification, *Biotechnol Progr*, 24 (2008) 1297-1303.
- [127] N. Ozturk, N. Bereli, S. Akgol, A. Denizli, High capacity binding of antibodies by poly(hydroxyethyl methacrylate) nanoparticles, *Colloid Surface B*, 67 (2008) 14-19.
- [128] L. Borlido, A.M. Azevedo, A.G. Sousa, P.H. Oliveira, A.C. Roque, M.R. Aires-Barros, Fishing human monoclonal antibodies from a CHO cell supernatant with boronic acid magnetic particles, *J Chromatogr B*, 903 (2012) 163-170.
- [129] J.P.S. Aniceto, C.M. Silva, Simulated Moving Bed Strategies and Designs: From Established Systems to the Latest Developments, *Sep Purif Rev*, 44 (2015) 41-73.
- [130] A. Rajendran, G. Paredes, M. Mazzotti, Simulated moving bed chromatography for the separation of enantiomers, *J Chromatogr A*, 1216 (2009) 709-738.
- [131] K. Vaňková, Z. Onderková, M. Antořová, M. Polakovič, Design and economics of industrial production of fructooligosaccharides, *Chem Pap*, 62 (2008).
- [132] H.J. Van Walsem, M.C. Thompson, Simulated moving bed in the production of lysine, *J Biotechnol*, 59 (1997) 127-132.
- [133] M. Bisschops, L. Frick, S. Fulton, T. Ransohoff, Single-Use, Continuous-Countercurrent, Multicolumn Chromatography, *Bioprocess Int*, 7 (2009) 18.
- [134] T. Müller-Späth, L. Aumann, L. Melter, G. Ströhlein, M. Morbidelli, Chromatographic separation of three monoclonal antibody variants using multicolumn countercurrent solvent gradient purification (MCSGP), *Biotechnol Bioeng*, 100 (2008) 1166-1177.
- [135] T. Müller-Späth, M. Krättli, L. Aumann, G. Ströhlein, M. Morbidelli, Increasing the activity of monoclonal antibody therapeutics by continuous chromatography (MCSGP), *Biotechnol Bioeng*, 107 (2010) 652-662.

- [136] T. Müller-Späth, L. Aumann, G. Ströhlein, H. Kornmann, P. Valax, L. Delegrange, E. Charbaut, G. Baer, A. Lamproye, M. Jöhnck, M. Schulte, M. Morbidelli, Two step capture and purification of IgG2 using multicolumn countercurrent solvent gradient purification (MCSGP), *Biotechnol Bioeng*, 107 (2010) 974-984.
- [137] S. Zobel, C. Helling, R. Ditz, J. Strube, Design and Operation of Continuous Countercurrent Chromatography in Biotechnological Production, *Ind Eng Chem Res*, 53 (2014) 9169-9185.
- [138] O. Shinkazh, D. Kanani, M. Barth, M. Long, D. Hussain, A.L. Zydney, Countercurrent tangential chromatography for large-scale protein purification, *Biotech Bioeng*, 108 (2011) 582-591.
- [139] A.L. Zydney, Continuous downstream processing for high value biological products: A Review, *Biotech Bioeng*, 113 (2016) 465-475.
- [140] F. Hilbrig, R. Freitag, Continuous annular chromatography, *J Chromatogr B*, 790 (2003) 1-15.
- [141] A. Buchacher, G. Iberer, A. Jungbauer, H. Schwinn, D. Josic, Continuous Removal of Protein Aggregates by Annular Chromatography, *Biotechnol Progr*, 17 (2001) 140-149.
- [142] J.H. Vogel, H. Nguyen, M. Pritschet, R. Van Wegen, K. Konstantinov, Continuous annular chromatography: General characterization and application for the isolation of recombinant protein drugs, *Biotech Bioeng*, 80 (2002) 559-568.
- [143] M.C. Lay, C.J. Fee, J.E. Swan, Continuous Radial Flow Chromatography of Proteins, *Food Bioprod Process*, 84 (2006) 78-83.
- [144] C. Cabanne, M. Raedts, E. Zavadzky, X. Santarelli, Evaluation of radial chromatography versus axial chromatography, practical approach, *J Chromatogr B*, 845 (2007) 191-199.
- [145] A. Demirci, F. Leu, F.J. Bailey, Comparison of Radial and Axial Flow Chromatography for Monoclonal Antibody Downstream Processing at Bench and Pilot Scales, *Am J Biochem Biotechnol*, 8 (2012) 255-262.
- [146] A. Kinna, B. Tolner, E.M. Rota, N. Titchener-Hooker, D. Nesbeth, K. Chester, IMAC capture of recombinant protein from unclarified mammalian cell feed streams, *Biotech Bioeng*, 113 (2016) 130-140.
- [147] M.C. García, M.L. Marina, M. Torre, Perfusion chromatography: an emergent technique for the analysis of food proteins, *J Chromatogr A*, 880 (2000) 169-187.
- [148] H.L. Knudsen, R.L. Fahrner, Y. Xu, L.A. Norling, G.S. Blank, Membrane ion-exchange chromatography for process-scale antibody purification, *J Chromatogr A*, 907 (2001) 145-154.
- [149] R. Ghosh, Protein separation using membrane chromatography: opportunities and challenges, *J Chromatogr A*, 952 (2002) 13-27.
- [150] V. Orr, L. Zhong, M. Moo-Young, C.P. Chou, Recent advances in bioprocessing application of membrane chromatography, *Biotechnol Adv*, 31 (2013) 450-465.
- [151] A. Nascimento, S.A.S.L. Rosa, M. Mateus, A.M. Azevedo, Polishing of monoclonal antibodies streams through convective flow devices, *Sep Purif Technol*, 132 (2014) 593-600.
- [152] J.X. Zhou, T. Tressel, U. Gottschalk, F. Solamo, A. Pastor, S. Dermawan, T. Hong, O. Reif, J. Mora, F. Hutchison, M. Murphy, New Q membrane scale-down model for process-scale antibody purification, *J Chromatogr A*, 1134 (2006) 66-73.
- [153] R. Hahn, M. Panzer, E. Hansen, J. Mollerup, A. Jungbauer, Mass transfer properties of monoliths, *Sep Sci Technol*, 37 (2002) 1545-1565.
- [154] G. Carta, A. Jungbauer, *Protein Chromatography: Process Development and Scale-up*, Wiley-VCH, Weinheim, 2010.
- [155] A. Jungbauer, R. Hahn, Monoliths for fast bioseparation and bioconversion and their applications in biotechnology, *J Sep Sci*, 27 (2004) 767-778.
- [156] T. Barroso, A. Hussain, A.C.A. Roque, A. Aguiar-Ricardo, Functional monolithic platforms: Chromatographic tools for antibody purification, *Biotechnol J*, 8 (2013) 671-681.
- [157] T. Barroso, A.C.A. Roque, A. Aguiar-Ricardo, Bioinspired and sustainable chitosan-based monoliths for antibody capture and release, *RSC Adv*, 2 (2012) 11285-11294.
- [158] K.K.R. Tetala, T.A. van Beek, Bioaffinity chromatography on monolithic supports, *J Sep Sci*, 33 (2010) 422-438.
- [159] H. Alkan, N. Bereli, Z. Baysal, A. Denizli, Antibody purification with protein A attached supermacroporous poly(hydroxyethyl methacrylate) cryogel, *Biochem Eng J*, 45 (2009) 201-208.
- [160] N. Bereli, L. Uzun, H. Yavuz, A. Elkak, A. Denizli, Antibody purification using porous metal-chelated monolithic columns, *J Appl Polym Sci*, 101 (2006) 395-404.
- [161] Z. Ma, S. Ramakrishna, Electrospun regenerated cellulose nanofiber affinity membrane functionalized with protein A/G for IgG purification, *J Membrane Sci*, 319 (2008) 23-28.
- [162] L. Zhang, T.J. Menkhaus, H. Fong, Fabrication and bioseparation studies of adsorptive membranes/felts made from electrospun cellulose acetate nanofibers, *J Membrane Sci*, 319 (2008) 176-184.

- [163] Y. Bondar, H.J. Kim, S.H. Yoon, Y.J. Lim, Synthesis of cation-exchange adsorbent for anchoring metal ions by modification of poly(glycidyl methacrylate) chains grafted onto polypropylene fabric, *React Funct Polym*, 58 (2004) 43-51.
- [164] S. Kaur, Z. Ma, R. Gopal, G. Singh, S. Ramakrishna, T. Matsuura, Plasma-induced graft copolymerization of poly(methacrylic acid) on electrospun poly(vinylidene fluoride) nanofiber membrane, *Langmuir*, 23 (2007) 13085-13092.
- [165] M. Fernandez-Lahore, M. Grasselli, Composite material, in Google Patents, 2010.
- [166] P.R. Gavara, R. Cabrera, R.R. Vennapusa, M. Grasselli, M. Fernandez-Lahore, Preparation, characterization, and process performance of composite fibrous adsorbents as cation exchangers for high throughput and high capacity bioseparations, *J Chromatogr B*, 903 (2012) 14-22.
- [167] P.R. Gavara, *Fibrous Adsorbents as Novel Chromatography Matrices for Enhancing Industrial Downstream Processing of Bioproducts in: School of Engineering and Sciences Jacobs University* -, Bremen, Germany, 2012.
- [168] P.R. Gavara, N.S. Bibi, M.L. Sanchez, M. Grasselli, M. Fernandez-Lahore, Chromatographic Characterization and Process Performance of Column-Packed Anion Exchange Fibrous Adsorbents for High Throughput and High Capacity Bioseparations, *Processes* 3(2015) 204-221.
- [169] T. Arakawa, D. Ejima, T. Li, J.S. Philo, The critical role of mobile phase composition in size exclusion chromatography of protein pharmaceuticals, *J Pharm Sci*, 99 (2010) 1674-1692.
- [170] M. Kuczewski, N. Fraud, R. Faber, G. Zarbis-Papastoitsis, Development of a polishing step using a hydrophobic interaction membrane adsorber with a PER.C6®-derived recombinant antibody, *Biotech Bioeng*, 105 (2010) 296-305.
- [171] J. Wang, J. Zhou, Y.K. Gowtham, S.W. Harcum, S.M. Husson, Antibody purification from CHO cell supernatant using new multimodal membranes, *Biotechnol Progr*, 33 (2017) 658-665.
- [172] M. Kuczewski, E. Schirmer, B. Lain, G. Zarbis-Papastoitsis, A single-use purification process for the production of a monoclonal antibody produced in a PER.C6 human cell line, *Biotechnol J*, 6 (2011) 56-65.
- [173] A.A. Shukla, C. Jiang, J. Ma, M. Rubacha, L. Flansburg, S.S. Lee, Demonstration of Robust Host Cell Protein Clearance in Biopharmaceutical Downstream Processes, *Biotechnol Progr*, 24 (2008) 615-622.
- [174] S. Ghose, Y. Tao, L. Conley, D. Cecchini, Purification of monoclonal antibodies by hydrophobic interaction chromatography under no-salt conditions, *mAbs*, 5 (2013) 795-800.
- [175] S. Curtis, K. Lee, G.S. Blank, K. Brorson, Y. Xu, Generic/matrix evaluation of SV40 clearance by anion exchange chromatography in flow-through mode, *Biotech Bioeng*, 84 (2003) 179-186.
- [176] L. Norling, S. Lute, R. Emery, W. Khuu, M. Voisard, Y. Xu, Q. Chen, G. Blank, K. Brorson, Impact of multiple re-use of anion-exchange chromatography media on virus removal, *J Chromatogr A*, 1069 (2005) 79-89.
- [177] M. Phillips, J. Cormier, J. Ferrence, C. Dowd, R. Kiss, H. Lutz, J. Carter, Performance of a membrane adsorber for trace impurity removal in biotechnology manufacturing, *J Chromatogr A*, 1078 (2005) 74-82.
- [178] J.X. Zhou, F. Solamo, T. Hong, M. Shearer, T. Tressel, Viral clearance using disposable systems in monoclonal antibody commercial downstream processing, *Biotech Bioeng*, 100 (2008) 488-496.
- [179] B. D. Kelley, S.A. Tobler, P. Brown, J.L. Coffman, R. Godavarti, T. Iskra, M. Switzer, S. Vunnum, Weak partitioning chromatography for anion exchange purification of monoclonal antibodies, *Biotech Bioeng*, 101 (2008) 553-566.
- [180] A. Brown, J. Bill, T. Tully, A. Radhamohan, C. Dowd, Overloading ion-exchange membranes as a purification step for monoclonal antibodies, *Biotechnol Appl Biochem*, 56 (2010) 59-70.
- [181] M. Brgles, J. Clifton, R. Walsh, F. Huang, M. Rucevic, L. Cao, D. Hixson, E. Müller, D. Josic, Selectivity of monolithic supports under overloading conditions and their use for separation of human plasma and isolation of low abundance proteins, *J Chromatogr A*, 1218 (2011) 2389-2395.
- [182] A. Arunakumari, J. Wang, in: U. Gottschalk (Ed.) *Process Scale Purification of Antibodies*, Wiley and Sons, Hoboken, 2009, pp. 103.
- [183] P. Gagnon, in: A. Shukla, M. Etzel, S. Gadam (Eds.) *Process Scale Separation for the Biopharmaceutical Industry*, CRC Press, Boca Raton, 2007, pp. 491.
- [184] T. Ishihara, T. Kadoya, S. Yamamoto, Application of a chromatography model with linear gradient elution experimental data to the rapid scale-up in ion-exchange process chromatography of proteins, *J Chromatogr A*, 1162 (2007) 34-40.
- [185] P.K. Ng, J. He, M.A. Snyder, Separation of protein mixtures using pH-gradient cation-exchange chromatography, *J Chromatogr A*, 1216 (2009) 1372-1376.
- [186] N. Lendero, J. Vidic, P. Brne, V. Frankovic, A. Strancar, A. Podgornik, Characterization of ion exchange stationary phases via pH transition profiles, *J Chromatogr A*, 1185 (2008) 59-70.

- [187] T.M. Pabst, G. Carta, pH transitions in cation exchange chromatographic columns containing weak acid groups, *J Chromatogr A*, 1142 (2007) 19-31.
- [188] J.E. Hale, D.E. Beidler, Purification of Humanized Murine and Murine Monoclonal Antibodies Using Immobilized Metal-Affinity Chromatography, *Anal Biochem*, 222 (1994) 29-33.
- [189] R.R. Prasanna, M.A. Vijayalakshmi, Characterization of metal chelate methacrylate monolithic disk for purification of polyclonal and monoclonal immunoglobulin G, *J Chromatogr A*, 1217 (2010) 3660-3667.
- [190] K. Kráčalíková, G. Tishchenko, M. Bleha, Effect of the matrix structure and concentration of polymer-immobilized Ni²⁺-iminodiacetic acid complexes on retention of IgG1, *J Biochem Biophys Meth*, 67 (2006) 7-25.
- [191] P. Přikryl, D. Horák, M. Tichá, Z. Kučerová, Magnetic IDA-modified hydrophilic methacrylate-based polymer microspheres for IMAC protein separation, *J Sep Sci*, 29 (2006) 2541-2549.
- [192] G. Tishchenko, J. Dybal, K. Mészárosová, Z. Sedláková, M. Bleha, Purification of the specific immunoglobulin G1 by immobilized metal ion affinity chromatography using nickel complexes of chelating porous and nonporous polymeric sorbents based on poly(methacrylic esters): Effect of polymer structure, *J Chromatogr A*, 954 (2002) 115-126.
- [193] M.B. Ribeiro, M. Vijayalakshmi, D. Todorova-Balvay, S.M.A. Bueno, Effect of IDA and TREN chelating agents and buffer systems on the purification of human IgG with immobilized nickel affinity membranes, *J Chromatogr B*, 861 (2008) 64-73.
- [194] M. Karataş, S. Akgöl, H. Yavuz, R. Say, A. Denizli, Immunoglobulin G depletion from human serum with metal-chelated beads under magnetic field, *Int J Biol Macromol*, 40 (2007) 254-260.
- [195] L. Tan, W.-B. Lai, C.T. Lee, D.S. Kim, W.-S. Choe, Differential interactions of plasmid DNA, RNA and endotoxin with immobilised and free metal ions, *J Chromatogr A*, 1141 (2007) 226-234.
- [196] L. Opitz, J. Hohlweg, U. Reichl, M.W. Wolff, Purification of cell culture-derived influenza virus A/Puerto Rico/8/34 by membrane-based immobilized metal affinity chromatography, *J Virol Methods*, 161 (2009) 312-316.
- [197] T. Zimmerman, C. Petit Frère, M. Satzger, M. Raba, M. Weisbach, K. Döhn, A. Popp, M. Donzeau, Simultaneous metal chelate affinity purification and endotoxin clearance of recombinant antibody fragments, *J Immunol Methods*, 314 (2006) 67-73.
- [198] P. Gagnon, Purification of monoclonal antibodies by mixed-mode chromatography, in: U. Gottschalk (Ed.) *Process Scale Purification of Antibodies*, John Wiley and Sons, Inc., 2009.
- [199] A. Tiselius, S. Hjertén, Ö. Levin, Protein chromatography on calcium phosphate columns, *Arch Biochem Biophys*, 65 (1956) 132-155.
- [200] F. Hilbrig, R. Freitag, Isolation and purification of recombinant proteins, antibodies and plasmid DNA with hydroxyapatite chromatography, *Biotechnol J*, 7 (2012) 90-102.
- [201] P. Gagnon, Improved antibody aggregate removal by hydroxyapatite chromatography in the presence of polyethylene glycol, *J Immunol Methods*, 336 (2008) 222-228.
- [202] L. Guerrier, I. Flayeux, E. Boschetti, A dual-mode approach to the selective separation of antibodies and their fragments, *J Chromatogr B*, 755 (2001) 37-46.
- [203] P. Gagnon, Monoclonal antibody purification with hydroxyapatite, *New Biotechnol*, 25 (2009) 287-293.
- [204] P. Gagnon, C.-W. Cheung, P.J. Yazaki, Cooperative multimodal retention of IgG, fragments, and aggregates on hydroxyapatite, *J Sep Sci*, 32 (2009) 3857-3865.
- [205] Y. Murakami, K. Sugo, M. Hirano, T. Okuyama, Surface chemical analysis and chromatographic characterization of polyethylenimine-coated hydroxyapatite with various amount of polyethylenimine, *Talanta*, 85 (2011) 1298-1303.
- [206] N. Charef, L. Arrar, A. Lamaaoui, H. Boudjellal, A. Baghiani, N. Hanachi, S. Boumerfeg, S. Khennouf, M.S. Mubarak, Effect of adsorbed metal ions and buffer nature on IgG separation from human plasma by column chromatography using an ion exchange resin, Amberlite IRC-718, *J Appl Polym Sci*, 115 (2010) 324-329.
- [207] D. Gao, L.L. Wang, D.Q. Lin, S.J. Yao, Evaluating antibody monomer separation from associated aggregates using mixed-mode chromatography, *J Chromatogr A*, 1294 (2013) 70-75.
- [208] I.T.L. Bresolin, M. Borsoi-Ribeiro, J.R. Caro, F.P.d. Santos, M.P.d. Castro, S.M.A. Bueno, Adsorption of human serum proteins onto TREN-agarose: Purification of human IgG by negative chromatography, *J Chromatogr B*, 877 (2009) 17-23.
- [209] S.C. Burton, D.R.K. Harding, Hydrophobic charge induction chromatography: salt independent protein adsorption and facile elution with aqueous buffers, *J Chromatogr A*, 814 (1998) 71-81.
- [210] J. Chen, J. Tetrault, A. Ley, Comparison of standard and new generation hydrophobic interaction chromatography resins in the monoclonal antibody purification process, *J Chromatogr A*, 1177 (2008) 272-281.

- [211] E. Boschetti, Antibody separation by hydrophobic charge induction chromatography, *Trends Biotechnol*, 20 (2002) 333-337.
- [212] T. Arakawa, M. Futatsumori-Sugai, K. Tsumoto, Y. Kita, H. Sato, D. Ejima, MEP HyperCel chromatography II: binding, washing and elution, *Protein Express Purif*, 71 (2010) 168-173.
- [213] W. Schwart, D. Judd, M. Wysocki, L. Guerrier, E. Birck-Wilson, E. Boschetti, Comparison of hydrophobic charge induction chromatography with affinity chromatography on protein A for harvest and purification of antibodies, *J Chromatogr A*, 908 (2001) 251-263.
- [214] K. Swinnen, A. Krul, I. Van Goidsenhoven, N. Van Tichelt, A. Roosen, K. Van Houdt, Performance comparison of protein A affinity resins for the purification of monoclonal antibodies, *J Chromatogr B*, 848 (2007) 97-107.
- [215] S. Vunnum, G. Vedantham, B. Hubbard, Protein A-based Affinity Chromatography, in: U. Gottschalk (Ed.) *Process Scale Purification of Antibodies*, Wiley, 2009.
- [216] J. Deisenhofer, Crystallographic refinement and atomic models of a human Fc fragment and its complex with fragment B of protein A from *Staphylococcus aureus* at 2.9- and 2.8-Å resolution, *Biochemistry*, 20 (1981) 2361-2370.
- [217] T. Alm, Interaction-Engineered Three-Helix Bundle Domains for Protein Recovery and Detection, in: School of Biotechnology, Royal Institute of Technology, Stockholm: KTH, 2010, pp. 79.
- [218] A.M. Ramos-de-la-Pena, J. Gonzalez-Valdez, O. Aguilar, Protein A chromatography: Challenges and progress in the purification of monoclonal antibodies, *J Sep Sci*, (2019).
- [219] B. Nilsson, T. Moks, B. Jansson, L. Abrahmsen, A. Elmlad, E. Holmgren, C. Henrichson, T.A. Jones, M. Uhlen, A synthetic IgG-binding domain based on staphylococcal protein A, *Protein Eng*, 1 (1987) 107-113.
- [220] A.A. Kosky, U.O. Razzaq, M.J. Treuheit, D.N. Brems, The effects of alpha-helix on the stability of Asn residues: deamidation rates in peptides of varying helicity, *Protein Sci*, 8 (1999) 2519-2523.
- [221] M. Linhult, S. Gülich, T. Gråslund, A. Simon, M. Karlsson, A. Sjöberg, K. Nord, S. Hober, Improving the tolerance of a protein A analogue to repeated alkaline exposures using a bypass mutagenesis approach, *Proteins*, 55 (2004) 407-416.
- [222] H. Watanabe, H. Matsumaru, A. Ooishi, S. Honda, Structure-based histidine substitution for optimizing pH-sensitive *Staphylococcus* protein A, *J Chromatogr B*, 929 (2013) 155-160.
- [223] N. Kruljec, T. Bratkovic, Alternative Affinity Ligands for Immunoglobulins, 28 (2017) 2009-2030.
- [224] J. Gonzalez-Valdez, A. Yoshikawa, J. Weinberg, J. Benavides, M. Rito-Palomares, T.M. Przybycien, Toward improving selectivity in affinity chromatography with PEGylated affinity ligands: the performance of PEGylated protein A, *Biotechnol Progr*, 30 (2014) 1364-1379.
- [225] B.I. Editors, Comparing Protein A Resins for Monoclonal Antibody Purification: A prototype Protein A resin is evaluated for purification performance, reusability, and cost performance., *BioPharm Int*, 26 (2013).
- [226] H. Utsunomiya, M. Ichinose, K. Tsujimoto, Y. Katsuyama, H. Yamasaki, A.H. Koyama, D. Ejima, T. Arakawa, Co-operative thermal inactivation of herpes simplex virus and influenza virus by arginine and NaCl, *Int J Pharm*, 366 (2009) 99-102.
- [227] J. Bach, L. Connell-Crowley, Clearance of the rodent retrovirus, XMuLV, by protein A chromatography, *Biotechnol Bioeng*, 112 (2015) 743-750.
- [228] M. Holstein, K. Cotoni, N. Bian, Protein A Intermediate Wash Strategies, *BioProcess Int*, 13 (2015) 56-62.
- [229] D. Ejima, R. Yumioka, K. Tsumoto, T. Arakawa, Effective elution of antibodies by arginine and arginine derivatives in affinity column chromatography, *Anal Biochem*, 345 (2005) 250-257.
- [230] Y.D. Clonis, Affinity chromatography matures as bioinformatic and combinatorial tools develop, *J Chromatogr A*, 1101 (2006) 1-24.
- [231] R. Li, V. Dowd, D.J. Stewart, S.J. Burton, C.R. Lowe, Design, synthesis, and application of a protein A mimetic, *Nat Biotechnol*, 16 (1998) 190-195.
- [232] S.F. Teng, K. Sproule, A. Husain, C.R. Lowe, Affinity chromatography on immobilized "biomimetic" ligands. Synthesis, immobilization and chromatographic assessment of an immunoglobulin G-binding ligand, *J Chromatogr B*, 740 (2000) 1-15.
- [233] G. El Khoury, L.A. Rowe, C.R. Lowe, Biomimetic affinity ligands for immunoglobulins based on the multicomponent Ugi reaction, *Methods Mol Biol*, 800 (2012) 57-74.
- [234] J. Qian, G. El Khoury, H. Issa, K. Al-Qaoud, P. Shihab, C.R. Lowe, A synthetic Protein G adsorbent based on the multi-component Ugi reaction for the purification of mammalian immunoglobulins, *J Chromatogr B*, 898 (2012) 15-23.
- [235] C. Chen, G.E. Khoury, C.R. Lowe, Affinity ligands for glycoprotein purification based on the multi-component Ugi reaction, *J Chromatogr B*, 969 (2014) 171-180.

- [236] L. Rowe, G. El Khoury, C.R. Lowe, A benzoboroxole-based affinity ligand for glycoprotein purification at physiological pH, *J Mol Recognit*, 29 (2016) 232-238.
- [237] R. dos Santos, S.A.S.L. Rosa, M.R. Aires-Barros, A. Tover, A.M. Azevedo, Phenylboronic acid as a multi-modal ligand for the capture of monoclonal antibodies: development and optimization of a washing step, *J Chromatogr A*, 1355 (2014) 115-124.
- [238] R.J. Carvalho, J. Woo, M.R. Aires-Barros, S.M. Cramer, A.M. Azevedo, Phenylboronate chromatography selectively separates glycoproteins through the manipulation of electrostatic, charge transfer, and cis-diol interactions, *Biotechnol J*, 9 (2014) 1250-1258.
- [239] A.G. Gomes, A.M. Azevedo, M.R. Aires-Barros, D.M.F. Prazeres, Studies on the adsorption of cell impurities from plasmid-containing lysates to phenyl boronic acid chromatographic beads, *J Chromatogr A*, 1218 (2011) 8629-8637.
- [240] A.E. Ivanov, H.A. Panahi, M.V. Kuzimenkova, L. Nilsson, B. Bergenstahl, H.S. Waqif, M. Jahanshahi, I.Y. Galaev, B. Mattiasson, Affinity Adhesion of Carbohydrate Particles and Yeast Cells to Boronate-Containing Polymer Brushes Grafted onto Siliceous Supports, *Chem-Eur J*, 12 (2006) 7204-7214.
- [241] X.C.S. Liu, W.H., Boronate Affinity Chromatography, in: D.S. Hage (Ed.) *Handbook of Affinity Chromatography*, CRC Press, 2005, pp. 215-229.
- [242] L. Liu, Antibody Glycosylation and Its Impact on the Pharmacokinetics and Pharmacodynamics of Monoclonal Antibodies and Fc-Fusion Proteins, *J Pharm Sci*, 104 (2015) 1866-1884.
- [243] E. Ucakurk, Analysis of glycoforms on the glycosylation site and the glycans in monoclonal antibody biopharmaceuticals, *J Sep Sci*, 35 (2012) 341-350.
- [244] R. Jefferis, Glycosylation of recombinant antibody therapeutics, *Biotechnol Prog*, 21 (2005) 11-16.
- [245] B. Zhang, S. Mathewson, H. Chen, Two-dimensional liquid chromatographic methods to examine phenylboronate interactions with recombinant antibodies, *J Chromatogr A*, 1216 (2009) 5676-5686.
- [246] L.I. Bosch, T.M. Fyles, T.D. James, Binary and ternary phenylboronic acid complexes with saccharides and Lewis bases, *Tetrahedron*, 60 (2004) 11175-11190.
- [247] G. Springsteen, B. Wang, A detailed examination of boronic acid–diol complexation, *Tetrahedron*, 58 (2002) 5291-5300.
- [248] L. Ren, Z. Liu, M. Dong, M. Ye, H. Zou, Synthesis and characterization of a new boronate affinity monolithic capillary for specific capture of cis-diol-containing compounds, *J Chromatogr A*, 1216 (2009) 4768-4774.
- [249] X.-C. Liu, Boronic Acids as Ligands for Affinity Chromatography, *Chinese Journal of Chromatography*, 24 (2006) 73-80.
- [250] M.B. Smith, J. March, *March's Advanced Organic Chemistry: Reactions, Mechanisms, and Structure*, 6th Edition ed., John Wiley & Sons, Inc., 2007.
- [251] S.A.S.L. Rosa, R. dos Santos, M.R. Aires-Barros, A.M. Azevedo, Phenylboronic acid chromatography provides a rapid, reproducible and easy scalable multimodal process for the capture of monoclonal antibodies, *Sep Purif Technol*, 160 (2016) 43-50.
- [252] A.L. Grilo, M. Mateus, M.R. Aires-Barros, A.M. Azevedo, Monoclonal antibodies production platforms: an opportunity study of a non protein A chromatographic platform based on process economics, *Biotechnol J*, (2017).
- [253] P. Damborský, J. Švitel, J. Katrlík, Optical biosensors, *Essays Biochem*, 60 (2016) 91-100.
- [254] F. Cheng, M.Y. Li, H.Q. Wang, D.Q. Lin, J.P. Qu, Antibody-ligand interactions for hydrophobic charge-induction chromatography: a surface plasmon resonance study, *Langmuir*, 31 (2015) 3422-3430.
- [255] K.P.M. Geuijen, L.A. Halim, H. Schellekens, R.B. Schasfoort, R.H. Wijffels, M.H. Eppink, Label-Free Glycoprofiling with Multiplex Surface Plasmon Resonance: A Tool To Quantify Sialylation of Erythropoietin, *Anal Chem*, 87 (2015) 8115-8122.
- [256] W. Wang, B. Soriano, Q. Chen, Glycan profiling of proteins using lectin binding by Surface Plasmon Resonance, *Anal Biochem*, 538 (2017) 53-63.
- [257] K.P.M. Geuijen, C. Oppers-Tiemissen, D.F. Egging, P.J. Simons, L. Boon, R.B.M. Schasfoort, M.H.M. Eppink, Rapid screening of IgG quality attributes – effects on Fc receptor binding, *FEBS Open Bio*, 7 (2017) 1557-1574.
- [258] S.R. Gallant, A. Kundu, S.M. Cramer, Modeling non-linear elution of proteins in ion-exchange chromatography, *J Chromatogr A*, 702 (1995) 125-142.
- [259] J.C. Bellot, J.S. Condoret, Modelling of liquid chromatography equilibria, *Process Biochem*, 28 (1993) 365-376.
- [260] F.S. Marques, G.L. Silva, M.E. Thrash Jr, A.C. Dias-Cabral, Lysozyme adsorption onto a cation-exchanger: Mechanism of interaction study based on the analysis of retention chromatographic data, *Colloid Surface B*, 122 (2014) 801-807.

- [261] A. Katiyar, S.W. Thiel, V.V. Gulians, N.G. Pinto, Investigation of the mechanism of protein adsorption on ordered mesoporous silica using flow microcalorimetry, *J Chromatogr A*, 1217 (2010) 1583-1588.
- [262] T. Blaschke, A. Werner, H. Hasse, Microcalorimetric study of the adsorption of native and mono-PEGylated bovine serum albumin on anion-exchangers, *J Chromatogr A*, 1277 (2013) 58-68.
- [263] G.L. Silva, F.S. Marques, M.E. Thrash Jr, A.C. Dias-Cabral, Enthalpy contributions to adsorption of highly charged lysozyme onto a cation-exchanger under linear and overloaded conditions, *J Chromatogr A*, 1352 (2014) 46-54.
- [264] P.A. Aguilar, A. Twarda, F. Sousa, A.C. Dias-Cabral, Thermodynamic study of the interaction between linear plasmid deoxyribonucleic acid and an anion exchange support under linear and overloaded conditions, *J Chromatogr A*, 1372 (2014) 166-173.
- [265] F.-Y. Lin, W.-Y. Chen, M.T.W. Hearn, Thermodynamic analysis of the interaction between proteins and solid surfaces: application to liquid chromatography, *J Mol Recognit*, 15 (2002) 55-93.
- [266] I. Mihelic, A. Podgornik, T. Koloini, Temperature influence on the dynamic binding capacity of a monolithic ion-exchange column, *J Chromatogr A*, 987 (2003) 159-168.
- [267] D. Haidacher, A. Vailaya, C. Horváth, Temperature effects in hydrophobic interaction chromatography, *PNAS*, 93 (1996) 2290-2295.
- [268] M.A. Esquibel-King, A.C. Dias-Cabral, J.A. Queiroz, N.G. Pinto, Study of hydrophobic interaction adsorption of bovine serum albumin under overloaded conditions using flow microcalorimetry, *J Chromatogr A*, 865 (1999) 111-122.
- [269] A.C. Dias-Cabral, J.A. Queiroz, N.G. Pinto, Effect of salts and temperature on the adsorption of bovine serum albumin on polypropylene glycol-Sepharose under linear and overloaded chromatographic conditions, *J Chromatogr A*, 1018 (2003) 137-153.
- [270] A.C. Dias-Cabral, A.S. Ferreira, J. Phillips, J.A. Queiroz, N.G. Pinto, The effects of ligand chain length, salt concentration and temperature on the adsorption of bovine serum albumin onto polypropyleneglycol-Sepharose, *Biomed Chromatogr*, 19 (2005) 606-616.
- [271] D.S. Gill, D.J. Roush, K.A. Shick, R.C. Willson, Microcalorimetric characterization of the anion-exchange adsorption of recombinant cytochrome b5 and its surface-charge mutants, *J Chromatogr A*, 715 (1995) 81-93.
- [272] A.C. Dias-Cabral, N.G. Pinto, J.A. Queiroz, Studies on hydrophobic interaction adsorption of bovine serum albumin on polypropylene glycol-sepharose under overloaded conditions, *Sep Sci Technol*, 37 (2002) 1505-1520.
- [273] K. Chiad, S.H. Stelzig, R. Gropeanu, T. Weil, M. Klapper, K. Müllen, Isothermal Titration Calorimetry: A Powerful Technique To Quantify Interactions in Polymer Hybrid Systems, *Macromolecules*, 42 (2009) 7545-7552.
- [274] G.R. Behbehani, A.A. Saboury, A. Divsalar, Thermodynamic study of the binding of calcium and magnesium ions with myelin basic protein using the extended solvation theory, *Acta Bioch Bioph Sin*, 40 (2008) 964-969.
- [275] F.P. Schmidtchen, in: C.A. Schalley (Ed.) *Analytical Methods in Supramolecular Chemistry*, Wiley-VCH: Weinheim, 2006.
- [276] M.M. Pierce, C.S. Raman, B.T. Nall, Isothermal Titration Calorimetry of Protein-Protein Interactions, *Methods*, 19 (1999) 213-221.
- [277] G. Holdgate, S. Fisher, W. Ward, The Application of Isothermal Titration Calorimetry to Drug Discovery in: J.E. Ladbury, M.L. Doyle (Eds.) *Biocalorimetry 2: Applications of Calorimetry in the Biological Sciences*, Wiley, 2004.
- [278] S. Schumacher, *Saccharide Recognition – Boronic Acids as Receptors in Polymeric Networks*, in: *Physical chemistry at the Faculty of Mathematics and Natural Sciences, Universität Potsdam, Postdam*, 2011.
- [279] M.R. Mirani, F. Rahimpour, Thermodynamic modelling of hydrophobic interaction chromatography of biomolecules in the presence of salt, *J Chromatogr A*, 1422 (2015) 170-177.
- [280] F.-Y. Lin, C.-S. Chen, W.-Y. Chen, S. Yamamoto, Microcalorimetric studies of the interaction mechanisms between proteins and Q-Sepharose at pH near the isoelectric point (pI): Effects of NaCl concentration, pH value, and temperature, *J Chromatogr A*, 912 (2001) 281-289.
- [281] F.-Y. Lin, W.-Y. Chen, R.-C. Ruaan, H.-M. Huang, Microcalorimetric studies of interactions between proteins and hydrophobic ligands in hydrophobic interaction chromatography: effects of ligand chain length, density and the amount of bound protein, *J Chromatogr A*, 872 (2000) 37-47.
- [282] E.A. Lewis, K.P. Murphy, in: G.E. Nienhaus (Ed.) *Methods in Molecular Biology*, Humana Press Inc., Totowa NJ, 2003.
- [283] J. Korfhagen, A.C. Dias-Cabral, M.E. Thrash, Nonspecific Effects of Ion Exchange and Hydrophobic Interaction Adsorption Processes, *Sep Sci Technol*, 45 (2010) 2039-2050.

- [284] J. Kim, R.J. Desch, S.W. Thiel, V.V. Gulians, N.G. Pinto, Energetics of lysozyme adsorption on mesostructured cellular foam silica: Effect of salt concentration, *J Chromatogr A*, 1218 (2011) 6697-6704.
- [285] R.J. Desch, J. Kim, S.W. Thiel, Interactions between biomolecules and an iron-silica surface, *Micropor Mesopor Mat*, 187 (2014) 29-39.
- [286] J.C.S. Cardoso, Understanding ion exchange chromatography adsorption mechanisms under different conditions, in: *Biocologia*, Universidade da Beira Interior, Covilhã, 2016.
- [287] A. Schön, B.R. Clarkson, M. Jaime, E. Freire, Temperature stability of proteins: Analysis of irreversible denaturation using isothermal calorimetry, *Proteins*, 85 (2017) 2009-2016.
- [288] Malvern, Instruments, Limited, Characterization of biopharmaceutical stability with Differential Scanning Calorimetry: Candidate selection for developability, *Whitepaper*, (2017) 1-16.
- [289] B. Beyer, A. Jungbauer, Conformational changes of antibodies upon adsorption onto hydrophobic interaction chromatography surfaces, *J Chromatogr A*, 1552 (2018) 60-66.
- [290] W. Krepper, P. Satzer, B.M. Beyer, A. Jungbauer, Temperature dependence of antibody adsorption in protein A affinity chromatography, *J Chromatogr A*, 1551 (2018) 59-68.
- [291] R. Ueberbacher, E. Haimer, R. Hahn, A. Jungbauer, Hydrophobic interaction chromatography of proteins: V. Quantitative assessment of conformational changes, *J Chromatogr A*, 1198-1199 (2008) 154-163.

Chapter II - Thermodynamic evaluation of the mechanisms underlying the adsorption of monoclonal antibodies in phenylboronate chromatography: The influence of different mobile phase modulators¹

Abstract: Phenylboronate chromatography has been employed for bioseparation applications, though details concerning the mechanisms of interaction between the ligand and large macromolecules as monoclonal antibodies (mAbs) remain widely unknown. Here, the phenomena underlying the adsorption of an anti-human IL-8 (anti-IL8) mAb onto an *m*-aminophenylboronic acid (*m*-APBA) ligand, in the absence and in the presence of different mobile phase modulators, is investigated. On-line flow microcalorimetry (FMC) was applied to measure instantaneous heat energy transfers, providing insights about the role of specific and non-specific interactions involved in the adsorptive process under different pH values and in the absence or presence of salts such as NaCl, NaF, MgCl₂ and (NH₄)₂SO₄. Results showed that the adsorption of anti-IL8 mAb to *m*-APBA is enthalpically driven ($\Delta H_{\text{ads}} < 0$), as expected for the predominant reversible esterification reaction between boronates and *cis*-diol-containing molecules. Nevertheless, for all mobile phase modulators studied, shifts in thermogram profiles were observed, as a decrease from 55% to 75% in the net heat of adsorption (ΔH_{ads}), when increasing the pH from 7.5 to the pH values of 8.5 and 9.0. The ΔH_{ads} obtained at conditions where the ligand was poorly negatively charged (pH 7.5) was approximately -243 ± 38 kJ/mol, in the absence and presence of NaCl, and -352.3 ± 29.5 kJ/mol, when using NaF, MgCl₂ and (NH₄)₂SO₄ as mobile phase modulators. Overall, the outcomes of this work suggest that (i) whereas the binding of the PBA ligand to mAb molecules has been described for decades as being affinity-based, this interaction presents multimodal behaviour and (ii) the salt tolerance of the bond under study could be enhanced using mobile phase modulators as NaF, MgCl₂ and (NH₄)₂SO₄ by the promotion of the specific *cis*-diol interactions and reduction of the non-specific interactions contribution to the anti-IL8 mAb adsorption onto the ligand. The last feature was more noticeable at pH values above ligand's pKa, mainly by the ability of NaF and (NH₄)₂SO₄ to diminish electrostatic interactions between ligand and biomolecule, when compared to the commonly used NaCl.

Keywords: Monoclonal antibodies, Adsorption process, Phenylboronate chromatography, Mobile phase modulators, Flow microcalorimetry

¹ The work present in this chapter resulted in the articles: (1) **Rosa, S.A.S.L.**, da Silva, C.L., Aires-Barros, M.R., Dias-Cabral, A.C., Azevedo, A.M., 2018. Thermodynamics of the adsorption of monoclonal antibodies in phenylboronate chromatography: affinity versus multimodal interactions. *Journal of Chromatography A*, 1569, 118-127 and, (2) **Rosa, S.A.S.L.**, Wagner, Alexandra, da Silva, C.L., Aires-Barros, M.R., Azevedo, A.M., Dias-Cabral, A.C., 2019. Mobile phase modulators as salt tolerance enhancers in phenylboronate chromatography: thermodynamic evaluation of the mechanisms underlying the adsorption of monoclonal antibodies. *Biotechnology Journal*, 14(10): e1800586.

II.1. Background

Phenylboronate chromatography has been extensively used for the capture of *cis*-diol containing molecules. However, detailed knowledge about the mechanisms of interaction between the ligand and complex biomolecules such as monoclonal antibodies (mAbs) is limited and needs deeper investigation.

The phenylboronic acid (PBA) is the most commonly used ligand in boronate chromatography, and it was first described as an affinity ligand able to promote the specific capture and effective enrichment of target *cis*-diol containing molecules from carbohydrates and glycoproteins (e.g. mAbs) [1, 2] to nucleotides and nucleic acids [3-5]. The affinity is based on the ability of the ligand to establish a pair of covalent bonds with diol groups *via* a reversible esterification reaction [6]. In the case of mAbs, this interaction occurs with the N-linked oligosaccharides present at the Fc region of each heavy chain [7, 8].

Interestingly, PBA ligand can be present in two different conformations, both able to bind diol compounds [9]. At pH values below its pKa (8.8), the boronic acid adopts a trigonal form, which can be converted in a tetrahedral boronate anion upon hydroxylation of the ligand, at pH values higher than the ligand pKa. The latter conformation presents a higher equilibrium constant (K_{tet}) and consequently, a higher stability when compared to the trigonal form (K_{trig}), predominant in acidic and neutral environments [10]. Nevertheless, due to the nature of PBA, the adsorption of *cis*-diol containing molecules can also be driven by non-specific interactions. Since PBA ligands are aromatic, these can establish hydrophobic and π - π interactions. Secondary interactions such as ionic, through coulombic attraction or repulsion effects, are also possible to occur, as well as hydrogen bonding and charge transfer interactions. The latter are more prone to take place under acidic/neutral conditions with the empty orbital of the trigonal uncharged form of the boron acting as an electron acceptor for a coordination interaction that will enable Lewis acid-base interactions with proteins [2, 11]. Considering all the interactions described, the multimodal behaviour of the synthetic ligand phenylboronic acid (PBA) has been studied in the last years [2, 4] with some works describing exciting results about the PBA potential for the capture of mAbs [12, 13].

Therefore, the challenge lies in understanding and consequently predicting the adsorption behaviour of proteins, including mAbs, onto PBA-chromatographic matrices. In order to depict the complex phenomena involved, the evaluation of the interaction between solutes and the chromatographic matrices is critical. The knowledge acquired in this context will contribute towards a better understanding of the process, essential to ensure process consistency under the quality attributes established by the Quality by Design (QbD) initiative [14]. Consequently, a deeper understanding of the phenomena involved in mAbs adsorption, combined with the economic advantages of employing the PBA ligand [15], could change the paradigm in mAbs downstream processing pushing the industry to adopt such chromatographic process either for mAb capture and/or polishing steps or even as a pre-chromatographic step for a longer life-time of the costly protein A resin. Isothermal titration calorimetry (ITC) [16, 17], surface plasma resonance [18], confocal laser scanning microscopy (CLSM) [19], attenuated total reflectance-Fourier transform infrared (ATR-FTIR) spectroscopy [20], nuclear magnetic resonance (NMR) [21, 22], small-angle x-ray scattering (SAXS) [23, 24] and flow microcalorimetry (FMC)

[25-27] are some of the techniques that have been employed to study the mechanisms behind the adsorption of biomolecules. From the up mentioned techniques, only few can operate *in situ*, *i.e.* in the chromatographic column and consequently, account directly for the dynamics of the chromatographic process. One of these techniques is FMC, which is able to simulate a packed-bed chromatographic system at a micro-scale. The heat signal profile obtained can provide an overview on the driving forces of the adsorption of biomolecules from small proteins [25, 28, 29] to larger molecules such as mAbs [27] and pDNA [26].

The aim of this work was to understand the complex phenomena underlying the adsorption of a full anti-human IL-8 mAb ($pI \geq 9.3$) obtained from a clarified supernatant of Chinese Hamster Ovary (CHO) cell cultures, towards the synthetic *m*-aminophenylboronic acid (*m*-APBA) ligand ($pK_a = 8.8$). To this end, as well as to elucidate the role of non-specific interactions during the adsorptive process, FMC was exploited as an emergent tool for thermodynamic *in-situ* and *on-line* evaluation of the mechanisms associated with the adsorption of an IL-8 mAb in boronate chromatography. Considering the ligand structure and possible conformations of *m*-APBA, studies were performed in the absence and presence of different mobile phase modulators such as sodium chloride (NaCl), sodium fluoride (NaF), magnesium chloride ($MgCl_2$) and ammonium sulfate ($(NH_4)_2SO_4$) at ionic strengths of 0.15 M and under different pH values as 7.5, 8.5, 9.0, except otherwise stated.

II.2. Material and Methods

II.2.1. Chemicals

Tris(hydroxymethyl)aminomethane (Tris), sodium citrate monobasic, 4-(2-hydroxyethyl)-1-piperazinepropanesulfonic acid (EPPS) and 2-(cyclohexylamino)ethanesulfonic acid (CHES) were purchased from Sigma–Aldrich (St. Louis, MO, USA). 4-(2-hydroxyethyl)-1-piperazineethanesulfonic acid (HEPES), sodium chloride (NaCl) and hydrochloric acid were obtained from Fisher Scientific (Waltham, MA, USA). Ammonium sulfate, sodium azide, sodium phosphate monobasic anhydrous and sodium phosphate dibasic were acquired from Panreac (Barcelona, Spain). Sodium fluoride was purchased from Merck (Darmstadt, Germany) and sodium hydroxide from José Manuel Gomes dos Santos Lda. (Odivelas, Portugal). All chemicals used were analytical or HPLC grade. Water used in all experiments was obtained from a Milli-Q purification system (Millipore, Bedford, MA, USA).

II.2.2. Production, purification, concentration and diafiltration of anti-IL8 mAb

Anti-human interleukin-8 (anti-IL8) monoclonal antibodies (from IgG1 family) were produced by CHO DP-12 clone#1934 (ATCC CRL-12445) using DHFR minus/methotrexate selection method (LGC Standards, Middlesex, UK). CHO DP-12 cells were grown in serum-free medium formulated with 0.1% Pluronic® F-68 and without L-glutamine, phenol red, hypoxanthine or thymidine (ProCHO™5, Lonza Group Ltd, Belgium). The cell culture medium was supplemented as described in [12, 13]. The cultures were carried out in single or multi T-175 flasks (BD Falcon, Franklin Lakes, NJ) at 37°C and 5% CO₂ with an initial cell density of 2.8×10^4 cells/cm². Cell passages were performed every 6 to 8 days. Cell supernatants were centrifuged at 350 *g* for 7 minutes, collected and storage at -20 °C. The produced

anti-IL8 mAb presents an isoelectric point (pI) of ~9.3, and its concentration in the serum-free cell culture supernatants varied between 50 and 100 mg/L.

Afterwards, anti-IL8 mAb purification was performed by protein A affinity chromatography using a HiTrap MabSelect Xtra pre-packed 1 mL column from GE Healthcare (Illinois, Chicago). Chromatographic runs were performed in two different ÄKTA systems: (i) an ÄKTA pure 25 L, from GE Healthcare (Section II.3.1.) and (ii) an ÄKTA Purifier 10, from Amersham Biosciences (Uppsala, Sweden) (Section II.3.2.). 150 mM NaCl in 20 mM phosphate at pH 7.2 and 100 mM sodium citrate at pH 3-3.6 were used as adsorption and elution buffers, respectively. To avoid denaturation of the eluted mAb, 10% (v/v) 1 M Tris-HCl at pH 8 was added to the elution fractions collected. Prior to injection, the column was equilibrated with 10 column volumes (CVs) of the adsorption buffer. The cell culture supernatants were directly injected at 1 mL/min using a S9 sample pump, when working with the ÄKTA pure 25 L system or using a third line of the ÄKTA Purifier 10. Before elution, the unbound or weakly bound samples were washed-out with 5 CVs of adsorption buffer. The bound material was eluted following a step gradient of 20-30 CVs. Column regeneration was achieved with a step gradient of 10% (v/v) elution buffer for 5 CVs followed by a second equilibration step with 5 CVs of adsorption buffer. The data collection and processing were accomplished using Unicorn 6.3 and Unicorn 5.11 softwares, depending on the ÄKTA system used. Chromatographic parameters such as conductivity, pH and UV absorbance at 280 nm of the outlet sample were continuously measured. Flow-through and eluted samples were collected using a F9-R or a Frac-950 fraction collector, and further analysed for IgG concentration determination.

Elution fractions from anti-IL8 mAb purification were then pooled (final volume of 30 mL), concentrated and diafiltered in 20 mM HEPES, pH 7.5 using Amicon Ultra-15 centrifugal filter units (MWCO of 50 kDa) from Merck Millipore, for 20 min at 4000 g in a swinging-bucket rotor centrifuge. The process was repeated 4 to 5 times. Buffer exchange to the different adsorption buffers under study was further performed using Amicon Ultra-4 or Ultra-0.5 centrifugal filter units (MWCO of 10 kDa) also from Merck Millipore. The units were used for 3 to 4 cycles of 10 min at 4000 g and 14000 g, respectively. After these steps, the final concentration of the mAb solutions were 1 and 5 mg/mL.

II.2.3. Flow Microcalorimetry (FMC) assays

Thermodynamic studies were performed in a flow microcalorimeter (Microscal FMC 4 Vi, Microscal Limited, London, UK), operated in heat conduction mode. The 171 μ L microcalorimeter cell is interfaced with two highly sensitive thermistors capable of detecting power changes with a magnitude of 10^{-7} W, resulting in an energy resolution in the order of 10^{-9} J. The flow-rate through the cell is controlled by precision syringe pumps (Harvard Apparatus, UK). A block heater is used to monitor and control the cell temperature. The FMC is also equipped with a multiport valve and an automated injection system, as with a conductivity monitor and a UV detector from Pharmacia (Uppsala, Sweden).

Data acquisition, storage and processing were achieved using CALDOS 4 software (Microscal, Limited, UK). The calibration factor was obtained from the correlation between the areas of the peaks and the energy of heat pulses (3 mJ) resulting from electrical impulses of known power and duration. Peak de-convolution and peak area determination were performed with PeakFit 4.12 software (Seasolve

Software Inc., San Jose, USA) using the Exponentially Modified Gaussian (EMG) model. The latter was employed due to its ability to model asymmetric signals. The exothermic and endothermic contributions to the overall heat of adsorption were calculated from the area of the respective de-convoluted peaks.

II.2.3.1. Evaluation of the adsorption of anti-IL8 mAb

Anti-IL8 mAb adsorption studies were performed in the Microscal FMC 4 Vi equipment, using the resin Aminophenylboronate P6XL from Prometic Bioseparations Ltd. (Cambridge, UK) with a ligand density of 76 $\mu\text{mol/g}_{\text{moisture gel}}$. Different adsorption buffers were screened in order to understand the thermodynamic phenomena involved in the adsorption process of anti-IL8 mAb onto *m*-APBA agarose beads at different pH values and salt types at ionic strengths of 0 and 0.15 M, using at least two independent replicated assays per each condition. The tested adsorption buffers were: (i) 20 mM HEPES, pH 7.5; (ii) 20 mM HEPES, 150 mM NaCl, pH 7.5; (iii) 20 mM HEPES, 150 mM NaF, pH 7.5; (iv) 20 mM HEPES, 50 mM MgCl₂, pH 7.5; (v) 20 mM HEPES, 50 mM (NH₄)₂SO₄, pH 7.5, (vi) 20 mM EPPS, pH 8.5; (vii) 20 mM EPPS, 150 mM NaCl, pH 8.5; (viii) 20 mM EPPS, 150 mM NaF, pH 8.5; (ix) 20 mM EPPS, 50 mM MgCl₂, pH 8.5; (x) 20 mM EPPS, 50 mM (NH₄)₂SO₄, pH 8.5, (xi) 20 mM CHES, pH 9.0; (xii) 20 mM CHES, 150 mM NaCl, pH 9.0; (xiii) 20 mM CHES, 150 mM NaF, pH 9.0; (xiv) 20 mM CHES, 50 mM MgCl₂, pH 9.0 and (xv) 20 mM CHES, 50 mM (NH₄)₂SO₄, pH 9.0; (xvi) 20 mM CHES, pH 9.5; (xvii) 20 mM CHES, 150 mM NaCl, pH 9.5; (xviii) 20 mM CHES, pH 10.0; (xix) 20 mM CHES, 150 mM NaCl, pH 10.0. Elution was performed with 1.5 M Tris-HCl, pH 8.5 since Tris has been reported to effectively disrupt specific and non-specific interactions with *m*-APBA [30]. Before injection, the cell was equilibrated overnight with the chosen adsorption buffer. Diafiltered solutions of anti-IL8 mAb (5 mg/mL) were then injected using a sample loop of 100 μL . The unbound or weakly bound material were washed-out with 17 CVs and, the strongly bound material was eluted following a step gradient with the elution buffer for 17 CVs. All the steps were performed at a constant flow-rate of 1.5 mL/h. The flow-through and eluted fractions were collected in conical tubes, and further analysed for IgG mass balance. Absorbance was monitored at 280 nm. Cleaning-in-place was accomplished with 0.5 M NaOH between each injection.

II.2.3.2. Thermodynamic profiling of cis-diol interactions using D-sorbitol

In order to obtain and confirm the thermodynamic profiles of typical *cis*-diol esterification, D-sorbitol adsorption studies were conducted with the resin Aminophenylboronate P6XL. The measurements were performed in duplicate for each condition. 20 mM of D-sorbitol was added to the adsorption buffers (i), (ii), (vi), (vii), (xi) and (xii) of the previous section. The samples were injected at a flow-rate of 1.5 mL/h, using a sample loop of 100 μL . Cleaning-in-place was accomplished with 0.5 M NaOH between each injection.

II.2.4. Structural characterization of anti-IL8 mAb

For all the conditions tested, anti-IL8 mAb was characterized in terms of secondary and tertiary structure by circular dichroism (CD) [31, 32] and fluorescence [33, 34] measurements, respectively. The hydrodynamic diameter (d_H) was also evaluated by dynamic light scattering (DLS).

II.2.4.1. Circular Dichroism

The secondary structure of the anti-IL8 mAb was evaluated by circular dichroism using an Applied Photophysics spectropolarimeter (Leatherhead, United Kingdom), model PiStar-180 containing a Peltier temperature control unit (Melcor MTCA). Suprasil Quartz cells from Hellma with an optical path of 1 mm were used. Far-UV (195–250 nm) measurements consisted of an accumulation of 6 scans with an integration time of 1.15 s and a scan rate of approximately 0.87 nm/s. The monochromator bandwidth was set to 5 nm and the analysis performed at room temperature. Each spectrum was corrected with the corresponding control. Samples were prepared in 5 mM of the different buffers under study with a mAb concentration of 0.3 mg/mL (2 μ M). The mean residue ellipticity was calculated considering a mean residue weight of 113.16 Da [35].

II.2.4.2. Fluorescence measurements

Fluorescence measurements were performed in order to assess the tertiary structure of the anti-IL8 mAb. Samples were prepared in 5 mM of the different buffers under study with a mAb concentration of 0.375 mg/mL (2.5 μ M). The intrinsic fluorescence spectra characteristics of tryptophan and tyrosine were exploited using a Varian (Palo Alto, CA, USA) Cary Eclipse fluorescence spectrophotometer. Emission and excitation spectra of tryptophan were measured at λ_{ex} = 296 nm and λ_{em} = 310 and 440 nm with the photomultiplier at 700 nm. Tyrosine spectra were evaluated at λ_{ex} = 280 nm and λ_{em} = 295 and 440 nm with the photomultiplier at 650 nm. The excitation and emission slits were set at 5 nm. Measurements consisted on the average of three consecutive readings obtained using a quartz cuvette with an optical path of 10 mm.

II.2.4.3. Dynamic light scattering

The hydrodynamic diameter (d_H) of anti-IL8 mAb was obtained by dynamic light scattering (DLS) using a Zetasizer Nano-ZS system (Malvern Instruments Ltd., UK). Samples of 1 mL of anti-IL8 mAb with a final concentration of 0.375 mg/mL (2.5 μ M) were analyzed in the different buffers study. Measurements were performed in polystyrene (PS) disposable cuvettes at 25 °C using solvent and protein refraction indexes of 1.333 and 1.450, respectively. Each sample was measured three times using the multimodal mode. Anti-IL8 mAb hydrodynamic diameters were calculated from the correlation function using the dispersion technology software. Results obtained were presented considering the number of particles in solution.

II.2.5. Contribution of matrix and resin components to the adsorption of anti-IL8: interaction studies

Complementary studies were performed in order to determine which types of interaction are involved in the adsorptive process of anti-IL8 mAb onto the aminophenylboronate P6XL resin. For such analyses, different chromatographic resins were used: (i) HiTrap Phenyl Fast Flow (high sup) 1 mL pre-packed column (GE Healthcare); (ii) Sepharose 6 Fast Flow (GE Healthcare) and (iii) Aminophenylboronate P6XL (Prometic Bioseparations Ltd) with three independent replicated assays

being performed. The last two resins were packed on Tricorn™ 5/50 glass columns (GE Healthcare) with a resin volume of 1 mL. At all cases, the columns were equilibrated with 10 CVs of the adsorption buffer. A volume of 100 µL of purified and diafiltered anti-IL8 mAb (1 mg/mL) was then injected, except otherwise stated. The loop was emptied with three times its volume and the unbound or weakly bound anti-IL8 mAb was washed-out with 10 CVs of adsorption buffer. The bound anti-IL8 mAb was eluted following a step gradient of 10 CVs. When stated, a stripping was performed using a step gradient of 10 CVs. Cleaning-in-place was achieved with 5 CVs of 0.5 M NaOH followed by 10 CVs of water and a re-equilibration step of 5 CVs with adsorption buffer. All the steps were performed at a constant flow-rate of 1.0 mL/min. The adsorption buffers used for screening are the same used for the FMC studies and listed in Section II.2.3.1., except otherwise stated. The buffer used to elute the anti-IL8 mAb, at all conditions, was 1.5 M Tris-HCl, pH 8.5, if not explicitly stated otherwise. In boronate chromatography assays, different strategies were followed. Firstly, in order to evaluate the contribution of ionic interaction in the anti-IL8 adsorption in presence of NaCl, different adsorption conditions were tested. Different buffers as (i) 20 mM HEPES, pH 7.5; (ii) 20 mM EPPS, pH 8.5 and (iii) 20 mM CHES, pH 9.0 were used at different salt concentrations such as 300, 450, 600, 750 mM and 1 M NaCl. In the case of the studies where the adsorption is performed with buffers containing the mobile phase modulators NaF, MgCl₂ and (NH₄)₂SO₄, the salt tolerance of the bond between the anti-IL8 mAb and the ligand was assessed by using the buffers previously mentioned but as elution buffers. The stripping of the column was achieved using 1.5 M Tris-HCl, pH 8.5.

All chromatographic runs were performed in an ÄKTA Purifier 10 system from Amersham Biosciences (Uppsala, Sweden). The data collection and processing were accomplished using Unicorn 5.1 software. Conductivity, pH and UV absorbance at 280 nm were continuously measured at the sample outlet. Flow-through and eluted samples were collected using a Frac-950 fraction collector from GE Healthcare, and further analysed for IgG content.

II.2.6. Anti-IL8 quantification

The concentration of anti-IL8 mAb present in the elution pool obtained from protein A chromatography was determined measuring the UV absorbance at 280 nm in microtiter plate readers as the (i) xMark equipped with the MPM 6 software, both from Bio-Rad (Hercules, CA, USA) (Section II.3.1.) and the (ii) Spectra Max from Molecular Devices (Sunnydale, CA, USA) (Section II.3.2.). The measurements were performed using UV-Star® 96-well microplates from Greiner Bio-One (Kremsmünster, Austria). On the other hand, the anti-IL8 mAb content on the samples obtained during FMC analyses and the complementary studies, described in Section II.2.5., was determined by analytical protein A chromatography using a POROS A ImmunoDetection sensor cartridge from Applied Biosystems (Foster City, CA, USA). The adsorption buffer was composed by 50 mM phosphate, 150 mM NaCl, pH 7.4 and the elution buffer was composed by 12 mM HCl, 150 mM NaCl, pH 2–3. Analyses were performed in (i) a LC-2010HT HPLC system from Shimadzu Corporation (Tokyo, Japan) and in (ii) an ÄKTA Purifier 10 system with an A-900 Autosampler as reported in [12]. Absorbance was monitored at 215 nm. For both quantification methods, calibration curves were obtained using a commercial human IgG solution (product name: Gammanorm®) from Octapharma (Lachen, Switzerland).

II.2.7. Total protein quantification

The total protein content was determined by the Bradford method using a Coomassie assay reagent and bovine gamma globulin (BGG) as protein standard, both from Pierce (Rockford, IL, USA). Absorbance was measured at 595 nm in a SpectraMax microplate reader from Molecular Devices (Sunnyvale, CA, USA). Protein purity was assessed by the ratio between the concentration of IgG determined by protein A HPLC and total protein content determined using the Bradford method.

II.3. Results and Discussion

The adsorption of the purified anti-IL8 mAb (purity of $99 \pm 1\%$) was performed using HEPES buffer due to its ability to favour the binding of *cis*-diol-containing compounds to PBA medium [10, 36]. This ability has been described to be due to B-N coordination between the boronic acid and the tertiary amines from HEPES in solution, which enables the capture of *cis*-diol-containing compounds under neutral conditions [12, 37]. EPPS and CHES were also selected as buffers due to the similarity that they share with HEPES in terms of chemical structure (Figure II.1).

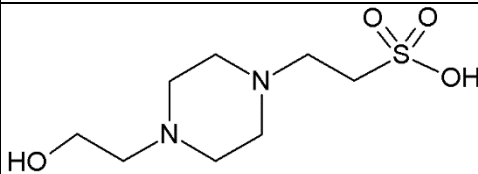
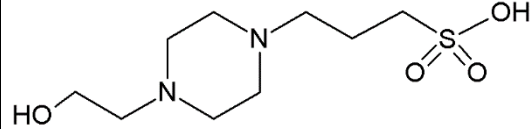
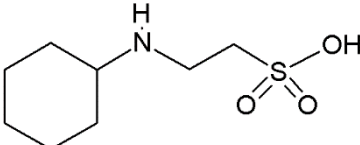
Buffers	Chemical structure	pKa (25 °C)	Useful pH range
HEPES		7.5	6.8 – 8.2
EPPS		8.0	7.3– 8.7
CHES		9.3	8.6 – 10.0

Figure II.1 Chemical structure and characteristics of the buffers used in anti-IL8 mAb adsorption studies onto a phenylboronate chromatographic agarose-based support.

Additionally, a structural evaluation of the anti-IL8 mAb was performed under each condition studied. Circular dichroism and fluorescence measurements were carried out with the goal of evaluating possible changes in the secondary and tertiary structure of the anti-IL8 mAb, respectively. The results revealed that no modifications have occurred (Figures II.S1.1-2 and II.S2.1-2 in Supplementary Material). In terms of hydrodynamic diameter (d_H), evaluated by dynamic light scattering, no significant changes were also observed (Figure II.S1.3 and II.S2.3 in Supplementary Material).

II.3.1. Evaluation of the adsorption of anti-IL8 mAb in the absence of added salt and in presence of NaCl

Considering the *m*-APBA pKa (8.8) and the isoelectric point of the anti-IL8 mAb (≥ 9.3), working pH values of 7.5, 8.5, 9.0, 9.5 and 10 were chosen to perform the adsorption studies. Each pH value was evaluated at two different salt concentrations, namely 0 and 150 mM NaCl, with the latter simulating physiological conductivity and often being reported as a possible suppressor of non-specific interactions [38].

II.3.1.1. Flow Microcalorimetry (FMC) studies

Flow microcalorimetry (FMC) allows the determination of the net heat of adsorption (ΔH_{ads}) of mAbs towards the *m*-APBA ligand as the sum of the endothermic and/or exothermic contribution of the different events detected. The results obtained are summarized in Table II.1.

In general, results obtained show that anti-IL8 mAb adsorption on P6XL resin is enthalpically driven ($\Delta H_{\text{ads}} < 0$) (ΔH_{ads} , Table II.1). The ΔH_{ads} values obtained were significantly higher when compared to the ones obtained by isothermal titration calorimetry (ITC) for hydrophobic charge-induction chromatography using a 4-mercaptoethyl-pyridine (MEP) multimodal ligand (-0.43 ± 0.03 kJ/mol) [16] or to systems comprising other proteins and ligands [25]. This could be due to the fact that the interaction between boronic acids or boronate ligands and *cis*-diols containing molecules relies on a reversible esterification reaction and other enthalpically driven processes, not evaluated by ITC. In ITC, thermodynamic quantities are not obtained under the conditions existing in the column but extrapolated to standard-state values.

The thermodynamic profiles obtained for each condition tested are presented in Figure II.2, where distinct peaks were observed, thus suggesting the occurrence of different events during and after the adsorption process. In order to depict the underlying mechanisms involved and once the peak symmetry test [39] indicated an overlap of the observed peaks, thermogram profiles were de-convoluted. The de-convoluted heat signals for all the experiments in the absence (A, C, E, G and I) and presence of NaCl (B, D, F, H and J) are also represented in Figure II.2, for the different pH conditions tested. Dilution heat contribution was null (data not shown) and, consequently, no corrections had to be performed to the different heat signals obtained. In Figures II.2A to II.2G are illustrated the results obtained using conditions where no flow-through was observed, which can, consequently, be used to study the adsorption process of the anti-IL8 mAb towards *m*-APBA and to depict the underlying mechanisms involved. The thermogram obtained at pH 7.5 and in the absence of salt (Figure II.2A) shows only one positive peak characteristic of an exothermic event (heat released to the environment). All the other thermograms exhibit two peaks. At pH values lower than the *m*-APBA pKa (Figures II.2B-D) and at pH 9 in absence of salt (Figure II.2E), the first peak is also positive and consequently representative of an exothermic event. However, the second peak is either related to another exothermic event (positive peak) or to an endothermic event (negative peak), depending on the pH and ionic strength. At pH 9.0 and pH 9.5 in presence of salt (Figures II.2F and II.2H) and at pH 10.0 (Figures II.2I and II.2J), a

complete shift is observed in thermogram profiles. In these, the first peak is negative and thus illustrative of an endothermic event and the second peak is a positive peak, representative of an exothermic event. Nevertheless, it is important to notice that at pH 9.5 in presence of salt, a flow-through value of around 70% was obtained and at pH 10 nearly no anti-IL8 mAb adsorption occurred (Table II.1).

These results show that both pH and the presence of NaCl modulate the mechanisms involved in anti-IL8 mAb's adsorption. The pH value was already expected to be a modulatory element since the ligand structure suffers conformational changes with the pH. Indeed, the boron atom can adopt a trigonal or a tetrahedral form, depending on the working pH. At a pH below the *m*-APBA pKa (8.8), the trigonal form of *m*-APBA predominates, while at pH values above the pKa, the tetrahedral boronate anion structure is dominant [9]. Although the equilibrium constant is usually higher for the tetrahedral form (K_{tet}) than for the trigonal form (K_{trig}), both structures are capable of interacting with *cis*-diol-containing molecules *via* esterification reactions [10].

Furthermore, the de-convoluted thermograms obtained were analysed considering the possible interactions between the anti-IL8 mAb and the *m*-APBA ligand. PBA ligands have an aromatic moiety that confers these the ability to establish hydrophobic, π - π and cation- π interactions, in addition to the primary *cis*-diol interactions [3, 40]. Secondary electrostatic interactions with the boronate anion are also possible, as well as hydrogen bonding and charge transfer interactions [2, 41].

Table II.1 Heat of adsorption for the anti-human IL-8 mAb onto P6XL resin considering a sample loop, adsorbent volumes and a protein loading of 100 μ L, 171 μ L and 5 mg/mL, respectively. All experiments were performed under a flow-rate of 1.5 mL/h. The amount of mAb in the flow-through (not binding to the column) is given as percentage of the total mass of mAb loaded into the column. ΔH^I , ΔH^{II} and ΔH^{III} were determined by integration of the individual peaks obtained from the de-convolution of thermograms using PeakFit software (Figure II.2). Results are displayed as mean \pm STDV. I and FT stand for ionic strength and flow-through, respectively. RSD stands for relative standard deviation. n.a. – not applicable.

Buffer	pH	I (M)	FT (%)	Exothermic events (kJ/mol)		Endothermic events (kJ/mol)	Net heat of adsorption (kJ/mol)	
				ΔH^I	ΔH^{II}	ΔH^{III}	ΔH_{ads}	RSD (%)
20 mM HEPES	7.5	0	0	-282.1 \pm 61.1	0	0	-282.1 \pm 61.1	22
		0.15	0	-205.2 \pm 26.4	-27.2 \pm 22.8	0	-232.4 \pm 24.6	11
20 mM EPPS	8.5	0	0	-187.6 \pm 29.9	-29.6 \pm 2.9	0	-217.2 \pm 32.8	15
		0.15	0	-370.2 \pm 117.7	0	170.8 \pm 83.2	-199.4 \pm 34.6	17
20 mM CHES	9.0	0	0	-664.2 \pm 212.5	0	380.8 \pm 153.9	-283.4 \pm 58.6	21
		0.15	0	-280.4 \pm 69.0	0	198.2 \pm 82.7	-82.22 \pm 13.7	17
	9.5	0	0	-837.7 \pm 223.8	0	538.0 \pm 222.6	-299.7 \pm 1.2	0.40
		0.15	70 \pm 4	-662.4 \pm 247.7	0	515.6 \pm 211.6	-146.8 \pm 36.0	25
10.0	0	97 \pm 4	n.a.	0	n.a.	\approx 0	n.a.	
	0.15	92 \pm 3	n.a.	0	n.a.			

$$\Delta H_{ads} = \Delta H^I + \Delta H^{II} + \Delta H^{III}$$

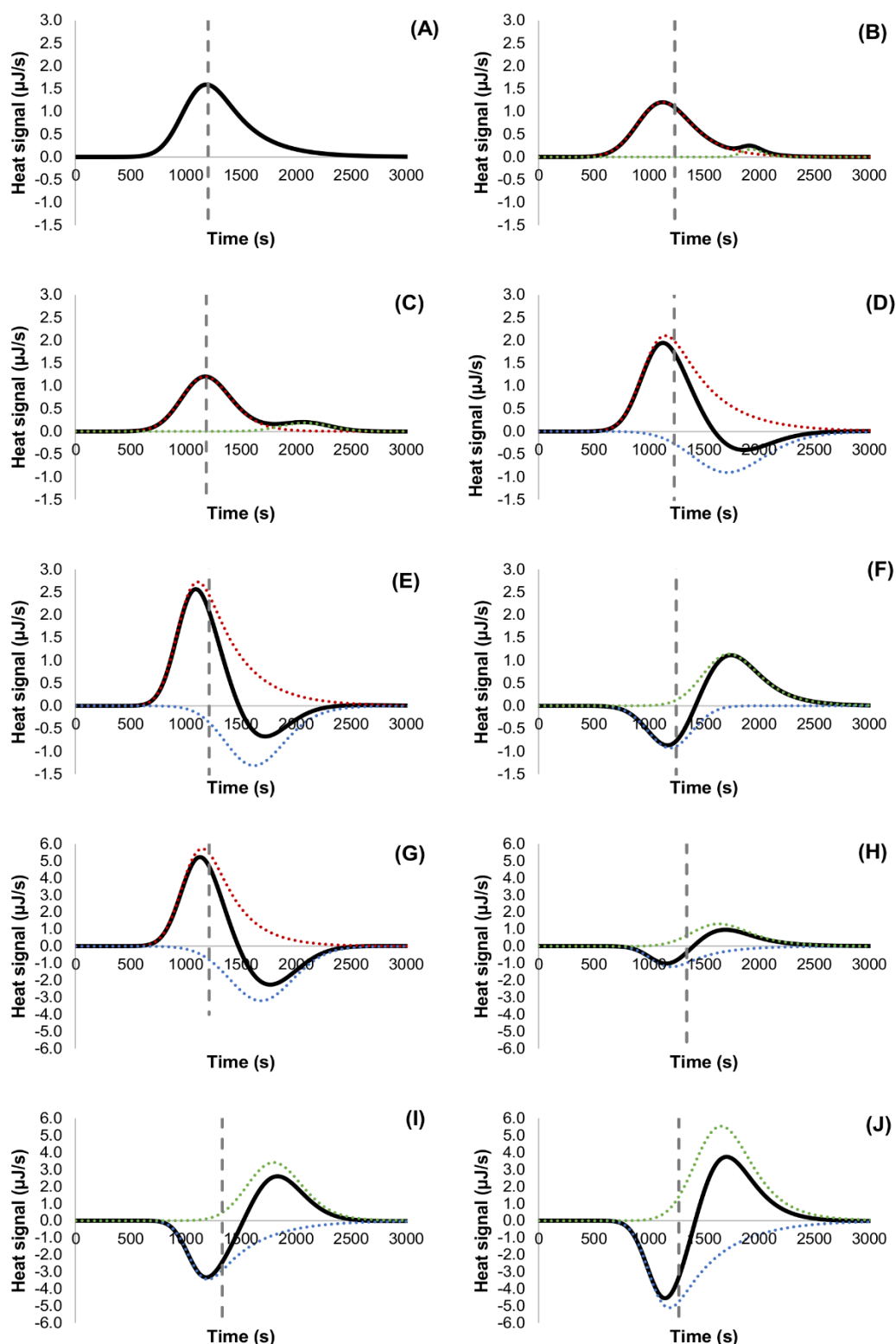


Figure II.2 PeakFit de-convolution of thermograms obtained for the anti-human IL-8 mAb (5 mg/mL) adsorption onto P6XL resin at different pH values, in the absence and in the presence of 150 mM NaCl. Injection loop: 100 μ L. Mobile phase flow-rate: 1.5 mL/h. (A) 20 mM HEPES, pH 7.5, (B) 20 mM HEPES, 150 mM NaCl, pH 7.5, (C) 20 mM EPPS, pH 8.5, (D) 20 mM EPPS, 150 mM NaCl, pH 8.5, (E) 20 mM CHES, pH 9.0, (F) 20 mM CHES, 150 mM NaCl, pH 9.0, (G) 20 mM CHES, pH 9.5, (H) 20 mM CHES, 150 mM NaCl, pH 9.5, (I) 20 mM CHES, pH 10, (J) 20 mM CHES, 150 mM NaCl, pH 10. Curves presented are for total peak fit (black line) and peaks resulting from de-convolution (endothermic peaks – blue dotted lines, exothermic peaks – red and green dotted lines). Vertical dashed lines represent the time where the protein-containing plug of solution is replaced with protein-free mobile phase.

II.3.1.1.1. FMC studies in the absence of added salt

The thermograms obtained in the absence of salt are exhibited in Figures II.2A, 2C, 2E, 2G and 2I, respectively for pH 7.5, 8.5, 9.0, 9.5 and 10.0. At pH 7.5, the thermogram shows a unique exothermic peak (Figure II.2A) that can be attributed to the *cis*-diol esterification reaction, and thus to the formation of a pair of covalent bonds between the anti-IL8 mAb and *m*-APBA hydroxyl groups. The contribution of non-specific interactions, as cation- π interactions (Section II.3.1.2.1.) and/or hydrogen bonding (Section II.3.1.2.2.), can be also considered having in mind that *cis*-diol esterification, as a covalent interaction, will be thermodynamically more favoured. However, at pH 8.5, a second non-overlapping exothermic peak can be observed (Figure II.2C). Since this second peak occurs after the protein-containing solution being replaced by the mobile phase and no flow-through is observed, this event is known to be related to anti-IL8 mAb reorganization at the surface. At pH 8.5, both trigonal and tetrahedral conformations will be present (*m*-APBA $pK_a = 8.8$) and anti-IL8 mAb molecules primarily adsorbed to the boronic acid ligands (trigonal conformation, dominant form) can be re-absorbed by free hydroxylated boronate ligands (tetrahedral conformation, minor form) that establish more thermodynamically stable interactions ($K_{\text{trig}} < K_{\text{tet}}$).

When the pH is further increased to 9.0 (Figure II.2E), the second exothermic peak, observed at pH 8.5, gives place to an endothermic overlapping peak. This change in the FMC profile is probably related to the presence of the boronate anion in the ligand structure, which is able to promote electrostatic interactions. For these interactions to occur, water and ions have to be released from the surface of the adsorbent and protein, which requires consumption of energy and originates an increase of entropy [42, 43]. According to the literature, the FMC profile characteristic of an ion-exchange interaction involves a first endothermic peak (related to the desolvation entropic process) overlapped with an exothermic peak (related with the electrostatic interaction itself) [25, 26]. Although in the present situation we could not isolate the exothermic peak resulting from the electrostatic interactions by de-convolution, a 2 to 4-fold increase in the ΔH of the exothermic signal is observed when the pH is increased from 7.5 and 8.5 to 9.0 (ΔH° , Table II.1). The presence of ion-exchange interactions is further corroborated by the constant net heat of adsorption observed as the pH is increased to 9.0 (Figures II.2A, 2C, 2E and ΔH_{ads} , Table II.1) and the consequent increment on the contribution of entropy to adsorption. Since the equilibrium constant, K_{tet} , observed at pH 9.0, is higher than the K_{trig} , observed at lower pH conditions [18], the ΔG of adsorption will be more negative for the tetrahedral form ($\Delta G = -RT \ln K$). Thus, according to the expression for the Gibbs free energy change ($\Delta G = \Delta H - T\Delta S$), a concomitant increase in entropy is expected for the adsorption to occur considering the constant net heat of adsorption observed throughout the tested conditions. Hydrophobic interactions are another type of secondary interactions that could be promoted by increasing the working pH and that involve an increase of entropy (Section II.3.1.2.1.). Typically, for values around the pI , protein molecules have relatively smaller hydrodynamic diameters and thinner hydration layers on the surface due to their low net charge [44, 45], which can favour short-range interactions such as hydrophobic interactions. Dynamic light scattering analyses (Figure II.S1.3 in Supplementary Material) confirmed that the anti-IL8 mAb presents the lowest hydrodynamic diameter (d_H) between pH 9.0 and 9.5. The aforementioned short-range interactions

between the anti-IL8 mAb and the aromatic boronic acid ligand could promote entropically driven non-specific adsorption by π - π and/or cation- π interactions, depending on the working pH. In Sections II.3.1.2.1. and II.3.1.2.3., it is shown that ionic interactions associated with cation- π and electrostatic interactions play a major role in the adsorption of the anti-IL8 mAb to the PBA ligand, when compared to pure hydrophobic effects. This leads us to conclude that at pH 9.0 there is a significant influence of ionic interactions in the adsorption process, in addition to the *cis*-diol esterification.

At pH 9.5, repulsive interactions also have to be considered since both ligand and anti-IL8 mAb (pI 9.3) are negatively charged [46], which can contribute to the observed increase in the ΔH of the endothermic peak (ΔH^{III} , Table II.1). At pH 10.0, anti-IL8 mAb molecules were not retained in the column and, consequently, the net heat of adsorption for this process is approximately zero (ΔH_{ads} , Table II.1).

II.3.1.1.2. FMC studies in the presence of NaCl

In the presence of salt, considerable changes in the thermogram profiles can be seen in Figure II.2 (II.2B, 2D, 2F, 2H and 2J obtained, respectively, at pH 7.5, 8.5, 9.0, 9.5 and 10.0). From pH 7.5 to pH 9.0 (Figures II.2B, 2D and 2F), a drastic change in the profile can be observed, together with a decrease of about 60 to 70% in the net heat of adsorption (ΔH_{ads} , Table II.1). At pH 7.5 and 8.5, a first exothermic peak characteristic of the *cis*-diol interaction between mAbs and PBA ligands is observed in the thermograms (Figures II.2B and 2D). Nevertheless, the events associated with the second peak lead to the formation of an exothermic peak at pH 7.5 (Figure II.2B), and of an endothermic peak at pH 8.5 (Figure II.2D). The observed thermograms are similar to the ones obtained in the absence of salt at pH 8.5 and 9.0 (Figures II.2C and 2E), respectively, suggesting that the addition of NaCl, as the increase in the pH, also results in the promotion of non-specific interactions. Since $\text{pH} < \text{pK}_a$, charge transfer interactions can occur between the chloride ion in the bulk solution and the uncharged boron in the ligand (trigonal conformation). This boron atom contains an empty orbital, which can serve as an electron acceptor for a coordination interaction, enabling Lewis acid–base interactions to occur [11]. Consequently, at pH 7.5, the second exothermic peak could be related to the re-adsorption of anti-IL8 mAb molecules to free tetrahedral PBA ligands (B-Cl form) rather than to its adsorption to PBA ligands in its trigonal conformation. At pH 8.5, the overlapping endothermic peak observed is probably due to the presence of PBA ligands in their tetrahedral conformation (not only to B-Cl coordination but also due to the shift in the acid-base equilibrium caused by the increase in pH), which promote electrostatic attractive forces between the positively charged protein and the negatively charged boronate ligand. Nevertheless, it is observed a decrease of the heat signal for the exothermic peak at pH 8.5 in presence of NaCl when compared to pH 9.0 in absence of salt (ΔH^{I} , Table II.1; Figures II.2D and 2E, respectively). This can be explained by the salt shielding effect towards mAb molecules promoted by the NaCl, that masks the electrostatic attractive forces between the protein and the adsorbent [47].

A total switch in the thermogram profile was observed at pH 9.0 (Figure II.2F), which exhibits a profile characteristic of ionic interactions [25, 26]. In this case, as in others described in Sections II.3.1.1.1. and II.3.1.1.2., no flow-through was observed and it is known that *cis*-diol esterification occurs since elution of the bound anti-IL8 mAb is triggered by the addition of a *cis*-diol competitor (1.5 M Tris-

HCl, pH 8.5). Nevertheless, *cis*-diol esterification contribution to the adsorption process is not exclusive and seems to be considerably reduced. Parallel experiments have demonstrated a decrease on salt tolerance of the ligand at pH values higher than PBA pKa, with a fraction of the anti-IL8 mAb not being adsorbed at salt concentrations ≥ 300 mM (Section II.3.1.2.3.). It is important to notice that, at this condition, the ligand is in its tetrahedral form and bears a negative charge while the anti-IL8 mAb molecule is positively charged and thus electrostatic interactions can be promoted. The predominance of the electrostatic interactions explains the decrease of about 60 to 70% in the net heat of adsorption when compared with conditions where *cis*-diol interactions are favoured (ΔH_{ads} , Table II.1).

Heat measurements performed above the pI value for anti-IL8 mAb, at pH 9.5 and 10.0 (Figures II.2H and 2J), show thermogram profiles very similar to the one acquired at pH 9.0 (Figure II.2F), however, with flow-through values of around 70% and 100% at pH 9.5 and 10.0, respectively (Table II.1).

II.3.1.1.3. Thermodynamic profiling of *cis*-diol interactions using D-sorbitol

In order to confirm if the first exothermic peak obtained in the majority of the thermograms presented in Section II.3.1.1. (Figure II.2) can be attributed to the *cis*-diol esterification reaction, the thermodynamics of the interaction between D-sorbitol and *m*-APBA was studied. D-sorbitol was chosen since the described affinity relies on *cis*-diol reversible esterification and it has an affinity constant towards PBA ($K_{eq\ D-sorbitol} = 370\ M^{-1}$) higher than other carbohydrates such as D-mannitol ($K_{eq\ D-mannitol} = 120\ M^{-1}$) [36]. The assays were performed at a concentration of 20 mM, which is the minimum amount of D-sorbitol that is used in elution processes promoted by competition. In terms of net heat of adsorption, all results obtained were considerably lower (up to 100x) than those obtained for anti-IL8 mAb adsorption studies, with endothermic events having a more important contribution in D-sorbitol adsorption (ΔH_{ads} , Table II.2 vs II.1 and Figure II.3 vs II.2).

Table II.2 Heat of adsorption for D-sorbitol onto P6XL resin considering a sample loop, adsorbent volumes and a loading of 100 μ L, 171 μ L and 20 mM (3.64 mg/mL), respectively. All experiments were performed under a flow-rate of 1.5 mL/h. ΔH^I , ΔH^{II} and ΔH^{III} were determined from the de-convoluted thermograms by PeakFit software (Figure II.3). Results are displayed as mean \pm STDV. I and RSD stand for ionic strength and relative standard deviation, respectively.

Buffer	pH	I (M)	Exothermic events (kJ/mol)		Endothermic events (kJ/mol)	Net heat of adsorption (kJ/mol)	
			ΔH^I	ΔH^{II}	ΔH^{III}	ΔH_{ads}	RSD (%)
20 mM HEPES	7.5	0	-3.76 \pm 0.16	0	3.69 \pm 0.17	-0.07 \pm 0.00	4.1
		0.15	-5.81 \pm 0.49	0	5.37 \pm 0.27	-0.44 \pm 0.21	49
20 mM EPSS	8.5	0	-1.74 \pm 0.04	-1.33 \pm 0.01	2.70 \pm 0.15	-0.37 \pm 0.10	26
		0.15	-1.43 \pm 0.31	-2.31 \pm 0.50	3.06 \pm 0.21	-0.68 \pm 0.01	2.1
20 mM CHES	9.0	0	-3.61 \pm 0.42	-2.48 \pm 0.07	5.21 \pm 0.20	-0.88 \pm 0.15	17
		0.15	-4.59 \pm 0.15	-1.51 \pm 0.08	3.71 \pm 0.33	-2.39 \pm 0.10	4.2

$$\Delta H_{ads} = \Delta H^I + \Delta H^{II} + \Delta H^{III}$$

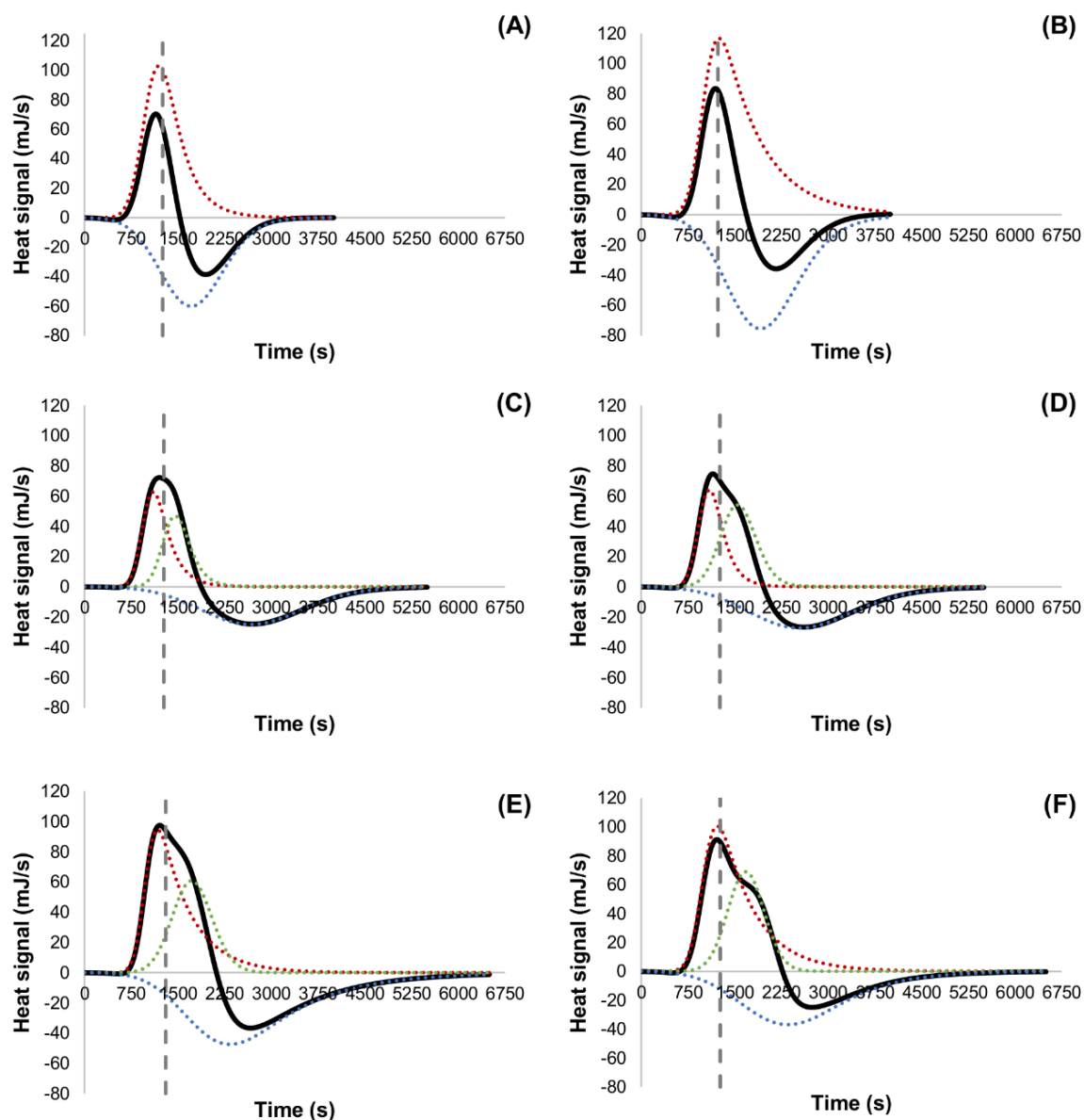


Figure II.3 PeakFit de-convolution of thermograms obtained for 20 mM (3.64 mg/mL) D-sorbitol adsorption onto P6XL resin at different pHs, in absence and in presence of 150 mM NaCl. Injection loop: 100 μ L. Mobile phase flow-rate: 1.5 mL/h. (A) 20 mM HEPES, pH 7.5, (B) 20 mM HEPES, 150 mM NaCl, pH 7.5, (C) 20 mM EPPS, pH 8.5, (D) 20 mM EPPS, 150 mM NaCl, pH 8.5, (E) 20 mM CHES, pH 9.0, (F) 20 mM CHES, 150 mM NaCl, pH 9.0. Curves showed are for total peak fit (black line) and peaks resulting from de-convolution (endothermic peaks – blue dotted lines, exothermic peaks – red and green dotted lines). Vertical dashed lines represent the time where the protein-containing plug of solution is replaced with protein-free mobile phase.

By analysing the de-convoluted thermograms, it was observed that the spreading of the heat signal was larger as the working pH increased (Figure II.3). Nevertheless, the first peak observed was an exothermic peak, characteristic of the *cis*-diol esterification, which started at the same time and had the same profile as the first exothermic peak observed for the anti-IL8 mAb adsorption process. Also, the time at which the solute-containing plug was replaced by mobile phase is relatively the same for both molecules, *i.e.*, anti-IL8 mAb (Figure II.2) and D-sorbitol (Figure II.3). These facts led us to conclude that all the events occurring after the plug, *i.e.*, after the maximum of the first exothermic peak, are not related

to the anti-IL8 mAb adsorption itself but with additional phenomena that occur upon the main adsorption process. Moreover, the first exothermic peak displayed in the thermodynamic analysis of the D-sorbitol adsorption at pH 9.0 in the presence of 150 mM NaCl (Figure II.3F) corroborates that *cis*-diol esterification still arise at this condition, being part of the adsorptive process (Section II.3.1.2.3.). In comparison, at this condition, a total shift of the thermogram profile was observed for the anti-IL8 mAb (Figure II.2F), reinforcing the presence of other type of interactions than besides the *cis*-diol esterification.

II.3.1.2. Contribution of matrix and resin components to the adsorption of anti-IL8 mAb: interaction studies

Control runs using phenyl Sepharose 6 FF, Sepharose 6 FF and Aminophenylboronate P6XL resins were performed to evaluate the importance of non-specific interactions in the anti-IL8 mAb adsorption process, respectively with (i) the phenyl group of the PBA molecule, (ii) the bare resin and (iii) the negative charge present in the ligand at pH higher than *m*-APBA pKa.

II.3.1.2.1. Evaluation of aromatic interactions

The contribution of aromatic interactions to the adsorption of anti-IL8 mAb onto the *m*-APBA ligand was studied using phenyl Sepharose 6 FF (Figure II.4A) at different pH values (7.5, 8.5, 9.0, 9.5, 10.0) and NaCl concentrations (0 and 150 mM NaCl). A strong retention is observed at pH 7.5, 8.5 and 9.0 when no NaCl is present in the adsorption buffer (Figure II.4B), suggesting that aromatic interactions may play an important role in the adsorptive process, for pH values lower than the anti-IL8 mAb pI. This effect is particularly relevant at pH 7.5, at which $96 \pm 6\%$ of the mAb was adsorbed against $86 \pm 2\%$ at pH 8.5 and $89 \pm 3\%$ at pH 9.0. This retention is probably due to cation- π interactions between the positively charged anti-IL8 mAb and the electron-rich π system of the phenyl ring present in the ligand (Figure II.4A). At pH values higher than the isoelectric point of the anti-IL8 mAb (pH 9.5 and 10.0), almost no mAb (around 1%) was retained on the column (Figure II.4B). At these pH values, the anti-IL8 mAb molecule is negatively charged being repelled by the aromatic π system. When 150 mM NaCl was present in the adsorption buffer, the majority of anti-IL8 mAb ($97 \pm 1\%$) was collected in the flow-through fractions (Figure II.4B). These results demonstrate that aromatic interactions are negligible under these conditions, which indicates that the shielding effect exerted by NaCl is sufficient to suppress the attractive forces of a cation- π interaction. In sum, the results obtained with phenyl-Sepharose 6 FF demonstrate the relevance of cation- π interactions in phenylboronate chromatography at adsorption conditions where the pH is lower than the anti-IL8 mAb pI and no salt is added.

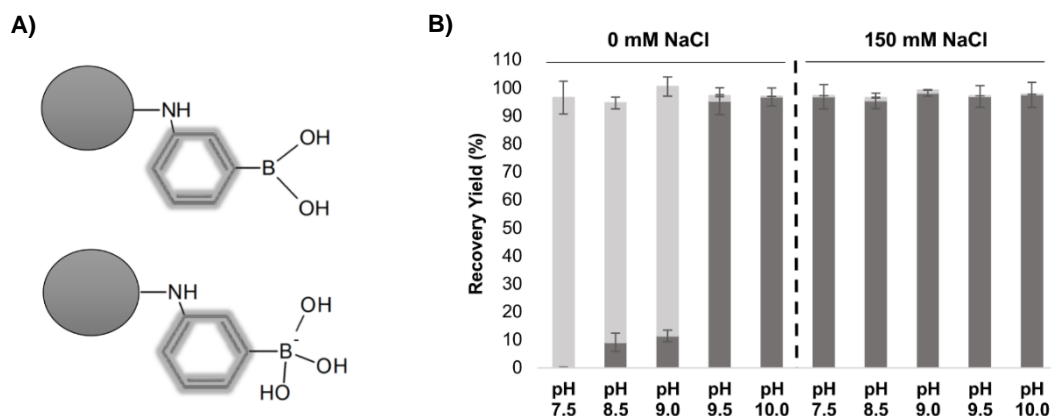


Figure II.4 Contribution of the phenyl group to the interaction between *m*-APBA agarose-based supports and the anti-IL8 mAb. Studies were performed under different pH and salt concentrations using a phenyl-Sepharose 6 FF resin. (A) Schematics of boronic acid (top) and boronate anion (bottom) structures. The ligand group under study is highlighted. (B) Recovery yields of purified anti-IL8 mAb in flow-through (■) and elution (■) fractions. Results are displayed as mean \pm STDV.

II.3.1.2.2. Evaluation of hydrogen bonding and van der Waals interactions

The non-specific interaction of the anti-IL8 mAb with the matrix of the stationary phase (agarose) through hydrogen bonding and van der Waals interactions was studied using bare Sepharose 6 FF beads, at different pH values (7.5, 8.5 and 9.0) and NaCl concentrations (0 and 150 mM NaCl) (Figure II.5). Using bare Sepharose 6 FF beads (Figure II.5A), no retention was observed whenever 150 mM NaCl was present in the adsorption buffer (Figure II.5B). Once again, a small concentration of salt shows to be able to eliminate any type of non-specific interactions between the ligand and the anti-IL8 mAb. In this case, considering the agarose structure, the non-specific interactions present should be van der Waals interactions and hydrogen bonding between the hydroxyl groups from agarose and the mAb molecule. In the absence of salt in the adsorption buffer, the anti-IL8 mAb was moderately adsorbed to the Sepharose 6 FF beads (Figure II.5B). At pH 7.5, $66 \pm 2\%$ of anti-IL8 mAb was retained against the $15 \pm 3\%$ adsorbed, on average, at pH 8.5 and 9.0. These non-specific interactions are predominant at pH 7.5, with van der Waals forces driven by permanent dipole-induced dipole interactions potentially playing an important role in the anti-IL8 mAb adsorption to the Sepharose 6 FF beads.

Overall, the results demonstrate the moderate importance of van der Waals forces, in particular permanent dipole-induced dipole interactions, in anti-IL8 mAb retention during phenylboronate chromatography, especially at pH 7.5. At this condition, anti-IL8 mAb has a high positive net charge and only the trigonal form of *m*-APBA is present, which presents less steric hindrance than the tetrahedral conformation. This would enable short-range interactions between the mAb molecules and the agarose matrix through hydrogen bonding and van der Waals interactions.

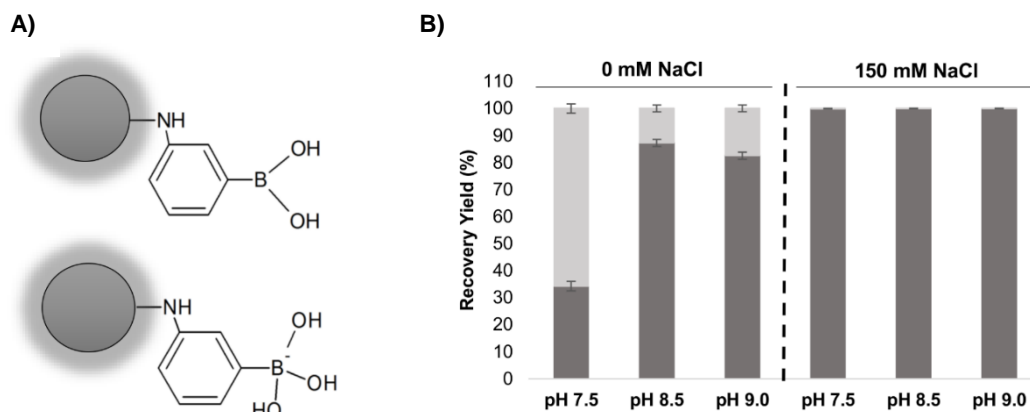


Figure II.5 Contribution of the bare resin to the interaction between *m*-APBA agarose-based supports and the anti-IL8 mAb. Studies were performed under different pH and salt concentrations using a Sepharose 6 FF resin. (A) Schematics of boronic acid (top) and boronate anion (bottom) structures. The ligand group under study is highlighted. (B) Recovery yields of purified anti-IL8 mAb in flow-through (■) and elution (□) fractions. Results are displayed as mean ± STDV.

II.3.1.2.3. Evaluation of ionic interactions: salt tolerance studies

Phenylboronate chromatography has been widely reported as an affinity process, especially under alkaline conditions (pH higher than ligand's pKa). Nonetheless, in Section II.3.1.1., the thermogram obtained for pH 9.0 in the presence of NaCl (Figure II.2F) suggested that *cis*-diol interactions were not exclusive and that electrostatic interactions could be playing an important role, thus raising questions concerning the magnitude of the affinity interaction and the salt tolerance of *m*-APBA, under the pH conditions studied. Considering the conformational changes of the ligand due to pH changes (Figure II.6A) and the results presented in Section II.3.1.1., salt tolerance studies were performed using the *m*-APBA P6XL resins at pH 7.5, 8.5 and 9.0 at increasing salt concentrations (up to 1 M NaCl) and revealed new insights for phenylboronate chromatography (Figure II.6B).

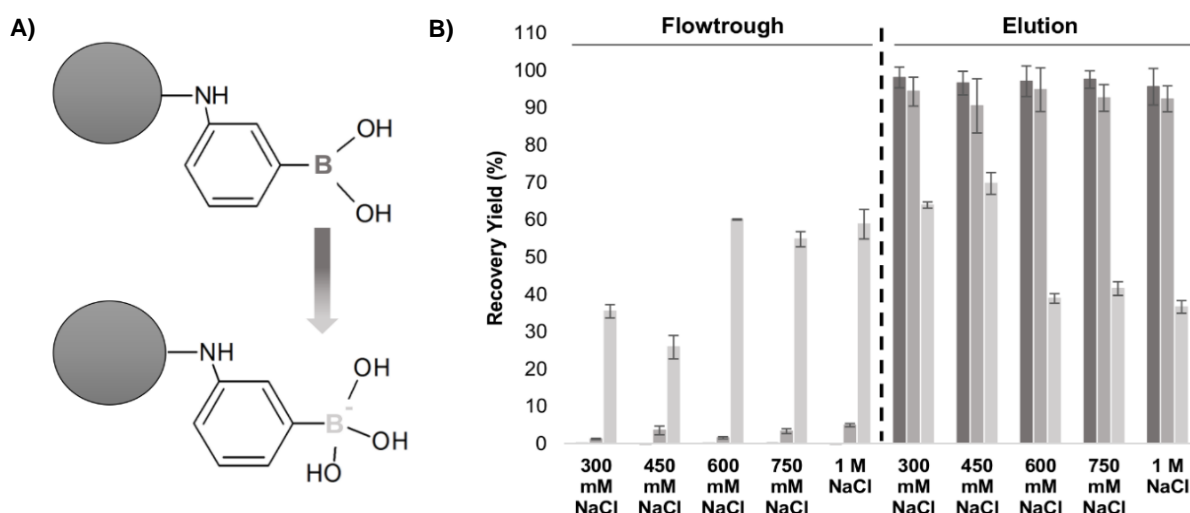


Figure II.6 Evaluation of the contribution of the negative charge present in the ligand (C) to the interaction between *m*-APBA agarose-based supports and the anti-IL8 mAb. Studies were performed under different pH and salt concentrations using an Aminophenylboronate P6XL resin. (A) Schematics of boronic acid (top) and boronate anion (bottom) structures. The ligand groups under study are highlighted. (B) Recovery yields of purified anti-IL8 mAb in flow-through and elution fractions. Buffers composition at pH 7.5 (■), pH 8.5 (■) and 9.0 (□) was 20 mM HEPES, 20 mM EPPS and 20 mM CHES, respectively. Results are displayed as mean ± STDV.

Results showed a high salt tolerance of the trigonal form of *m*-APBA at both pH 7.5, with no flow-through detected at salt concentrations ranging from 300 mM to 1 M NaCl, and pH 8.5, with only $3 \pm 2\%$ of anti-IL8 mAb not being retained for all salt concentrations studied (Figure II.6B). The obtained results are in accordance with the ones described in Sections II.3.1.2.1. and II.3.1.2.2., for pH 7.5 and pH 8.5, which indicates that NaCl has the ability to mitigate non-specific interactions promoted by cation- π interactions, van der Waals forces and hydrogen bonding, thus enhancing the specific *cis*-diol esterification between the anti-IL8 mAb and the ligand. On the other hand, at pH 9.0, the majority of PBA ligand molecules are in the tetrahedral conformation. In this case, the anti-IL8 mAb, although positively charged, presents a low charge density (the pH is very close to the pI). These features, allied with the increment of the salt shielding effect, led to an average anti-IL8 mAb recovery of $31 \pm 7\%$, in the flow-through fractions, for salt concentrations ranging from 300 to 450 mM NaCl (Figure II.6B). When increasing the salt concentration from 600 mM to 1 M NaCl, the average anti-IL8 mAb recovery in the flow-through increased to $58 \pm 3\%$, on average (Figure II.6B). It is important to notice that at 150 mM NaCl, no flow-through was observed. However, the thermogram profile (Figure II.2F) already indicated that electrostatic interactions were involved in the adsorptive process of anti-IL8 mAb with a profile characteristic of an ion-exchange interaction being observed. This profile involves a first endothermic peak (related to the desolvation process) overlapped with an exothermic peak (related with the electrostatic interaction itself). Still, at pH 9.0, *cis*-diol interactions are present and anti-IL8 mAb molecules that engage in the esterification reaction are further recovered after elution with 1.5 M Tris-HCl. Nevertheless, at pH 9.0, the predominant type of interaction is in fact ionic, as suggested by both FMC and salt tolerance studies.

II.3.2. Evaluation of the adsorption of anti-IL8 mAb in presence of different mobile phase modulators

Different strategies to manipulate the separation selectivity in boronate chromatography have been commonly used and may include (i) choosing the appropriate binding buffer composition and (ii) designing and meticulously choosing the proper stationary phases. In the present work, the first strategy was followed. Thus, enhancers of *cis*-diol esterification, such as sodium fluoride (NaF) and magnesium chloride (MgCl_2) were selected [48, 49] and the impact of using a kosmotropic salt as ammonium sulfate ($(\text{NH}_4)_2\text{SO}_4$), studied. The overall goals are: (i) to understand the influence of such mobile phase modulators on the adsorption of a purified anti-IL8 mAb (purity of $99 \pm 1\%$) onto *m*-APBA agarose beads and, (ii) to establish a comparison with the contribution of sodium chloride (NaCl) to the same adsorptive process, presented in Section II.3.1.. Hence, all the solutions were prepared in order to meet the ionic strength (I) of a buffer containing 150 mM NaCl ($I=0.15$). The aforementioned studies were performed at pH values of 7.5, 8.5 and 9.0, considering the *m*-APBA pKa (8.8) and the isoelectric point of the anti-IL8 mAb (≥ 9.3); conditions at which no anti-IL8 mAb was detected in the flow-through fractions.

II.3.2.1. Flow Microcalorimetry (FMC) studies

The results show that anti-IL8 mAb adsorption on P6XL resin in the presence of the different salts tested (Table II.3) is enthalpically driven ($\Delta H_{\text{ads}} < 0$), similarly to what was observed in Section II.3.1.. Also, the net heat of adsorption (ΔH_{ads}) values determined are of the same order of magnitude that the ones obtained previously in Section II.3.1. indicating the presence of the reversible esterification reaction between biomolecule and ligand, in its boronic acid or boronate forms, and probably other enthalpically driven processes as explored in Section II.3.1.. On the other hand, the presence of the mobile phase modulators under study (NaF, MgCl₂ and (NH₄)₂SO₄) originated thermograms with profiles rather distinct from the ones obtained in the presence of NaCl (Figure II.7 vs Figure II.2) suggesting that different mechanisms of interaction might occur. Also, when analysing and comparing the thermograms obtained in the presence of NaF, MgCl₂ and (NH₄)₂SO₄, it is possible to perceive differences within profiles with the majority of the thermograms presenting distinct peaks, which suggest the occurrence of different events during and after the adsorption process (Figure II.7). The de-convoluted heat signals for the experiments in presence of NaF (A, B and C), MgCl₂ (D, E and F) and (NH₄)₂SO₄ (G, H and I), at the different pH values studied (pH 7.5, 8.5 and 9.0), are also represented in Figure II.7.

Thermograms obtained at pH 7.5 in the presence of MgCl₂ and (NH₄)₂SO₄ (Figures II.7D and II.7G) show only one positive peak, characteristic of an exothermic event. However, two positive overlapped peaks are observed in the presence of NaF (Figure II.7A). At pH 8.5 (Figures II.7B, 7E and 7H) and at pH 9.0, in the presence of (NH₄)₂SO₄ (Figure II.7I), the existence of enthalpic events with an endothermic character, involved in the interaction between the anti-IL8 mAb and the ligand, is more prominent when comparing to the results obtained in Section II.3.1.. The thermograms obtained at these conditions present three peaks, where the first and third peaks represent exothermic events and the second peak an endothermic event (negative peak). Despite the similarities between the thermograms in terms of profiles, it is interesting to notice that the duration of the overall process is different. For instance, analysing the results obtained at pH 8.5, it is notorious that the duration of the overall adsorptive process in the presence of (NH₄)₂SO₄ is shorter than the ones taking place in the presence of NaF and MgCl₂, by this order. Nevertheless, the time at which the protein-containing solution is replaced with protein-free mobile phase shows that the heat events involved in the binding of anti-IL8 mAb are the same in the presence of NaF and MgCl₂ (Figures II.7B and II.7E). In the presence of (NH₄)₂SO₄ at both pH 8.5 and 9.0, it can be seen that the events that make part of the adsorption process might be different at some extent since the plug occurs near the maximum of the second exothermic peak and a higher endothermic contribution to the interaction is observed (Figures II.7H and II.7I, Table II.3). Considering the thermograms obtained in the presence of NaF and MgCl₂ at pH 9.0 (Figures II.7C and II.7F), both exhibit profiles characteristic of ionic interactions [25, 26] suggesting that the pH has a key role in modulating the adsorption process, also in the presence of these salts.

Table II.3 Heat of adsorption for the anti-human IL-8 mAb onto P6XL resin considering a sample loop, adsorbent volumes and a protein loading of 100 μ L, 171 μ L and 5 mg/mL, respectively. All experiments were performed under a flow-rate of 1.5 mL/h and at a constant ionic strength of 0.15. No flow-through was observed in all the conditions tested. ΔH^I , ΔH^{II} and ΔH^{III} were determined by integration of the individual peaks obtained from the de-convolution of thermograms using PeakFit software (Figure II.7). Results are displayed as mean \pm STDV. RSD stands for relative standard deviation.

Buffer	pH	Salt	Salt concentration (mM)	Exothermic events (kJ/mol)		Endothermic events (kJ/mol)	Net heat of adsorption (kJ/mol)	
				ΔH^I	ΔH^{II}	ΔH^{III}	ΔH_{ads}	RSD (%)
20 mM HEPES	7.5	NaF	150	-254.2 \pm 8.84	-131.4 \pm 19.6	0	-385.6 \pm 19.4	5.0
		MgCl ₂	50	-342.0 \pm 47.2	0	0	-342.0 \pm 47.2	14
		(NH ₄) ₂ SO ₄	50	-329.5 \pm 18.2	0	0	-329.5 \pm 18.2	5.5
20 mM EPPS	8.5	NaF	150	-33.79 \pm 1.80	-250.3 \pm 17.5	109.3 \pm 2.90	-174.8 \pm 16.4	9.4
		MgCl ₂	50	-55.86 \pm 9.52	-287.8 \pm 42.3	252.3 \pm 38.4	-91.35 \pm 12.7	14
		(NH ₄) ₂ SO ₄	50	-76.10 \pm 7.40	-1141 \pm 282.7	1130 \pm 278	-87.22 \pm 3.03	3.5
20 mM CHES	9.0	NaF	150	-625.4 \pm 4.65	0	506.4 \pm 23.1	-119.1 \pm 14.1	12
		MgCl ₂	50	-557.9 \pm 6.70	0	449.1 \pm 11.2	-108.8 \pm 4.38	4.0
		(NH ₄) ₂ SO ₄	50	-75.34 \pm 2.21	-970.0 \pm 360.8	907.7 \pm 358	-137.7 \pm 0.45	0.33

$$\Delta H_{ads} = \Delta H^I + \Delta H^{II} + \Delta H^{III}$$

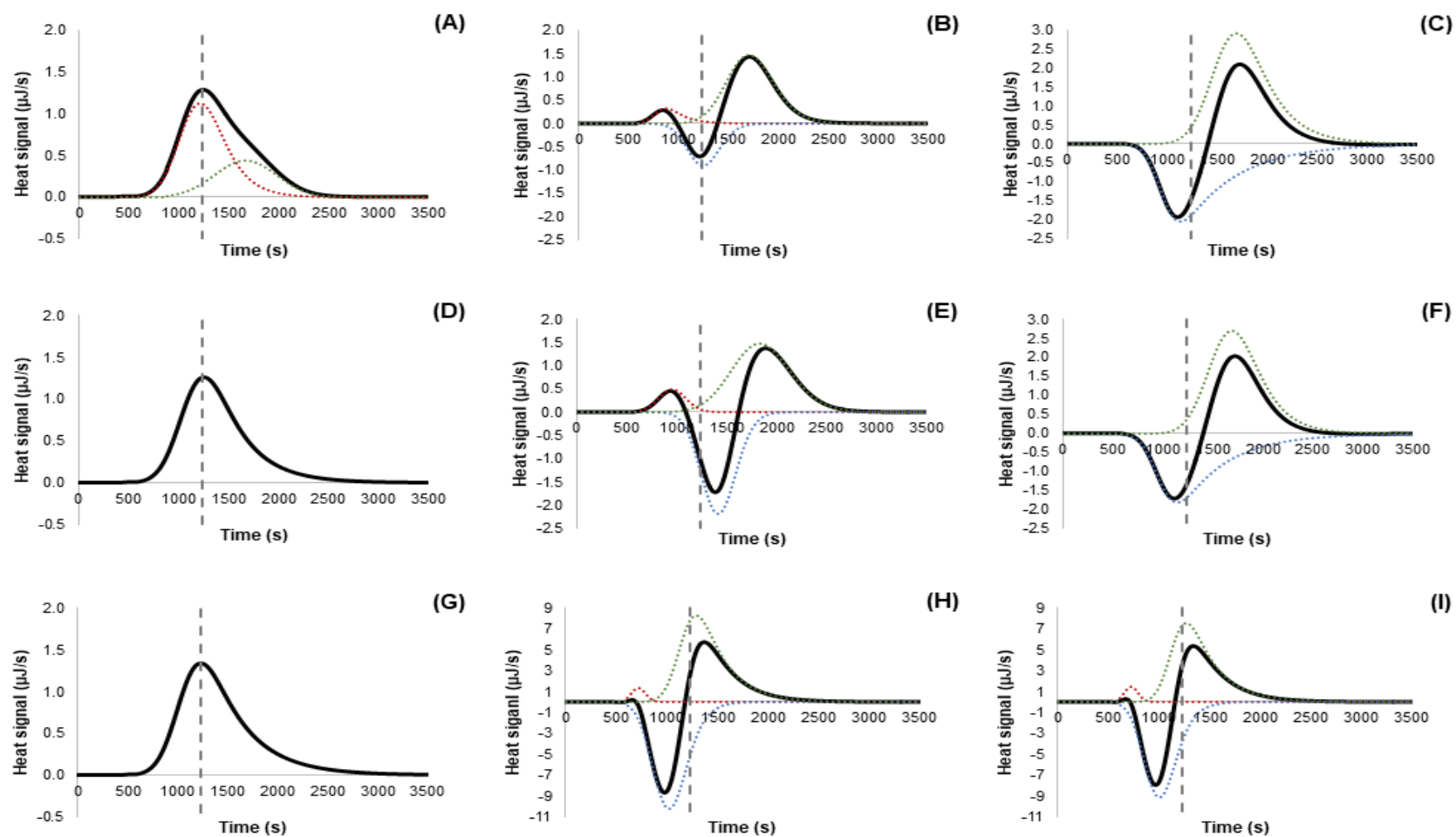


Figure II.7 PeakFit de-convolution of thermograms obtained for the anti-IL8 mAb (5 mg/mL) adsorption onto P6XL resin at different pH values (pH 7.5, 8.5 and 9.0) and salt types (NaF, MgCl₂ and (NH₄)₂SO₄). Injection loop: 100 μL. Mobile phase flow-rate: 1.5 mL/h. (A) 20 mM HEPES, 150 mM NaF, pH 7.5, (B) 20 mM EPPS, 150 mM NaF, pH 8.5, (C) 20 mM CHES, 150 mM NaF, pH 9.0, (D) 20 mM HEPES, 50 mM MgCl₂, pH 7.5, (E) 20 mM EPPS, 50 mM MgCl₂, pH 8.5, (F) 20 mM CHES, 50 mM MgCl₂, pH 9.0, (G) 20 mM HEPES, 50 mM (NH₄)₂SO₄, pH 7.5, (H) 20 mM EPPS, 50 mM (NH₄)₂SO₄, pH 8.5 and (I) 20 mM CHES, 50 mM (NH₄)₂SO₄, pH 9.0. Curves represented are for total peak fit (black line) and peaks resulting from de-convolution (endothermic peaks – blue dotted lines and exothermic peaks – red and green dotted lines). Vertical dashed lines represent the time at which the protein-containing plug of solution is replaced with protein-free mobile phase.

II.3.2.2. Adsorption studies in presence of a Lewis base - NaF

In terms of heat profiles, considerable changes were observed in the presence of NaF at pH 7.5, 8.5 and 9.0 (Figures II.7A, 7B and 7C, respectively). The successive increment on the working pH resulted in profile changes that were accompanied by a decrease of around 55% and 70% in the net heat of adsorption (ΔH_{ads} , Table II.3). This kind of response was also observed in the presence of NaCl, from pH 7.5 to pH 9.0 (ΔH_{ads} , Table II.1).

Inorganic anions such as fluoride have been used to modulate the retention of *cis*-diol containing compounds. The coordination effect of this Lewis base has been shown to enhance the complexation of saccharides with boronate under less basic conditions [3] which can be corroborated by the increment on the net heat of adsorption at pH 7.5 in presence of NaF, when comparing to the values obtained at the conditions studied in Section II.3.1.1.2. (ΔH_{ads} , Table II.3 vs Table II.1). Nevertheless, it is interesting to note that, at pH 7.5, the enthalpy values of the first exothermic peaks obtained in the presence of NaF and NaCl are similar (ΔH^I , Table II.3 vs Table II.1). As mentioned in Section II.3.1.1.2., this exothermic peak results mainly from the *cis*-diol esterification reaction between the anti-IL8 mAb and the trigonal form of the *m*-APBA ligand, predominant at this condition. The second exothermic peak could be justified by the presence of fluoroboronates ($R-B(OH)_2F$), as illustrated in Figure II.8B. At pH 7.5, the anti-IL8 mAb adsorbed to trigonal boronic acids (major form) can thus re-adsorb onto free tetrahedral fluoroboronates (minor form) that establish more thermodynamically stable interactions ($K_{trig} < K_{tet}$). The overlapping nature of this peak as the time at which the protein-containing solution is replaced with protein-free mobile phase occurs, indicates that the events are taking place simultaneously and that a small part of the interaction between some anti-IL8 mAb molecules and the ligand is performed within the tetrahedral conformation (Figure II.7A).

Thermogram profiles obtained at pH 8.5 and 9.0 (Figures II.7B and II.7C) demonstrate that endothermic events have a major role in the adsorption process under study, which is in accordance with the lower ΔH_{ads} , exhibited in Table II.3. The profile changes are probably related to the increased presence of the boronate anion in the ligand structure (mainly due to the shift in the acid-base equilibrium caused by the increase in the pH), which is able to promote electrostatic interactions with the anti-IL8 mAb. For this type of interactions to occur, water and ions have to be released from the surface of the adsorbent and protein, which leads to a consumption of energy and to an increase of entropy [42, 43]. At pH 9.0, the ligand will be predominantly present in its tetrahedral forms – the ones obtained by hydroxylation of the boronic acid or by B-F coordination (Figures II.8A and II.8B). At this pH, considering the formal charge of the boronate anion, all the structures are prone to participate in ionic interactions with the anti-IL8 mAb. However, salt tolerance studies performed, using increasing NaCl concentrations (300 mM to 1 M NaCl), showed that at all pH conditions, the ligand presents high salt tolerance. Even at pH 9.0, in average, only $2.2 \pm 0.8\%$ of anti-IL8 mAb was not retained (Figure II.9). This fact demonstrates, once more, the ability of NaF to promote the specific interactions between the boronate and *cis*-diol containing molecules at all pH values, in comparison to the use of NaCl. The salt tolerance of the ligand at pH 9.0, in the presence of NaCl, is, by far, smaller, with anti-IL8 mAb losses of around 58% being observed when 1 M NaCl is added (Section II.3.1.2.3.). These findings are mostly due to the

type of interaction that occur between the mobile phase modulator and the ligand. In the presence of NaF, the *cis*-diol interactions are predominant, also at pH 9.0, since the effective negative charge of the boron turns to be less available to be part of an ionic interaction with the anti-IL8 mAb [50]. As the B-F bond is an ionic bond and the fluoride ion is the most electronegative of the atoms present, it is expected that the boron gets less negatively charged or even positively charged [51]. This can happen because during binding, there is a complete transfer of valence electrons between atoms. On the other hand, the B-O and O-H bonds are strong polar covalent chemical bonds and the B-Cl is a polar bond [51]. Since the difference in electronegativity between these atoms is smaller, the effective negative charge of the boron anion is more available for the establishment of electrostatic interactions with the anti-IL8 mAb.

Furthermore, the contribution of the matrix and the phenyl group constituent of the *m*-APBA ligand towards the adsorption process was evaluated. The results showed that non-specific interactions with (i) the bare bead composed by Sepharose and (ii) the phenyl ring intrinsic to the *m*-APBA structure were mitigated in the presence of NaF, at all pH conditions tested (data not shown). The same had been already reported to occur in the presence of NaCl [12, 13] with the results of Sections II.3.1.2.1 and II.3.1.2.2. corroborating these statements.

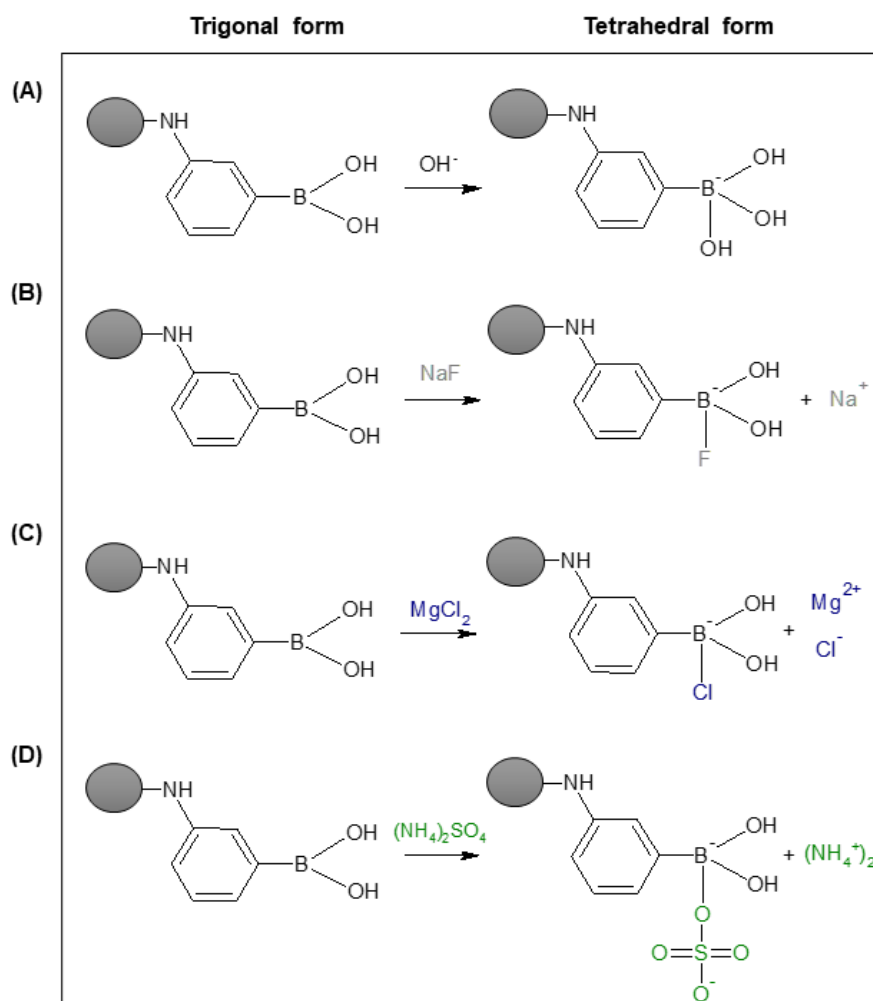


Figure II.8 Schematics on the influence of the pH (A) and the presence of the mobile phase modulators NaF (B), MgCl_2 (C) and $(\text{NH}_4)_2\text{SO}_4$ (D) on the *m*-APBA ligand conformation.

II.3.2.3. Adsorption studies in presence of a chaotropic salt - $MgCl_2$

The addition of $MgCl_2$ to the mobile phase resulted in thermogram profiles similar to the ones obtained in the presence of NaF, except at pH 7.5 (Figures II.7D, 7E and 7F). Nonetheless, the net heat of adsorption value determined at this pH is very similar to the one obtained in presence of NaF (ΔH_{ads} , Table II.3). At pH 7.5, it was expected to observe two exothermic peaks, coincident with the presence of the PBA ligand in the trigonal and tetrahedral forms, the latter obtained through B-Cl coordination leading to the formation of a tetrahedral chloroboronate ($R-B(OH)_2Cl$) (Figure II.8C). Both ligand conformations may be present; however, the contribution of the tetrahedral form seems to be negligible since no second exothermic peak is observed in the thermogram (Figure II.7D). The presence of only one exothermic peak can be justified by the ability that divalent cations as Mg^{2+} have to stabilize the anionic boronate complex through the formation of an ion pair [52-54]. This shielding of the negative charge of the chloroboronate is certainly beneficial to the anti-IL8 mAb adsorption onto the ligand through the specific *cis*-diol esterification. However, the specificity of the interaction can be compromised by an increase in the divalent cation concentration since it can also contribute to the intensification of non-specific interactions promoted by coordination interactions between the hydroxyl groups of *m*-APBA and the magnesium ion [52, 54]. These conclusions are in accordance with results obtained from experiments performed using the same buffer composition but with bare and phenyl-Sepharose beads, that showed no anti-IL8 mAb adsorption onto the bare beads nor towards the phenyl ring, at pH 7.5 (data not shown). Nevertheless, a very small contribution of hydrophobic effects was observed at pH 8.5 and 9.0 with $5.7 \pm 0.1\%$ of the anti-IL8 mAb being adsorbed onto the phenyl-Sepharose resin, on average. It is known that magnesium is also likely to cause a redistribution of the π electron cloud over the ligand, thus possibly affecting π - π complexation [52].

Similar to what was observed at pH 9.0 in the presence of NaF and NaCl, a decrease of about 70% in net heat of adsorption was observed in the presence of $MgCl_2$ at pH 8.5 and 9.0 (ΔH_{ads} , Table II.3). Despite of the decrease in ΔH_{ads} observed at pH 8.5, the high salt tolerance of the ligand was maintained (data not shown). Nevertheless, at pH 9.0, the ligand presented a slight decrease on its salt tolerance due to the existence of electrostatic interactions promoted by hydroxylation of the boron atom and B-Cl coordination (Figures II.8A and 8C, respectively). Indeed, the presence of this type of interactions was already expected. The thermogram obtained was similar to the ones obtained, at the same pH in presence of NaF (Figure II.7F vs II.7C) and NaCl (Figure II.2F), reinforcing the idea that the pH is the major modulatory element of the adsorption process, also in the presence of these salts. Parallel experiments were performed in order to corroborate such conclusions using increasing NaCl concentrations (300 mM to 1 M) on the elution buffer, which led to an increase on the loss of anti-IL8 mAb – around $8.7 \pm 0.4\%$ in the presence of 1 M NaCl (Figure II.9). Nevertheless, the addition of the different type of salts seems to have some modulatory effect. Comparing the addition of NaCl to the mobile phase, described in Section II.3.1., to the addition of $MgCl_2$ in this work, the presence of the magnesium cation led to a drastic increase in the salt tolerance of the bond between the anti-IL8 mAb and the ligand (Figure II.9 vs II.6). Since the B-Cl coordination can occur in both cases (*i.e.* in the presence of $MgCl_2$ and NaCl, as shown in Figure II.8C), it can be reaffirmed that is not the anion but the

metal cation that determines the salt tolerance modulation. In addition to the shielding effect of the anion boron charge achieved with Mg^{2+} , it may be possible to have the divalent cation interacting with the anti-IL8 mAb decreasing the ionic repulsion between carboxylates (e.g. from aspartic and glutamic acid residues) and the boronate ligand [52]. Nevertheless, this last type of interactions can occur with any negatively charged protein present. In this way, when evaluating the performance of the ligand with an artificial mixture and/or a real cell culture supernatant, the presence of $MgCl_2$ could be important to promote the binding of the anti-IL8 mAb but could also be responsible for the adsorption of some protein impurities which will lead to a decrease in the selectivity of the ligand towards glycoproteins such as mAbs.

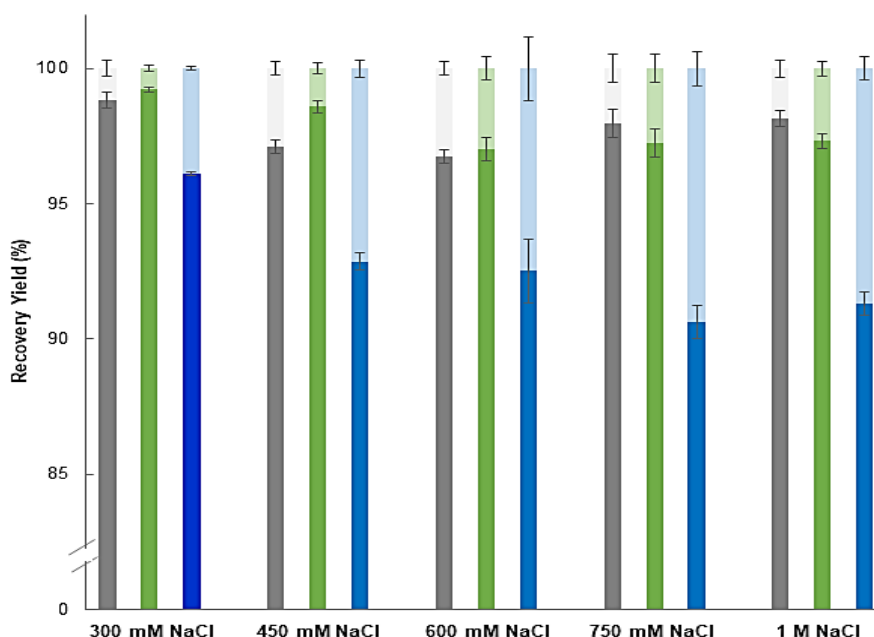


Figure II.9 Evaluation of the boronate anion contribution for ionic interactions between the aminophenylboronate P6XL resin and anti-IL8 mAb at pH 9.0 using different salts – NaF, 150 mM (■), $(NH_4)_2SO_4$, 50 mM (■) and $MgCl_2$, 50 mM (■). Recovery yields of purified anti-IL8 in elution (lighter colors) and stripping fractions (darker colors) using boronate chromatography. Adsorption and elution studies were performed with buffers containing 20 mM CHES, pH 9.0. Column stripping was accomplished with 1.5 M Tris-HCl, pH 8.5. Results are displayed as mean \pm STDV.

II.3.2.4. Adsorption studies in presence of a kosmotropic salt - $(NH_4)_2SO_4$

The thermogram profiles obtained in the presence of $(NH_4)_2SO_4$ (Figures II.7G, 7H and 7I) demonstrate that the type of events involved in the adsorption of anti-IL8 mAb onto the *m*-APBA ligand, at pH 8.5 and 9.0, are predominantly the same. The exception occurred at pH 7.5 where only one exothermic peak was obtained, as observed in the presence of $MgCl_2$ (Figure II.7G vs II.7D). The presence of the SO_4^{2-} anion can lead to the formation of negatively charged tetrahedral sulfoboronates ($R-B(OH)_2SO_4$) (Figure II.8D). The latter can be obtained by the coordination of the SO_4^{2-} anion and the trigonal uncharged form of the ligand. The described interaction is achieved by charge transfer from the SO_4^{2-} anion to the boron with an empty orbital present in the ligand, at pH 7.5. However, the existence of just one exothermic peak show that the presence negatively charged boron as no impact in the

interaction between the anti-IL8 mAb and the ligand. This fact could be due to the ability that NH_4^+ cations have to stabilize the negative charge of the boron, as occurred in the presence of Mg^{2+} , by the establishment of a hydrogen bond between the boronate anion and the protonated N-atom, as previously described [55]. Moreover, the values of net heat of adsorption obtained at pH 7.5 and in the presence of 50 mM $(\text{NH}_4)_2\text{SO}_4$ are in line with those obtained with other salt types at the same pH (ΔH_{ads} , Table II.3), indicating the prevalence of a reversible esterification between the trigonal form of boronic acid and the *cis*-diol containing anti-IL8 mAb.

When analysing the net heat of adsorption (ΔH_{ads}) obtained at pH 8.5 and 9.0, it can be concluded that, again, the increase of the pH value modulates the interaction between the anti-IL8 and the ligand. Similar to what was obtained in presence of NaF and MgCl_2 , a decrease between 60 to 75% is observed in the ΔH_{ads} values when comparing the values obtained at pH 7.5 to the ones obtained at pH values of 8.5 and 9.0 (ΔH_{ads} , Table II.3). It is also possible to observe a shift in the thermogram profiles when the working pH is increased from 7.5 to pH values of 8.5 and 9.0 (Figure II.7G vs 7H and 7I), as previously indicated. Thermogram profiles obtained at pH 8.5 and 9.0 are the same and similar to the ones obtained in the presence of NaF and MgCl_2 at pH 8.5, with the main differences residing in the intensity of the last two peaks and in the duration of each event and of the overall process (Figure II.7H vs Figures II.7B and 7E). The latter difference shows that during the adsorption process under study, a series of events that turns the process more endothermic should occur. These events could be related to the strong solvation energy characteristic of kosmotropic ions such as SO_4^{2-} , associated with a high solvation capacity of the salt and therefore to a low solvation of the anti-IL8 mAb [56]. Such features are more pronounced as the salt concentration is increased, but can also occur at lower concentrations [57], especially for large biomolecules as mAbs. Since at pH 8.5 and 9.0, the tetrahedral boronate is the predominant conformation of the ligand, non-specific interactions such as electrostatic interactions, are able to occur. The increased intensities of heat signals, as the higher contribution of entropic events to the adsorption process, could be related to the release of water molecules and ions from the surfaces of the adsorbent and protein, necessary to the establishment of the electrostatic interactions [42, 43]. Nevertheless, it is interesting to observe that the de-convoluted peaks, especially the first exothermic peak, do not differ between pH values of 8.5 and 9.0 in terms of heat signal (Figure II.7 and ΔH^1 , Table II.3), suggesting that no major differences exist in the adsorption process within these conditions.

Moreover, additional experiments showed that the use of $(\text{NH}_4)_2\text{SO}_4$ acted as a suppressor of non-specific interactions that could occur between the anti-IL8 mAb and the bare and phenyl-Sepharose beads, at all the pH conditions under study (data not shown). Also, it was concluded that the ability of the *m*-APBA ligand to establish *cis*-diol esterification interactions with the anti-IL8 mAb was enhanced at pH 9.0, when compared to the results achieved in the presence of MgCl_2 (Figure II.9) and, particularly, NaCl (Figure II.6). The percentage of the anti-IL8 mAb eluted with 1 M NaCl was only of $2.7 \pm 0.3\%$ at pH 9.0, a very similar result to one obtained in the presence of NaF (Figure II.9). This result could be explained by the coordination of SO_4^{2-} to the boron (Figure II.8D). The difference in electronegativity between the boron and the sulfate anion will turn the negative charge of the boron less available to participate in electrostatic interactions with anti-IL8 mAb molecules. In this case, we are not in the presence of an ionic bond, as in the B-F case (Figure II.8B), but the polar covalent bonds B-O (strong)

and S-O are sufficient to delocalize the negative charge of the boron to the negative oxygen atom, as a result of the SO_4^{2-} coordination (Figure II.8D). The same could also be valid when using phosphate buffers and, indeed, an increase in the affinity of PBA towards uncharged *cis*-diol containing molecules was reported by others, using increasing concentrations of this buffer [49]. HPO_4^{2-} and PO_4^{3-} behave like as Lewis bases, coordinating with the boron atom [49, 55]. As result of the coordination process, the negative charge of the boron will be delocalized to the phosphorus atom as to its adjacent oxygen atoms.

II.4. Conclusions

In this work, it was shown that FMC is highly valuable to illustrate and thermodynamically quantify the mechanisms underlying the adsorption of anti-IL8 mAbs towards PBA, including the role of non-specific effects. The knowledge acquired about the adsorption mechanisms contributes towards a better understanding on how to manipulate the environmental conditions in order to increase the salt tolerance of the bond between PBA and the anti-IL8 mAb. It was shown that such feature can be accomplished by, on one hand, promoting the specific *cis*-diol interactions between PBA and the anti-IL8 mAb and, on the other hand, by diminishing the non-specific interactions involved in the adsorptive process, especially at pH values above the ligand pKa.

For the adsorption studies of anti-IL8 mAb on the *m*-APBA ligand in absence of salt and in presence of NaCl, the ΔH_{ads} obtained for conditions where *cis*-diol interactions are predominant was approximately -243 ± 38 kJ/mol whereas at pH 9.0, 150 mM NaCl – condition under which *cis*-diol esterification is not the main interaction – a value of -82 ± 14 kJ/mol was achieved. For the latter, the decrease in ΔH_{ads} and the total shift observed in the thermogram were indicative of the presence of electrostatic interactions between the protein and the ligand, which was also corroborated by salt tolerance studies. The results also demonstrate the multimodal behaviour of the interaction and not only the affinity-based esterification process that has been described for years. Additional studies also confirmed that anti-IL8 mAb adsorption to *m*-APBA depends on the pH and salt concentration of the adsorption buffer and that a salt concentration of 150 mM is sufficient to mitigate non-specific interactions. The interaction between *m*-APBA and anti-IL8 mAb showed high salt tolerance with retentions between 97 and 100% being observed at pH values lower than the pKa of the ligand and salt concentrations up to 1 M NaCl. When *m*-APBA is present in the tetrahedral conformation, it also behaves as a cation exchanger and, consequently, a lower salt tolerance is observed. Adsorption yields of $67 \pm 4\%$ were obtained with 300 to 450 mM NaCl, against only $39 \pm 3\%$ in the presence of 600 mM to 1 M NaCl. The remaining anti-IL8 mAb was retained by the specific *cis*-diol interaction, which is still present, revealing the multimodal character of this ligand, especially at pH 9.0.

The adsorption process in presence of different mobile phase modulators such as NaF, MgCl_2 and $(\text{NH}_4)_2\text{SO}_4$ was also characterized as enthalpically driven at all conditions tested, as expected. However, the ΔH_{ads} obtained at pH 7.5 was slightly higher - approximately -352.3 ± 29.5 kJ/mol – than the values obtained in absence of salt or presence of NaCl. These results corroborate the fact that such salts could enhance the complexation of saccharides with boronate under less basic conditions. Nevertheless, as

the pH increases and reaches the pKa, the structure of the ligand changes from a trigonal neutral conformation to a tetrahedral negatively charged conformation and the ΔH_{ads} decreases from 55% to 75% at pH 8.5 and 9.0. The reduction in ΔH_{ads} and thermogram shifts that occurred with the increase in the pH, show that FMC is able to disclose the impact that ligand conformational changes and formal charges have on anti-IL8 mAb adsorption. However, only when performing parallel experiments, it could be concluded that the salt tolerance of the ligand was improved using different mobile phase modulators. The use of salts, such as NaF, MgCl₂ and (NH₄)₂SO₄, demonstrated to mitigate non-specific interactions with the agarose matrix and with the phenyl group present on the *m*-APBA ligand structure, except in the presence of MgCl₂ at pH 8.5 and 9.0. The results obtained for these conditions showed a slight contribution of the hydrophobic moiety of the ligand in the adsorption of the anti-IL8 mAb, with $5.7 \pm 0.1\%$ of the anti-IL8 mAb being adsorbed to a phenyl-Sepharose resin. Experiments concerning the evaluation of the salt tolerance at pH 9.0, demonstrated that electrostatic interactions, between the protein and the ligand, were diminished by the use of the mobile phase modulators tested. In some cases, this decrease was associated with the ability that some cations (Mg²⁺ and NH₄⁺) have to stabilize the boron anion or with differences in the electronegativity between the anions used (F⁻ and SO₄²⁻) and the boron atom. The decrease in the electrostatic interactions contribution to the adsorptive process of the anti-IL8 mAb was of high importance to the increase of the ligand salt tolerance, with the best results being obtained in the presence of NaF and (NH₄)₂SO₄.

Overall, the information retrieved through FMC and other analytical techniques provide us a better understanding of the biomolecular phenomena involved in *m*-APBA – anti-IL8 mAb interaction. A deeper knowledge about the underlying mechanisms of this adsorption process could contribute towards the effective integration of boronate chromatography in the current mAb downstream processing platform. Moreover, the use of FMC in combination with other analytical methods, (e.g. surface plasmon resonance and small-angle X-ray scattering) can be foreseen with the aim of significantly shortening chromatography process development by designing and developing models that can be applied to better fit and predict the biomolecular phenomena.

II.5. References

- [1] A.E. Ivanov, H.A. Panahi, M.V. Kuzimenkova, L. Nilsson, B. Bergenståhl, H.S. Waqif, M. Jahanshahi, I.Y. Galaev, B. Mattiasson, Affinity Adhesion of Carbohydrate Particles and Yeast Cells to Boronate-Containing Polymer Brushes Grafted onto Siliceous Supports, *Chem-Eur J*, 12 (2006) 7204-7214.
- [2] R.J. Carvalho, J. Woo, M.R. Aires-Barros, S.M. Cramer, A.M. Azevedo, Phenylboronate chromatography selectively separates glycoproteins through the manipulation of electrostatic, charge transfer, and cis-diol interactions, *Biotechnol J*, 9 (2014) 1250-1258.
- [3] L. Ren, Z. Liu, M. Dong, M. Ye, H. Zou, Synthesis and characterization of a new boronate affinity monolithic capillary for specific capture of cis-diol-containing compounds, *J Chromatogr A*, 1216 (2009) 4768-4774.
- [4] A.G. Gomes, A.M. Azevedo, M.R. Aires-Barros, D.M.F. Prazeres, Studies on the adsorption of cell impurities from plasmid-containing lysates to phenyl boronic acid chromatographic beads, *J Chromatogr A*, 1218 (2011) 8629-8637.
- [5] I. Percin, N. Idil, A. Denizli, RNA purification from *Escherichia coli* cells using boronated nanoparticles, *Colloid Surface B*, 162 (2018) 146-153.
- [6] X.C.S. Liu, W.H., Boronate Affinity Chromatography, in: D.S. Hage (Ed.) *Handbook of Affinity Chromatography*, CRC Press, 2005, pp. 215-229.

- [7] E. Ucakturk, Analysis of glycoforms on the glycosylation site and the glycans in monoclonal antibody biopharmaceuticals, *J Sep Sci*, 35 (2012) 341-350.
- [8] L. Liu, Antibody Glycosylation and Its Impact on the Pharmacokinetics and Pharmacodynamics of Monoclonal Antibodies and Fc-Fusion Proteins, *J Pharm Sci*, 104 (2015) 1866-1884.
- [9] B. Zhang, S. Mathewson, H. Chen, Two-dimensional liquid chromatographic methods to examine phenylboronate interactions with recombinant antibodies, *J Chromatogr A*, 1216 (2009) 5676-5686.
- [10] L.I. Bosch, T.M. Fyles, T.D. James, Binary and ternary phenylboronic acid complexes with saccharides and Lewis bases, *Tetrahedron*, 60 (2004) 11175-11190.
- [11] D.G. Hall, Structure, Properties, and Preparation Of Boronic Acid Derivatives. Overview of Their Reactions and Applications, 2nd ed., Wiley-VCH Verlag GmbH & Co. KGaA, Weinheim, Germany, 2011.
- [12] R. dos Santos, S.A.S.L. Rosa, M.R. Aires-Barros, A. Tover, A.M. Azevedo, Phenylboronic acid as a multi-modal ligand for the capture of monoclonal antibodies: development and optimization of a washing step, *J Chromatogr A*, 1355 (2014) 115-124.
- [13] S.A.S.L. Rosa, R. dos Santos, M.R. Aires-Barros, A.M. Azevedo, Phenylboronic acid chromatography provides a rapid, reproducible and easy scalable multimodal process for the capture of monoclonal antibodies, *Sep Purif Technol*, 160 (2016) 43-50.
- [14] A.T. Hanke, M. Ottens, Purifying biopharmaceuticals: knowledge-based chromatographic process development, *Trends Biotechnol*, 32 (2014) 210-220.
- [15] A.L. Grilo, M. Mateus, M.R. Aires-Barros, A.M. Azevedo, Monoclonal antibodies production platforms: an opportunity study of a non protein A chromatographic platform based on process economics, *Biotechnol J*, (2017).
- [16] X.-M. Yuan, D.-Q. Lin, Q.-L. Zhang, D. Gao, S.-J. Yao, A microcalorimetric study of molecular interactions between immunoglobulin G and hydrophobic charge-induction ligand, *J Chromatogr A*, 1443 (2016) 145-151.
- [17] M. Yu, S. Zhang, Y. Zhang, Y. Yang, G. Ma, Z. Su, Microcalorimetric study of adsorption and disassembling of virus-like particles on anion exchange chromatography media, *J Chromatogr A*, 1388 (2015) 195-206.
- [18] F. Cheng, M.Y. Li, H.Q. Wang, D.Q. Lin, J.P. Qu, Antibody-ligand interactions for hydrophobic charge-induction chromatography: a surface plasmon resonance study, *Langmuir*, 31 (2015) 3422-3430.
- [19] J. Hubbuch, M.R. Kula, Confocal laser scanning microscopy as an analytical tool in chromatographic research, *Bioproc Biosyst Eng*, 31 (2008) 241-259.
- [20] M. Boulet-Audet, S.G. Kazarian, B. Byrne, In-column ATR-FTIR spectroscopy to monitor affinity chromatography purification of monoclonal antibodies, *Sci Rep*, 6 (2016) 30526.
- [21] W.K. Chung, A.S. Freed, M.A. Holstein, S.A. McCallum, S.M. Cramer, Evaluation of protein adsorption and preferred binding regions in multimodal chromatography using NMR, *Proc Natl Acad Sci USA*, 107 (2010) 16811-16816.
- [22] K. Srinivasan, S. Parimal, M.M. Lopez, S.A. McCallum, S.M. Cramer, Investigation into the Molecular and Thermodynamic Basis of Protein Interactions in Multimodal Chromatography Using Functionalized Nanoparticles, *Langmuir*, 30 (2014) 13205-13216.
- [23] J. Plewka, G.L. Silva, R. Tscheliessnig, H. Rennhofer, C. Dias-Cabral, A.L. Jungbauer, H. C., Antibody adsorption in protein-A affinity chromatography-in-situ measurement of nanoscale structure by small-angle X-ray scattering, *J Sep Sci*, (2018).
- [24] G.L. Silva, J. Plewka, H. Lichtenegger, A.C. Dias-Cabral, A.T. Jungbauer, R., The pearl necklace model in Protein A chromatography - molecular mechanisms at the resin interface, *Biotechnol Bioeng*, 116 (2019) 76-86.
- [25] G.L. Silva, F.S. Marques, M.E. Thrash Jr, A.C. Dias-Cabral, Enthalpy contributions to adsorption of highly charged lysozyme onto a cation-exchanger under linear and overloaded conditions, *J Chromatogr A*, 1352 (2014) 46-54.
- [26] P.A. Aguilar, A. Twarda, F. Sousa, A.C. Dias-Cabral, Thermodynamic study of the interaction between linear plasmid deoxyribonucleic acid and an anion exchange support under linear and overloaded conditions, *J Chromatogr A*, 1372 (2014) 166-173.
- [27] G.F. Lopes da Silva, J. Plewka, R. Tscheliessnig, H. Lichtenegger, A. Jungbauer, A.C.M. Dias-Cabral, Antibody binding heterogeneity of Protein A resins, *Biotechnol J*, Accepted Author Manuscript (2019).
- [28] F.S. Marques, G.L. Silva, M.E. Thrash Jr, A.C. Dias-Cabral, Lysozyme adsorption onto a cation-exchanger: Mechanism of interaction study based on the analysis of retention chromatographic data, *Colloid Surface B*, 122 (2014) 801-807.

- [29] A. Katiyar, S.W. Thiel, V.V. Guliants, N.G. Pinto, Investigation of the mechanism of protein adsorption on ordered mesoporous silica using flow microcalorimetry, *J Chromatogr A*, 1217 (2010) 1583-1588.
- [30] A.M. Azevedo, A.G. Gomes, L. Borlido, I.F. Santos, D.M. Prazeres, M.R. Aires-Barros, Capture of human monoclonal antibodies from a clarified cell culture supernatant by phenyl boronate chromatography, *J Mol Recognit*, 23 (2010) 569-576.
- [31] L. Borlido, A.M. Azevedo, M.R. Aires-Barros, Extraction of Human IgG in Thermo-Responsive Aqueous Two-Phase Systems: Assessment of Structural Stability by Circular Dichroism, *Sep Sci Technol*, 45 (2010) 2171-2179.
- [32] S.M. Kelly, T.J. Jess, N.C. Price, How to study proteins by circular dichroism, *Biochim Biophys Acta*, 1751 (2005) 119-139.
- [33] A. Bhambhani, J.M. Kissmann, S.B. Joshi, D.B. Volkin, R.S. Kashi, C.R. Middaugh, Formulation design and high-throughput excipient selection based on structural integrity and conformational stability of dilute and highly concentrated IgG1 monoclonal antibody solutions, *J Pharm Sci*, 101 (2012) 1120-1135.
- [34] V. Filipe, A. Hawe, J.F. Carpenter, W. Jiskoot, Analytical approaches to assess the degradation of therapeutic proteins, *TrAC - Trend Anal Chem*, 49 (2013) 118-125.
- [35] E.O. Saphire, P.W.H.I. Parren, R. Pantophlet, M.B. Zwick, G.M. Morris, P.M. Rudd, R.A. Dwek, R.L. Stanfield, D.R. Burton, I.A. Wilson, Crystal Structure of a Neutralizing Human IgG Against HIV-1: A Template for Vaccine Design, *Science*, 293 (2001) 1155-1159.
- [36] G. Springsteen, B. Wang, A detailed examination of boronic acid–diol complexation, *Tetrahedron*, 58 (2002) 5291-5300.
- [37] D. Li, Y. Chen, Z. Liu, Boronate affinity materials for separation and molecular recognition: structure, properties and applications, *Chem Soc Rev*, 44 (2015) 8097-8123.
- [38] K. Tsumoto, D. Ejima, A.M. Senczuk, Y. Kita, T. Arakawa, Effects of salts on protein–surface interactions: applications for column chromatography, *J Pharm Sci*, 96 (2007) 1677-1690.
- [39] M.A. Esquibel-King, A.C. Dias-Cabral, J.A. Queiroz, N.G. Pinto, Study of hydrophobic interaction adsorption of bovine serum albumin under overloaded conditions using flow microcalorimetry, *J Chromatogr A*, 865 (1999) 111-122.
- [40] X.-C. Liu, Boronic Acids as Ligands for Affinity Chromatography, *Chinese Journal of Chromatography*, 24 (2006) 73-80.
- [41] M.B. Smith, J. March, *March's Advanced Organic Chemistry: Reactions, Mechanisms, and Structure*, 6th Edition ed., John Wiley & Sons, Inc., 2007.
- [42] M.E. Thrash, J.M. Phillips, N.G. Pinto, An Analysis of the Interactions of BSA with an Anion-Exchange Surface Under Linear and Non-Linear Conditions, *Adsorption*, 10 (2005) 299-307.
- [43] J. Korfhagen, A.C. Dias-Cabral, M.E. Thrash, Nonspecific Effects of Ion Exchange and Hydrophobic Interaction Adsorption Processes, *Sep Sci Technol*, 45 (2010) 2039-2050.
- [44] D. Gao, D.-Q. Lin, S.-J. Yao, Mechanistic analysis on the effects of salt concentration and pH on protein adsorption onto a mixed-mode adsorbent with cation ligand, *J Chromatogr B*, 859 (2007) 16-23.
- [45] H.-F. Xia, D.-Q. Lin, Z.-M. Chen, S.-J. Yao, Influences of Ligand Structure and pH on the Adsorption with Hydrophobic Charge Induction Adsorbents: A Case Study of Antibody IgY, *Sep Sci Technol*, 46 (2011) 1957-1965.
- [46] M.E. Thrash, Jr., N.G. Pinto, Flow microcalorimetric measurements for bovine serum albumin on reversed-phase and anion-exchange supports under overloaded conditions, *J Chromatogr A*, 908 (2001) 293-299.
- [47] F.-Y. Lin, C.-S. Chen, W.-Y. Chen, S. Yamamoto, Microcalorimetric studies of the interaction mechanisms between proteins and Q-Sepharose at pH near the isoelectric point (pI): Effects of NaCl concentration, pH value, and temperature, *J Chromatogr A*, 912 (2001) 281-289.
- [48] P. Muhammad, D. Li, Z. Liu, Boronate Affinity Chromatography, in: R.A. Meyers (Ed.) *Encyclopedia of Analytical Chemistry*, John Wiley and Sons, Inc, 2015, pp. 1-18.
- [49] M.B. Espina-Benitez, J. Randon, C. Demesmay, V. Dugas, Back to BAC: Insights into Boronate Affinity Chromatography Interaction Mechanisms, *Sep Purif Rev*, 47 (2018) 214-228.
- [50] R. Glaser, N. Knotts, Coordinate Covalent C → B Bonding in Phenylborates and Latent Formation of Phenyl Anions from Phenylboronic Acid, *The Journal of Physical Chemistry A*, 110 (2006) 1295-1304.
- [51] R.H. Petrucci, W.S. Harwood, J.D. Madura, *General Chemistry: Principles and Modern Applications*, Pearson/Prentice Hall, 2007.
- [52] B.M. Brena, F. Batista-Viera, L. Rydén, J. Porath, Selective adsorption of immunoglobulins and glycosylated proteins on phenylboronate-agarose, *J Chromatogr A*, 604 (1992) 109-115.

- [53] R. Tuytten, F. Lemière, E.L. Esmans, W.A. Herrebout, B.J. van der Veken, B.U.W. Maes, E. Witters, R.P. Newton, E. Dudley, Role of Nitrogen Lewis Basicity in Boronate Affinity Chromatography of Nucleosides, *Anal Chem*, 79 (2007) 6662-6669.
- [54] M.A. Wimmer, G. Lochnit, E. Bassil, K.H. Mühling, H.E. Goldbach, Membrane-Associated, Boron-Interacting Proteins Isolated by Boronate Affinity Chromatography, *Plant Cell Physiol*, 50 (2009) 1292-1304.
- [55] J.A. Peters, Interactions between boric acid derivatives and saccharides in aqueous media: Structures and stabilities of resulting esters, *Coordin Chem Rev*, 268 (2014) 1-22.
- [56] Z. Yang, Hofmeister effects: an explanation for the impact of ionic liquids on biocatalysis, *J Biotechnol*, 144 (2009) 12-22.
- [57] O. Esue, A.X. Xie, T.J. Kamerzell, T.W. Patapoff, Thermodynamic and structural characterization of an antibody gel, *mAbs*, 5 (2013) 323-334.

II.6. Supplementary Material

II.S1. Structural characterization of anti-IL8 mAb in the absence of added salt and in presence of NaCl

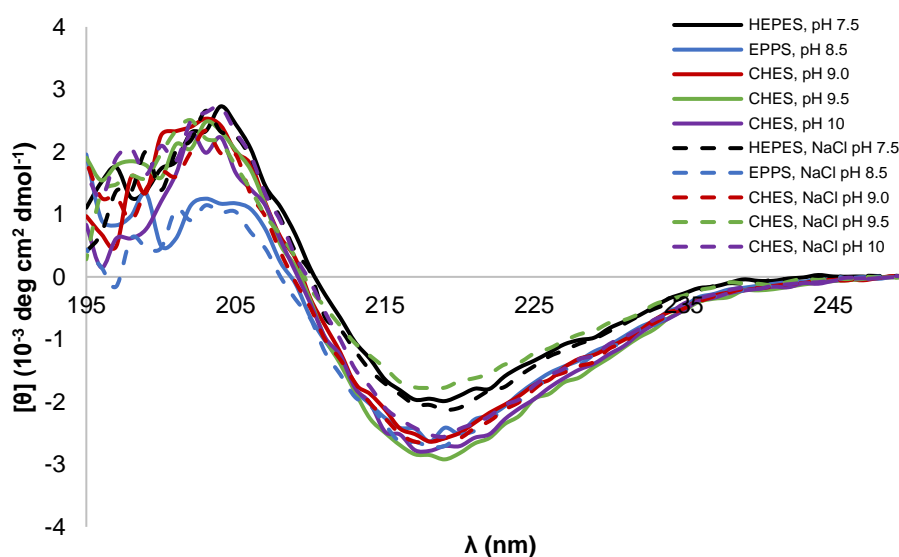


Figure II.S1.1. Anti-IL8 mAb far UV circular dichroism spectra at different pH and salt concentrations – 0 (solid lines) and 150 mM NaCl (dashed lines). Buffers concentration used was 5 mM for all conditions tested.

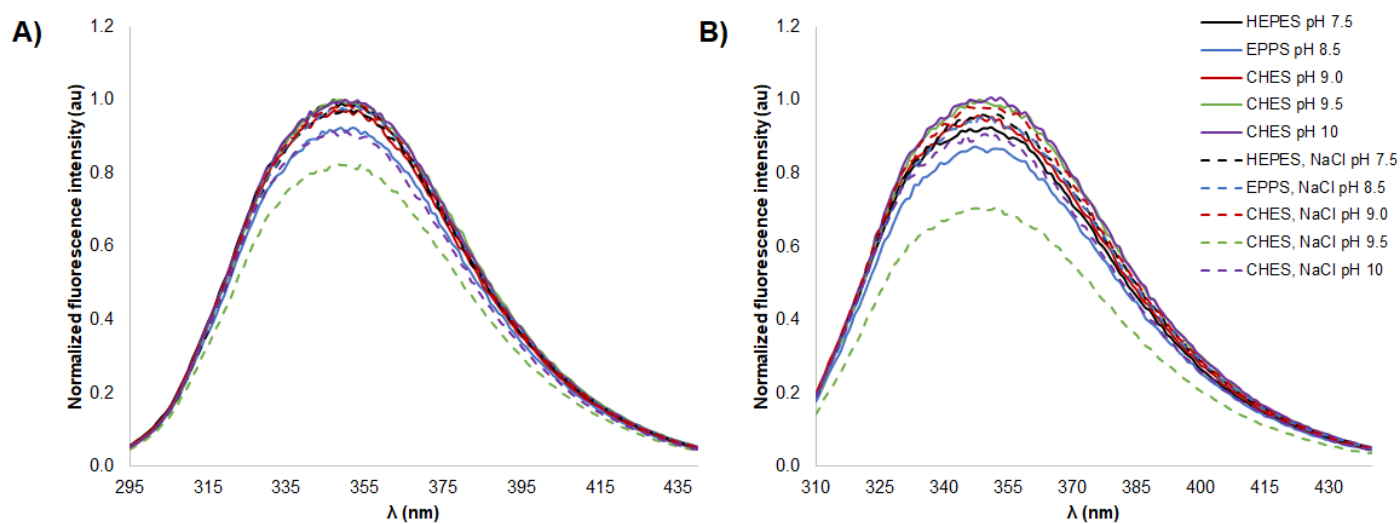


Figure II.S1.2. Fluorescence spectra of (A) Tyrosine at an excitation wavelength of 280 nm and (B) Tryptophan at an excitation wavelength of 296 nm at different pH and salt concentrations – 0 (solid lines) and 150 mM NaCl (dashed lines). Buffers concentration used was 5 mM for all conditions tested. $\lambda(\text{max})$ obtained were similar for all the conditions in both analysis - $\lambda(280 \text{ nm}) = 349.74 \pm 1.08$ and $\lambda(296 \text{ nm}) = 348.96 \pm 1.25$.

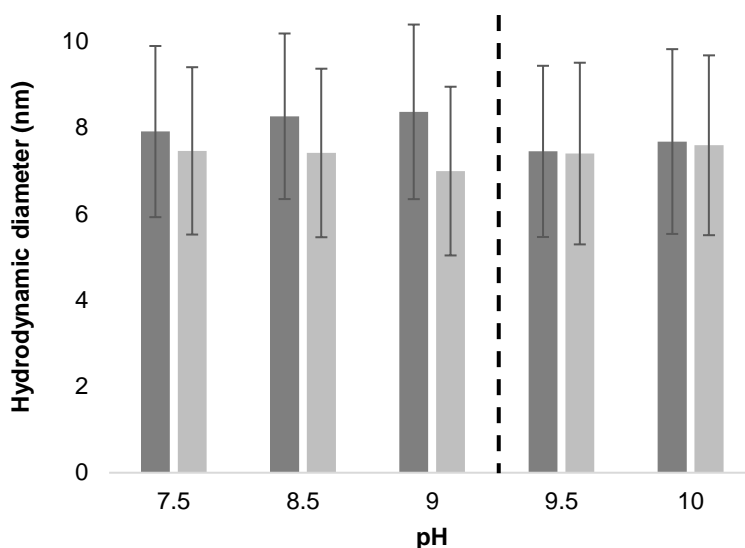


Figure II.S1.3 Size analysis of anti-IL8 mAb at the different working pH and salt concentrations – 0 (dark grey) and 150 mM NaCl (light grey) by dynamic light scattering. Buffer systems used were composed by HEPES for pH 7.5, EPPS for pH 8.5 and CHES for the pH values of 9.0, 9.5 and 10, at a concentration of 20 mM. Results are presented as mean of the hydrodynamic diameter \pm STDV. Results are represented considering the number of particles in solution. The dashed line corresponds to the anti-IL8 mAb pI (≥ 9.3).

II.S2. Structural characterization of anti-IL8 mAb studies in presence of different mobile phase modulators

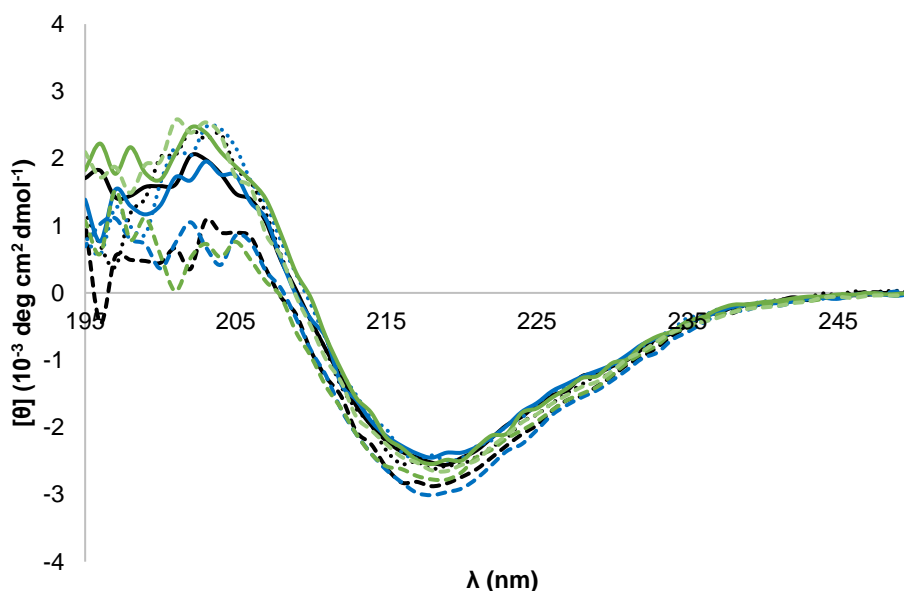


Figure II.S2.1. Anti-IL8 mAb far UV circular dichroism spectra at different pH - 7.5 (full lines), 8.5 (dashed lines) and 9.0 (dotted lines) - and salts – NaF, 150 mM (black lines), MgCl₂, 50 mM (blue lines) and (NH₄)₂SO₄, 50 mM (green lines). Buffer systems used were composed by HEPES for pH 7.5, EPPS for pH 8.5 and CHES for pH 9.0 at a concentration of 5 mM.

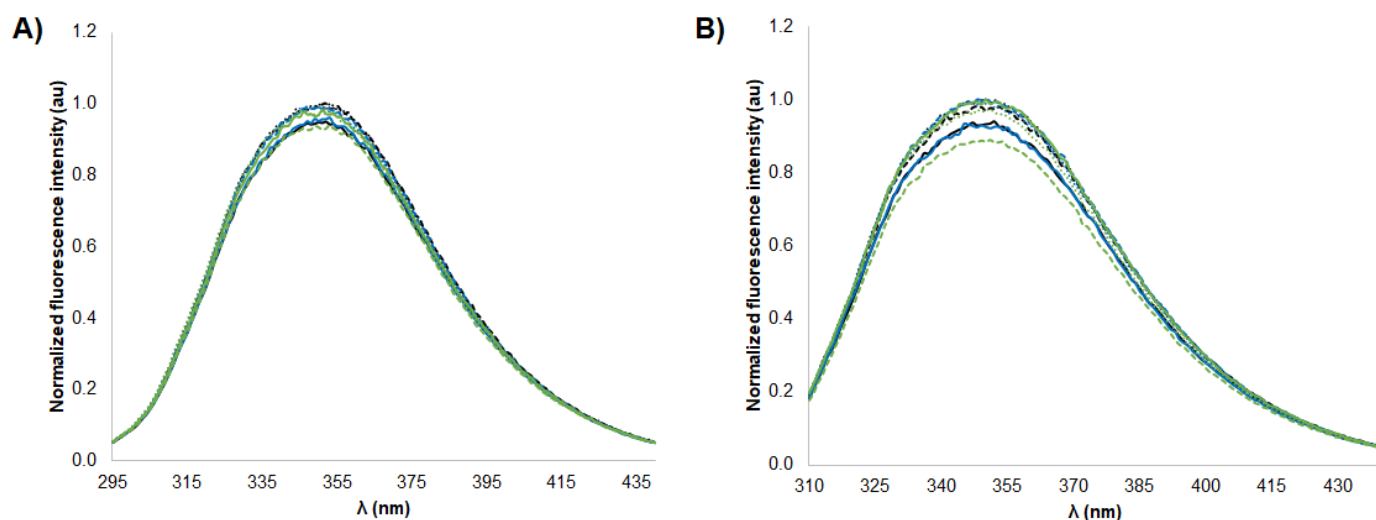


Figure II.S2.2 Fluorescence spectra of (A) Tyrosine at an excitation wavelength of 280 nm and (B) Tryptophan at an excitation wavelength of 296 nm at different pH values - 7.5 (full lines), 8.5 (dashed lines) and 9.0 (dotted lines) - and salts – NaF, 150 mM (black lines), $MgCl_2$, 50 mM (blue lines) and $(NH_4)_2SO_4$, 50 mM (green lines). Buffer systems used were composed by HEPES for pH 7.5, EPPS for pH 8.5 and CHES for pH 9.0 at a concentration of 5 mM. $\lambda(\max)$ obtained were similar for all the conditions in both analysis - $\lambda(280\text{ nm})= 351.48 \pm 1.14$ and $\lambda(296\text{ nm})= 349.36 \pm 1.32$.

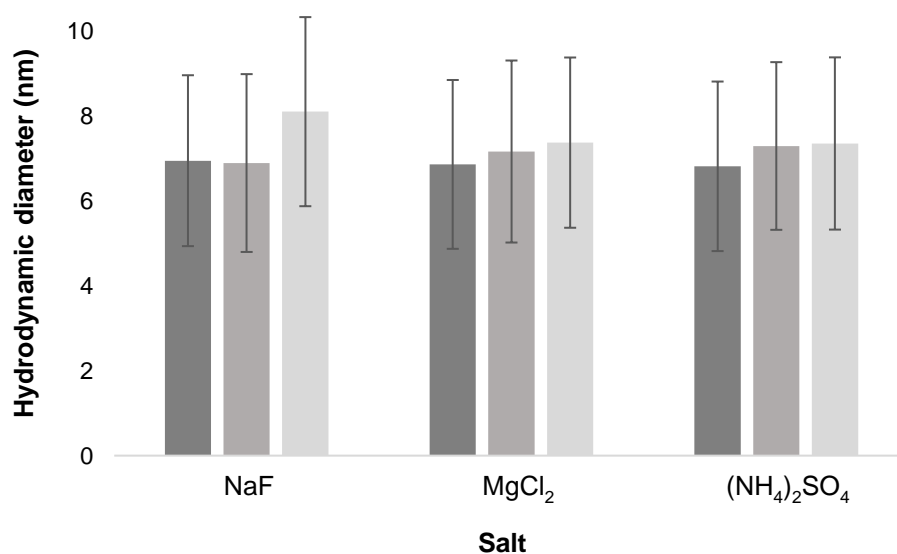


Figure II.S2.3 Size analysis of anti-IL8 mAb at the different working pH - 7.5 (■), 8.5 (■) and 9.0 (■) - and salts – NaF (150 mM), $MgCl_2$ (50 mM) and $(NH_4)_2SO_4$ (50 mM) performed by dynamic light scattering. Buffer systems used were composed by HEPES for pH 7.5, EPPS for pH 8.5 and CHES for the pH value of 9.0, at a concentration of 20 mM. Results are presented as mean of the hydrodynamic diameter \pm STDV. Results are represented considering the number of particles in solution.

Chapter III - Phenylboronic acid chromatography as a rapid, reproducible and easy scalable multimodal process for the capture of monoclonal antibodies²

Abstract: In this work, phenylboronic acid (PBA) was thoroughly investigated as a synthetic and multimodal ligand for the purification of immunoglobulins G (IgG) directly from Chinese Hamster Ovary (CHO) cell culture supernatants. Firstly, the study was focused on the development of a washing step and in the optimization of the elution step using a serum-containing supernatant with anti-human IL-8 monoclonal antibodies (anti-IL8 mAbs). From the different conditions tested, best recoveries - 99% - and purifications – protein purity of 81% and a purification factor of 16 out of a maximum of 20 - were achieved using 100 mM D-sorbitol in 10 mM Tris-HCl as washing buffer and 0.5 M D-sorbitol with 150 mM NaCl in 10 mM Tris-HCl as elution buffer. The purification outcome was also compared with protein A chromatography that revealed a recovery of 99%, 87% protein purity and 29 out of a maximum of 33 purification factor. Following the main purification, purified IgG was characterized in terms of isoelectric point, size and activity. Secondly, and considering the results achieved, in order to test whether the conditions found can be used to purify other mAbs, a proof of concept was performed using two different mAbs from serum-free CHO cell cultures. The mAbs chosen are both IgG1 and are relevant to the health sector. The first - the anti-IL8 mAb – is currently in Phase 1 of clinical development aiming cancer treatment and the second could become a promise to the hepatitis C virus (HCV) treatment. At last, the feasibility of scaling-up PBA chromatography for the purification of anti-IL8 mAbs from clarified serum-free CHO cell cultures was addressed. Column performance optimization regarding superficial velocity and feed volume was performed with the best results being achieved with superficial velocities of 5.1, 15.3 and 25.5 cm/min in the adsorption, wash and elution steps, respectively. The column volume was scale-up 100 times from 0.4 cm³ (laboratory scale) to 4, 16 and 40 cm³ (preparative scale). This 100-fold scale-up was successfully achieved with a recovery yield of 97.7%, a protein purity of 82.6% and a gDNA removal higher than 96%. Overall results suggest that using PBA chromatography for mAbs purification is simple, reproducible, robust and scalable without compromising the target molecule integrity and purity.

Keywords: Monoclonal antibodies, Downstream processing, Multimodal chromatography, Phenylboronic acid chromatography, Scale-up

² The work present in this chapter have been published as: (1) dos Santos, R.*, **Rosa, S.A.S.L.***, Aires-Barros, M.R., Tover, A., Azevedo, A.M., 2014. Phenylboronic acid as a multi-modal ligand for the capture of monoclonal antibodies: Development and optimization of a washing step. *Journal of Chromatography A*, 1355, 115-124 and, (2) **Rosa, S.A.S.L.***, dos Santos, R.*, Aires-Barros, M.R., Azevedo, A.M., 2016. Phenylboronic acid Chromatography provides a Rapid, Reproducible and Easy Scalable Multimodal Process for the Capture of Monoclonal Antibodies. *Separation and Purification Technology Journal* **160**, 43-50. *The authors contributed equally.

III.1. Background

Therapeutic applications of monoclonal antibodies (mAbs) in human medicine are increasingly becoming the best choice to treat cancers, autoimmune diseases and inflammatory disorders. Such reality is creating a demand translated in expected worldwide sales of around \$125 billion by 2020-22 [1, 2], more than 70 mAbs based product have been approved by the regulatory agencies (FDA, EMA), and in a large number of mAbs in clinical development [3]. HuMax-IL8 mAb, from Bristol-Myers Squibb, is an example of such investment. In Phase 1 of clinical development, it has been indicated for the treatment of patients with advanced malignant solid tumours [4].

As the number of mAbs on the market and in development has accelerated over the years and with biosimilars gaining ground, majorly due to the losing patent exclusivity of therapeutics such as Adalimumab and Trastuzumab, both in 2018 [5], the design of mAbs manufacturing processes has been more and more challenged. On one hand, the emergence of biosimilars is driving a desire to achieve a lower cost of goods and globalize biologics manufacturing and, on the other hand, progresses at process upstream led to the achievement of high titres of mAbs in mammalian cell cultures [3] that are causing the increase of constraints on downstream processing, where the capture is the critical step. Due to the conserved domains of mAbs, a general purification process based on a common sequence of unit operations is currently employed by many companies [6]. The heart of the process is the protein A chromatography capture, which despite being highly stable, reliable, and reproducible, is considered to be a productivity bottleneck and especially expensive, representing up to 25% of the total mAbs manufacturing process [7, 8]. The formation of product aggregates under low pH standard elution conditions is also one of the major drawbacks of this chromatographic step [9]. The aforementioned driving forces have resulted in significant evolution in process platform approaches aiming the search for cheap, stable and easy-to-use alternatives for protein A. These include novel affinity-based separations that have emerged from the development of synthetic ligands including biomimetic peptides obtained by combinatorial libraries and artificial ligands generated by *de novo* process designs [10, 11], and promising strategies like multimodal chromatography [12-14].

One unique synthetic ligand is phenylboronic acid (PBA), used in boronate affinity chromatography [15]. The PBA ligand was first reported as an affinity ligand able to selective bind to 1,2-*cis*-diol containing molecules by *cis*-diol esterification [16]. MAb's bear two N-linked oligosaccharide chains at the 297-asparagine residue of the CH2 domain of the Fc region, and despite some heterogeneity found in the terminal sugars attached, mannose, galactose, fucose and N-acetylneuraminic acid typically present contain *cis*-diol groups, thus making PBA ligands suitable for mAbs purification [15, 17]. In acidic solutions, boronic acids adopt a trigonal planar form which can revert to a tetrahedral boronate anion upon hydroxylation in alkaline conditions. Both the acid and its conjugate base can bind to diol compounds [18]. However, since the equilibrium constant for the tetrahedral (K_{tet}) is usually higher than that of the trigonal form (K_{trig}), complexes are less stable in acidic conditions [19]. This esterification is stronger if the two hydroxyl groups of the diol are on adjacent carbon atoms and in an approximately coplanar configuration, such as 1,2-*cis*-diol [20]. Ligands as PBA are aromatic and thus also able to establish hydrophobic and π - π interactions. Secondary ionic interactions between boronates and diols

are also possible through coulombic attraction or repulsion effects, hydrogen bonding by the hydroxyl groups and charge transfer interactions. The latter is more prone to occur in acidic conditions, since in the trigonal uncharged form, the boron atom has an empty orbital and can thus serve as an electron receptor for a coordination interaction, enabling Lewis acid-base interactions to occur [21].

The aim of the present work is to evaluate the potential of PBA as an alternative multimodal ligand for the direct purification of different mAbs from clarified CHO cell culture supernatants. Previous work have already shown the ability of PBA to bind antibodies highlighting that non-specific interactions could play an important role in the binding of proteins to the PBA ligand [18, 22, 23]. Also, the development and optimization of a washing step will be emphasized since it is an important feature to increase the final purity. The selectivity of the PBA ligand was evaluated with the purified fractions being fully characterized in terms of product yield, purity and IgG activity. Special attention is given to the elucidation of the binding and elution mechanisms. At last, the effect of the working superficial velocity on process performance was assessed, and a series of loading and scale-up studies were implemented in order to evaluate the feasibility of using PBA chromatography for the purification of mAbs in an industrial setting.

III.2. Materials and Methods

III.2.1. Chemicals

Tris(hydroxymethyl)aminomethane (Tris), sodium chloride (NaCl), D-sorbitol, 4-(2-hydroxyethyl)-1-piperazineethanesulfonic acid (HEPES), sodium azide (NaN_3) were purchased from Sigma–Aldrich (St. Louis, MO, USA). Sodium phosphate monobasic anhydrous and sodium phosphate dibasic were obtained from Panreac Quimica Sau (Barcelona, Spain), and hydrochloric acid from Fluka (Buchs, Switzerland). All other chemicals were of analytical or HPLC grade. All solutions were prepared using purified water from a Milli-Q® system (Millipore, Bedford, MA, USA).

III.2.2. IgG production

III.2.2.1. Anti-human interleukin-8 monoclonal antibodies

Anti-human interleukin-8 (anti-IL8) monoclonal antibodies (mAbs) were produced by CHO DP-12 clone#1934 (ATCC CRL-12445) using DHFR minus/methotrexate selection method (LGC Standards, Middlesex, UK). CHO DP-12 cells were grown in 75% (v/v) serum-free media (ProCHO™5, Lonza Group Ltd, Belgium) and 25% (v/v) DMEM (Dulbecco's Modified Eagle's Medium) (Gibco®, Carlsbad, CA, USA) supplemented with 10% (v/v) ultra-low IgG fetal bovine serum (FBSUL, Gibco®). 200 nM methotrexate (MTX) was present in both culture media to maintain selective pressure. ProCHO™5 was supplemented with 4 mM L-glutamine (Gibco®), 2.1 g/dm³ NaHCO₃ (Sigma-Aldrich), 10 mg/dm³ recombinant human insulin (Lonza), 0.07% (v/v) lipids (Lonza) and 1% (v/v) antibiotics (100 U/cm³ penicillin and 100 µg/cm³ streptomycin) (Gibco®). The DMEM used contains 4.5 g/dm³ D-glucose, 4 mM L-glutamine, and 1 mM sodium pyruvate. After resuspension of DMEM powder, 1.5 g/dm³ NaHCO₃, 2 mg/dm³ recombinant human insulin, 35 mg/dm³ L-proline (all from Sigma-Aldrich), 0.1% (v/v) of a trace element A, 0.1% (v/v) of a trace element B (both from Cellgro®, Manassas, VA, USA) and 1%

antibiotics (v/v) (100 U/cm³ penicillin and 100 µg/dm³ streptomycin) were added. The cultures were carried out in T-175 or T-75 flasks (BD Falcon, Franklin Lakes, NJ) at 37 °C and 5% CO₂ with an initial cell density of 2.8x10⁴ cells/cm². Cell passages were performed every 4 days. Cell supernatants were collected by centrifugation at 350 g for 7 minutes, and storage at -20 °C. In each passage, cells were washed with phosphate buffered saline (PBS, Gibco®) and detached from the flask by adding Accutase® solution (Sigma-Aldrich) for 3 minutes at 37 °C. Cell number and viability were determined using the Trypan Blue (Gibco®) exclusion method. This culture was maintained for several months and the mAb concentration varied between 40 and 91 mg/dm³.

Anti-IL-8 mAbs were also produced in serum-free media, using only ProCHO™5, prepared as described above. In this specific case, the reagent TrypLE™ (Gibco®) Select was used in substitution of Accutase®, previously referred. Cultures were performed as described for the serum-media but with cell passages every 6 days. This culture was also maintained for several months and the mAb concentration varied between 48 and 130 mg/dm³.

III.2.2.2. Anti-human recombinant hepatitis C virus subtype 1b monoclonal antibodies

Anti-human recombinant hepatitis C virus (HCV) subtype 1b monoclonal antibodies were from mouse hybridoma cells expressing a mouse anti-recombinant hepatitis C virus subtype 1b nonstructural protein 5B (NS5B) RNA-dependent RNA polymerase (RdRp) monoclonal antibody. The mRNA of antibody variable regions was isolated and for reconstruction of full antibody, the corresponding cDNA fragments were cloned into the Icosagen Cell Factory proprietary QMCF expression vector containing IgG1 antibody constant regions. The QMCF plasmid contains the mouse polyomavirus (Py) DNA replication origin which in combination with the Epstein-Barr virus (EBV) EBNA-1 protein binding site, as nuclear retention element, ensures stable propagation of plasmids in the QMCF cells [24]. The chimeric antibody was expressed by the QMCF cell line CHOEBNALT85, developed from CHO-S cell line (Invitrogen™, Carlsbad, CA, USA) which have been adapted for suspension growth in chemically defined serum-free medium. The cells were grown in a mix of two serum-free media, (i) CD CHO medium (Gibco®) and (ii) 293 SFM II medium (Gibco®) with the addition of CHO CD efficient feed B and feed A with glutamine using an *in-house* procedure (Icosagen Cell Factory OÜ) in the presence of G418 (700 µg/cm³) to select expression plasmid containing pool of the cells. After antibiotic selection, 5 vials of expression cell bank were generated (10⁷ cells/vial) and kept at liquid nitrogen. For antibody production, one vial from the expression cell bank of the chimeric antibody was thawed in 25 cm³ fresh medium in order to achieve a cell culture density of 2x10⁶ cells/cm³. G418 (Geneticin®, Carlsbad, CA, USA) was added after 24 hours and the culture was expanded to 4.0 dm³ final volume. For production, the temperature was lowered to 30 °C and the culture was repeatedly fed. The culture was harvested 13 days after the beginning of production phase, the cell culture supernatant was filtrated and further stored at -20 °C. The antibody concentration in the supernatant was 150 mg/ dm³ and the total soluble protein concentration 252 mg/dm³.

III.2.3. Monoclonal antibodies purification

Purification of mAbs was performed using different resins: (i) controlled porous glass (CPG) beads functionalized with 3-aminophenyl boronate (ProSep®-PB media, EMD Millipore, UK); (ii) CPG beads functionalized with recombinant native protein A (ProSep® ultra plus chromatography media, EMD Millipore, UK); (iii) non-functionalized CPG beads; (iv) HiTrap Phenyl Fast Flow (High Sub) pre-packed 1 cm³ column (GE Healthcare). The first three resins were packed on Tricorn™ 5/20 empty glass columns (GE Healthcare) with 0.4 cm³ of resin, except otherwise stated. All chromatographic runs were performed in ÄKTA Purifier 10 system from Amersham Biosciences (Uppsala, Sweden), except stated differently. Data acquisition and processing was accomplished using a Unicorn 5.1 software. Chromatographic parameters such as conductivity, pH and UV absorbance at 280 nm of the outlet sample were continuously measured.

III.2.3.1. Phenylboronic acid chromatography

III.2.3.1.1. Development and optimization of wash and elution steps

All chromatographic runs were performed with an adsorption buffer composed by 20 mM HEPES, 150 mM NaCl at pH 7.5, except otherwise stated. Different wash and elution buffers were screened to determine the condition that lead to higher IgG yield and purity, using three independent replicated assays. The tested wash buffers were: (i) 10 mM Tris-HCl, pH 7.5; (ii) 10 mM Tris-HCl, 100 mM D-sorbitol, pH 7.5; (iii) 10 mM Tris-HCl, 200 mM D-sorbitol, pH 7.5; (iv) 10 mM Tris-HCl, 150 mM NaCl, pH 7.5; and (v) 10 mM Tris-HCl, 100 mM D-sorbitol, 150 mM NaCl, pH 7.5. The tested elution buffers included: (i) 1.5 M Tris-HCl, pH 7.5; (ii) 10 mM Tris-HCl, 0.5 M D-sorbitol, pH 7.5; (iii) 10 mM Tris-HCl, 150 mM NaCl, pH 7.5; (iv) 10 mM Tris-HCl, 0.5 M D-sorbitol, 150 mM NaCl, pH 7.5.

Before injection, the column was equilibrated with 10 column volumes (CVs) of the adsorption buffer. The supernatants were directly injected at 1 cm³/min, and the 2 cm³ sample loop was emptied with three-times its volume. After the unbound or weakly bound material were washed-out with 2 CVs of the adsorption buffer, bound material was first eluted following a step gradient with the washing buffer for 10 CVs at 1 cm³/min. The strongly bound material was eluted following a step gradient with the elution buffer for 10 CVs at 1 cm³/min. The flow-through, wash and eluted fractions were collected using Frac-950 fraction collector from GE Healthcare, and further analysed for IgG and protein content.

III.2.3.1.2. Scale-up process optimization

All runs were performed at pH 7.5 using (i) 20 mM HEPES with 150 mM NaCl as adsorption buffer, (ii) 100 mM D-sorbitol in 10 mM Tris-HCl as washing buffer, and (iii) 0.5 M D-sorbitol with 150 mM NaCl in 10 mM Tris-HCl as elution buffer. The purification methodology applied was described in the previous section (Section III.2.3.1.1.), except when a new approach is presented.

III.2.3.1.2.1. Superficial velocities studies

Different superficial velocities were tested along the chromatographic run - flow-through, wash and elution. The velocities evaluated were 5.1, 15.2 and 25.5 cm/min. As a first approach, all the

chromatographic steps – adsorption, wash and elution – were performed at the same velocity. Then, in a second study, the adsorption superficial velocity was set at 5.1 cm/min and the superficial velocity of the wash and elution steps were altered. Samples were analysed for IgG and protein content.

III.2.3.1.2.2. Loading studies

Different load volumes of clarified CHO DP-12 supernatant (5, 12.5 and 25 CVs) were injected at the optimal superficial velocities determined: adsorption at 5.1 cm/min, wash at 15.3 cm/min and elution at 25.5 cm/min. A 50 cm³ Superloop (GE Healthcare) was used for the 25 CVs loading assays. Collected samples were analysed for IgG, protein and gDNA content.

III.2.3.1.3. Process scale-up

The scale-up of PBA chromatography was performed in three steps. In the first step, a Tricorn™ 5/200 glass columns (GE Healthcare) was packed with 4 cm³ of resin; in the second step, a Tricorn™ 10/200 glass column (GE Healthcare) was packed with 16 cm³ of resin; and in the last step a HiScale 16 20BH column (GE Healthcare) was packed with 40 cm³ of resin. All chromatographic runs were performed in ÄKTA Purifier 100 system from GE Healthcare.

In the first scale-up step, the column height was increased from 2 to 20 cm, while the i.d. was maintained at 0.5 cm. The column volume was increased 10 times from an initial volume of 0.4 cm³ to a final volume of 4 cm³ [25]. The flow rates of each chromatographic step were maintained at 1, 3 and 5 cm³/min. In the second scale-up step, the column height was maintained at 20 cm, while the i.d. and final volume were increased to 1 cm and 16 cm³, respectively [25]. The working flow rates were also increased to 4, 12 and 20 cm³/min, respectively, for the adsorption, wash and elution step. The final scale-up, was performed maintaining the column height at 20 cm and increasing the i.d. to 1.6 cm, to a resin volume of 40 cm³, accomplishing a final 100-fold scale-up. The working flow rates were increased accordingly to 10.2, 30.7 and 51.2 cm³/min, respectively, for the adsorption, wash and elution steps [26]. Flow-through, wash and elution fractions were collected using Frac-920 fraction collector from GE Healthcare, and further analysed for IgG, protein, CHO host cell proteins and genomic DNA content. Productivity was calculated as described elsewhere [27].

III.2.3.2. Protein A chromatography

Purification by protein A chromatography was performed using as adsorption buffer 10 mM phosphate buffered saline (PBS, Sigma-Aldrich) at pH 7.4 and as elution buffer 100 mM glycine-HCl (Bio-Rad, Hercules, CA, USA), at pH 2. To avoid denaturation of the eluted antibodies, 1 M Tris-HCl at pH 8 was added to the elution fractions collected. Prior to injection, the column was equilibrated with 5 CVs of the adsorption buffer. The supernatants were directly injected at 1 cm³/min. Before elution, the unbound or weakly bound samples were washed-out with 2 CVs of adsorption buffer. The bound material was eluted following a step gradient of 5 CVs. Flow-through and eluted samples were collected using Frac-950 fraction collector from GE Healthcare, and further analyzed for IgG and protein content.

III.2.3.3. CPG and phenyl-Sepharose chromatography

Both types of chromatography were performed as controls, using as adsorption buffer 20 mM HEPES, 150 mM NaCl at pH 7.5, as wash buffer 10 mM Tris-HCl, 100 mM D-sorbitol at pH 7.5 and as elution buffer 0.5 M D-sorbitol, 150 mM NaCl in 10 mM Tris-HCl at pH 7.5. Prior to injection, the columns were equilibrated with 10 CVs of the adsorption buffer. The supernatants were directly injected at 1 cm³/min using a 2 cm³ loop. Before elution, the unbound or weakly bound samples were washed-out with 2 CVs of adsorption buffer. Bound material was first eluted following a step gradient with washing buffer for 10 CVs at 1 cm³/min, and strongly bound material was eluted following a step gradient with elution buffer for 10 CVs at 1 cm³/min. Flow-through, wash and eluted samples were collected using Frac-950 fraction collector from GE Healthcare, and further analysed for IgG and protein content.

III.2.4. IgG quantification

The concentration of IgG was determined by analytical protein A chromatography using a PA ImmunoDetection sensor cartridge from Applied Biosystems (Foster City, CA, USA) as described elsewhere [28]. The adsorption buffer was composed by 50 mM phosphate, 150 mM NaCl, pH 7.4 and the elution buffer by 12 mM HCl, 150 mM NaCl, pH 2–3. An IgG calibration curve was obtained using human IgG (product name: Gammanorm®) from Octapharma (Lachen, Switzerland) prepared in binding buffer. Samples were previously diluted at least 5 times with adsorption buffer. Analyses were performed in an ÄKTA Purifier system with an A-900 Autosampler fitted with a 500 µL loop. Absorbance was monitored at 215 nm.

III.2.5. Total protein quantification

The total protein content was determined by the Bradford method using a Coomassie assay reagent provided by Pierce (Rockford, IL, USA). The protein standard used was bovine serum albumin (BSA) from Pierce. The protein concentration determined for fractions with high IgG content were corrected by the co-relation factor - 0.63 – specific for human IgG [29]. When working with serum-free CHO DP-12 cell culture supernatants, the protein standard used was bovine gamma globulin (BGG), also from Pierce (Rockford, IL, USA). Absorbance was measured at 595 nm in a microplate reader from Molecular Devices (Sunnyvale, CA, USA). Protein purity was assessed by the ratio between the concentration of IgG determined by protein A HPLC and the concentration of total protein determined using the Bradford method.

III.2.6. Protein gel electrophoresis

Sodium dodecyl sulfate–polyacrylamide gel electrophoresis (SDS–PAGE) was performed to evaluate the purity of the fractions collected. Samples were diluted with loading buffer (62.5 mM Tris-HCl, pH 6.2, 2% (w/v) SDS, 10% (v/v) glycerol, 0.01% (w/v) bromophenol) prior to be exposed to denaturation conditions with 100 mM dithiothreitol, from Sigma-Aldrich, at 100 °C for 10 minutes. Afterwards, samples were applied in a 12% acrylamide gel, prepared from a 40% acrylamide/bis stock solution (29:1) from Bio-Rad. The samples were ran at 90 mV using as running buffer composed by 192 mM glycine, 25 mM Tris-HCl and 0.1% SDS, pH 8.3. Gels were stained with Coomassie Brilliant Blue

(Pharmacia, Uppsala, Sweden), followed by silver nitrate staining, when necessary. Images were acquired with a GS-800 calibrated densitometer from Bio-Rad (Hercules, CA, USA).

III.2.7 Host cell proteins quantification

Host cell proteins (HCP) were quantified using a CHO Host Cell Proteins 3rd Generation ELISA kit from Cygnus Technologies (Southport, NC, USA). Samples were diluted in Sample Diluent Buffer, also from Cygnus Technologies. The absorbance was measured at 450 nm and 650 nm in a SpectraMax microplate reader from Molecular Devices.

III.2.8. CHO genomic DNA quantification

CHO genomic DNA (gDNA) content was determined by real-time PCR according to the conditions described in [30]. Reactions were conducted using a LightCycler® from Roche Applied Science (Manheim, Germany). The primers NV1_F (5'-ACAGGTTTCTGCTTCTGGCT) and NV1_R (5'-CATCAGCTGACTGGTTCACA) were synthesized by STAB Vida (Costa da Caparica, Portugal) [31]. Genomic DNA was extracted from non-plasmid containing CHO cell cultures (3x10⁶ cells/cycle) using Wizard Genomic DNA isolation kit from Promega (Madison, WI, USA).

III.2.9. IgG characterization

III.2.9.1. Isoelectric focusing

Isoelectric focusing (IEF) was performed in order to compare the initial feed sample and the elution fraction obtained from protein A and PBA chromatography. Isoelectric focusing (IEF) was performed in a Pharmacia PhastSystem separation module using PhastGel® IEF 3-9 with 50x46x0.45 mm (GE Healthcare). Gels were run at 2000 V for 410 Vh, after a 75 Vh prefocusing step at 2000 V and sample application at 200 V for 15 Vh. Afterwards, gels were stained with silver nitrate.

III.2.9.2. High performance size-exclusion chromatography

High performance size-exclusion chromatography (SEC-HPLC) was performed in order to assess the IgG aggregates content on the feed sample as in the samples resulting from the purification process. The samples were loaded undiluted and run in isocratic mode in a TSK-Gel Super SW3000 column equipped with a TSK-GEL Super SW guard column, both from Tosoh Bioscience (Stuttgart, Germany) at 0.35 cm³/min for 30 minutes with 50 mM phosphate, 300 mM NaCl, pH 7.0. Absorbance was monitored at 215 nm. HPLC purity was calculated by the ratio between the IgG peak area and the total area of the chromatogram less the contribution of the buffers' composition.

III.2.9.3. Competitive enzyme linked immunosorbent assay

To evaluate the anti-IL-8 monoclonal antibodies activity after purification, a competitive ELISA was performed in 96-well ELISA plates using a Quantikine® Human CXCL8/IL-8 kit from R&D systems (Minneapolis, MN, USA). The plate was coated with assay diluent RD1-85 followed by the addition of IL-8 standard (1 mg/dm³) in order to saturate the plate. Incubation took place for two hours at room temperature. The plate was then aspirated and washed for four consecutive times. Once the plates were

saturated, the anti-IL-8 antibodies produced by CHO DP-12 were added to the wells. A calibration curve was constructed based on IgG concentration obtained from HPLC quantification and diluted with calibrator diluent RD5P. The incubation took place for one hour at room temperature, and the wells were further washed as previously described. Following, the anti-IL-8 conjugate was added and incubated for one hour at room temperature, and after washed as previously described. The substrate solution was added to the plate and incubated for 30 minutes at room temperature and protected from light. The reaction ended by adding the stop solution. The absorbance was measured at 450 nm and 570 nm in a microplate reader from Molecular Devices. Final results were obtained by subtracting the outcome from the measurement at 570 nm to the one obtained at 450 nm.

III.3. Results and Discussion

III.3.1. Development and optimization of wash and elution steps

III.3.1.1. Dynamic binding capacity evaluation

Dynamic binding capacity (DBC) of the PBA resin was determined by frontal analysis. The experiments were conducted by continuously feeding solutions of IgG in 20 mM HEPES, 150 mM NaCl, pH 7.5, with concentrations ranging from 1 to 10 g/dm³. The DBC calculated at 10% breakthrough yielded an average value of 13.2 ± 1.4 mg IgG/cm³ resin. After eluting bound IgG, the total binding capacity (TBC) was quantified by off-line protein A HPLC, returning a TBC of 18.1 ± 1.6 mg IgG/cm³ resin. For the protein A chromatography media - ProSep® Ultra Plus, the DBC for IgG was already characterized by the supplier as 50 mg IgG/cm³ resin [32].

III.3.1.2. Optimization studies

III.3.1.2.1. Adsorption step

HEPES has been reported to favor the binding of *cis-diol* containing compounds to PBA media, regardless its concentration [19, 33]. Hence, all the optimization studies were performed using 20 mM HEPES as adsorption buffer. The salt concentration was set at 150 mM NaCl not only to simulate the supernatant's conductivity and avoid diafiltration of the feedstock but also because previous studies have demonstrated that under these conditions binding of IgG is maximized with recoveries higher than 90% being obtained [15, 23] and non-specific interactions with the bare matrix are mitigated [23]. The binding of IgG to the PBA media was then evaluated using 20 mM HEPES, 150 mM NaCl at two different pH values, namely 7.5 and 8.5. Using the adsorption buffer at pH 7.5 led however to a slightly higher IgG adsorption ($99 \pm 2\%$) than at pH 8.5 ($93 \pm 5\%$), and thus pH 7.5 was set as the adsorption pH further avoiding adjustment of the feedstock pH and thus eliminating pre-conditioning steps and minimizing additional costs.

III.3.1.2.2. Washing step studies

In a first approach, a previously reported binding-elution operation mode was tested using as elution buffer, a high concentration of Tris-HCl (1.5 M) at pH 7.5 in order to disrupt any interaction with PBA media [15]. This run showed a yield of about $99 \pm 2\%$, but the protein purity of the recovered IgG was considerably low ($18 \pm 1\%$). In order to increase the purity of the eluted samples, an additional step was inserted in the chromatographic run giving rise to a purification process based on a binding-wash-elution mode. A two-step elution was thus applied where the first elution was design to wash-out impurity proteins that bound to PBA media through less specific interactions and the second elution would release the IgG from the column with a considerable higher purity.

In a first attempt, 10 mM of Tris-HCl at pH 7.5 was used as wash buffer as it has been reported to shield non-specific interactions with the PBA ligand [34, 35] and also due to its buffering capacity. Results showed that no IgG was lost but no purity improvement was obtained (Table III.1).

Table III.1. Performance parameters (recovery yield, protein purity and purification factor - PF) of IgG purification from a clarified serum-containing CHO DP-12 cell supernatant by PBA chromatography using 20 mM HEPES, 150 mM NaCl as adsorption buffer, different wash buffers and step elution with 1.5 M Tris-HCl. All buffers are at pH 7.5. Results are displayed as mean \pm STDV. W: wash buffer, E: elution buffer.

Buffer	Yield (%)	Purity ¹ (%)	PF ²
W: 10 mM Tris-HCl	0.3 ± 0.4	n.d.	n.d.
E: 1.5 M Tris-HCl	99.4 ± 0.4	25.4 ± 0.6	$6.2 \pm 0.1/24.4$
W: 10 mM Tris-HCl, 100 mM D-sorbitol	0.9 ± 1.2	n.d.	n.d.
E: 1.5 M Tris-HCl	98.3 ± 1.2	85.0 ± 2.0	$13.3 \pm 0.3/15.6$
W: 10 mM Tris-HCl, 200 mM D-sorbitol	4.8 ± 0.8	n.d.	n.d.
E: 1.5 M Tris-HCl	95.3 ± 0.3	80.1 ± 4.9	$15.4 \pm 0.9/19.3$
W: 10 mM Tris-HCl, 150 mM NaCl	0.4 ± 0.0	n.d.	n.d.
E: 1.5 M Tris-HCl	97.3 ± 1.7	68.7 ± 5.5	$6.6 \pm 0.5/9.6$
W: 10 mM Tris-HCl, 100 mM D-sorbitol, 150 mM NaCl	98.4 ± 0.7	n.d.	n.d.
E: 1.5 M Tris-HCl	1.6 ± 0.7	0.9 ± 0.5	$0.2 \pm 0.1/18.1$

n.d. - not determined.

¹ Ratio between IgG and total protein concentration.

² Ratio between final and initial protein purity. As different supernatants have been used in the several runs the maximum PF is given after the STDV.

Subsequently, the wash buffer (10 mM Tris-HCl pH 7.5) was supplemented with low concentrations of *cis*-diol competitors, namely 100 mM of D-sorbitol, in order to evaluate the capacity of this carbohydrate to compete with bound impurities. D-sorbitol was selected in detriment of other carbohydrates such as D-mannitol since it has a higher affinity constant towards PBA ($K_{eqD-sorbitol} = 370 \text{ M}^{-1}$ vs. $K_{eqD-mannitol} = 120 \text{ M}^{-1}$ [33]) making it a stronger competitor in both PB configurations (trigonal and tetrahedral). Also, among the multiple hydroxyls in D-sorbitol, 3,4- and 4,5-dihydroxyls in the middle of the chain, can readily form a co-planar configuration due to the low energy barriers of 1.202 - 1.489 kcal/mol [18]. The washing step performed with 100 mM D-sorbitol in 10 mM Tris-HCl at pH 7.5, turned to allow an efficient removal of impurities, with protein purity reaching 85%, and with a very low concentration of leached IgG ($0.9 \pm 1.2\%$) (Figure III.1A). To further improve the washing step, a higher concentration of D-sorbitol, 200 mM in the same buffer, was also tested. The results, however,

evidenced a higher loss of IgG ($5 \pm 1\%$), thus demonstrating that the D-sorbitol strength as competitor is dependent on its concentration. The increase of D-sorbitol concentration can efficiently promote leaching of bound protein impurities but at higher concentrations IgG can also be eluted due to the promotion of 1,2-*cis*-diol interactions between D-sorbitol and PBA that leads to the disruption of the IgG-PBA bond. Indeed, as shown in Chapter II, *cis*-diol esterification between the ligand and solutes as D-sorbitol or IgG is one of the prevalent interactions observed at this working condition (pH 7.5). Interestingly, a lower IgG purity was obtained when compared with washing step performed with 100 mM D-sorbitol (80% vs 85%) revealing that other interactions may be responsible for the adsorption of IgG to PBA. In fact, at the working pH (7.5), other interactions such as electrostatic, hydrophobic and charge transfer can play an important role in both IgG-PBA and impurities-PBA bonds. In order to evaluate the importance of electrostatic interactions, 150 mM NaCl in 10 mM Tris at pH 7.5 was tested as wash buffer. Nevertheless, it was observed that very few proteins were washed out showing that the majority of the bound proteins were not adsorbed solely by electrostatic interactions (Figure III.1B). A lower protein purity was thus obtained comparing with the wash done with 100 mM D-sorbitol (69% vs 85%) (Figure III.1A vs III.1B).

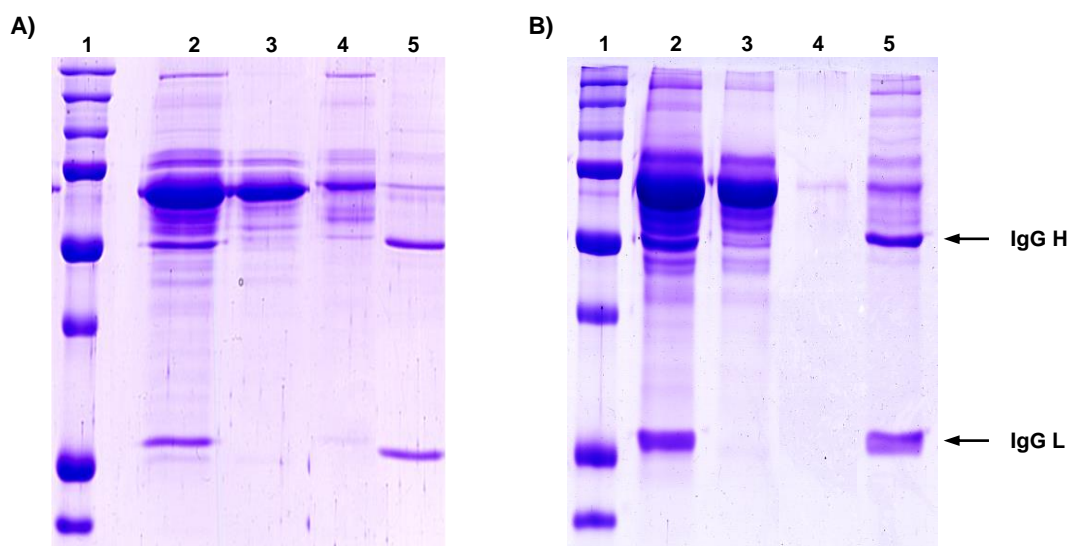


Figure III.1 Coomassie Blue stained SDS-PAGE of fractions collected during IgG purification from a clarified serum-containing CHO DP-12 cell supernatant by PBA chromatography using different wash buffers: (A) 100 mM D-sorbitol, 10 mM Tris-HCl, pH 7.5 and (B) 150 mM NaCl, 10 mM Tris-HCl, pH 7.5. In both runs the adsorption buffer was 20 mM HEPES, 150 mM NaCl, pH 7.5 and the elution buffer, 1.5 M Tris-HCl, pH 7.5. Lanes ID: 1: Precision Plus Protein™ Dual Color Standards (from top to bottom: 200, 150, 100, 75, 50, 37, 25 and 20 kDa); 2: feed sample of CHO DP-12 supernatant; 3: flow-through fraction; 4: wash fraction; 5: elution fraction. Position of IgG heavy (H) (50 kDa) and light (L) (25 kDa) chains are indicated in the right side of the gel. The concentration of IgG in lane 5A and 5B was 52 mg/dm^3 and 86 mg/dm^3 , respectively.

Finally, a last run was carried out where all the components previously evaluated were added together in the wash buffer: 100 mM D-sorbitol with 150 mM NaCl in 10 mM Tris-HCl at pH 7.5. However, in this case, practically all IgG was eluted in the washing step along with the feedstock impurities (Table III.1) thus revealing a synergic effect between *cis*-diol interactions (elution by D-sorbitol) and electrostatic interactions (elution by NaCl) towards the IgG-PBA bond at pH 7.5. The latter could occur between the positively charged antibodies and the negative charged boronate form, considering however that at the

working pH the presence of the tetrahedral conformation is lower than the trigonal form, or with the silica backbone, namely with the silanol groups that at the working pH are negatively charged (pKa 4.9 for isolated silanol groups). Cation- π interactions can also be established with the phenyl aromatic ring present in the 3-aminophenyl boronate ligand. Nonetheless, charge transfer interactions that may also occur between Lewis bases and PBA can act as promoters of the esterification between *cis*-diol compounds and PBA, being responsible for the specificity of the IgG towards PBA at the current working pH (7.5). Boronic acids, as a result of their deficient valence (sp_2 hybridization state) contain an empty p-orbital and adopt a trigonal form with coplanar geometry. In this conformation, the uncharged boronic acid serves as an electron receptor for charged transfer interaction. Unprotonated amines and carboxylic groups, present in IgG structure, can donate a pair of electrons to the boron atom that adopts a tetrahedral conformation [20]. In this way, the interaction between PBA and *cis*-diol compounds turns more specific since the equilibrium constant of the esterification reaction for tetrahedral complexes formation has been reported to be much higher than for trigonal complexes [19]. In sum, from the studies conducted, it was possible to determine that the most efficient wash buffer is composed by 100 mM D-sorbitol in 10 mM Tris-HCl at pH 7.5. Moreover, high recovery yields were achieved, which is the most important parameter for an initial capture step. Hence, in further studies, this buffer composition will be used for IgG purification by PBA chromatography.

III.3.1.2.3. Elution step studies

Tris-HCl at high concentrations has been reported to effectively disrupt specific and non-specific interactions with PB [15], however a high concentration of a salt as Tris may influence the activity and protein integrity of biomolecules such as mAbs [36]. With the aim to replace the elution buffer used, 1.5 M Tris-HCl at pH 7.5, by another equally effective competitor, different experiments were performed. In a first trial, a high concentration of D-sorbitol (0.5 M) in 10 mM Tris-HCl at pH 7.5 was used as elution buffer, however it was observed that IgG was retained in the column and in order to elute it an additional stripping step was performed using 1.5 M Tris-HCl (Table III.2). The use of 0.5 M D-sorbitol as elution buffer has thus failed to elute IgG because D-sorbitol competes only with the *cis*-diol interactions. This result suggests that, after the washing step, the interaction of IgG with PBA has been altered by the washing conditions since previously a concentration of 200 mM D-sorbitol, in the wash buffer, leached some IgG (5%) while 0.5 M D-sorbitol hardly had any effect in IgG elution (2.8%).

Table III.2. Performance parameters (recovery yield, protein purity and purification factor - PF) of IgG purification from a clarified serum-containing CHO DP-12 cell supernatant by PBA chromatography using 20 mM HEPES, 150 mM NaCl as adsorption buffer, 100 mM D-sorbitol in 10 mM Tris-HCl as wash buffer and different elution buffers. All buffers are at pH 7.5. Results are displayed as mean \pm STDV. W: wash buffer, E: elution buffer.

Buffer	Yield (%)	Purity ¹ (%)	PF ²
W: 100 mM D-sorbitol, 10 mM Tris-HCl	1.8 \pm 1.1	n.d.	n.d.
E: 0.5 M D-sorbitol, 10 mM Tris-HCl	2.8 \pm 0.4	2.54 \pm 0.3	0.2 \pm 0.0/8.5
W: 100 mM D-sorbitol, 10 mM Tris-HCl	4.9 \pm 1.5	n.d.	n.d.
E: 150 mM NaCl, 10 mM Tris-HCl	75.1 \pm 8.0	43.6 \pm 2.1	9.5 \pm 0.5/21.5
W: 100 mM D-sorbitol, 10 mM Tris-HCl	0.5 \pm 0.5	n.d.	n.d.
E: 0.5 M D-sorbitol, 150 mM NaCl, 10 mM Tris-HCl	99.4 \pm 0.5	80.8 \pm 1.5	15.9 \pm 0.3/19.7

n.d. - not determined.

¹ Ratio between IgG and total protein concentration.

² Ratio between final and initial protein purity. As different supernatants have been used in the several runs the maximum PF is given after the STDV.

To better evaluate the IgG interaction with PBA, 150 mM NaCl in 10 mM Tris-HCl at pH 7.5 was used for elution. In this condition, 75% of IgG was recovered (Table III.2). Nonetheless when the same buffer was used in the washing step, no IgG left the column being only eluted in the elution step. Once again, the results reinforce that after the washing step a change in the IgG-PBA bond occurred showing that, in this step, IgG was bonded to the resin mainly by electrostatic interactions. An additional trial using 0.5 M D-sorbitol with 150 mM NaCl in 10 mM Tris-HCl at pH 7.5 was then evaluated (Figure III.2A). The results obtained showed to be possible to replace 1.5 M Tris-HCl without compromising IgG yield (99% vs 98%) and purity (81% vs 85%) (Table III.2; Figure III.2B). In addition, since IgG has been adsorbed and eluted with 150 mM NaCl, a synergic effect between NaCl and *cis*-diol competitors (Tris-HCl or D-sorbitol) has allowed to mitigate all the interactions between IgG and PBA, namely the *cis*-diol, charge transfer and electrostatic interactions. In line with the previous results, these further reinforce the hypothesis of IgG being adsorbed to the resin by different types of interaction, which are disrupted by the addition of NaCl, Tris-HCl and D-sorbitol. Furthermore, considering the size and high number of functional groups present in glycoproteins, such as IgG, multiple interactions are in fact expected to occur.

In conclusion, an elution buffer containing 0.5 M D-sorbitol, 150 mM NaCl in 10 mM Tris-HCl at pH 7.5 is also an efficient solution to elute IgG. Furthermore, contrary to a high concentrated Tris-HCl buffer (1.5 M) that can decrease the IgG stability [36], D-sorbitol has been reported to stabilize IgG [33, 37]. Moreover, D-sorbitol is used in a lower molar concentration (0.5 M) than Tris, thus represents an important economic improvement that can account up to 80% savings in the final buffer cost.

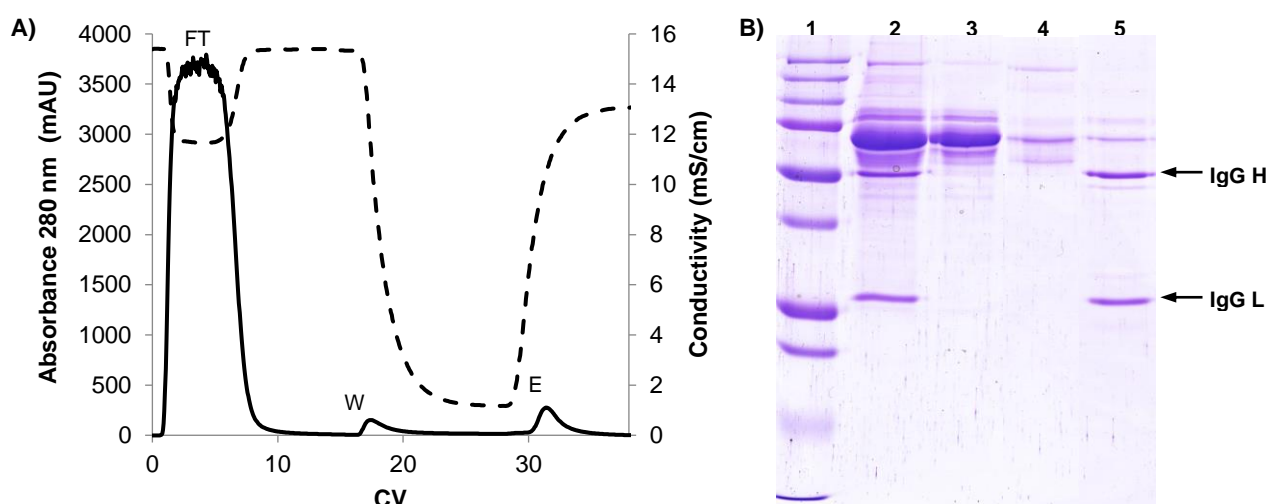


Figure III.2 (A) Chromatographic profile of IgG purification by PBA chromatography from a clarified serum-containing CHO DP-12 cell supernatant, using as adsorption buffer 20 mM HEPES, 150 mM NaCl, pH 7.5, wash buffer 100 mM D-sorbitol, 10 mM Tris-HCl, pH 7.5 and as elution buffer 0.5 M D-sorbitol, 150 mM NaCl, 10 mM Tris, pH 7.5. Absorbance at 280 nm (mAU) – black line, conductivity (mS/cm) – dashed black line, FT: Flow-through; W: Wash; E: Elution. (B) Coomassie Blue stained SDS-PAGE of fractions collected during IgG purification from clarified CHO DP-12 cell supernatant by PBA chromatography using the same buffers as in (A). Lanes ID: 1: Precision Plus Protein™ Dual Color Standards (from top to bottom: 200, 150, 100, 75, 50, 37, 25, 20, and 10 kDa); 2: feed sample of CHO DP-12 supernatant; 3: flow-through fraction; 4: wash fraction; 5: elution fraction. Position of IgG heavy (H) (50 kDa) and light (L) (25 kDa) chains are indicated in the right side of the gel. The concentration of IgG in lane 5B was 41 mg/dm³.

III.3.1.3. Matrix and resin interactions

To evaluate if the unspecific interaction with the resin backbone or with the phenyl group present in the PBA molecule played an important role in the IgG purification by PBA chromatography, control runs using either a bare CPG resin or phenyl-Sepharose were performed using the optimized conditions for PBA chromatography. In both runs, almost all loaded IgG (99%) was collected in the flow-through fractions (Table III.3). With CPG beads, no interaction has occurred between the silanol groups and IgG, under the adsorption conditions, meaning that resin by itself does not have any effect in the binding of IgG. On the other hand, phenyl-Sepharose chromatography also revealed that the majority of IgG (99%) did not interact with the phenyl group. However, very small portions of IgG were lost in the washing (0.9%) and elution (0.1%) steps. This result suggested that, under the condition used in PBA chromatography, hydrophobic interactions do not play a major role in IgG interaction with the PBA-resin.

Table III.3 Performance parameters of IgG purification from a clarified serum-containing CHO DP-12 cell supernatant by CPG and phenyl-Sepharose chromatography. All the buffers used were at pH 7.5. Results are displayed as mean ± STDV. A: adsorption buffer; W: wash buffer; E: elution buffer.

Resin	Buffer	Yield (%)	Purity ¹ (%)	PF ²
CPG	A: 20 mM HEPES, 150 mM NaCl	99.3 ± 0.1	n.d.	n.d.
	W: 100 mM D-sorbitol, 10 mM Tris-HCl	0.3 ± 0.1	n.d.	n.d.
	E: 0.5 M D-sorbitol, 150 mM NaCl, 10 mM Tris-HCl	0.5 ± 0.0	0.9 ± 0.0	0.2 ± 0.0 / 21.7
Phenyl-Sepharose	A: 20 mM HEPES, 150 mM NaCl	99.0 ± 0.2	n.d.	n.d.
	W: 100 mM D-sorbitol, 10 mM Tris-HCl	0.9 ± 0.2	n.d.	n.d.
	E: 0.5 M D-sorbitol, 150 mM NaCl, 10 mM Tris-HCl	0.1 ± 0.1	0.1 ± 0.1	0.0 ± 0.0 / 17.7

¹ Ratio between IgG and protein concentration.

² Ratio between final and initial protein purity. As different supernatants have been used in the several runs the maximum PF is given after the STDV.

III.3.1.4. Phenylboronic acid vs protein A

Since protein A chromatography is the golden standard in the downstream processing of mAbs, a comparison between IgG purification by protein A and PBA chromatography was performed. Both ligands originated very similar results, with recovery yields around 99%, namely $99.4 \pm 0.5\%$ for PBA and $99.5 \pm 0.9\%$ for protein A. Slightly higher purities were obtained for protein A, namely $87.0 \pm 2.3\%$ for the eluate from protein A and $80.8 \pm 1.5\%$ for the eluate from PBA. Figure III.3 corroborates this observation, where no other proteins are detected in the eluted fraction from protein A (Figure III.3A, lane 3) while in the elution fractions from PBA some impurities can be observed (Figure III.3B, lanes 3-S and 3-T). Nonetheless one can conclude that PBA-chromatography is an interesting alternative to protein A, despite the calculated DBC for PBA being 4 times lower than the DBC determined for the protein A resin (50 mg IgG/cm³ resin).

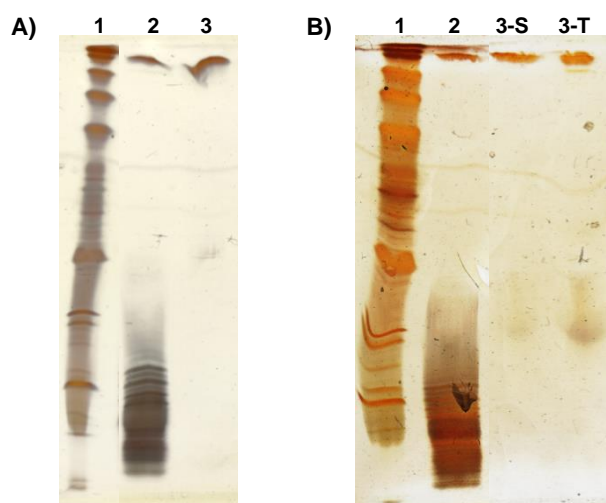


Figure III.3 Silver stained IEF gel of the fractions collected after the purifications of IgG from serum-containing CHO DP-12 cell culture supernatants by (A) Protein A affinity chromatography and (B) PBA chromatography using as elution buffer 0.5 M D-sorbitol, 150 mM NaCl in 10 mM Tris-HCl, pH 7.5 (S) or 1.5 M Tris-HCl, pH 7.5 (T). Lanes ID: 1: pI broad standards (from bottom to top: Amylglicosidase - 3.50 pI (Native); Methyl red (dye) - 3.75 (pI Native); Trypsin inhibitor - 4.55 (pI Native); b-Lactoglobulin A - 5.20 (pI Native); Carbonic anhydrase B (bovine) - 5.85 (pI Native); Carbonic anhydrase B (human) - 6.55 (pI Native); Myoglobin, acidic band - 6.85 (pI Native); Myoglobin, basic band - 7.35 (pI Native); Lentil lectin, acidic - 8.15 (pI Native); Lentil lectin, middle - 8.45 (pI Native); Lentil lectin, basic - 8.65 (pI Native) and Trypsinogen - 9.30 (pI Native)); 2: feed sample of CHO DP-12 supernatant; 3: elution fraction from Protein A purification; 3S: elution fraction from PBA chromatography (0.5 M D-sorbitol, 150 mM NaCl in 10 mM Tris-HCl, pH 7.5); 3T: elution fraction from PBA chromatography (1.5 M Tris-HCl, pH 7.5).

III.3.1.4.1. IgG characterization

Some antibody characteristics, such as pI, presence of aggregates and biological activity, were determined before and after purification by protein A and PBA chromatography. Three different techniques were used: (i) isoelectric focusing (IEF); (ii) size-exclusion chromatography (SEC); and (iii) competitive enzyme-linked immunosorbent assay (cELISA), in order to establish if the antibody maintains the same characteristics after purification. Regarding PBA chromatography, two elution buffers, 0.5 M D-sorbitol with 150 mM NaCl in 10 mM Tris-HCl and 1.5 M Tris-HCl both at pH 7.5, were compared.

The anti-IL8 mAb purified by both PBA and protein A chromatography maintained the same pI (9.3) as in the CHO DP-12 feedstock (Figure III.3). Also, comparing the lanes of the eluted fractions with 0.5 M D-sorbitol, 150 mM NaCl, 10 mM Tris-HCl, pH 7.5 and with 1.5 M Tris-HCl, pH 7.5, it is possible to acknowledge the presence of an acid protein, not visible in the lane of the eluted fraction from the protein A column thus corroborating the results previously obtained in Section III.3.1.4..

Size exclusion chromatography was performed in order to evaluate if IgG aggregates were present or formed along the purification process. In the feedstock chromatogram no IgG aggregates were identified. Regarding, protein A or PBA chromatography the same results were achieved with no IgG aggregates developed during both downstream procedures (Figure III.S1, Supplementary Material). Nevertheless, comparing the three chromatographic conditions evaluated, different HPLC purities have been calculated. The highest value – $88.1 \pm 0.3\%$ – was obtained for the PBA chromatography using 0.5 M D-sorbitol, 150 mM NaCl, 10 mM Tris-HCl, pH 7.5 as elution buffer. For protein A and PBA chromatography using 1.5 M Tris-HCl as elution buffer, HPLC purities were very similar ($61.4 \pm 0.3\%$ vs $58.4 \pm 1.1\%$). This apparent decrease in purity is probably due to the higher salt concentration in the later fractions.

The biological activity of the purified antibodies was further evaluated by a cELISA (Figure III.4). The elution fractions obtained from protein A and PBA chromatography using the two elution buffers (1.5 M Tris-HCl, pH 7.5 and 0.5 M D-sorbitol, 150 mM NaCl, 10 mM Tris-HCl, pH 7.5) were analyzed. The antibody elution fractions from protein A and PBA chromatography using the D-sorbitol elution buffer presented a high and similar activity ($78.7 \pm 8.7\%$ vs. $77.7 \pm 2.3\%$), meaning that none of the buffer constituents diminished or interfere with the anti-IL8 mAb biological activity. However, when the fraction eluted with 1.5 M Tris-HCl was analyzed, the anti-IL8 mAb activity was only $42.8 \pm 2.1\%$. This lower activity could be either due to changes in the 3D structure induced by the elution buffer during IgG storage or due to interference of the high salt concentration in the ELISA assay. In this case, both hypotheses should be considered since a high concentration of Tris-HCl may lead to IgG denaturation and consequent loss of activity and/or may also interfere in the recognition events occurring in the micro-wells, leading to inaccurate results [36].

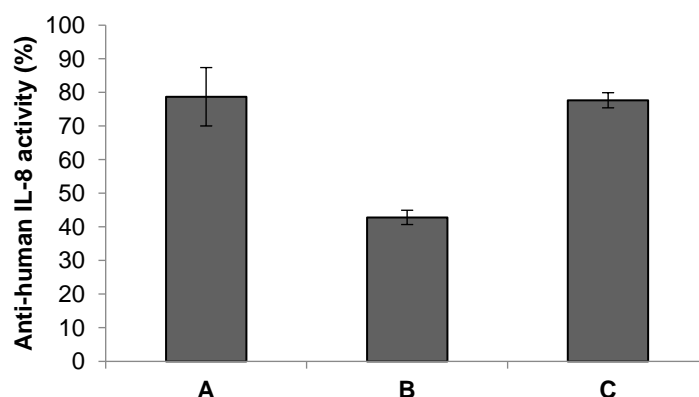


Figure III.4 Activity of purified anti-IL8 monoclonal antibodies from clarified serum-containing CHO DP-12 cell culture supernatants determined by competitive ELISA. (A) Elution fraction from protein A chromatography; (B) Elution fraction from PBA chromatography using as elution buffer 1.5 M Tris-HCl, all at pH 7.5; C – Elution fraction from PBA chromatography using as elution buffer 0.5 M D-sorbitol, 150 mM NaCl in 10 mM Tris-HCl, all at pH 7.5. Results are displayed as mean \pm STDV.

III.3.1.5. Proof of concept

III.3.1.5.1. Anti-IL8 mAbs from serum-free cell cultures

Anti-IL8 antibodies produced in serum-free conditions were also purified using the condition previously optimized. When comparing with the purification of the same mAb from the serum-containing supernatant, the recovery yield obtained was the same (99.5%). However, the protein purity of the eluted fractions was much higher for the anti-IL8 mAb produced in serum-free media, reaching 100% and a purification factor of 1.6 (Table III.4). The purification factor is considerably lower since the initial feedstock is much more pure than the ones containing serum. The high yield and purity are in agreement with in the SDS-PAGE gels in Figure III.5A, where no IgG loss is observed in both flow-through and wash fractions. In terms of aggregates, results show that no IgG aggregation occurs as result of the purification process developed (Figure III.S2, Supplementary Material).

III.3.1.5.2. Anti-recombinant HCV subtype 1b mAbs from serum-free cell cultures

To test whether the conditions found for the purification of anti-IL8 mAb can be used to purify other mAbs, an anti-recombinant hepatitis C virus subtype 1b (anti-HCV) mAb produced in a low protein-content medium was also purified using the optimized conditions determined for PBA chromatography. The performance parameters obtained are summarized in Table III.4. Curiously, the recovery yield obtained (86%) was considerably below the ones obtained previously for the purification of the anti-IL8 mAb because a portion of IgG was lost in the washing step (13%). This loss, easily observed in the SDS-PAGE in Figure III.5B, can be due to structural differences between the anti-HCV and the anti-IL-8 antibody. Although both mAbs belong to IgG1 class, minimal structural differences may lead to different interactions between IgG and PBA, leading to a loss during the washing step. Nonetheless, the performance parameters and SDS-PAGE gel show that the purification of the anti-HCV mAb can be successfully accomplished using PBA chromatography with a final purity of 95%.

Table III.4 Performance parameters regarding the purification by PBA chromatography of anti-IL-8 and anti-HCV mAbs produced in serum-free media. All buffers are at pH 7.5. Results are displayed as mean \pm STDV. A: adsorption buffer; W: wash buffer; E: elution buffer.

MAb	Buffer	Yield (%)	Purity ¹ (%)	PF ²
Anti-IL-8	A: 20 mM HEPES, 150 mM NaCl	0.5 \pm 0.1	n.d.	n.d.
	W: 100 mM D-sorbitol, 10 mM Tris-HCl	0.0 \pm 0.0	n.d.	n.d.
	E: 0.5 M D-sorbitol, 150 mM NaCl, 10 mM Tris-HCl	99.5 \pm 0.1	100 \pm 5.2	1.6 \pm 0.07/ _{1.6}
Anti-HCV	A: 20 mM HEPES, 150 mM NaCl	1.1 \pm 1.9	n.d.	n.d.
	W: 100 mM D-sorbitol, 10 mM Tris-HCl	13.4 \pm 0.6	n.d.	n.d.
	E: 0.5 M D-sorbitol, 150 mM NaCl, 10mM Tris-HCl	85.5 \pm 2.5	94.9 \pm 2.1	1.9 \pm 0.0/ _{2.0}

n.d – not determined.

¹ Ratio between IgG and protein concentration.

² Ratio between final and initial protein purity. As different supernatants have been used in the several runs the maximum PF is given after the STDV.

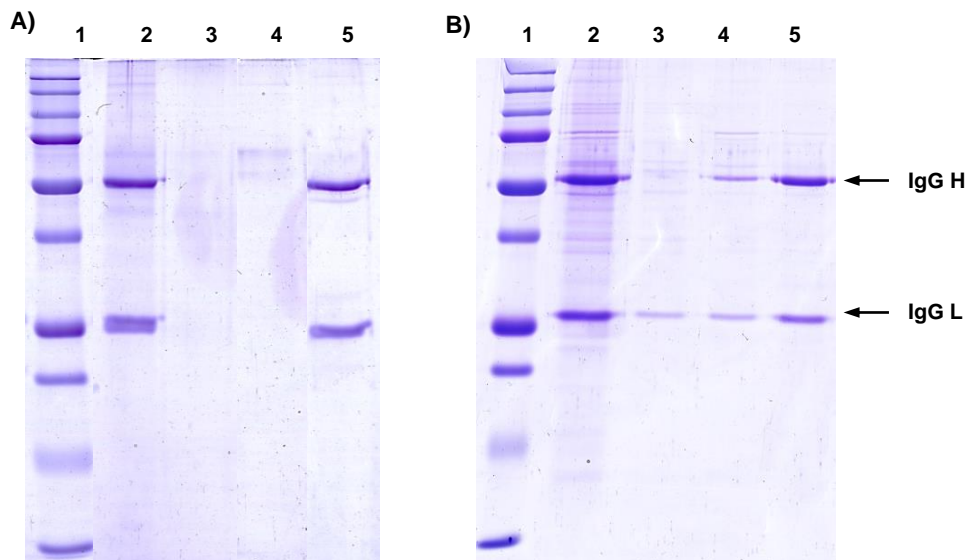


Figure III.5 Coomassie Blue stained SDS-PAGE of fractions collected during the purification by PBA chromatography of (A) anti-IL8 mAb from clarified serum-free media CHO DP-12 cell culture supernatants and (B) anti-HCV mAb from clarified serum-free CHOEBNALT85 cell culture supernatants, using as adsorption buffer 20 mM HEPES with 150 mM NaCl at pH 7.5, as wash buffer 100 mM D-sorbitol in 10 mM Tris-HCl at pH 7.5 and as elution buffer 0.5 M D-sorbitol with 150 mM NaCl in 10 mM Tris-HCl at pH 7.5. Lanes ID: 1: Precision Plus Protein™ Dual Color Standards (from top to bottom: 250, 150, 100, 75, 50, 37, 25, 20, 15 and 10 kDa); 2: feed sample of serum-free CHO supernatants; 3: flow-through fraction; 4: wash fraction; 5: elution fraction. Position of IgG heavy (H) (50 kDa) and light (L) (25 kDa) chains are indicated in the right side of the gel. The concentration of IgG in lane 5A and 5B was 66 mg/dm³ and 117 mg/dm³, respectively.

To determine if the anti-HCV mAb also retains its main characteristics after the purification process, IEF and SEC analysis were performed for the purified fraction obtained by both PBA and protein A chromatography. According to the IEF analysis (Figure III.6), the feed sample of CHOEBNALT85 supernatant show the presence of four distinct isoforms with distinct pI values. The formation of these isoforms is due to the technology used to produce this mAb, the QMCF technology which is a stable episomal expression system that uses an appropriate episomal expression vector. The production of the anti-HCV mAb was performed using a double-expression cassette vectors. QMCF antibody expression vectors are containing constant regions of different human IgG isoforms which allows easily antibodies to switch between different isoforms by cloning of the antibody variable region-encoding cDNAs into desired antibody background. These isoforms may vary in size, superficial charge, disulfide bonds, number of disulfide bonds in the hinge region, glycosylation, activity, among other characteristics. These differences may lead to different interactions between each isoform and the PBA media, turning possible their separation. The majority of the impurity proteins were removed in the washing step, together with one of the isoforms (Figure III.6, lane 3) that does not appear in the elution fraction (Figure III.6, lane 4). Since different isoforms could have different therapeutic behavior, it is of great interest evaluate this unexplored ability of the PBA ligands for multimodal chromatography. Therefore, the washing step showed to be useful not only to wash-out unspecific bond proteins, but also that with PBA chromatography is possible to differentiate IgG isoforms and elute one among four different. At last, the elution fractions were in line with the previous purification of the serum-containing CHO DP-12 cell culture supernatant (Figure III.3). When comparing the elution fraction obtained with 0.5 M D-sorbitol,

150 mM NaCl in 10 mM Tris-HCl at pH 7.5 (Figure III.6B, lane 4) and with 1.5 M Tris-HCl at pH 7.5, it was possible to observe an impurity protein in the later with a pI of around 7.35 - 8.15 that does not appear in the other elution conditions (data not shown). On the other hand, protein A was not able to separate any isoforms, since the interaction occurs with a conserved region in the Fc domain.

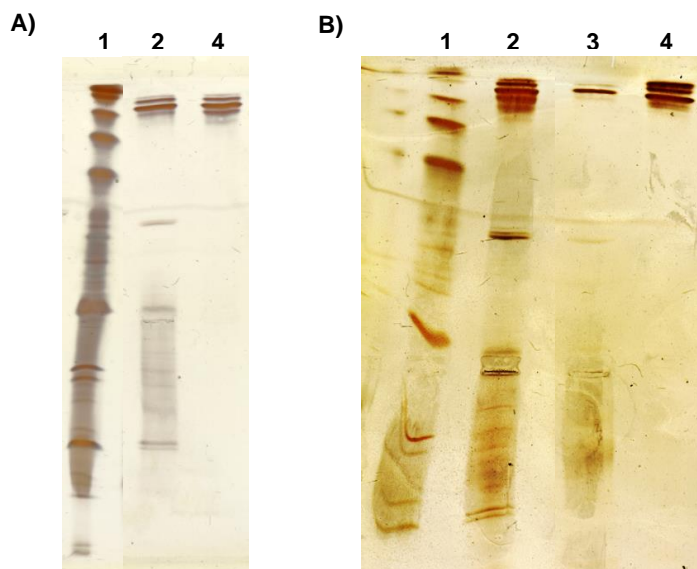


Figure III.6 Silver stained IEF gel of the fractions collected during the purifications of the anti-HCV mAb by (A) Protein A affinity chromatography and (B) PBA chromatography (wash buffer: 100 mM D-sorbitol in 10 mM Tris-HCl at pH 7.5). Lanes ID: 1: pI broad standards (from bottom to top: Amylglucosidase - 3.50 pI (Native); Methyl red (dye) - 3.75 (pI Native); Trypsin inhibitor - 4.55 (pI Native); b-Lactoglobulin A - 5.20 (pI Native); Carbonic anhydrase B (bovine) - 5.85 (pI Native); Carbonic anhydrase B (human) - 6.55 (pI Native); Myoglobin, acidic band - 6.85 (pI Native); Myoglobin, basic band - 7.35 (pI Native); Lentil lectin, acidic - 8.15 (pI Native); Lentil lectin, middle - 8.45 (pI Native); Lentil lectin, basic - 8.65 (pI Native) and Trypsinogen - 9.30 (pI Native)); 2: feed sample of CHOEBNALT85 supernatant; 3: wash fraction; 4: elution fraction.

SEC analysis was also performed for anti-HCV antibodies in order to calculate the HPLC purity and specially to ascertain aggregate formation (Figure III.S3, Supplementary Material). Accordingly, the highest HPLC purity was obtained with protein A, reaching $80.1 \pm 1.3\%$ against $68.9 \pm 5.8\%$ obtained with PBA. The main reason for this difference relies probably in the fact that in the PBA purification, an isoform was eluted in the wash fraction, representing $31.2 \pm 4.8\%$ of the total IgG eluted. From the chromatogram of the CHOEBNALT85 supernatant, it was not possible to establish if aggregates were present or not in the initial feedstock. For the protein A chromatography, a considerable amount of IgG aggregates ($5.6 \pm 0.2\%$) was present in addition to the IgG monomers ($80.1 \pm 1.3\%$). These aggregates showed a higher MW than expected (459 kDa) suggesting that trimers had been formed probably due to the low pH used in the elution step. Also, a tailing of the IgG peak was present, suggesting that some impurities may also be present. For the PBA chromatography, IgG aggregates were also observed in the elution fraction but at a lower percentage ($3.5 \pm 0.6\%$). As previously, larger aggregated complexes were present. Tailing was observed, coherent with the protein smear observed in the SDS-PAGE (Figure III.5B, lane 5) above the IgG heavy chain band (>50 kDa). The presence of aggregates can be due to the chromatography method used, such as linear velocity and elution conditions, or could have been formed prior to purification, due to storage and shipping conditions [38].

III.3.2. Scale-up process optimization

With the feasibility of using PBA chromatography for the capture of mAbs directly from animal cell culture supernatants being demonstrated in Section III.3.1., raised the motivation to design a scale-up process for mAbs purification. The high recovery yields obtained are in accordance with the study of Carvalho *et al.* (2014), who thoroughly investigated the behaviour of basic, neutral and acidic proteins during PBA chromatography. Accordingly, the binding of basic proteins to PB reaches nearly 100% for pH above 7 [39].

In order to accomplish a successful scale-up, studies regarding (i) superficial velocity, (ii) feed volume and (iii) reproducibility were performed using serum-free CHO DP-12 cell culture supernatants. An evaluation of the binding capacities towards feed residence time was also carried out. Those studies were conducted in a small-scale column with 0.4 cm³ of resin.

III.3.2.1. Dynamic binding capacity studies

In order to understand the relationship between the DBC and residence time, frontal analysis was performed (Figure III.7A). Residence times of 0.4, 0.8, 2 and 4 minutes were evaluated, covering those applied in all steps of the scale-up process (4, 1.4 and 0.8 minutes in adsorption, wash and elution, respectively). The experiments were conducted by continuously feeding solutions of 0.75 and 1 mg IgG/cm³ in 20 mM HEPES, 150 mM NaCl, pH 7.5.

The DBC was calculated at 10% breakthrough and it was noticed an increase in DBC with the increment in the residence time. It was also observed that higher residence times led to the higher breakthrough curve slopes (Figures III.7B and III.7D). Also, with the increment on residence time, capacity utilization increased from around 30% (8.0 ± 0.5 mg IgG/ cm³ resin) to almost 90% (21.8 ± 3.8 mg IgG/ cm³ resin), at the higher residence time (Figure III.7C), reaching nearly a steady-state operation mode. The total binding capacity (TBC) was quantified by off-line protein A HPLC, returning a TBC of 26.8 ± 2.5 mg IgG/ cm³ resin. For the ProSep[®] Ultra Plus chromatography media, the DBC has been described as 50 mg IgG/ cm³ resin (10% breakthrough at 3 – 6 min residence time) [32].

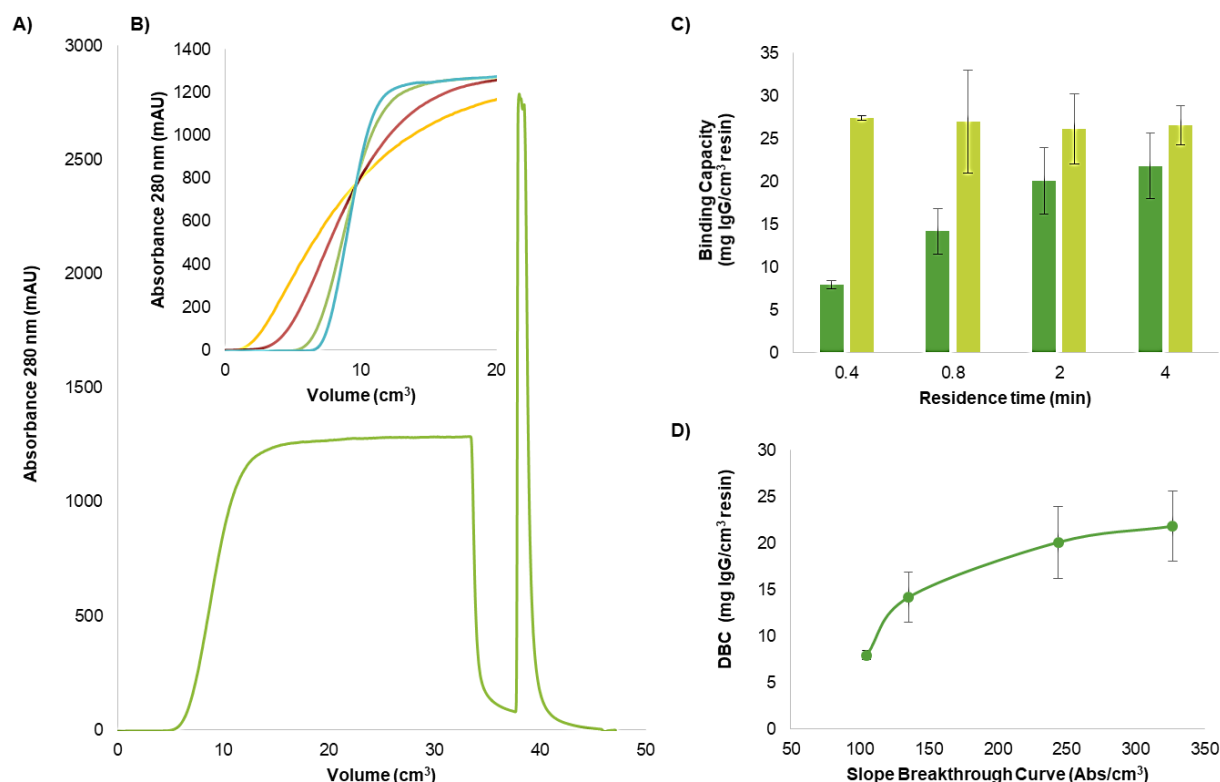


Figure III.7 Effect of residence time in the dynamic binding capacity of PBA resin. (A) Frontal analysis for a residence time of 2 minutes and a pure IgG feedstock of 1 g/dm³. Absorbance at 280 nm (—). (B) Schematic of the breakthrough curves for the different residence times tested – 0.4 (—), 0.8 (—), 2 (—) and 4 minutes (—) – using an IgG feedstock of 1 g/dm³. (C) Dynamic (■) and Total (■) binding capacities for the different residence times tested. (D) Relation between the calculated DBC and the slope of the respective breakthrough curves, displayed in (B). Results are displayed as mean ± STDV.

III.3.2.2. Superficial velocity studies

In a scale-up process, superficial velocity should be maintained among the different scales. In a Section III.3.1., mAbs purification using PBA was accomplished with a superficial velocity of 5.1 cm/min. However, the use of this superficial velocity along the scale-up process would lead to longer chromatographic runs, turning the capture step in a very time-consuming process. To minimize productivity bottlenecks, different superficial velocities were tested in order to verify the possibility of increasing the throughput without compromising the performance parameters.

Three different working superficial velocities were thus tested, namely 5.1, 15.2 and 25.5 cm/min which correspond to flow rates of 1, 3 and 5 cm³/min. It was observed that with the increase on the superficial velocity, a reduction on the residence time led to a less effective adsorption of anti-IL8 mAbs, with recovery yields decreasing from 97.0 ± 0.1%, at 5.1 cm/min, to 77.4 ± 3.5% as the superficial velocity increased to 25.5 cm/min (Table III.5). Losses were mainly observed during the adsorption step. Protein purity also decreased from 83.8 ± 3.5%, at 5.1 cm/min, to 62.2 ± 11.1%, at 25.5 cm/min, most likely as a consequence of the decrease in yield, since the removal of proteins increased from 49.3 ± 1.7% (at 5.1 cm/min) to 70.1 ± 0.2% (at 25.5 cm/min). These results thus indicate that adsorption should be performed at 5.1 cm/min in order to maintain an adequate binding of IgG. However, increasing only the superficial velocity of the wash and elution steps may not compromise the performance parameters

(Table III.5). In fact, the results obtained using 5.1, 15.3 and 25.5 cm/min in the adsorption, wash and elution steps, respectively, were very similar to the ones obtained when all the steps were performed at 5.1 cm/min (Table III.5). These results were corroborated by the SDS-PAGE gels that show that the flow-through, wash and elution fractions have the same protein profile (Figure III.8). It was therefore demonstrated the ability to perform PBA multimodal chromatography for anti-IL8 mAbs purification at higher superficial velocities. In addition, for the 20 cm height columns, the expended time was diminished almost 3 times in comparison with the original run at 5.1 cm/min.

Table III.5 Effect of superficial velocity in the performance parameters (recovery yield, protein purity and protein removal) of IgG purification from clarified CHO DP-12 cell supernatants by PBA chromatography at a scale of 0.4 cm³. IgG concentration in the feedstock was 74 mg/dm³. Results are displayed as mean ± STDV.

Superficial velocity (cm/min)			Yield (%)	Purity ¹ (%)	Protein Removal ² (%)
Adsorption	Wash	Elution			
5.1	5.1	5.1	97.0 ± 0.1	83.8 ± 3.5	49.3 ± 1.7
15.3	15.3	15.3	86.7 ± 2.9	80.7 ± 7.6	64.6 ± 0.7
25.5	25.5	25.5	77.4 ± 3.5	62.2 ± 11.1	70.1 ± 0.2
5.1	5.1	25.5	96.4 ± 0.1	86.4 ± 0.0	58.3 ± 2.1
5.1	15.3	15.3	96.1 ± 0.7	84.3 ± 7.7	56.0 ± 3.1
5.1	15.3	25.5	96.1 ± 0.9	87.3 ± 3.6	58.0 ± 2.4

¹ Ratio between IgG and total protein concentration.

² Difference between the total amount of protein in the feedstock and in the elution pools divided by the same total amount of protein on the feedstock.

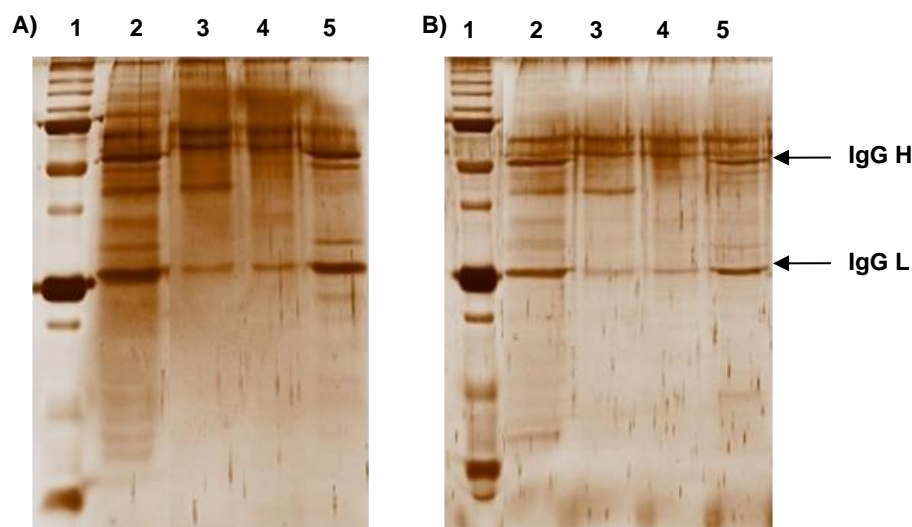


Figure III.8 Silver stained SDS-PAGE of fractions collected during IgG purification from clarified serum-free CHO DP-12 cell culture supernatants, by PBA chromatography. IgG concentration on the feedstock was of 74 mg/dm³. (A) Superficial velocity study using 5.1 cm³/min in adsorption, wash and elution steps. (B) Superficial velocities study using 5.1, 15.3 and 25.5 cm³/min in adsorption, wash and elution steps, respectively. Lanes ID: 1: Precision Plus Protein™ Dual Color Standards (from top to bottom: 250, 200, 150, 100, 75, 50, 37, 25, 15, and 10 kDa); 2: feed sample of CHO DP-12 supernatant; 3: flow-through fraction; 4: wash fraction; 5: elution fraction. Position of IgG heavy (H) (50 kDa) and light (L) (25 kDa) chains are indicated in the right side of the gel.

HPLC-SEC and IEF analysis were conducted to ensure that IgG integrity was maintained. By HPLC-SEC analyses it was possible to confirm the absence of aggregation in all conditions demonstrating that the increase in superficial velocity did not have any effect in IgG aggregation nor in HPLC purity. For a constant velocity of 5.1 cm/min, $83.6 \pm 1.4\%$ HPLC purity was obtained and a similar result, $89.9 \pm 1.1\%$, was obtained using 5.1, 15.3 and 25.5 cm/min in the adsorption, wash and elution steps, respectively. IEF analyses showed that no differences on IgG charge and/or structure modifications were observed among the studies at different superficial velocities, with a pI of 9.3 maintained in all runs (data not shown).

III.3.2.3. Loading studies

Loading studies were performed by increasing the injected volume of the clarified serum-free CHO DP-12 supernatant feedstock from 5 to 25 CVs corresponding to 2 and 10 cm³ of supernatant, respectively. The results obtained are presented in Figure III.9 and show a slight decrease in the recovery yield of IgG for the 25 CVs feedstock volume to $86.7 \pm 2.8\%$, from an average value of $95.6 \pm 0.7\%$ for loading volumes of 5 and 12.5 CVs (respectively, 2 and 5 cm³ of supernatant), even though working below the DBC determined for the same residence time, was observed. This DBC value was however calculated using a commercially available pure IgG, while these studies have been performed with a clarified CHO cell culture supernatant, which contains impurities (e.g. sugars and lipids) that can compete with the antibody for the ligand binding, thus explaining the decrease in the recovery yield (Figure III.9B). For a loading volume of 25 CVs, there was also a decrease in purity from an average value of $87 \pm 0.1\%$, obtained at the lower loading volumes, to $67.7 \pm 6.0\%$. The results thus suggest that optimal loading volumes are between 5 and 12.5 CVs. Both presented high recovery yields, $96.1 \pm 0.9\%$ and $96.0 \pm 1.1\%$, and high purities, $87.3 \pm 3.6\%$ and $87.5 \pm 4.5\%$ respectively.

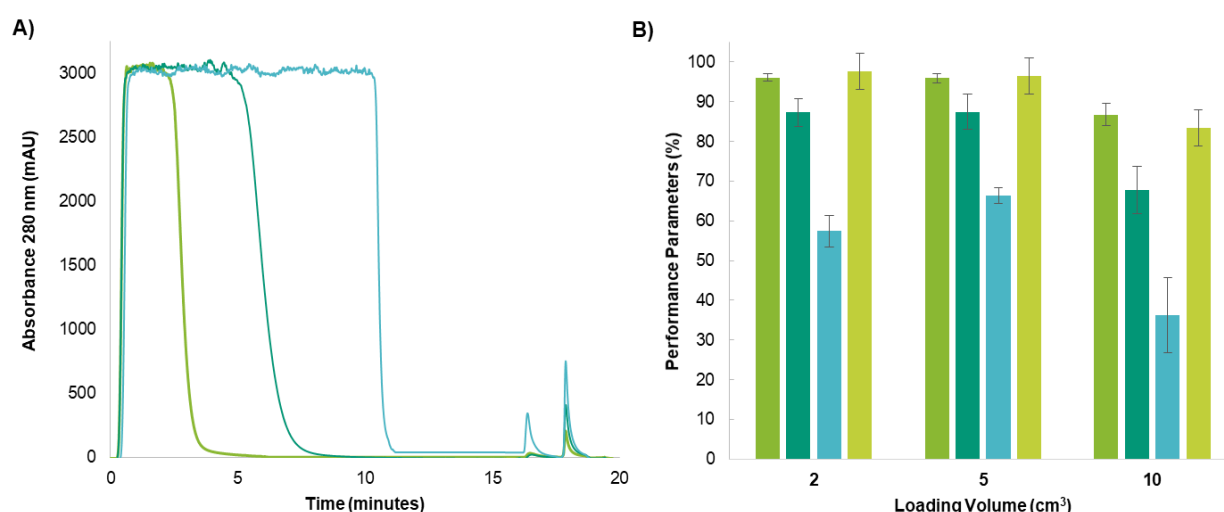


Figure III.9 Effect of different loading volumes in the (A) chromatographic profile: 2 cm³ (—), 5 cm³ (—) and 10 cm³ (—); and in the (B) performance parameters, namely recovery yield (■), protein purity (■), protein removal (■) and gDNA removal (■) of IgG purification from clarified serum-free CHO DP-12 cell culture supernatants, by PBA chromatography. IgG concentration on the feedstock was 58 mg/dm³. Results are displayed as mean \pm STDV (except for gDNA removal: \pm standard error). Protein purity was assessed by the ratio between IgG and total protein concentration. Protein and gDNA removal were determined by the difference between the total amount of molecules in the feedstock and in the elution pools divided by the same amount of molecules on the feedstock.

IgG structure was monitored by HPLC-SEC and no aggregation was observed. Regarding HPLC purity, similar results were obtained among the different loads applied. However, it was noticed a slight decrease in purity with the increase of volume loaded. The best result regarding HPLC purity was $89.9 \pm 1.1\%$ achieved with a load of 5 CVs, followed by $87.0 \pm 0.4\%$ for a 12.5 CVs load and $85.6 \pm 2.1\%$ for a 25 CVs load. A similar profile was observed regarding genomic DNA (gDNA) removal (Figure III.9B). DNA does not contain *cis*-diol groups and thus binding to PBA is not favourable. Nevertheless, it has been reported that DNA is able to bind to PBA under acidic conditions [40], which were not met in this study, and a high removal of the gDNA content was obtained at all conditions (Figure III.9B). The highest gDNA removal - 97.6% - was observed with the 5 CVs load followed by a 96.5% removal with the 12.5 CVs load. As expected, a lower gDNA removal - 83.5% - was obtained with the 25 CVs load.

Since PBA chromatography is being evaluated as an alternative capture step for mAbs purification and the best compromise between yield and purity was evidenced with the 5 CVs load volume (0.4 mg protein/cm³ resin), further studies were performed with this load volume.

III.3.2.4. Reproducibility performance

The run-to-run reproducibility was evaluated by loading several samples of clarified serum-free CHO DP-12 cell culture supernatants from the same lot and from different lots in a 0.4 cm³ column. The performance of anti-IL8 mAbs capture did not change significantly as shown by the consistency of the chromatograms depicted in Figure III.10, which show the same overall profile. The impurities that did not bind to PBA left the column in the flow-through fraction. The remaining impurities bound were removed in the wash step, and at last, IgG elution was performed. The protein A-HPLC analysis of the five feedstock samples, showed an average IgG yield of $95.5 \pm 3.4\%$ and protein purity of $86.6 \pm 5.9\%$, thus confirming the reproducibility of PBA chromatography for the capture of mAbs.

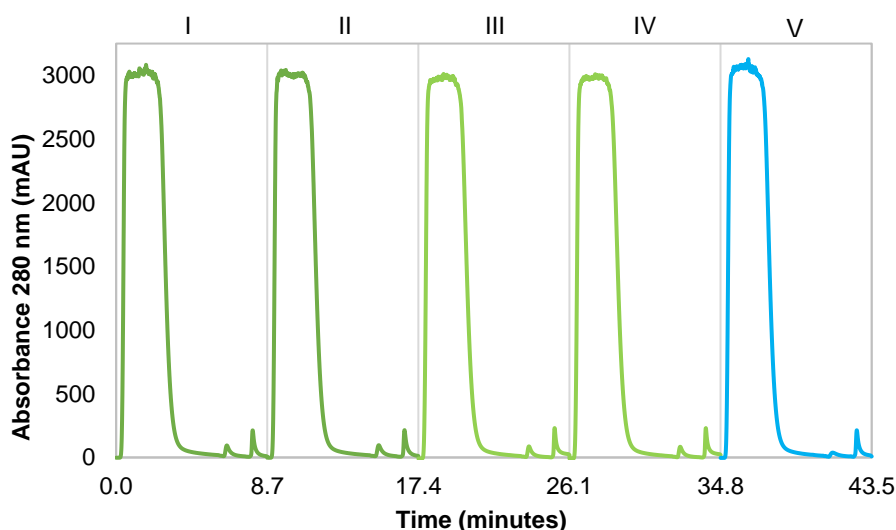


Figure III.10 Run-to run reproducibility demonstrated by chromatographic profiles of IgG capture from different clarified serum-free CHO DP-12 cell culture supernatants using PBA ligands. Each individual run took 8.7 minutes. IgG concentration in the different runs were: (I and II) 65 mg/dm³; 73.9 mg/dm³ (III and IV) and 58.3 mg/dm³ (V). I and II are duplicates as III and IV.

III.3.2.5. Process scale-up

In line with the previous results, a scale-up of the chromatographic process was performed with the goal of confirming the scalability of the process. A 100-fold scale-up was hence performed from a 0.4 cm³ column to a 40 cm³ column, passing through two intermediate volumes of 4 and 16 cm³ column (Figure III.11A). At all scales, the superficial velocity was maintained, as previously determined, at 5.1, 15.3 and 25.5 cm/min for the adsorption, wash and elution step, respectively.

Firstly, the scale-up was achieved by increasing the adsorbent volume ten-times, from 0.4 to 4 cm³ and the sample volume from 2 to 20 cm³ (5 CVs). The column height was increased from 2 to 20 cm while the internal diameter was maintained at 0.5 cm. This first scale-up was not conventional since the goal was to reach a typical process height [27]. The recovery yield obtained ($99.0 \pm 1.8\%$) was slightly higher than the one achieved at the smaller scale ($96.0 \pm 0.9\%$). Protein purity ($82.2 \pm 5.1\%$) and protein removal ($55.9 \pm 1.8\%$) were also similar between the two scales (Table III.5 and Figure III.11B). Considering these results, the next stage was to scale-up the 4 cm³ column 4-times by increasing the internal diameter from 0.5 to 1 cm, the adsorbent volume from 4 to 16 cm³ and the loading volume from 20 to 80 cm³. A recovery yield of $98.6 \pm 2.5\%$ was obtained with a protein purity of $82.7 \pm 5.8\%$ (Figure III.11B). In the final scale-up, the internal diameter was further increased to 1.6 cm, the column volume to 40 cm³ and the feed volumes to 204.8 cm³. The performance parameters obtained were very similar to the smaller scales: a yield of $97.7 \pm 0.1\%$ was obtained with a purity of $82.6 \pm 2.5\%$, translating a protein removal of $62.4 \pm 1.7\%$ (Figure III.11B). All the scale-up runs were performed in 75 min (Figure III.11A) and presented the same chromatographic profile - an initial flow-through peak of unbound material which contains the majority of the unbound proteins and other impurities, a second peak of bound material containing compounds that co-adsorbed with IgG during the adsorption step, and a third peak where more than 97% of anti-IL8 mAb was recovered. Overall, it was possible to demonstrate the reproducibility of PBA multimodal chromatography at different scales with yields higher than 97%, purities around 82% and protein removals of about 60%. The productivity of the chromatographic processes was $233 \pm 3 \text{ mg}\cdot\text{h}^{-1}\cdot\text{dm}^{-3}$ of PB-CPG resin for the three 20 cm height columns, which is in agreement with previously published values [41].

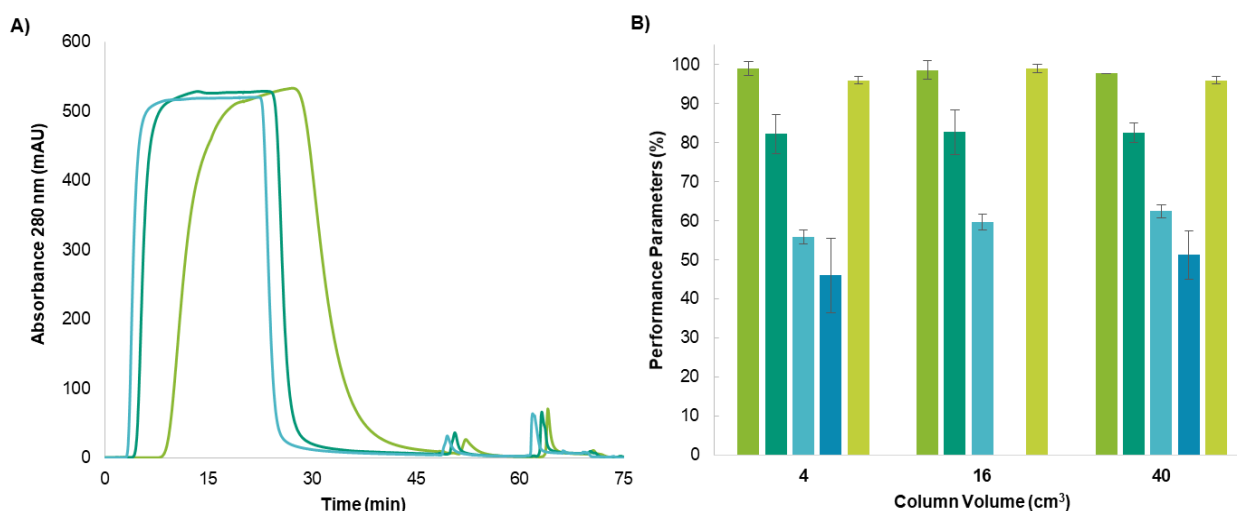


Figure III.11 (A) Chromatographic profiles at different scales: 4 cm³ (—), 16 cm³ (—) and 40 cm³ (—) and (B) performance parameters: recovery yield (■), protein purity (■), protein removal (■), HCP removal (■) and gDNA removal (■) obtained for the IgG capture from clarified serum-free CHO DP-12 cell culture supernatants by PBA chromatography. IgG concentration on the feedstock was 57.8 ± 0.3 mg/dm³. Results are displayed as mean \pm STDV (except for gDNA removal: \pm standard error). Protein purity was assessed by the ratio between IgG and protein concentration. Protein, HCP and gDNA removal were determined by the difference between the total amount of molecules in the feedstock and in the elution pools divided by the same total amount of molecules on the feedstock.

The purified anti-IL8 mAb was further characterized by size-exclusion chromatography (SEC) and isoelectric focusing (IEF). According to SEC analysis, no aggregates were present or formed during the purification process at all scales and the HPLC purities obtained were very consistent among the different scales, with an average value of $83.6 \pm 1.0\%$ being reached, which again demonstrates the scalability of the process. The overall charge of the purified anti-IL8 mAb was maintained according to IEF and the same pI (9.3) was obtained at all the scales and in the CHO DP-12 feedstock. The purified samples were additionally analysed in terms of gDNA and host cell proteins (HCP). In terms of gDNA, removals higher than 96% were achieved (Figure III.11B). Relatively to soluble protein removal values of around 60% were reached. Interestingly, HCP removal values obtained were of about 50%. This result shows that the majority of the removed proteins were CHO produced proteins, as expected since CHO-DP 12 cells were grown under serum-free conditions. However, the 50% of HCP removal is far from the values obtained for mAbs capture with PBA under elution with 1.5 M Tris-HCl (88%) with a different kind of support [30] or even with the traditional mAbs platform approach (99.5%). Still, for a single non-affinity method, a removal of this magnitude is quite expectable [27]. In order to overcome this excess of HCP present in the elution fraction, additional polishing steps are required, including ion exchange chromatography, hydrophobic interaction chromatography or multimodal chromatography. Previous studies already demonstrated that the combination of these three-column processes (ion-exchange, multimodal, or hydrophobic interaction) has a similar efficiency to an affinity-based process, in terms of yield and host cell proteins removal [42, 43]. Additionally, charged depth filters could be used prior to capture [44].

PBA could emerge as an alternative ligand to the standard protein A capture step since it presents similar recovery yields ($96.1 \pm 0.9\%$ vs $96.4 \pm 0.8\%$, respectively) and protein purities ($83.3 \pm 5.7\%$ vs $87.3 \pm 3.6\%$), and greater gDNA removals (97.6% vs 91.0%). Furthermore, PBA could overcome some

of the drawbacks of mAbs capture by protein A, mainly those related with (i) the high cost of the resin, (ii) ligand leaching, (iii) instability at high pH and (iv) the formation of product aggregates under low pH standard elution conditions [9, 45, 46]. Indeed, PBA is a small synthetic ligand, much cheaper than the biological protein A, and has demonstrated a very good performance for mAbs purification under physiological pH values that could prevent protein aggregation and ligand leaching phenomena. In addition, and as demonstrated in the current work, PBA multimodal chromatography can be performed at higher superficial velocities, unlike the standard protein A affinity chromatography [47-49]. Still, for industrial applications, additional points would need to be considered beyond the scope and possibilities of the present study, e.g. (i) the capacity to process high cell density cell culture supernatants that present high mAb and impurities titres, (ii) the advantages of applying a continuous process strategy as multicolumn countercurrent solvent gradient (MCSGP) or periodic countercurrent chromatography (PCC) to PBA chromatography and (iii) the evaluation of possible reversible or irreversible mAb conformational changes by differential scanning calorimetry (DSC) or circular dichroism (CD) and its implication in product quality.

III.4. Conclusions

The viability of using PBA for the direct capture of mAbs from clarified cell culture supernatants has been demonstrated, allowing high recovery yields as well as high impurity clearance. The optimization studies using PBA chromatography media, revealed that contrarily to what has been used for the purification of other glycoproteins using PB chromatography [15, 18, 50], the most efficient pH condition is below PBA pKa, namely at pH 7.5. The development and optimization of an additional washing step demonstrated to be essential in order to achieve a high purity. Nonetheless, the type of buffer, ionic strength, and pH of the wash buffer needs to be well-defined in order to minimize IgG losses. In addition, the implementation of a washing step showed the possibility of using PBA chromatography for isoform separation. The standard elution buffer, 1.5 M Tris-HCl [15] that leads to a lower biological activity, can be successfully replaced by an alternative competitor - 0.5 M D-sorbitol with 150 mM NaCl in 10 mM Tris-HCl. The latter allows recovering 99% of the anti-IL-8 mAb with a final protein purity of 81%, besides being economically more favorable. PBA chromatography was also successfully used to purify the same anti-IL-8 mAb but from a serum-free culture media and a second mAb produced by a different cell line. The results clearly show the feasibility of PBA chromatography for the purification of mAbs, yielding results comparable with ones obtained by protein A. The lower costs, stability and selectivity of this synthetic ligand may lead to the implementation of PBA chromatography as a new platform in the downstream processing of mAbs, either as a protein A replacement or as a pre-chromatographic step for a longer life-time of the high costly protein A resin.

The scalability of PBA chromatography was also successfully demonstrated with a 100-fold scale-up. PBA was effectively used as a multimodal ligand for the direct capture of anti-IL8 mAbs from a clarified serum-free CHO DP-12 cell culture supernatant at small to moderate scales thus supporting its application at larger scales. Working superficial velocities of the different chromatographic steps were optimized to allow a reduction of the chromatographic run time of about 3 times without compromising the performance parameters. The 100-fold scale-up was successfully accomplished with recovery yields

of about 97%, purities of 82% and removals of gDNA higher than 96% obtained at all the scales tested (0.4, 4, 16 and 40 cm³ columns). The DBC determined at 10% of breakthrough is lower than that of protein A chromatography (21.8 ± 3.8 mg IgG/cm³ resin vs > 50 mg IgG/cm³ resin, respectively). This low capacity could, however, be mitigated with further optimizations of the commercial ligand in terms of density and spacer arms structures [51-53].

Moreover, since boronic acids have the ability to recognize the 1,2-*cis*-diol compounds present in the glycan structure, it could be possible to purify antibody fragments lacking the Fc region proving that they are glycosylated in its Fv region, unlike protein A [30, 54]. PBA chromatography can therefore be described as a scalable, rapid, efficient and cost-effective multimodal process that has the potential to be used in an industrial setting. In fact, multimodal processes are being increasingly exploited and considered of high importance for the fractionation of complex biological mixtures, as pre-chromatographic and polishing steps or as capture alternatives [12, 55-57]. Compared with other types of chromatography, multimodal chromatography is particular advantageous in its salt-independent adsorption and simple elution by charge repulsion. Multimodal ligands, such as Capto MMC and MEP-Hypercel have been tested for mAbs purification, as an alternative to the affinity-based capture platform [14, 58]. Capto MMC presents similar characteristics to PB resin used in these studies, in terms of recovery yield, purity and also dynamic binding capacity (30 mg IgG/cm³ resin) [59]. However, the cost of the PBA silica-based resins is much lower than that of the Capto MMC (agarose-based). The physical bed stability is also higher using silica-based resins than agarose-based. Regarding the MEPHypercel, both PBA and Capto MMC present much higher recovery yields (>97% vs 86%) [12].

III.5. References

- [1] D.M. Ecker, S.D. Jones, H.L. Levine, The therapeutic monoclonal antibody market, *mAbs*, 7 (2015) 9-14.
- [2] S.S. Dewan, *Antibody Drugs: Technologies and Global Markets*, in BCC Research Report, October 2017.
- [3] A.A. Shukla, L.S. Wolfe, S.S. Mostafa, C. Norman, Evolving trends in mAb production processes, *Bioeng Transl Med*, 2 (2017) 58-69.
- [4] ClinicalTrials.gov, HuMax-IL8 (Interleukin8) in Patients With Advanced Malignant Solid Tumors, in, <https://clinicaltrials.gov/ct2/show/NCT02536469>, November 11, 2018.
- [5] M. Aitken, *Delivering on the Potential of Biosimilar Medicines: The Role of Functioning Competitive Markets*, in IMS Institute for Healthcare Informatics Report, March 2016.
- [6] H.F. Liu, J. Ma, C. Winter, R. Bayer, Recovery and purification process development for monoclonal antibody production, *mAbs*, 2 (2010) 480-499.
- [7] M.D. Costioli, C. Guillemot-Potelle, C. Mitchell-Logean, H. Broly, Cost of Goods Modeling and Quality by Design for Developing Cost-Effective Processes, *BioPharm Int*, 23 (2010).
- [8] M.A. Hashim, K.H. Chu, Modeling the performance of protein-A affinity columns using asymptotic solutions, *Sep Purif Technol*, 68 (2009) 279-282.
- [9] A.A. Shukla, B. Hubbard, T. Tressel, S. Guhan, D. Low, Downstream processing of monoclonal antibodies -Application of platform approaches, *J Chromatogr B*, 848 (2007) 28-39.
- [10] A.C.A. Roque, C.R. Lowe, M.Å. Taipa, *Antibodies and Genetically Engineered Related Molecules: Production and Purification*, *Biotechnol Progr*, 20 (2004) 639-654.
- [11] Y. Liu, Y. Lu, Z. Liu, Restricted access boronate affinity porous monolith as a protein A mimetic for the specific capture of immunoglobulin G, *Chem Sci*, 3 (2012) 1467-1471.
- [12] J. Pezzini, G. Joucla, R. Gantier, M. Toueille, A.M. Lomenech, C. Le Senechal, B. Garbay, X. Santarelli, C. Cabanne, Antibody capture by mixed-mode chromatography: a comprehensive study from determination of optimal purification conditions to identification of contaminating host cell proteins, *J Chromatogr A*, 1218 (2011) 8197-8208.

- [13] S. Maria, G. Joucla, B. Garbay, W. Dieryck, A.M. Lomenech, X. Santarelli, C. Cabanne, Purification process of recombinant monoclonal antibodies with mixed mode chromatography, *J Chromatogr A*, 1393 (2015) 57-64.
- [14] C. Zhang, D. Fredericks, E.M. Campi, P. Florio, C. Jespersgaard, C.B. Schjødt, M.T.W. Hearn, Purification of monoclonal antibodies by chemical affinity mixed mode chromatography, *Sep Purif Technol*, 142 (2015) 332-339.
- [15] A.M. Azevedo, A.G. Gomes, L. Borlido, I.F. Santos, D.M. Prazeres, M.R. Aires-Barros, Capture of human monoclonal antibodies from a clarified cell culture supernatant by phenyl boronate chromatography, *J Mol Recognit*, 23 (2010) 569-576.
- [16] X.C. Liu, W.H. Scouten, Boronate Affinity Chromatography, in: D.S. Hage (Ed.) *Handbook of Affinity Chromatography*, CRC Press, 2006, pp. 215-229.
- [17] M. Matsumoto, T. Shimizu, K. Kondo, Selective adsorption of glucose on novel chitosan gel modified by phenylboronate, *Sep Purif Technol*, 29 (2002) 229-233.
- [18] B. Zhang, S. Mathewson, H. Chen, Two-dimensional liquid chromatographic methods to examine phenylboronate interactions with recombinant antibodies, *J Chromatogr A*, 1216 (2009) 5676-5686.
- [19] L.I. Bosch, T.M. Fyles, T.D. James, Binary and ternary phenylboronic acid complexes with saccharides and Lewis bases, *Tetrahedron*, 60 (2004) 11175-11190.
- [20] X.-C. Liu, W.H. Scouten, Boronate Affinity Chromatography, in: P. Bailon (Ed.) *Affinity Chromatography*, Human Press, 2000.
- [21] D.G. Hall, Structure, Properties, and Preparation Of Boronic Acid Derivatives. Overview of Their Reactions and Applications, 2nd ed., Wiley-VCH Verlag GmbH & Co. KGaA, Weinheim, Germany, 2011.
- [22] B.M. Brena, F. Batista-Viera, L. Rydén, J. Porath, Selective adsorption of immunoglobulins and glycosylated proteins on phenylboronate-agarose, *J Chromatogr A*, 604 (1992) 109-115.
- [23] S.A.S.L. Rosa, C.L. da Silva, M.R. Aires-Barros, A.C. Dias-Cabral, A.M. Azevedo, Thermodynamics of the adsorption of monoclonal antibodies in phenylboronate chromatography: Affinity versus multimodal interactions, *J Chromatogr A*, 1569 (2018) 118-127.
- [24] T. Silla, I. Hääl, J. Geimanen, K. Janikson, A. Abroi, E. Ustav, M. Ustav, Episomal Maintenance of Plasmids with Hybrid Origins in Mouse Cells, *J Virol*, 79 (2005) 15277.
- [25] R.B. Carrillo, G., Scale-up and Commercial Production of Recombinant Proteins, in: R.M. Hatti-Kaul, Bo (Ed.) *Isolation and Purification of Proteins*, CRC Press, 2003, pp. 470-480.
- [26] A.V. Rathore, A., An Overview of Scale-up in Preparative Chromatography, in: A.V. Rathore, A. (Ed.) *Scale-up and Optimization in Preparative Chromatography: Principles and Biopharmaceutical Applications*, CRC Press, 2003, pp. 1-32.
- [27] H. Lars, Jagschies, G., Sofer, G., *Handbook of Process Chromatography: Development, Manufacturing, Validation and Economics*, 2nd ed., Academic Press, 2008.
- [28] A.M. Azevedo, P.A.J. Rosa, I.F. Ferreira, M.R. Aires-Barros, Integrated process for the purification of antibodies combining aqueous two-phase extraction, hydrophobic interaction chromatography and size-exclusion chromatography, *J Chromatogr A*, 1213 (2008) 154-161.
- [29] Thermo Scientific Pierce Protein Assay Technical Handbook, 2010, pp. 9.
- [30] L. Borlido, A.M. Azevedo, A.G. Sousa, P.H. Oliveira, A.C. Roque, M.R. Aires-Barros, Fishing human monoclonal antibodies from a CHO cell supernatant with boronic acid magnetic particles, *J Chromatogr B*, 903 (2012) 163-170.
- [31] P.M. Nissom, Specific detection of residual CHO host cell DNA by real-time PCR, *Biologicals*, 35 (2007) 211-215.
- [32] MerckMillipore, ProSep® Ultra Plus Chromatography Media brochure, 2012.
- [33] G. Springsteen, B. Wang, A detailed examination of boronic acid–diol complexation, *Tetrahedron*, 58 (2002) 5291-5300.
- [34] Y. Li, J.-O. Jeppsson, M. Jörntén-Karlsson, E. Linné Larsson, H. Jungvid, I.Y. Galaev, B. Mattiasson, Application of shielding boronate affinity chromatography in the study of the glycation pattern of haemoglobin, *J Chromatogr B*, 776 (2002) 149-160.
- [35] C. Quan, E. Alcalá, I. Petkovska, D. Matthews, E. Canova-Davis, R. Taticek, S. Ma, A study in glycation of a therapeutic recombinant humanized monoclonal antibody: where it is, how it got there, and how it affects charge-based behavior, *Anal Biochem*, 373 (2008) 179-191.
- [36] S. O. Ugwu, S. P. Apte, The Effect of Buffers on Protein Conformational Stability, *Pharmaceutical Technology*, (2004) 86-113.
- [37] M. Maury, K. Murphy, S. Kumar, A. Mauerer, G. Lee, Spray-drying of proteins: effects of sorbitol and trehalose on aggregation and FT-IR amide I spectrum of an immunoglobulin G, *Eur J Pharm Biopharm*, 59 (2005) 251-261.

- [38] M.E.M. Cromwell, E. Hilario, F. Jacobson, Protein aggregation and bioprocessing, *AAPS J*, 8 (2006) E572-E579.
- [39] R.J. Carvalho, J. Woo, M.R. Aires-Barros, S.M. Cramer, A.M. Azevedo, Phenylboronate chromatography selectively separates glycoproteins through the manipulation of electrostatic, charge transfer, and cis-diol interactions, *Biotechnol J*, 9 (2014) 1250-1258.
- [40] A.G. Gomes, A.M. Azevedo, M.R. Aires-Barros, D.M. Prazeres, Clearance of host cell impurities from plasmid-containing lysates by boronate adsorption, *J Chromatogr A*, 1217 (2010) 2262-2266.
- [41] A.G. Gomes, A.M. Azevedo, M.R. Aires-Barros, D.M. Prazeres, Validation and scale-up of plasmid DNA purification by phenyl-boronic acid chromatography, *J Sep Sci*, 35 (2012) 3190-3196.
- [42] D.K. Follman, R.L. Fahrner, Factorial screening of antibody purification processes using three chromatography steps without protein A, *J Chromatogr A*, 1024 (2004) 79-85.
- [43] S. Aldington, J. Bonnerjea, Scale-up of monoclonal antibody purification processes, *J Chromatogr B*, 848 (2007) 64-78.
- [44] Y. Yigzaw, R. Piper, M. Tran, A.A. Shukla, Exploitation of the Adsorptive Properties of Depth Filters for HCP Removal during Monoclonal Antibody Purification, *Biotechnol Progr*, 22 (2006) 288-296.
- [45] B. Kelley, Very Large Scale Monoclonal Antibody Purification: The Case for Conventional Unit Operations, *Biotechnol Progr*, 23 (2007) 995-1008.
- [46] A.M. Azevedo, P.A. Rosa, I.F. Ferreira, M.R. Aires-Barros, Chromatography-free recovery of biopharmaceuticals through aqueous two-phase processing, *Trends Biotechnol*, 27 (2009) 240-247.
- [47] H. Miyahara, R. Nakashima, M. Inoue, T. Katsuda, H. Yamaji, S. Katoh, Optimization and Performance of Silica-Based Media for Industrial-Scale Antibody Purification, *Chem Eng Technol*, 35 (2012) 157-160.
- [48] C.K. Ng, H. Osuna-Sanchez, E. Valery, E. Sorensen, D.G. Bracewell, Design of high productivity antibody capture by protein A chromatography using an integrated experimental and modeling approach, *J Chromatogr B*, 899 (2012) 116-126.
- [49] D. Low, R. O'Leary, N.S. Pujar, Future of antibody purification, *J Chromatogr B*, 848 (2007) 48-63.
- [50] D. Zanette, A. Soffientini, C. Sottani, E. Sarubbi, Evaluation of phenylboronate agarose for industrial-scale purification of erythropoietin from mammalian cell cultures, *J Biotechnol*, 101 (2003) 275-287.
- [51] S. Hober, K. Nord, M. Linhult, Protein A chromatography for antibody purification, *J Chromatogr B*, 848 (2007) 40-47.
- [52] G. Zhao, X.Y. Dong, Y. Sun, Ligands for mixed-mode protein chromatography: Principles, characteristics and design, *J Biotechnol*, 144 (2009) 3-11.
- [53] W. Bicker, J. Wu, H. Yeman, K. Albert, W. Lindner, Retention and selectivity effects caused by bonding of a polar urea-type ligand to silica: a study on mixed-mode retention mechanisms and the pivotal role of solute-silanol interactions in the hydrophilic interaction chromatography elution mode, *J Chromatogr A*, 1218 (2011) 882-895.
- [54] A. Nascimento, I.F. Pinto, V. Chu, M.R. Aires-Barros, J.P. Conde, A.M. Azevedo, Studies on the purification of antibody fragments, *Sep Purif Technol*, 195 (2018) 388-397.
- [55] M. Toueille, A. Uzel, J.F. Depoisier, R. Gantier, Designing new monoclonal antibody purification processes using mixed-mode chromatography sorbents, *J Chromatogr B*, 879 (2011) 836-843.
- [56] D. Gao, L.L. Wang, D.Q. Lin, S.J. Yao, Evaluating antibody monomer separation from associated aggregates using mixed-mode chromatography, *J Chromatogr A*, 1294 (2013) 70-75.
- [57] T. Müller-Späth, L. Aumann, G. Ströhlein, H. Kornmann, P. Valax, L. Delegrange, E. Charbaut, G. Baer, A. Lamproye, M. Jöhnck, M. Schulte, M. Morbidelli, Two step capture and purification of IgG2 using multicolumn countercurrent solvent gradient purification (MCSGP), *Biotechnol Bioeng*, 107 (2010) 974-984.
- [58] I.F. Pinto, M.R. Aires-Barros, A.M. Azevedo, Multimodal chromatography: debottlenecking the downstream processing of monoclonal antibodies, *Pharm Bioprocess*, 3 (2015) 263-279.
- [59] K.A. Kaleas, M. Tripodi, S. Revelli, V. Sharma, S.A. Pizarro, Evaluation of a multimodal resin for selective capture of CHO-derived monoclonal antibodies directly from harvested cell culture fluid, *J Chromatogr B*, 969 (2014) 256-263.

III.6. Supplementary Material

The elution fractions from protein A and PBA purifications of the serum-containing and serum-free CHO DP-12 cell culture supernatants as the serum-free CHOEBNALT85 cell culture supernatants were analyzed by SEC-HPLC as referred in Sections III.3.1.4.1, III.3.1.5.1. and III.3.1.5.2., respectively. The figures mentioned in those sections are presented as supplementary data for a better comprehension of the results.

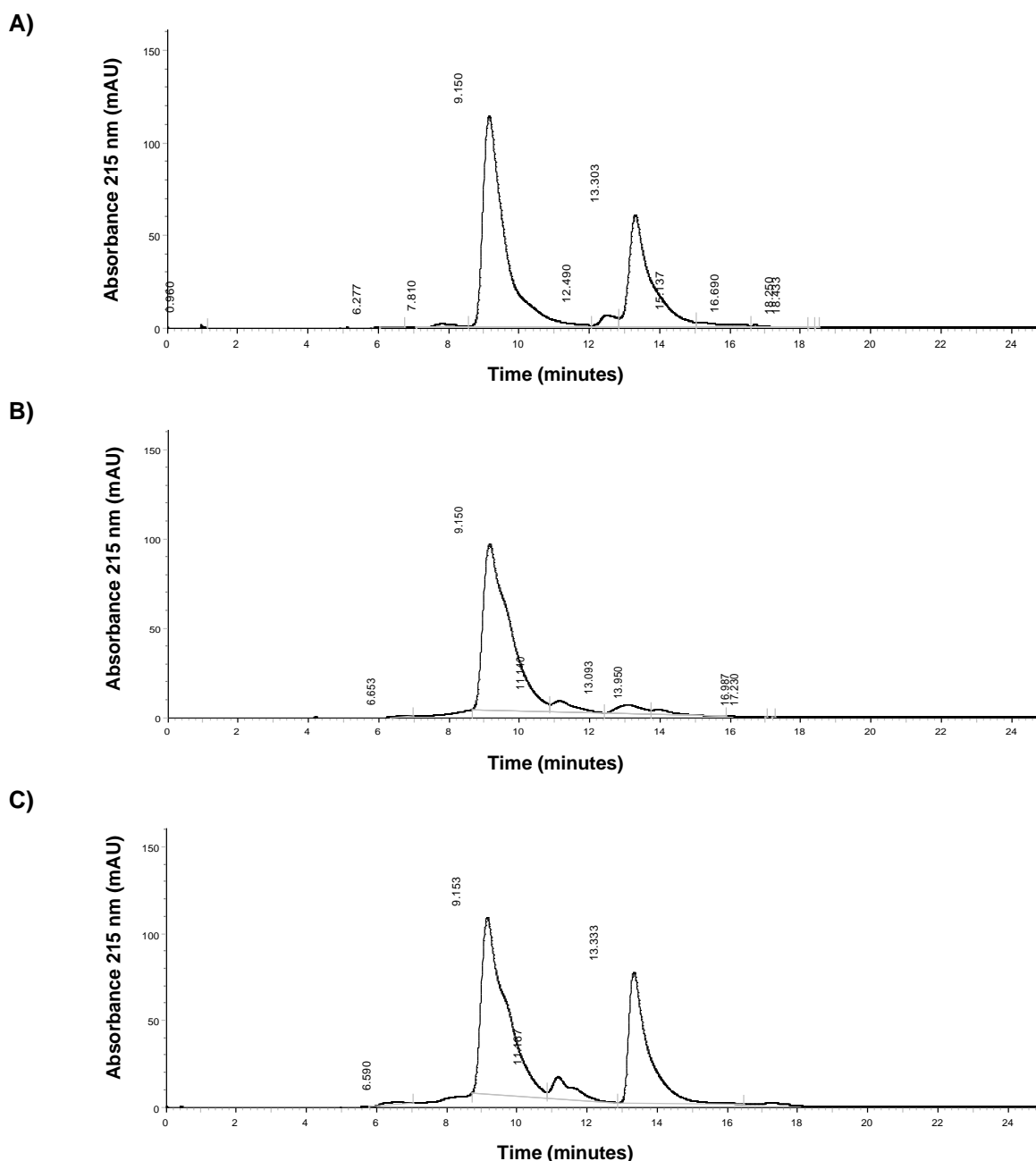


Figure III.S1 Analytical chromatogram from SEC-HPLC analysis of the purified IgG fractions from 2.5% serum-containing CHO DP-12 cell culture supernatants. (A) Protein A chromatography. Adsorption buffer: 10 mM PBS, pH 7.4; elution buffer: 100 mM glycine-HCl, pH 2. (B) PBA chromatography: Adsorption buffer: 20 mM HEPES, 150 mM NaCl, pH 7.5; wash buffer: 100 mM D-sorbitol in 10 mM Tris-HCl, pH 7.5; elution buffer: 0.5 M D-sorbitol and 150 mM NaCl in 10 mM Tris-HCl, pH 7.5. (C) PBA chromatography: Adsorption buffer: 20 mM HEPES, 150 mM NaCl, pH 7.5; wash buffer: 100 mM D-sorbitol in 10 mM Tris-HCl, pH 7.5; elution buffer: 1.5 M Tris-HCl, pH 7.5.

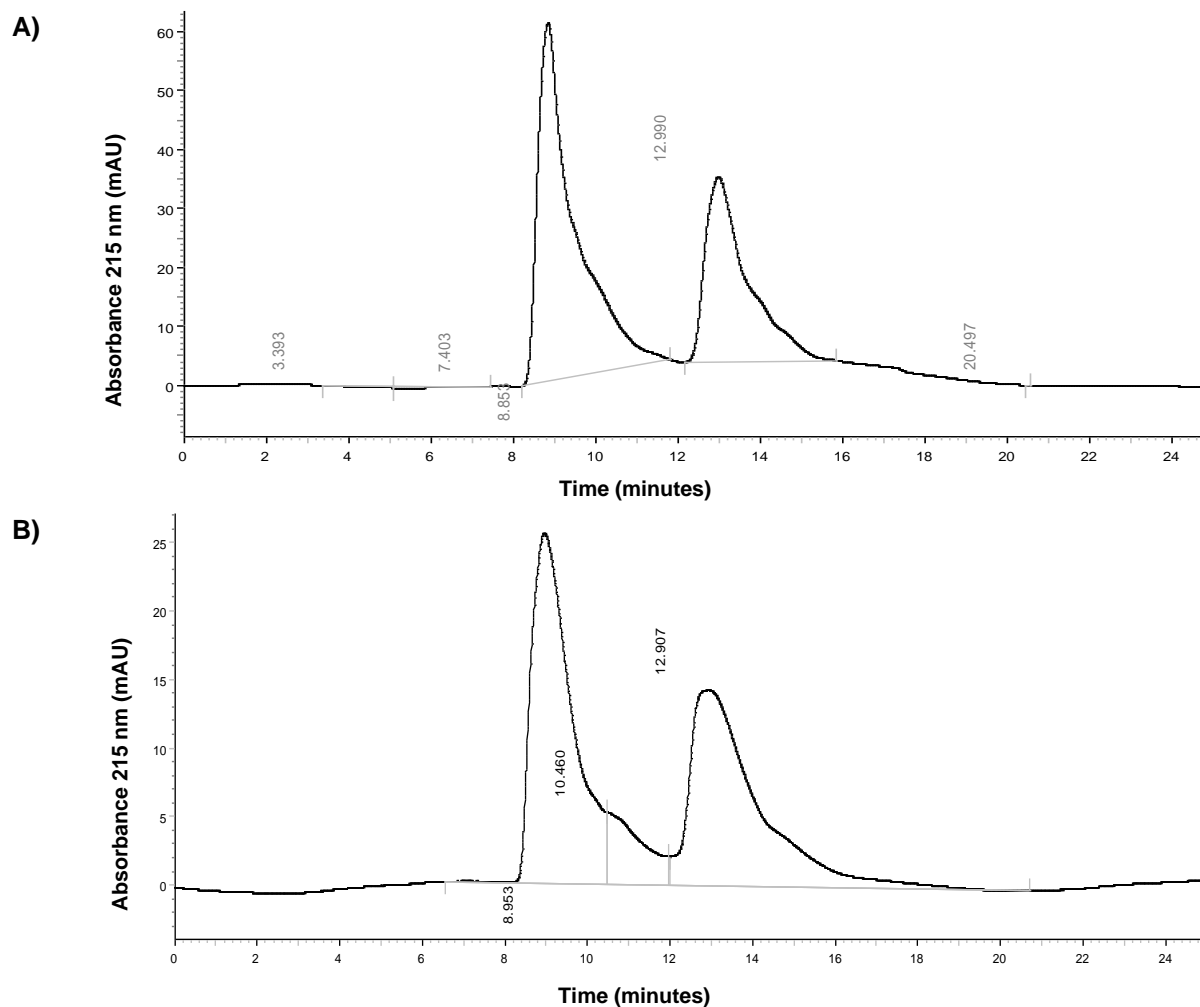


Figure III.S2 Analytical chromatogram from SEC-HPLC analysis of the purified IgG fractions from serum-free CHO DP-12 cell culture supernatants. (A) Protein A chromatography. Adsorption buffer: 10 mM PBS, pH 7.4; elution buffer: 100 mM glycine-HCl, pH 2. (B) PBA chromatography: Adsorption buffer: 20 mM HEPES, 150 mM NaCl, pH 7.5; wash buffer: 100 mM D-sorbitol in 10 mM Tris-HCl, pH 7.5; elution buffer: 0.5 M D-sorbitol and 150 mM NaCl in 10 mM Tris-HCl, pH 7.5.

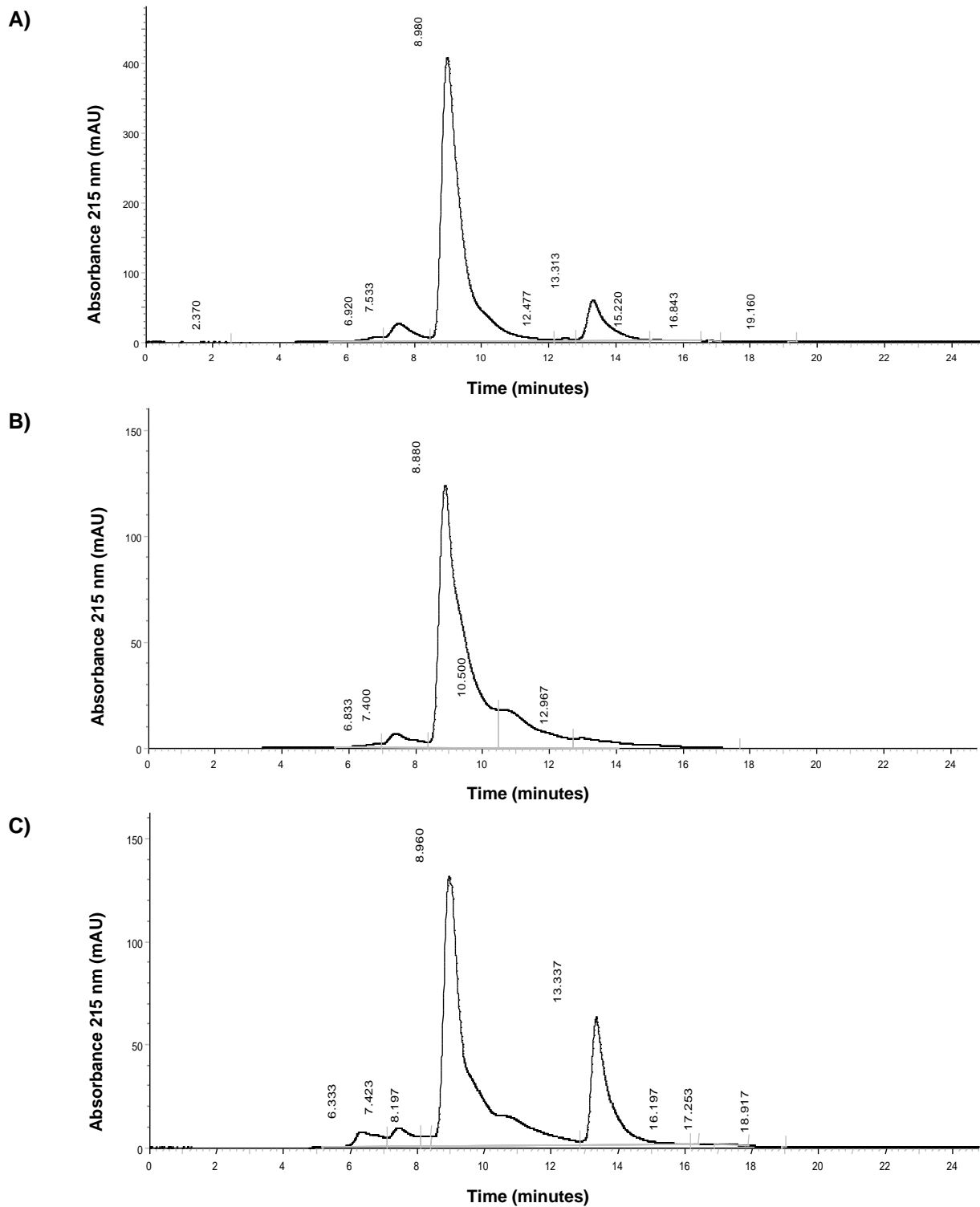


Figure III.S3 Analytical chromatogram from SEC-HPLC analysis of the purified IgG fractions from serum-free CHOEBNALT85 cell culture supernatants. (A) Protein A chromatography. Adsorption buffer: 10 mM PBS, pH 7.4; elution buffer: 100 mM glycine-HCl, pH 2. (B) PBA chromatography: Adsorption buffer: 20 mM HEPES, 150 mM NaCl, pH 7.5; wash buffer: 100 mM D-sorbitol in 10 mM Tris-HCl, pH 7.5; elution buffer: 0.5 M D-sorbitol and 150 mM NaCl in 10 mM Tris-HCl, pH 7.5.

Chapter IV - Exploring the selectivity of phenylboronate chromatography towards glycosylated and non-glycosylated proteins: proof of concept

Abstract: Boronate affinity chromatography has been extensively used for the capture and enrichment of *cis*-diol containing species such as glycoproteins. However, it has also been reported that this type of chromatography relies on a more complex system which presents a multimodal behaviour. Therefore, its application to the purification of proteins could be turned broader covering both glycosylated and non-glycosylated proteins. The choice of the experimental conditions (pH, conductivity and type of salt) has been described as essential for the manipulation of the selectivity of the ligand towards a type of proteins in detriment of the other. Thus, it is possible to envisaging the capacity of the *m*-aminophenylboronic acid (*m*-APBA) ligand to effectively separate different types of proteins from a complex mixture or even proteins of the same group but with tenuous differences in charge, for example. Herein, different elution strategies were carried out in order to explore phenylboronic acid (PBA) chromatography selectivity. In particular, the addition of displacers and application of pH gradients were investigated. From the different conditions screened, a Tris gradient at pH 9.0 and a citrate gradient at pH 5.0 provided the best *m*-APBA selective elution pattern, respectively for the glycosylated and acidic/neutral proteins under study. With the use of Tris, it was possible to selectively elute glycosylated proteins retained at alkaline pH by affinity *cis*-diol interaction. When the system was challenged with an artificial mixture of four different glycoproteins, the best separation result was achieved with a linear gradient rate of 0.6% Tris/min (≈ 3 mM Tris/min). Gradient elution was also performed for acidic/neutral proteins separation. In this case, proteins were selectively eluted at acidic pH using a citrate linear gradient, with a rate of 0.75% citrate/min (≈ 3.75 mM citrate/min) providing the best peaks separation. On the other hand, elution strategies considering pH gradients failed to promote selective elution of the different proteins under study. In the majority of the cases, the same protein was not completely eluted within a broad range of pH values indicating that changes in the ligand conformation and overall charge of proteins were not sufficient to promote the elution of such proteins and consequently, corroborating the presence of multimodal interactions between ligand and proteins. In sum, this work provides a broader understanding on PBA selectivity towards different types of proteins disclosing some of the mechanisms involved in the adsorption but especially in their desorption process.

Keywords: Protein purification, Glycosylated and non-glycosylated proteins, Phenylboronate chromatography, Elution studies, Selectivity analysis

IV.1. Background

Phenylboronate (PB) chromatography has been used since the 70s for the separation of a wide variety of sugar-containing compounds, such as carbohydrates [1, 2], glycoproteins [3, 4], glycolipids [5] and nucleic acids [6-8], using different types of supports, including not only the traditional beads but also magnetic nanoparticles [9], monoliths [10] and membrane adsorbers [11]. The core interaction in boronate chromatography is a reversible esterification reaction that occurs between the boronate ligand and a *cis*-diol containing molecule [12]. Several types of diols can react with boronic acids however, 1,2 *cis*-diol geometry has been reported as the most favourable for esterification [13, 14]. PB chromatography is mostly performed at alkaline conditions since it is known that the tetrahedral conformation of the ligand is more prone to establish the specific *cis*-diol interactions due to the higher association constant towards *cis*-containing molecules that presents ($K_{\text{tet}} > K_{\text{trig}}$) [15]. Nevertheless, the interaction between PB and diols is not as simple as it seems due to the multimodal nature of the ligand [16], *i.e.*, due to the ability of PB to participate in different type of interactions.

Multimodal chromatography is becoming a feasible strategy to obtain more efficient purification processes, as it could bring some advantages over single-mode chromatography. For example, the modulation and even enhancement of the selectivity in systems where it is desirable to separate proteins from closely related variants can be achieved by using multimodal chromatography [17]. Nevertheless, this type of chromatography is complex and more fundamental studies are needed to reveal the mechanisms of interactions involved. PB chromatography is a clear example of this complexity with several studies revealing non-specific interactions as driving forces for protein adsorption towards PB ligands as, for example, the *m*-APBA ligand [13, 18, 19]. Indeed, besides the *cis*-diol esterification reactions, several other types of interactions can play an important role in molecules adsorption towards the *m*-APBA ligand ($\text{pK}_a = 8.8$). At alkaline conditions ($\text{pH} > \text{pK}_a$), boronic acids are negatively charged presenting a tetrahedral conformation due to the hydroxylation of the boron atom, allowing the ligand to act also as cation exchanger. This behaviour can be noticed in some studies where NaCl was used to avoid the electrostatic repulsion of the target biomolecule [13, 19, 20], or to shield electrostatic interactions of impurities and increase selectivity towards the protein target [4, 20]. At acid or neutral conditions ($\text{pH} < \text{pK}_a$), the ligand adopts a trigonal conformation where the boron atom has an empty orbital, which can act as an electron receptor for charge transfer or coordination interactions. The phenyl moiety of PBA can also provide hydrophobic or aromatic interactions, as cation- π interactions, that can be established between the phenyl ring and positively charged molecules [19]. Nevertheless, low ionic strength is usually applied to avoid these secondary interactions [19, 20].

Considering the multitude of interactions that the *m*-APBA ligand can establish, the work developed by Carvalho *et al.* (2014) is of major importance to disclose the phenomena involved in the adsorption of proteins [18]. The exhaustive evaluation of the adsorption of glycosylated and non-glycosylated proteins onto PB resins demonstrated the ability of PB chromatography to selectively adsorb proteins that differ in terms of charge and presence of glycans in their structure. Through the manipulation of the adsorption conditions it was shown that is possible to modulate the predominant type of interactions established between ligand and proteins during the adsorptive process. For example, the majority of

glycoproteins adsorption was achieved at alkaline conditions through the esterification of their diol groups with the hydroxyl groups of the tetrahedral boronate of the ligand [4]. Nevertheless, the retention of proteins, glycosylated or not, at neutral and acidic conditions has also been reported using the *m*-APBA ligand [4, 18]. Although the uncharged trigonal form of the ligand is less susceptible to form electrostatic and *cis*-diol interactions with proteins, its ability to participate in charge transfer interactions is extremely important to achieve high adsorption yields of acidic to neutral glycoproteins at these conditions [18].

The knowledge retrieved can be thus used to identify possibilities to explore the selectivity of PB chromatography during the elution process. Glycoproteins majorly captured *via cis*-diol esterification should be further fractionated during elution based on electrostatic (*via* an ionic strength gradient) or charge transfer interactions (*via* pH or Lewis base gradients). On the other hand, proteins adsorbed mainly by charge transfer interactions should be selectively recovered by using Lewis base species in buffer formulation aiming to reversibly modify the ligand surface properties.

The aim of this work is to provide purification strategies for different classes of proteins using PB chromatography as to give some insights on the multimodal character of the interactions that occur during the adsorption but especially, through the desorption process of such proteins. Different elution strategies were thus applied in order to separate two different classes of proteins, namely, (i) glycoproteins, adsorbed at alkaline conditions, and (ii) neutral/acidic proteins, adsorbed at acidic conditions. The selectivity of the elution process was analysed by applying displacer or pH gradients.

IV.2. Materials and Methods

IV.2.1. Chemicals

2-(Cyclohexylamino)ethanesulfonic acid (CHES), 4-(2-hydroxyethyl)-1-piperazinepropanesulfonic acid (EPPS), 4-(2-hydroxyethyl)-1-piperazineethanesulfonic acid (HEPES), 3-morpholino-2-hydroxypropanesulfonic acid (MOPSO), 2-(N-morpholino)ethanesulfonic acid (MES), [(2-Hydroxy-1,1-bis(hydroxymethyl)ethyl)amino]-1-propanesulfonic acid (TAPS), Tris(hydroxymethyl)aminomethane (Tris), tri-sodium citrate dehydrate and sodium chloride were purchased from Sigma–Aldrich (St. Louis, MO, USA). Sodium acetate anhydrous was obtained from Merck (Darmstadt, Germany) and hydrochloric acid and glacial acetic acid from Fisher Scientific (Waltham, MA, USA). Sodium hydroxide was acquired from José Manuel Gomes dos Santos Lda. (Odivelas, Portugal). All chemicals used were analytical or HPLC grade. Water used in all experiments was obtained from a Milli-Q purification system (Millipore, Bedford, MA, USA).

IV.2.2. Biologics

A protein library composed by the following proteins was obtained from Sigma-Aldrich® (St. Louis, MO, USA): amyloglucosidase from *Aspergillus niger*, cellulase from *Trichoderma reesei*, invertase from *Saccharomyces cerevisiae*, pepsin from porcine stomach, and ribonuclease B (RNaseB) from bovine pancreas. The proteins from this library were divided, according to their features, in two major groups: (i) glycosylated (amyloglucosidase, cellulase, RNase B and invertase) and (ii) acidic/neutral proteins

(amyloglucosidase, cellulase and pepsin). Protein Data Bank identity and characteristics as the molecular weight, isoelectric point and relevant functions of these proteins can be found in Table IV.1.

IV.2.3. Phenylboronate chromatography: development and optimization of elution steps

Selectivity studies were performed in order to demonstrate the ability of phenylboronate chromatography to separate different types of proteins from a complex mixture or even proteins of the same group but with tenuous differences in charge. For such studies, two different chromatographic supports –silica and agarose beads – functionalized with *m*-aminophenylboronic acid (*m*-APBA) were used: (i) ProSep®-PB (EMD Millipore, UK) and (ii) Aminophenylboronate P6XL (Prometic Bioseparations Ltd), respectively. At least two independent replicated assays were performed. Both two resins were packed on Tricorn™ 5/50 glass columns (GE Healthcare) with a resin volume of 1 mL. All chromatographic runs were performed in an ÄKTA Purifier 10 system from Amersham Biosciences (Uppsala, Sweden). The data collection and processing were accomplished using Unicorn 5.1 software. Conductivity, pH and UV absorbance at 280 nm were continuously measured at the sample outlet. Samples were collected using a Frac-950 fraction collector from GE Healthcare, and further analysed by SDS-PAGE.

Glycoproteins separation studies were performed using an adsorption buffer at alkaline pH (pH 9.0), while studies aiming the separation of acidic and neutral proteins, comprising glycosylated and non-glycosylated proteins, were run using an acidic adsorption buffer (pH 4.0 or 5.0). Different elution strategies were then performed using either 1) a displacer gradient or 2) a pH gradient in order to explore the multimodal behaviour of the *m*-APBA ligand and understand its selectivity in order to enhance elution processes. The optimization studies were performed using the silica-based ProSep®-PB resin. Posteriorly, the agarose-based Aminophenylboronate P6XL resin was challenged with artificial protein mixtures of the aforementioned groups of proteins under the best conditions achieved during the optimization studies.

IV.2.3.1. Displacer gradients

Chromatographic runs, comprising the study of the behaviour of the *m*-APBA ligand towards the separation of glycoproteins, were performed using an adsorption buffer composed by 20 mM CHES, 300 mM NaCl at pH 9.0. In the case of the acidic/neutral proteins, the adsorption buffer used was 50 mM acetate, pH 5.0. These conditions were chosen considering a previous work from Carvalho *et al.*, (2014) in which several adsorption conditions were screened for the same type of proteins under study.

Table IV.1 Summary table of the most important characteristics of proteins to the current study. A glimpse about the function of each protein is also present. PDB ID stands for Protein Data Bank Identity. MW and pI stand for molecular weight and isoelectric point, respectively. ^a Product specifications provided by the supplier.

Protein	Abbreviation	Source	Type	PDB ID	MW (kDa)	pI	Protein group	Function	Ref.
Amyloglucosidase	AMY	<i>Aspergillus niger</i>	Glycosylated	3GLY	97	3.6	Glycoprotein Acidic-neutral	<ul style="list-style-type: none"> Converts starch to dextrins and glucose Capable of hydrolysing the α-D-(1-4) and α- (1,6) glucosidic bonds of starch and malto-oligosaccharides 	^a
Cellulase	CEL	<i>Trichoderma reesei</i>	Glycosylated	3QR3	65	5.7	Glycoprotein Acidic-neutral	<ul style="list-style-type: none"> Breakdown of cellulose molecules into monosaccharides such as beta-glucose, or shorter polysaccharides and oligosaccharides 	[21, 22]
Ribonuclease B	RNase B, RB	<i>Bos taurus</i>	Glycosylated	1RBB	15	8.8-9.7	Glycoprotein	<ul style="list-style-type: none"> Demonstration of N-linked deglycosylation; Source of N-glycans following enzymatic digestion 	[23, 24]
Invertase	INV	<i>Sacharomyces cerevisiae</i>	Glycosylated	4EQV	270	3.4 – 4.4	Glycoprotein	<ul style="list-style-type: none"> Catalyzes the following reaction: <i>Sucrose + H₂O > Glucose + Fructose</i> (Raffinose and methyl-b-D-fructofuranoside may also be used as substrates.) 	^a
Pepsin	PEP	<i>Porcine gastric mucosa</i>	Non-glycosylated	3PEP	35	2.2 – 3.0	Acidic-neutral	<ul style="list-style-type: none"> Peptidase that only hydrolyzes peptide bonds, not amide or ester linkages 	^a

IV.2.3.1.1. Displacer selection

In order to select the more adequate displacer, the adsorption buffers were supplemented with different compounds in order to obtain the elution buffers that will be screened. For the elution of glycoproteins, 0.5 M Tris, 0.5 M D-sorbitol, 0.5 M D-fructose, 0.5 M citrate and 0.5 M borate were added to the respective adsorption buffer. To the acidic/neutral proteins elution studies, 0.5 M Tris and 0.5 M citrate were the selected displacers.

Firstly, the column was equilibrated with 10 column volumes (CVs) of the adsorption buffer. Then, 100 µg of each protein, dissolved in adsorption buffer, was separately loaded using a loop of 100 µL at 1 mL/min, with the loop being emptied with three-times its volume. After the unbound or weakly bound material were washed-out with 5 CVs of the adsorption buffer and the bound material was eluted using a linear gradient of 20 CVs of length followed by a 5 CVs step gradient at 100% (v/v) of the elution buffer. The column was further regenerated using 1.5 M Tris-HCl pH 8.5 for 5 CVs. All the steps were conducted at 1 mL/min.

The percentage of protein recovered was calculated based on the areas of the eluted peaks obtained minus the areas of the *phantom* peaks generated by the elution buffers, when applicable.

IV.2.3.1.2. Linear gradients optimization

After selecting the best displacer to each set of proteins under study, the system was challenged using an artificial mixture of glycoproteins and other artificial mixture of acidic/neutral proteins. Hereupon, the need to optimize the separation of such proteins emerged. The adsorption procedure was maintained (see Section IV.2.3.1.) and each protein mixture prepared in order to be possible to inject 100 µg of each protein. A loop of 500 µL was then used and emptied with three-times its volume. The unbound or weakly bound material were washed-out with 5 CVs of the adsorption buffer. In the case of glycoproteins, the bound material was eluted using different linear gradients (see description below) followed by a 10 CVs step gradient at 100% (v/v) of the elution buffer. On the other hand, the elution of acidic/neutral proteins was accomplished with different linear gradients instantaneously followed by the regeneration of the column. In both cases, the column was regenerated using 1.5 M Tris-HCl pH 8.5 for 10 CVs. All the steps were conducted at 1 mL/min. For both protein groups, the elution evaluation comprised linear gradients of: (i) 20 CVs in length until reach 100% of the elution buffer at 5%/min, (ii) 20 CVs to reach 50% at 2.5%/min, (iii) 40 CVs to 50% at 1.25%/min and (iv) 40 CVs to 30% at 0.75%/min. All elution buffer percentages are given in a v/v ratio. To obtain a better separation of the glycoproteins under study, an additional linear gradient was tested: 25 CVs in length until reach 15% of the elution buffer at 0.6%/min. Afterwards, the conditions that allowed the best separation were tested with a 2.5-times higher protein loading using a loop of 1000 µL.

IV.2.3.1.3. Step gradients: Proof of concept

The knowledge acquired from the linear gradients performed as described in Section IV.2.3.1.2., gave tools for a better tuning of the separation of the aforementioned protein mixtures. Thus, the elution process was carried out using different step gradients leading to less diluted pools of each protein.

Again, the adsorption procedure was the described in Section IV.2.3.1., the protein mixtures injection carried out as referred in Section IV.2.3.1.2. and the unbound or weakly bound material washed-out with 5 CVs of the adsorption buffer. The elution of glycoproteins and acid/neutral proteins was conducted following a series of step gradients with 10 CVs of length. In the case of glycoproteins the steps performed were of 2%, 4.5%, 8.5%, 15% and 100% (v/v) of elution buffer. For the elution of the acidic/neutral proteins under study, steps of 1.5%, 4% and 15% (v/v) of elution buffer were used. Regeneration of the column was accomplished using 1.5 M Tris-HCl pH 8.5 for 10 CVs, in both cases. At last, systems were tested with a 2.5-times higher protein loading using a loop of 1000 μ L.

IV.2.3.2. pH gradients

With the aim of studying the ability of applying pH gradients to fractionate glycoproteins and acidic/neutral proteins using phenylboronate chromatography, different pH gradients were evaluated. The pH gradients selected were based on the work of Kröner and Hubbuch, (2013), which provides the generation of buffer compositions with linear titration curves to be applied to ion exchange chromatography as controllable and linear pH gradients [24]. The buffer compositions used in the present work are described in Table IV.1 with all the components being acidic buffers. One buffer formulation, BGly, was prepared aiming the separation of glycoproteins and other two others, BAN1 and BAN2, for the separation of acidic/neutral proteins.

Table IV.2 Buffer systems used to obtained linear pH gradients for the separation of glycoproteins (BGly) and acidic/neutral proteins (BAN1 and BAN2).

Buffer components	Buffer composition		
	BGly	BAN1	BAN2
9.4 mM CHES	x	x	x
4.6 mM TAPS			x
4.6 mM HEPES	x	x	
9.9 mM EPPS	x	x	x
8.7 mM MOPSO	x	x	x
11 mM MES	x	x	x
13 mM Acetate	x	x	x
300 mM NaCl	x		

Prior to injection, the columns were equilibrated with 10 CVs of adsorption buffer. The adsorption buffer used for the adsorption of glycoproteins was BGly at pH 9.0. In the case of acidic/neutral proteins, the adsorption was performed using BAN1 and BAN2 at acidic pH values. The adsorption of the acidic/neutral proteins onto the ProSep®-PB resin was carried out at pH 4.0, and at pH 5.0, when working with the P6XL resin. Such conditions were selected based on a previous study that show that at pH 4.0 is not possible to adsorb all proteins onto the P6XL resin [18]. Afterwards, 100 μ g of each protein was separately loaded at 1 mL/min using a loop of 100 μ L, with the loop being emptied with

three-times its volume. Protein solutions were obtained by dissolution of proteins in the selected adsorption buffer. The unbound or weakly bound material were washed-out with 5 CVs of the adsorption buffer and the bound material was eluted using a linear gradient of 15 CVs of length followed by a ten CVs step gradient at 100% (v/v) of the elution buffer. The column was further regenerated using 1.5 M Tris-HCl pH 8.5 for 10 CVs. All the steps were conducted at 1 mL/min. The buffers used for the elution of glycoproteins were BGly at pH 4.0 (ProSep®-PB) and at pH 5.0 (P6XL). For the elution of acidic/neutral proteins, BAN1 and BAN2 were employed at pH 9.0.

The percentage of protein recovered was determined based on the peak areas obtained in the chromatogram divided by the total peak area minus the areas of the *phantom* peaks generated by the elution buffers, when applicable.

IV.2.4. Protein gel electrophoresis

Sodium dodecyl sulfate–polyacrylamide gel electrophoresis (SDS–PAGE) was performed to qualitatively evaluate (i) the different commercial protein samples used, (ii) the artificial mixtures of proteins under study and (iii) the samples collected during all the chromatographic runs carried out. Samples were diluted with loading buffer (62.5 mM Tris-HCl, pH 6.2, 2% (w/v) SDS, 10% (v/v) glycerol, 0.01% (w/v) bromophenol) prior to be exposed to denaturation conditions with 100 mM dithiothreitol, from Sigma-Aldrich, at 100 °C for 5 minutes. The different commercial protein samples as the artificial mixtures were diluted in order to apply 5 µg of each protein in the gel. Samples collected from the chromatographic runs were previously concentrated, from 20 to 60-fold, using Amicon Ultra-15, 4 or 0.5 centrifugal filter units (MWCO of 3 or 10 kDa) from Merck Millipore. Afterwards, samples were applied in a 12% acrylamide gel, prepared from a 40% acrylamide/bis stock solution (29:1) from Bio-Rad. The samples were ran at 150 mV using as running buffer composed by 192 mM glycine, 25 mM Tris-HCl and 0.1% (w/v) SDS, pH 8.3. Gels were stained with Coomassie Brilliant Blue (Pharmacia, Uppsala, Sweden). Images were acquired with a GS-800 calibrated densitometer from Bio-Rad (Hercules, CA, USA).

IV.3. Results and Discussion

A protein library composed by five proteins was selected for this study. Among them, it can be found glycoproteins comprising a broad range of isoelectric points and acidic/neutral proteins that include glycosylated and non-glycosylated proteins. The list of proteins chosen is presented in Section IV.2.2.. Information regarding their molecular weight, isoelectric point and relevant functions is available in Table IV.1). To confirm the molecular weight as the purity and protein profile of each commercial protein under study, a SDS-PAGE was run (Figure IV.S1, Supplementary Material). The validation of the presence or absence of a glycosylation site on each protein was also carried out using a Pierce™ Glycoprotein Staining Kit confirming the information provided by the suppliers (data not shown).

The selection of the different proteins was performed aiming to prove the ability that PB chromatography has to adsorb and selectively elute proteins within the aforementioned groups. This work will be focused on the *m*-APBA ligand affinity behaviour towards *cis*-diol compounds, e.g.

glycoproteins, and also on its multimodal behaviour. The ligand multimodal character could be the key to a successful separation of glycoproteins with different charge profiles and to the widespread application of this type of chromatography to other protein classes such as non-glycosylated proteins. In order to proceed with such studies, two different elution strategies were tested, based on the use of 1) displacer or 2) pH gradients.

IV.3.1. Displacer gradient studies

Compounds as Tris, citrate, borate, D-fructose and D-sorbitol were tested in order to evaluate their performance as displacers for the selective elution of proteins adsorbed to PB resins. These studies were performed using linear gradients of the selected displacers which were chosen based on previous works which described effective protein elution from PB resins.

In the majority of the cases described in the literature, the elution process is driven by competition phenomena since most displacers are also able to perform *cis*-diol esterification with the *m*-APBA ligand:

- Tris has showed the ability to interact with the *m*-APBA ligand by tridentate interaction at alkaline pH, when applied as shielding reagent [25] or elution buffer [4, 7, 26];
- Citrate is a strong Lewis base comprising three carboxylic acid moieties and is also an α -hydroxyacid, being thus able to perform either charge-transfer or a coordination interaction with the trigonal conformation of the *m*-APBA ligand [27, 28];
- Borate has been reported as an important component of washing buffers, e.g. in anion exchange chromatography, allowing the separation of host glycoproteins that exhibit similar charge, size, and hydrophobicity characteristics to the target molecule [29];
- D-fructose and D-sorbitol are able to establish specific *cis*-diol interactions with *m*-APBA, leading to the selective elution of molecules adsorbed to the ligand by the same type of interactions, i.e. *cis*-diol containing molecules, such as glycoproteins [13, 20]. D-fructose and D-sorbitol were selected in detriment of other carbohydrates such as D-mannitol since they present higher affinity constants towards *m*-APBA ($K_{\text{eqD-sorbitol}} = 370 \text{ M}^{-1} > K_{\text{eqD-fructose}} = 160 \text{ M}^{-1} > K_{\text{eqD-mannitol}} = 120 \text{ M}^{-1}$ [30]) making them stronger competitors in both *m*-APBA configurations (trigonal and tetrahedral).

IV.3.1.1. Displacer gradient studies for the separation of glycosylated proteins

Glycosylated proteins were adsorbed to *m*-APBA ligand at alkaline conditions (pH 9.0) to promote the establishment of specific *cis*-diol interactions between the protein and ligand. 300 mM NaCl were added in order to suppress non-specific interactions that could occur between the negatively charged silanol groups present in bare beads, the phenyl group present in the ligand structure and proteins. These conditions were already reported to promote the adsorption of all glycoproteins under study towards the *m*-APBA ligand, regardless of their charge [18].

The first step in the development of an elution strategy was to evaluate the ability of PB chromatography to selectively elute different glycoproteins by screening the different selected displacers.

Results showed that citrate and borate were not able to elute the glycosylated proteins, which were only recovered during the regeneration step with 1.5 M Tris-HCl, pH 8.5 (data not shown). Citrate, as α -hydroxyacid, was expected to promote the elution of glycoproteins by coordination interactions with the hydroxyl groups linked to the negatively charged boron present on the ligand [28, 31]. However, citrate was not effective in the elution of the retained glycosylated proteins most likely due to its inability to compete with the high association constants achieved between the carbohydrate moieties present in glycoproteins and the *m*-APBA ligand. Borate is able to form complexes with sugar residues containing *cis*-diol groups. Nevertheless, it was not able to compete with the boronate ligand, failing to establish strong interactions with the adsorbed glycoproteins in order to promote their elution [29, 32].

Tris, D-fructose and D-sorbitol were however effective in eluting all proteins with 100% recovery, nevertheless, D-fructose and D-sorbitol did not provide any selectivity to the elution process, with all proteins being recovered at the same retention time (Figure IV.1). Tris was the only displacer able to selectively elute the proteins absorbed. According to Figure IV.1, the more acidic the protein is, the higher the concentration of Tris required to elute it. Nonetheless, the secondary interactions involved seem not to be predominantly of the electrostatic type. The presence of the negatively charge boron, characteristic of the tetrahedral conformation of the ligand, was expected to promote attractive electrostatic interactions between the ligand and glycoproteins as RNase B ($pI = 8.8-9.7$) due to its positive overall charge but the opposite was observed. Indeed, what is observed is that smaller glycoproteins (e.g. RNase B) are eluted at low concentrations of Tris and glycoproteins with higher molecular weights, such as invertase, are eluted at higher concentrations of Tris. Tris has been described as a shielding agent able to disrupt not only *cis*-diol interactions but also non-specific interactions as electrostatic. Therefore, it is reasonable to consider that a higher concentration of the agent is needed to achieve the complete shielding of proteins with higher molecular weights and consequently, promote their elution. Other explanations to the results obtained could rely on (i) the glycosylation profile as on (ii) the glycosylation occupancy or glycoform stoichiometry of each protein. Different glycosylation patterns and absolute protein glycosylation stoichiometry could promote different degrees of affinity regarding both adsorption and desorption process of proteins. For example, the result achieved for invertase could be related to its highly glycosylated structure. Invertase is composed by 50% (w/w) mannose and 3% (w/w) glucosamine [33] which will enhance the occurrence of specific *cis*-diol interactions between protein and ligand. Plus, the patches by which each glycoprotein adsorb to the *m*-APBA ligand could present specific electrostatic potential that may differ from the overall charge of the protein. D-sorbitol has also been reported to disrupt non-specific interaction at high concentrations [13] and to provide high recovery and purity in IgG purification [20], however this displacer did not provided the selectivity desired for this study.

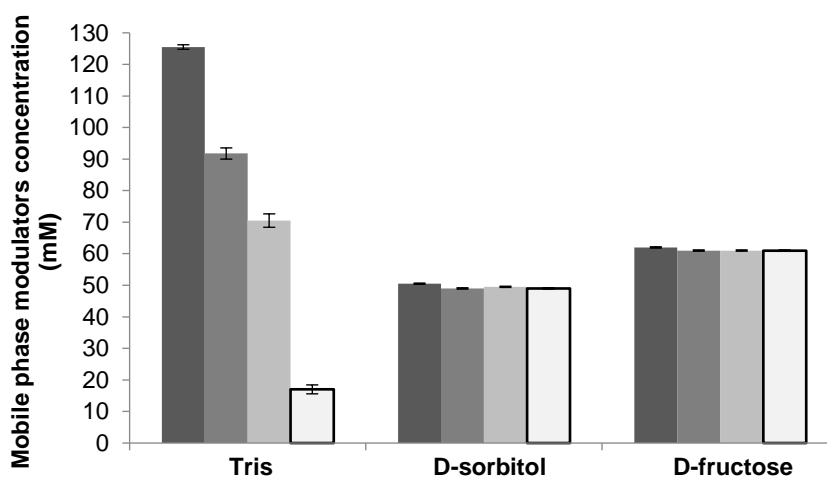


Figure IV.1 Mobile phase modulators concentration required to promote complete elution of the different glycoproteins under study. Studies were performed using a ProSep®-PB resin. Adsorption of glycoproteins was performed using 20 mM CHES, 300 mM NaCl, pH 9.0. Results are based on the mobile phase concentration present in the elution buffer at which was obtained the maximum peak height. Acidic invertase (■), acidic amyloglucosidase (■), neutral cellulase (■) and basic RNase B (□). Results are displayed as average \pm STDV.

Considering the promising results obtained using Tris as displacer, the fractionation of an artificial mixture, composed by all the glycoproteins previously described was tested, using the same linear gradient (from 0 to 0.5 M Tris). The resultant chromatogram exhibited two elution peaks with low resolution (C1, Figure IV.2A). In fact, it seems that the first peak observed could be masking two effective peaks. To enhance the resolution of the separation, different gradient slopes were tested from 5 to 0.6% Tris/min [34-36]. The decrease of the gradient slopes allowed to achieve a complete separation of the peaks (Figure IV.2A).

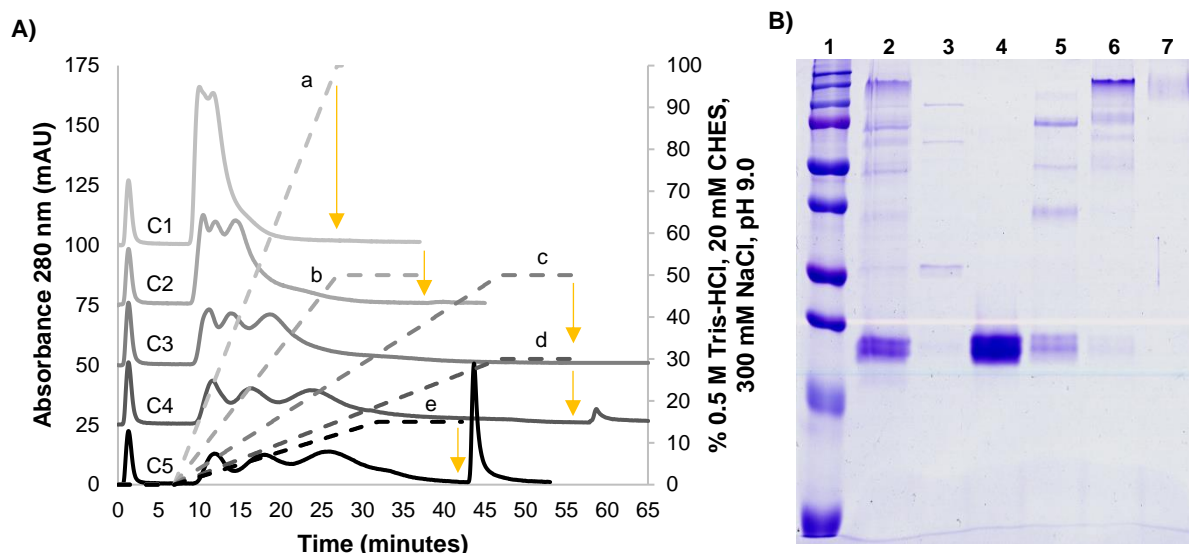


Figure IV.2 (A) Chromatograms obtained using a ProSep®-PB resin for the separation of an artificial mixture containing 1 mg/mL of each glycoprotein under study prepared in the adsorption buffer 20 mM CHES, 300 mM NaCl at pH 9.0. Five different gradient slopes were performed considering an elution buffer containing 0.5 M Tris as displacer agent (a-e). The gradients were performed under the rates of (a) 5 % Tris/min, (b) 2.5 % Tris/min, (c), 1.25 % Tris/min, (d) 0.75 % Tris/min and (e) 0.6 % Tris/min giving rise to five distinct chromatograms – C1 to C5, respectively. The times at which the system was imposed to start to pump 100% (v/v) of the elution buffer are marked with a yellow arrow. C5 presents five peaks denominated as flow-through (FT), peak 1 (P1), peak 2 (P2), peak 3 (P3) and peak 4 (P4), from left to right. (B) Coomassie Blue stained SDS-PAGE of the fractions collected during glycoproteins separation by PB chromatography using a ProSep®-PB resin and an elution gradient strategy accomplished by the use of 0.5 M Tris as displacer agent at a rate of 0.6% Tris/min. Lanes ID: 1: Precision Plus Protein™ Dual Color Standards (from top to bottom: 250, 200, 150, 100, 75, 50, 37, 25, 20 and 10 kDa); 2: artificial mixture containing 5 µg of each glycoprotein under study; 3: flow-through (FT) fraction; 4: P1; 5: P2; 6: P3; 7: P4.

Analysing all the chromatograms (Figure IV.2A) it is possible to understand that higher gradient slopes (a, b, and c) did not promoted an effective separation of invertase from the other glycoproteins present in the mixture. As previously discussed, invertase was the glycoprotein which elution was only possible at higher Tris concentrations (around 125 mM Tris). At higher rates, the percentages of elution buffer reached at the end of the elution process were very high (100% and 50% (v/v)) and, consequently, the concentrations of Tris reached were greater than 125 mM. Moreover, by applying higher rates of Tris the changes in the concentration of Tris along the elution process occurred faster which did not lead to the selectivity necessary to collect all glycoproteins in distinct peaks. Using the gradient slope d (0.75% Tris/min) is already possible to notice that part of the loaded invertase is eluted separately. However, it is only with a rate of 0.6% Tris/min (slope e, Figure IV.2A) that invertase is not co-eluted during the Tris gradient with other glycoproteins as amyloglucosidase (see Figure IV.1). The SDS-PAGE analysis of the fractions obtained by using a gradient slope of 0.6% Tris/min (Figure IV.2B) are in accordance with the results described when each protein was separately loaded into the column (Figure IV.1). RNase B was mostly eluted in the first elution peak (Figure IV.2B, line 4,). Cellulase was co-eluted with a minor fraction of RNase B in the second peak (Figure IV.2B, line 5). The majority of amyloglucosidase was collected in the third peak (Figure IV.2B, line 6) and invertase recovered in the fourth peak (Figure IV.2B, line 7) presenting high purity.

Although the previous results demonstrate the ability of PB chromatography to selective elute glycoproteins, the linear gradients used led to broad peaks (C5, Figure IV.2A) and consequently, to the collection of highly diluted protein samples. Stepwise elution was then tested aiming to increase the peak resolution as to decrease the dilution of proteins. For that purpose, concentrations of 2%, 4.5%, 8.5%, 15% and 100 % (v/v) of the elution buffer containing 0.5 M Tris were selected and indeed, the peaks obtained were better resolved than the ones acquired using a linear gradient elution (Figure IV.3A vs Figure IV.2A). Furthermore, the use of a series of step gradients revealed to be essential to obtain a more selective elution of glycoproteins. During the application of the linear gradient, RNase B was recovered in all the peaks collected (Figure IV.2B). Using a stepwise elution strategy, RNase B was majorly collected at a concentration of 2% (v/v) of elution buffer (Figures IV.3B and IV.5B). Cellulase was recovered using 4.5% (v/v) of elution buffer with a higher purification degree and amyloglucosidase was eluted at the step gradients of 8.5% (v/v) and 15% (v/v) (Figure IV.3B). Considering this result, process optimization could be further achieved removing the elution step using 8.5% (v/v) and applying only the step comprising the use of 15% (v/v) elution buffer. Invertase, as previously observed, was only recovered in the presence of 100% (v/v) elution buffer (Figure IV.3B).

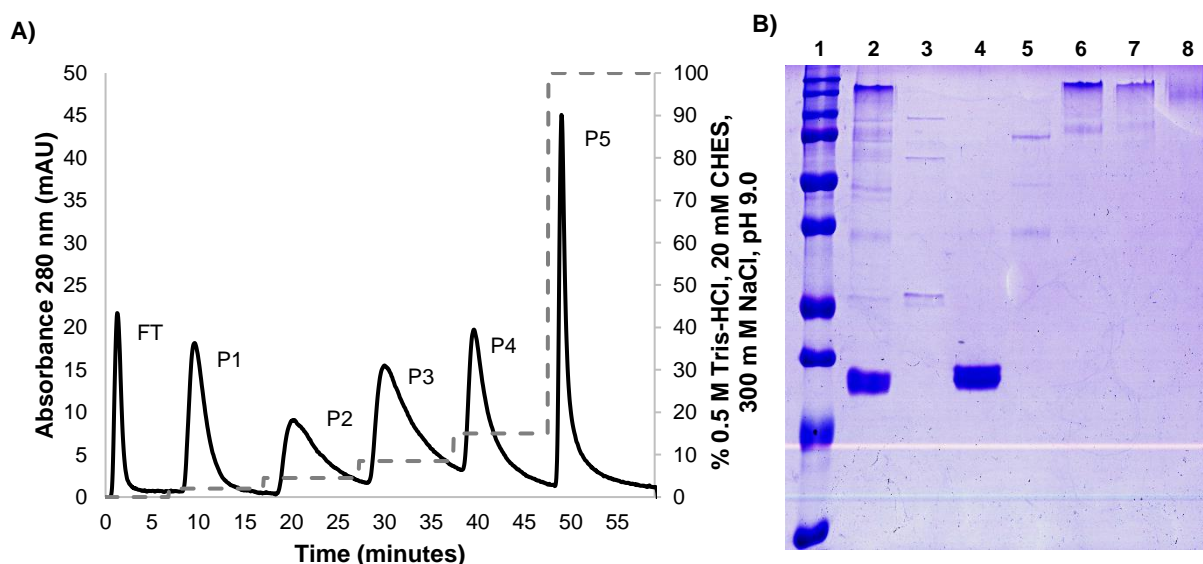


Figure IV.3 (A) Chromatograms obtained using a ProSep®-PB resin for the separation of an artificial mixture containing 1 mg/mL of each glycoprotein under study prepared in the adsorption buffer 20 mM CHES, 300 mM NaCl at pH 9.0. The elution process was performed using a series of step gradients – 2.0%, 4.5%, 8.5%, 15% and 100% (v/v). The elution buffer used was obtained by addition of 0.5 M Tris to the adsorption buffer. The chromatogram presents six peaks denominated as flow-through (FT), peak 1 (P1), peak 2 (P2), peak 3 (P3), peak 4 (P4) and peak 5 (P5), from left to right. (B) Coomassie Blue stained SDS-PAGE of the fractions collected during glycoproteins separation by PB chromatography using a ProSep®-PB resin and an elution strategy accomplished by the use of a series of step gradients – 2%, 4.5%, 8.5%, 15% and 100% (v/v). Lanes ID: 1: Precision Plus Protein™ Dual Color Standards (from top to bottom: 250, 200, 150, 100, 75, 50, 37, 25, 20 and 10 kDa); 2: artificial mixture containing 5 µg of each glycoprotein under study; 3: flow-through (FT) fraction; 4: P1; 5: P2; 6: P3; 7: P4; 8: P5.

Higher protein loads (2.5x) were tested in the linear and step gradient mode with similar results being achieved in terms of chromatographic profiles and protein separation efficacy (Figures IV.4 and IV.5).

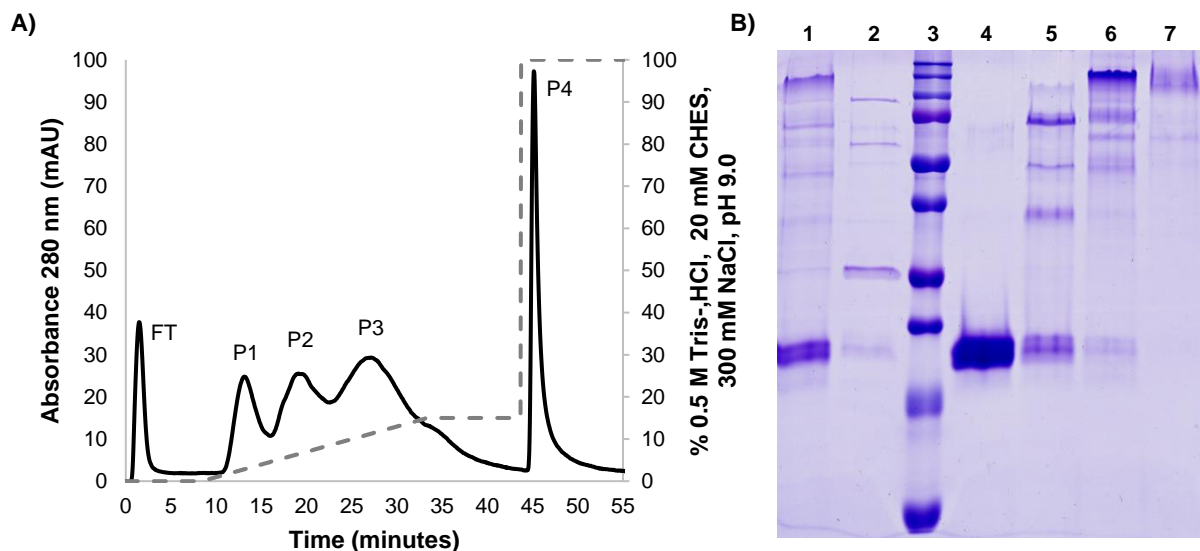


Figure IV.4 (A) Chromatograms obtained using a ProSep®-PB resin for the separation of an artificial mixture containing 2.5 mg/mL of each glycoprotein under study prepared in the adsorption buffer 20 mM CHES, 300 mM NaCl at pH 9.0. The elution process was performed using a linear gradient performed at a rate of 0.6% Tris/min. The elution buffer used was obtained by addition of 0.5 M Tris to the adsorption buffer. The chromatogram presents five peaks denominated as flow-through (FT), peak 1 (P1), peak 2 (P2), peak 3 (P3) and peak 4 (P4), from left to right. (B) Coomassie Blue stained SDS-PAGE of the fractions collected during glycoproteins separation by PB chromatography using a ProSep®-PB resin and an elution gradient strategy accomplished by the use of 0.5 M Tris as displacer agent at a rate of 0.6% Tris/min. Lanes ID: 1: artificial mixture containing 5 μ g of each glycoprotein under study; 2: flow-through (FT) fraction; 3: Precision Plus Protein™ Dual Color Standards (from top to bottom: 250, 200, 150, 100, 75, 50, 37, 25, 20 and 10 kDa); 4: P1; 5: P2; 6: P3; 7: P4.

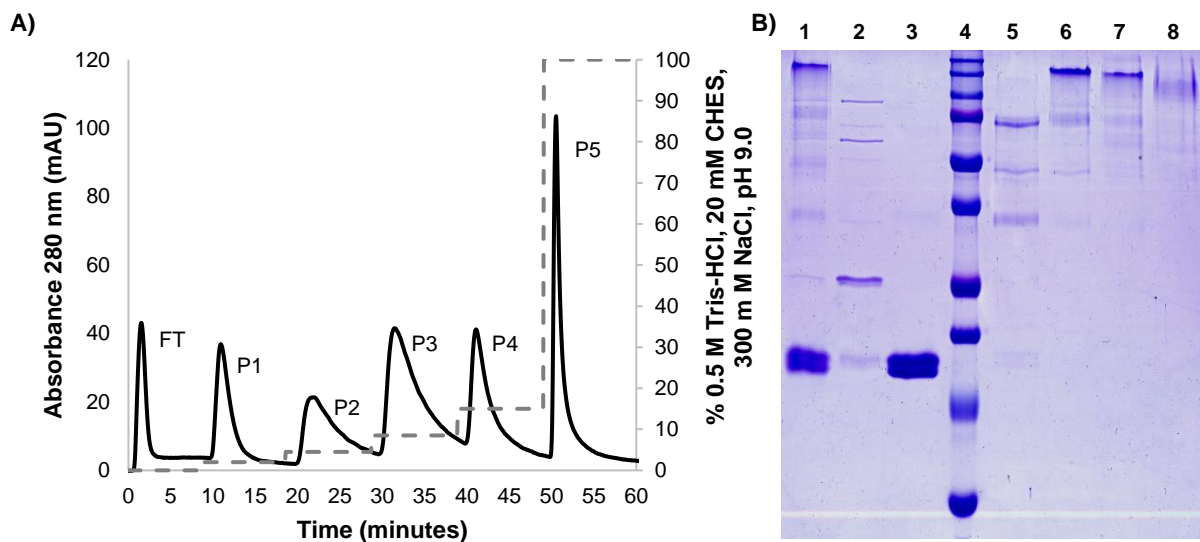


Figure IV.5 (A) Chromatograms obtained using a ProSep®-PB resin for the separation of an artificial mixture containing 2.5 mg/mL of each glycoprotein under study prepared in the adsorption buffer 20 mM CHES, 300 mM NaCl at pH 9.0. The elution process was performed using a series of step gradients – 2%, 4.5%, 8.5%, 15% and 100% (v/v). The elution buffer used was obtained by addition of 0.5 M Tris to the adsorption buffer. The chromatogram presents six peaks denominated as flow-through (FT), peak 1 (P1), peak 2 (P2), peak 3 (P3), peak 4 (P4) and peak 5 (P5), from left to right. (B) Coomassie Blue stained SDS-PAGE of the fractions collected during glycoproteins separation by PB chromatography using a ProSep®-PB resin and an elution strategy accomplished by the use of a series of step gradients – 2%, 4.5%, 8.5%, 15% and 100% (v/v). Lanes ID: 1: artificial mixture containing 5 μ g of each glycoprotein under study; 2: flow-through (FT) fraction; 3: P1; 4: Precision Plus Protein™ Dual Color Standards (from top to bottom: 250, 200, 150, 100, 75, 50, 37, 25, 20 and 10 kDa); 5: P2; 6: P3; 7: P4; 8: P5.

At last, an agarose-based resin P6XL was also tested. The results obtained from the application of the linear gradient at 0.6% Tris/min and of the series of step gradients can be found in the Section IV.S2 of the Supplementary Material (Figures IV.S2.1 and IV.S2.2, respectively).

IV.3.1.2. Displacer gradient studies for the separation of acidic to neutral proteins

Similarly to what was performed for the evaluation of the PB chromatography performance towards the selective separation of glycoproteins, studies regarding the fractionation of acidic and neutral proteins were also conducted. In this case, the goal was to understand the potential of the multimodal behaviour of the *m*-APBA ligand to selectively separate acidic to neutral proteins, glycosylated or not, from each other. The adsorption of the selected proteins (amyloglucosidase, cellulase and pepsin) was performed under acidic conditions, *i.e.* at a pH lower than the ligand's pKa, in order to promote their retention mostly through non-specific interactions such as charge transfer interactions. Since it was already reported that the use of 50 mM acetate at pH 5 promoted the binding of glycosylated and non-glycosylated proteins towards the ligand under study [18], the same buffer composition was used in this study as adsorption buffer.

For the development of the elution strategy, the use of displacers such as Tris and citrate were considered. The goal was to evaluate which could act as an effective displacer able to confer selectivity to the elution of acidic/neutral proteins. In a first attempt, 0.5 M Tris was prepared in 50 mM acetate at pH 5. Under this condition, none of proteins were eluted probably due to the protonated amine moiety of Tris which impaired the trident interaction with the *m*-APBA ligand. However, at alkaline conditions, when the amine is deprotonated (pKa \approx 8, 25 °C), Tris has been demonstrated to be highly effective in disrupting specific and non-specific interactions established with the ligand. Considering this, a second run of experiments were performed using 0.5 M Tris in 20 mM CHES at pH 8.5. The results obtained by the application of a linear gradient at a rate of 5% Tris/min were more promising with all proteins being 100% recovered. Nevertheless, Tris did not show the ability to confer selectivity to the elution process with all proteins being eluted in a narrow concentration range of Tris (86 to 95 mM of Tris) (data not shown).

Citrate was however able to elute the acidic to neutral proteins at considerable different ionic strengths (Figure IV.6). The first protein to be eluted was amyloglucosidase, followed by pepsin and cellulase (Figure IV.6). The order by which the elution occurred is most likely related to the overall charges of the proteins. At the working pH, amyloglucosidase and pepsin are negatively charged and cellulase positively charged. The *m*-APBA ligand is predominantly present in a trigonal conformation since acetate, a weak base, was used during the adsorption of proteins. When added during elution, citrate, a strong Lewis base, will bind to the boronic acids of the ligand through charge transfer interactions, *i.e.* Lewis acid-base interactions, established between one of the three carboxylic acid groups of the citrate and the empty orbital of the boron atom of the ligand. The establishment of such interaction will promote the presence of the tetrahedral conformation of the *m*-APBA ligand which presents a negatively charged boronate that can thus participate in electrostatic interactions (repulsive

or attractive) with the proteins already adsorbed leading to protein rearrangements [28]. The two remaining carboxylates of citrate coupled to the boron atom will also confer negative charges to the ligand [28]. The presence of the negatively charged silanol groups ($pK_a = 4.9$) present in the chromatographic support can be another source of negative charges. On the other hand, the presence of the tetrahedral conformation of the ligand could also enhance the *cis*-diol esterification between glycoproteins and the ligand since $K_{tet} > K_{trig}$. However, as can be implied by the results displayed in Figure IV.6, *cis*-diol interactions do not play a major role in the desorption process. If so, the elution of glycoproteins as amyloglucosidase and cellulase would occur at last or only after a regeneration step using 1.5 M Tris-HCl, pH 8.5.

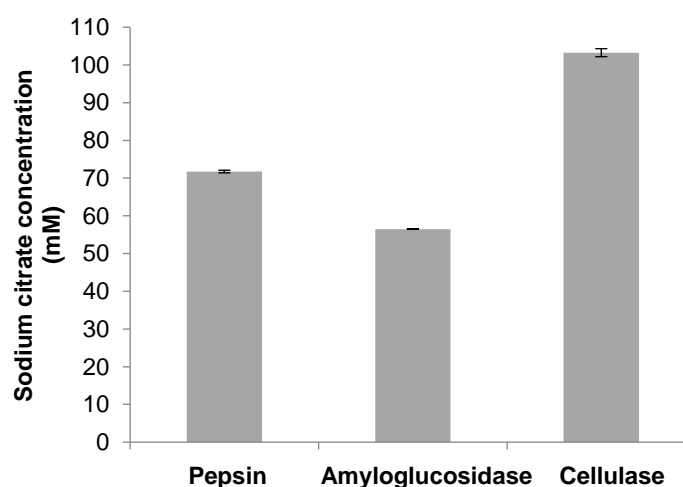


Figure IV.6 Sodium citrate concentration required to promote complete elution of the different acidic/neutral proteins under study. Studies were performed using a ProSep®-PB resin. Adsorption of acidic/neutral proteins was performed using 50 mM acetate, pH 5.0. Results are based on the sodium citrate concentration on the elution buffer at which was obtained the maximum peak height. Results are displayed as average \pm STDV.

Considering the type of interactions involved in the adsorption process as the isoelectric points of the acidic/neutral proteins, exhibited in Table IV.1, it was expected to collect pepsin in the first place. At pH 5, pepsin presents a more negative charge than amyloglucosidase. However, it is important to consider the molecular weight of the protein as well as the charge of the protein patch at which occur the interaction with the ligand, *i.e.* protein configuration. At last, the elution of positively charged cellulase was also accomplished using the citrate gradient at pH 5. This can be due to the proximity of the working pH to its pI - 5.0 vs 5.7, respectively - which not promoted electrostatic interactions strong enough to retain cellulase in the column.

In order to explore the ability of citrate to selectively promote the elution of acidic to neutral proteins, 100 μ L of an artificial mixture composed by 1 mg/mL of each protein was loaded into the PB column. The elution of this mixture was firstly conducted at a rate of 5% citrate/min. However, a selective separation was not achieved with the first eluted peaks appearing under the form of a doublet peak (C1, Figure IV.7A). The citrate gradient rate was then gradually decreased to 2.5 %, 1.25 %, and 0.75 % citrate/min, with the best protein separation being accomplished with the lowest gradient (C2-C4, Figure IV.7A). The gel electrophoresis carried out in order to analyse the peak fractions obtained using a rate

of 0.75% citrate/min corroborate that it was possible to achieve a good separation of the acidic/neutral proteins using the stated strategy (Figure IV.7B). The majority of amyloglucosidase elutes in the first elution peak (line 4, Figure IV.7B) being the remaining co-elute with pepsin during the second elution peak (line 5, Figure IV.7B). Cellulase is eluted in the broad third peak (line 6, Figure IV.7B). In the last peak, only a residual impurity present in the commercial cellulase was eluted (see Figure IV.S1 in Supplementary Material) which corroborates that all the acidic/neutral proteins can be eluted during the linear gradient employed with no need to resort to the regeneration buffer 1.5 M Tris-HCl, pH 8.5 (Figure IV.6). Contrarily to what was performed for the separation of glycoproteins, a lower rate as 0.6% citrate/min was not applied in this case. Even existing the possibility to improve the separation of amyloglucosidase from pepsin and *vice versa*, cellulase will get even more diluted which could impair the application of this elution strategy at industrial levels, *per se*.

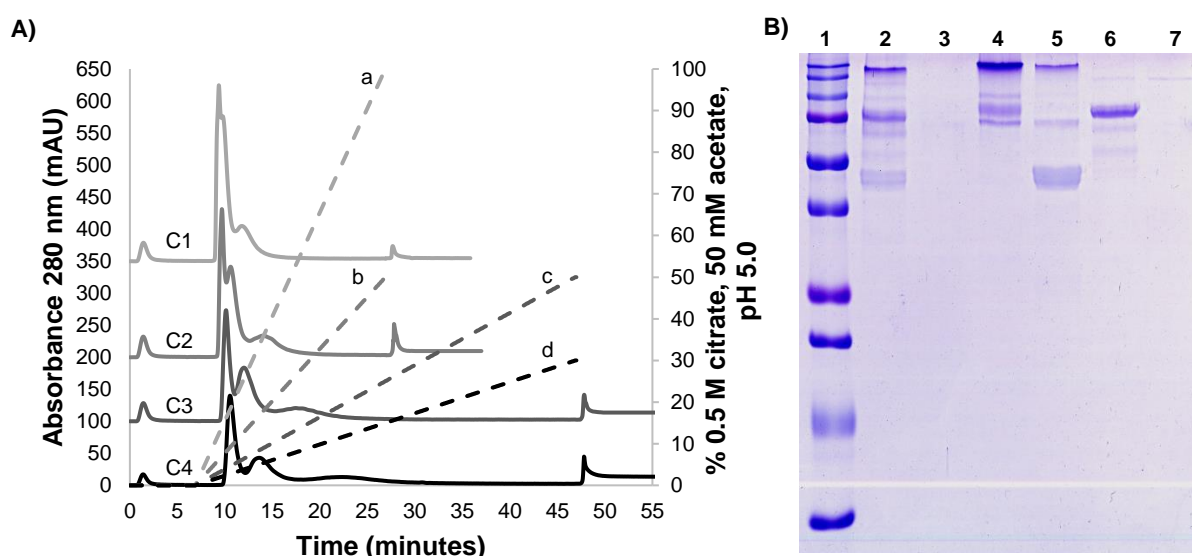


Figure IV.7 (A) Chromatograms obtained using a ProSep®-PB resin for the separation of an artificial mixture containing 1 mg/mL of each acidic/neutral protein under study prepared in the adsorption buffer 50 mM citrate at pH 5.0. Four different gradient slopes were applied considering an elution buffer containing 0.5 M citrate as displacer agent (a-d). The gradients were performed under the rates of (a) 5 % citrate/min, (b) 2.5 % citrate/min, (c), 1.25 % citrate/min and (d) 0.75 % citrate/min giving rise to four distinct chromatograms – C1 to C4, respectively. Immediately after the elution, the column regeneration was conducted using 1.5 M Tris-HCl, pH 8.5. C4 presents five peaks denominated as flow-through (FT), peak 1 (P1), peak 2 (P2), peak 3 (P3) and peak 4 (P4), from left to right. (B) Coomassie Blue stained SDS-PAGE of the fractions collected during acidic/neutral proteins separation by PB chromatography using a ProSep®-PB resin and an elution gradient strategy accomplished by the use of 0.5 M citrate as displacer agent at a rate of 0.75% citrate/min. Lanes ID: 1: Precision Plus Protein™ Dual Color Standards (from top to bottom: 250, 200, 150, 100, 75, 50, 37, 25, 20 and 10 kDa); 2: artificial mixture containing 5 µg of each acidic/neutral protein under study; 3: flow-through (FT) fraction; 4: P1; 5: P2; 6: P3; 7: P4.

A three-step elution gradient strategy was then implemented aiming the achievement of peaks with higher resolution and, consequently, more concentrated protein pools (Figure IV.8A). The goals were reached and improvements in separation achieved. As discussed previously, the two negatively charged proteins – amyloglucosidase and pepsin – were eluted at similar concentrations of citrate, namely 55 and 70 mM, respectively (Figure IV.6). This similarity did not turn possible to achieve a good peak separation using the linear gradient elution but was successfully achieved using a step gradient strategy. Using a step gradient elution, it was possible to effectively separate amyloglucosidase from pepsin

(Figure IV.8B) as to obtain cellulase in a more concentrated pool. Amyloglucosidase was mostly recovered in the first elution peak at 1.5% (v/v) of elution buffer, pepsin in the second at 4% (v/v) elution buffer and cellulase in the third at 15% (v/v). However, when performing the column regeneration, it was possible to observe that not all the cellulase was eluted using 15% (v/v) of elution buffer (Figure IV.8B). Nonetheless, the application of a step gradient is preferable at an industrial setting. The cellulase diluted pool obtained from the linear gradient strategy would have to go through a series of concentration steps which could (i) lead to a higher loss of cellulase, (ii) turn the downstream processing more expensive and (iii) induce changes in protein conformation leading to a decrease of their enzymatic activity.

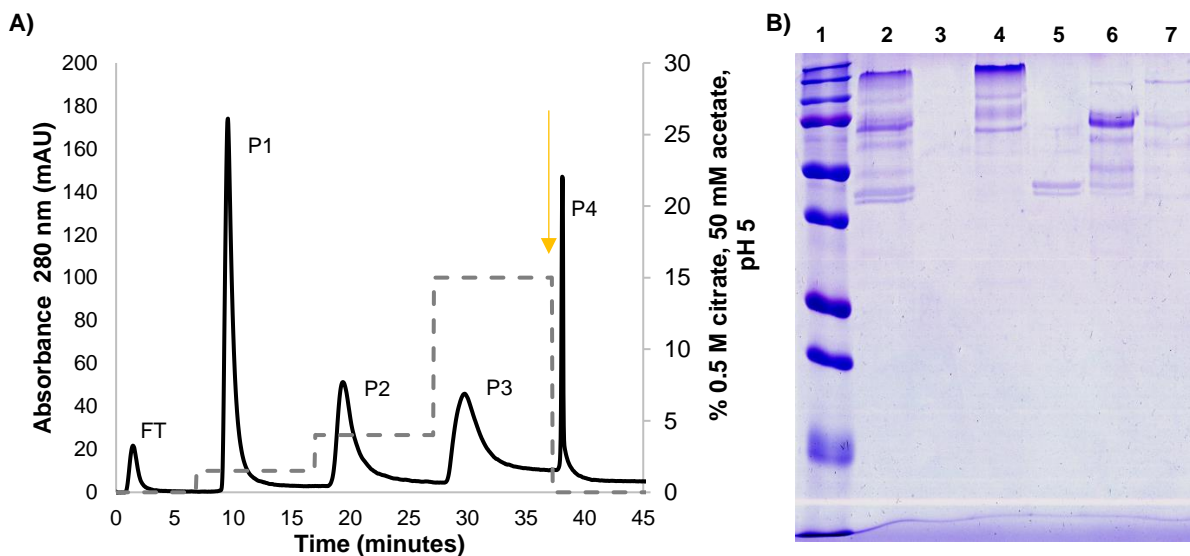


Figure IV.8 (A) Chromatograms obtained using a ProSep®-PB resin for the separation of an artificial mixture containing 1 mg/mL of each acidic/neutral protein under study prepared in the adsorption buffer 50 mM citrate at pH 5.0. The elution process was performed using a series of step gradients – 1.5%, 4%, and 15% (v/v). The elution buffer used was obtained by addition of 0.5 M citrate to the adsorption buffer. The chromatogram presents five peaks denominated as flow-through (FT), peak 1 (P1), peak 2 (P2), peak 3 (P3) and peak 4 (P4), from left to right. The time at which the system was imposed to start to pump 100% (v/v) of the regeneration buffer – 1.5 M Tris-HCl, pH 8.5 – is marked with a yellow arrow. (B) Coomassie Blue stained SDS-PAGE of the fractions collected during acidic/neutral proteins separation by PB chromatography using a ProSep®-PB resin and an elution strategy accomplished by the use of a series of step gradients – 1.5%, 4%, and 15% (v/v). Lanes ID: 1: Precision Plus Protein™ Dual Color Standards (from top to bottom: 250, 200, 150, 100, 75, 50, 37, 25, 20 and 10 kDa); 2: artificial mixture containing 5 µg of each acidic/neutral protein under study; 3: flow-through (FT) fraction; 4: P1; 5: P2; 6: P3; 7: P4.

Higher protein loads (2.5x) were also tested in the linear and step gradient modes with high reproducibility being achieved in terms of chromatographic profiles and protein separation efficacy (Figures IV.9 and IV.10).

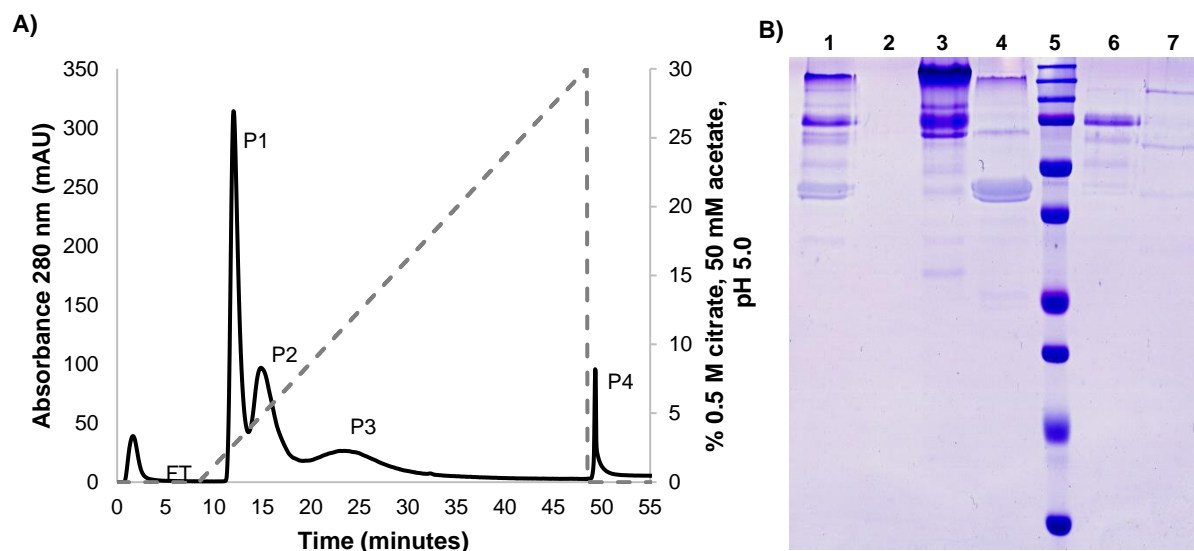


Figure IV.9 (A) Chromatogram obtained using a ProSep®-PB resin for the separation of an artificial mixture containing 2.5 mg/mL of each acidic/neutral protein under study prepared in the adsorption buffer 50 mM citrate at pH 5.0. The elution process was performed using a linear gradient performed at a rate of 0.75% citrate/min. The elution buffer used was obtained by addition of 0.5 M citrate to the adsorption buffer. Immediately after the elution, the column regeneration was conducted using 1.5 M Tris-HCl, pH 8.5. The chromatogram presents five peaks denominated as flow-through (FT), peak 1 (P1), peak 2 (P2), peak 3 (P3) and peak 4 (P4), from left to right. (B) Coomassie Blue stained SDS-PAGE of the fractions collected during acidic/neutral proteins separation by PB chromatography using a ProSep®-PB resin and an elution gradient strategy accomplished by the use of 0.5 M citrate as displacer agent at a rate of 0.75% citrate/min. Lanes ID: 1: artificial mixture containing 5 μ g of each cidic/neutral protein under study); 2: flow-through (FT) fraction; 3: P1; 4: P2; 5: Precision Plus Protein™ Dual Color Standards (from top to bottom: 250, 200, 150, 100, 75, 50, 37, 25, 20 and 10 kDa); 6: P3; 7: P4.

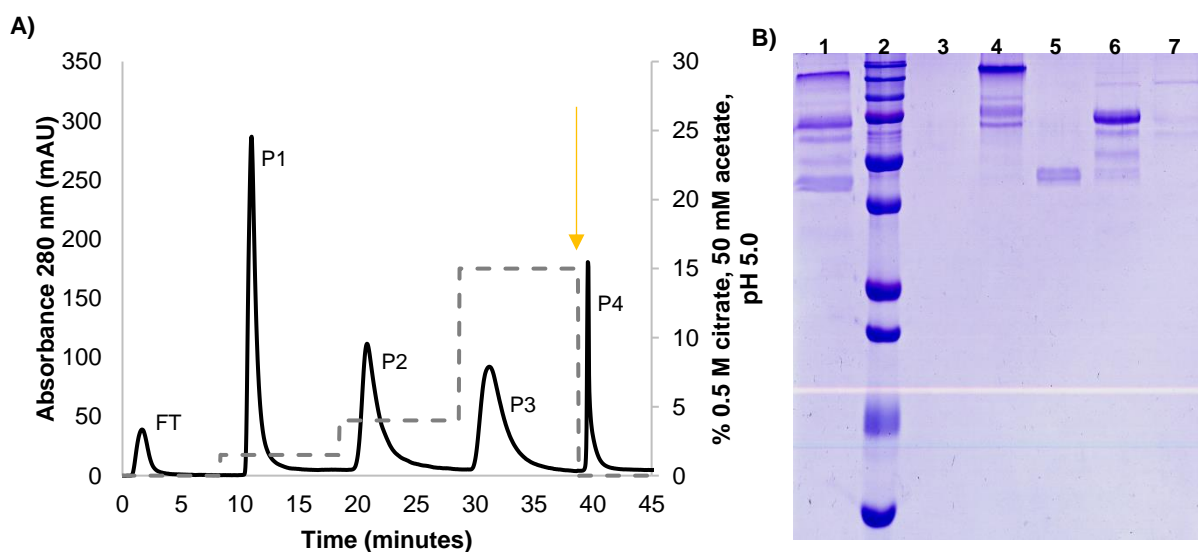


Figure IV.10 (A) Chromatogram obtained using a ProSep®-PB resin for the separation of an artificial mixture containing 2.5 mg/mL of each acidic/neutral protein under study prepared in the adsorption buffer 50 mM citrate at pH 5.0. The elution process was performed using a series of step gradients – 1.5%, 4%, and 15% (v/v). The elution buffer used was obtained by addition of 0.5 M citrate to the adsorption buffer. The chromatogram presents five peaks denominated as flow-through (FT), peak 1 (P1), peak 2 (P2), peak 3 (P3), and peak 4 (P4), from left to right. The time at which the system was imposed to start to pump 100% (v/v) of the regeneration buffer – 1.5 M Tris-HCl, pH 8.5 – is marked with a yellow arrow. (B) Coomassie Blue stained SDS-PAGE of the fractions collected during acidic/neutral proteins separation by PB chromatography using a ProSep®-PB resin and an elution strategy accomplished by the use of a series of step gradients – 1.5%, 4%, and 15% (v/v). Lanes ID: 1: artificial mixture containing 5 μ g of each acidic/neutral protein under study); 2: Precision Plus Protein™ Dual Color Standards (from top to bottom: 250, 200, 150, 100, 75, 50, 37, 25, 20 and 10 kDa); 3: flow-through (FT) fraction; 4: P1; 5: P2; 6: P3; 7: P4.

Also, in this case, an agarose-based resin P6XL was tested. The results obtained from the application of the linear gradient at 0.75% Tris/min and of the series of step gradients are present as Supplementary Material in the Section IV.S3 (Figures IV.S3.1 and IV.S3.2, respectively).

IV.3.2. pH gradient studies

m-APBA has been shown to be a pH dependent ligand. Therefore, elution strategies based on pH gradients were evaluated in order to fractionate the proteins under study, specifically by exploiting differences on their overall charge at the different pH values, and the ability to promote *cis*-diol interactions with the ligand due to the presence of carbohydrates in the structure of some. The pH gradients chosen were based on Kröner *et al.* (2003) studies [24].

For the glycoproteins elution study, a decreasing pH gradient was chosen. Since it has been described that the adsorption of glycoproteins towards the *m*-APBA ligand is enhanced at alkaline conditions, the pH gradient started at pH 9.0, and ended at acidic conditions (pH 4.0 or pH 5.0). The aim was to evaluate at which extent differences between the equilibrium constant towards carbohydrates of the tetrahedral (K_{tet}) and trigonal forms (K_{trig}) of the *m*-APBA ligand can promote the full recover of glycoproteins as to provide selectivity to the elution process. 300 mM NaCl was added to the buffer formulation – B Gly - to mitigate non-specific interaction that could occur between the silanol groups present in bare beads, the phenyl group present in the ligand structure and proteins, considering the results observed in Chapters II and III. However, it is important to consider that the addition of NaCl, as the high pH values ($pH > pK_a$), could result in the promotion of non-specific interactions, as reported in Chapter II. The presence of NaCl will promote the formation of a tetrahedral chloroboronate ($R-B(OH)_2Cl$) obtained through B-Cl coordination, mainly at lower pH values (low concentration of HO^-). Nevertheless, the trigonal conformation of the ligand will also be present at pH values lower than the pK_a of the ligand. It should also be considered that the presence NaCl can have a shielding effect towards proteins decreasing electrostatic repulsive effects between ligand and proteins. Therefore, the *cis*-diol esterification and secondary interactions such as electrostatic and charge transfer interactions between the ligand and proteins are expected to be involved in the adsorption and desorption processes of such biomolecules, acting synergistically.

In contrast, pH gradients applied to the acidic/neutral proteins were increasing gradients starting at pH 4.0 or pH 5.0 and finishing at basic conditions (pH 9.0). The two buffer formulations used – BAN 1 and BAN 2 – presented low ionic strength in order to favour the adsorption and desorption of proteins by secondary interactions. BAN2 differs from BAN1 by the addition of TAPS in detriment of the use of HEPES (see Table IV.2). TAPS, a Tris varied buffer, avoids the retention of glycosylated proteins at alkaline pH values but not at acidic conditions. Therefore, its use will not compromise the adsorption of glycosylated proteins but can increase the elution selectivity within the acidic/neutral proteins under study, as soon as the pH increases [24].

Moreover, two different chromatographic supports were analysed. ProSep®-PB and P6XL share the same ligand – *m*-APBA – but differ in the type of matrix – silica- and agarose-based, respectively. All linear gradients obtained presented high correlation coefficients (R^2). Buffers used for glycoprotein separation (B Gly), provided linear gradients with correlation coefficients of 0.9982 and 0.9965 using

ProSep®-PB and P6XL, respectively. In which regards the two BAN formulations, correlation coefficients of 0.9989 and 0.9979, with deviations lower than 0.001, were achieved using ProSep®-PB and P6XL, respectively. All the values acquired are comparable with the ones obtained by Kröner *et al.* (2003) using MonoQ and MonoS columns ($R^2 > 0.99$) [24].

IV.3.2.1. pH gradient studies for the separation of glycosylated proteins

The use of pH gradients aiming the understanding of the phenomena involved in desorption of glycoproteins revealed that proteins as RNaseB and invertase can be eluted at pH values of 6.65 ± 0.1 when ProSep®-PB was used as matrix (Figure IV.11A). On the other hand, both amyloglucosidase and cellulase were eluted only at regeneration conditions (1.5 M Tris-HCl) but at distinct pH values. Amyloglucosidase was eluted at a pH around 6.2 and cellulase at 7.2 (Figure IV.11A). Interestingly, amyloglucosidase was eluted at the same pH that RNase B and invertase however, only the presence of a displacer conducted to the recovery of such protein. The shielding effect conferred by the presence of NaCl, allied to the establishment of specific *cis*-diol esterification between protein and ligand during adsorption, was a key element to avoid amyloglucosidase elution throughout the pH gradient. The result achieved for cellulase is in line with other studies which demonstrated that this glycoprotein is adsorbed to a PB ligand within a broad pH range (pH 9.0 to pH 4.0).

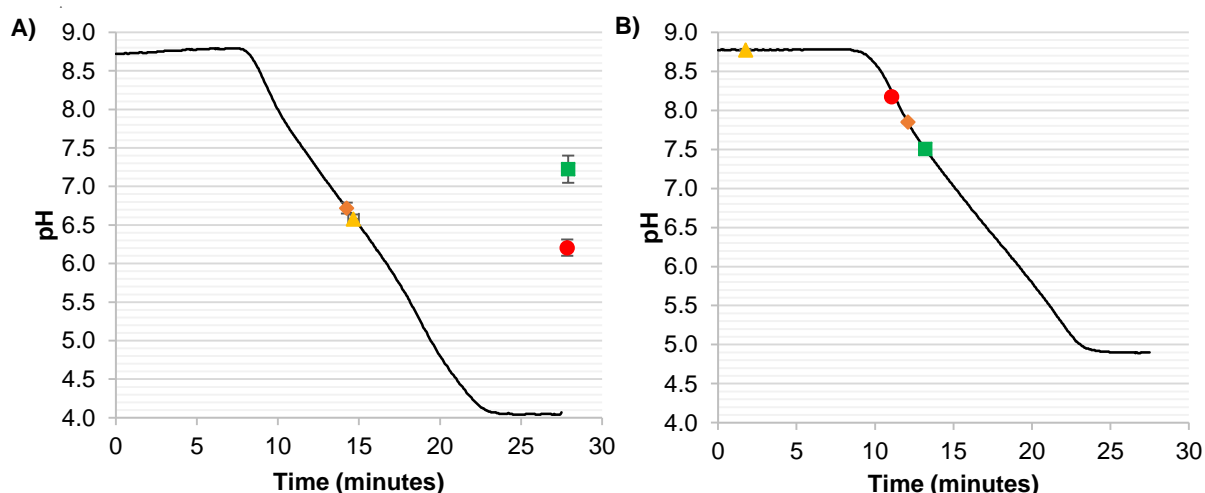


Figure IV.11 pH gradient curves obtained for the elution of glycosylated proteins from (A) ProSep®-PB and (B) P6XL matrices. pH gradients were performed using BGly buffer formulation, based on Kröner *et al.* (2013) [24]. Column regeneration was achieved using 1.5 M Tris-HCl, pH 8.5. 1 mg/mL of each glycosylated protein - amyloglucosidase (red circle), cellulase (green square), RNase B (yellow triangle) and invertase (orange diamond) - were separately loaded in each column. The elution points represented, correspond to the maximum peak height obtained.

Comparing the different supports used, it was possible to conclude that the one with an agarose core provided higher selectivity with the elution of glycoproteins being achieved at distinct pH values (Figure IV.11A vs IV.11.B). However, the difference within pH values (8.2 – 7.5) is too narrow in order to consider the application of a pH gradient as an elution strategy at the industrial setting (Figure IV.11B). The elution of glycoproteins at such pH values is co-related with what was observed in the work of

Carvalho *et al.* (2014) where a shorter pH range of adsorption were obtained using the P6XL resin [18]. Other distinct result relies on the elution of the glycoprotein RNase B. Using the agarose-base matrix, no adsorption of this protein is achieved demonstrating that secondary interactions could play a major role in the adsorption of RNase B, in detriment of *cis*-diol interactions, and posteriorly, in its elution.

A drawback related to the application of pH gradients to the elution steps in PB chromatography concerns the partial elution of proteins. Considering the results present in Figure IV.12, it is possible to observe that only invertase is completely recovered during the pH gradient when the agarose-based matrix – P6XL – is used (Figure IV.12B). In this case, the conformational changes that *m*-APBA suffers along the pH gradient seem to be sufficient to trigger the elution of such protein. Indeed, the equilibrium constant towards carbohydrates, present in glycoproteins, is higher when *m*-APBA is in its tetrahedral form ($K_{tet} > K_{trig}$) [28]. Decreasing the working pH will promote the presence of the *m*-APBA ligand in its trigonal form to which invertase has decreased affinity (Figure IV.12B). Amyloglucosidase and cellulase, on the other hand, were not completely eluted during the pH gradient. The remaining content of amyloglucosidase and cellulase, 25% and 70%, respectively, was then recovered at the regeneration step. These results, corroborate the ability that the trigonal form of the *m*-APBA has to establish esterification reactions with diols [28], at the same time that indicate that secondary interactions could be involved in the adsorption but also in desorption of glycoproteins in this chromatographic system. Results obtained using the silica-based resin ProSep®-PB, revealed that RNase B and invertase were partially eluted during the pH gradient (Figure IV.12A). The remaining 30% of RNase B and 65% of invertase were recovered with the addition of 1.5 M Tris-HCl, pH 8.5. These results are, at some extent, in line with was observed during IgG purification where only 7% of the glycoprotein was recovered after a pH drop until 2 [4].

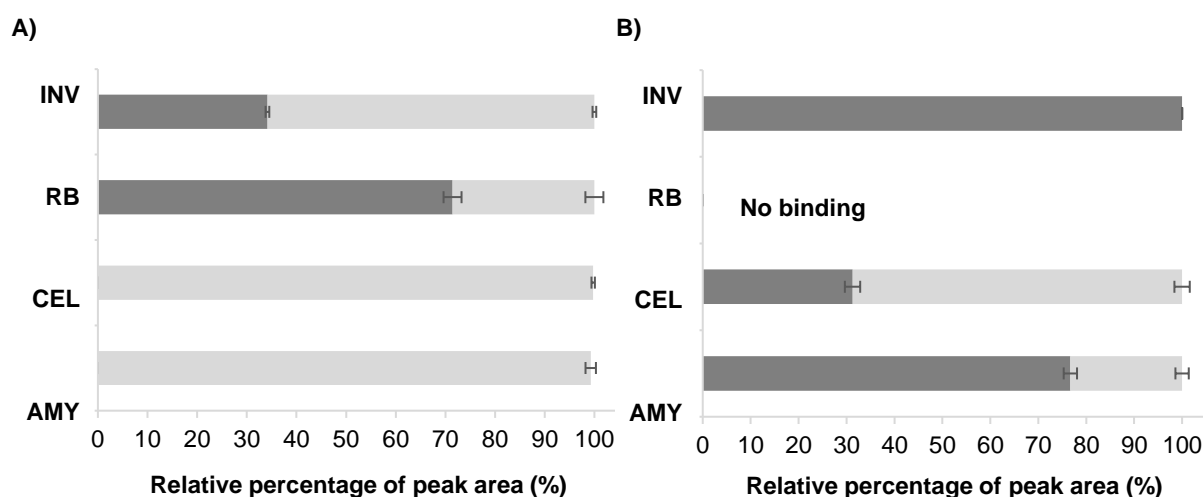


Figure IV.12 Percentage of each glycoprotein recovered from (A) ProSep®-PB and (B) P6XL matrices during the employed elution pH gradient (■) or at the regeneration step (▒). pH gradients were performed using B Gly buffer formulation, based on Kröner *et al.* (2013) [24]. Column regeneration was achieved using 1.5 M Tris-HCl, pH 8.5. 1 mg/mL of each glycosylated protein - amyloglucosidase (AMY), cellulase (CEL), RNase B (RB) and invertase (INV) - were separately loaded in each column. Results correspond to the ratio between the areas of the peaks obtained during the elution peak gradient and regeneration step and the total peak area of the chromatogram. Results are displayed as average \pm STDV.

In sum, it can be concluded that there are major differences in the phenomena involved in the adsorption and desorption of glycoproteins towards resins with the same ligand but different matrices. Again, features as backbone, ligand density, *m*-APBA spacer arm composition and extension could be in the basis of the differences observed.

IV.3.2.2. pH gradient studies for the separation of acidic to neutral proteins

The evaluation of the application of a pH gradient in the elution process of acidic and neutral proteins was also performed. In this case, the adsorption of proteins was performed at low pH values (pH 4 or 5) aiming to reduce the specific *cis*-diol interactions that could occur between the *m*-APBA ligand and glycoproteins. Therefore, protein adsorption will occur mainly by secondary interactions as charge transfer interactions. Hydrophobic and/or aromatic interactions could also occur between proteins and the phenyl moiety of the ligand although they are not expected to have representative effect.

The elution strategy employed followed an increasing pH gradient until reaching a pH value higher than the ligand's pKa (pH 9.0). Moreover, TAPS, a Tris varied buffer, was used as substituent of HEPES in buffer formulation BAN1 in order to try to understand if its use could promote a higher selectivity during the elution process (BAN2). However, the use of different buffer formulations did not result in substantial differences in the elution profiles when using the same type of resin (Figure IV.13).

Elution studies performed with ProSep®-PB resin show that amyloglucosidase and pepsin are eluted at slightly lower pH values when TAPS is used in the buffer composition (Figures IV.13A and IV.13B). However, the observed differences are not significant (around 0.25). The major difference within the use of TAPS in the elution buffer relies on the amount of amyloglucosidase recovered during the pH gradient. Amyloglucosidase is completely recovered during the pH gradient in the presence of TAPS (Figure IV.14B) confirming that the presence of the Tris varied buffer could promote the disruption of specific and non-specific interactions and thus, conducting to the full recovery of amyloglucosidase. However, in the absence of TAPS, the majority of amyloglucosidase, around 80%, was only recovered in the regeneration step (Figure IV.14A). Regarding the total amount of proteins recovered, analysing the Figures IV.14A and IV.14B, it is possible to observe that cellulase is only eluted at the regeneration step using 1.5 M Tris-HCl and that pepsin is fully recovered during the pH gradient using both buffer formulations – BAN1 and BAN2. The result obtained for cellulase show that, even at alkaline conditions, the electrostatic repulsion between the negatively charged cellulase (pI = 5.7) and the negatively charge boronate present on the ligand are not sufficient to disrupt or to compete with the *cis*-diol interactions established during the adsorption process. This *cis*-diol interaction occurs with the carbohydrates present in cellulase structure and the *m*-APBA ligand in its trigonal form. Pepsin, on the other hand, is a non-glycosylated protein and thus cannot interact with the ligand through *cis*-diol interactions. However, the adsorption of pepsin can be accomplished by secondary interactions that are disrupted during the increasing pH gradient. Here the electrostatic repulsion between protein and ligand did play a major role in the desorption process.

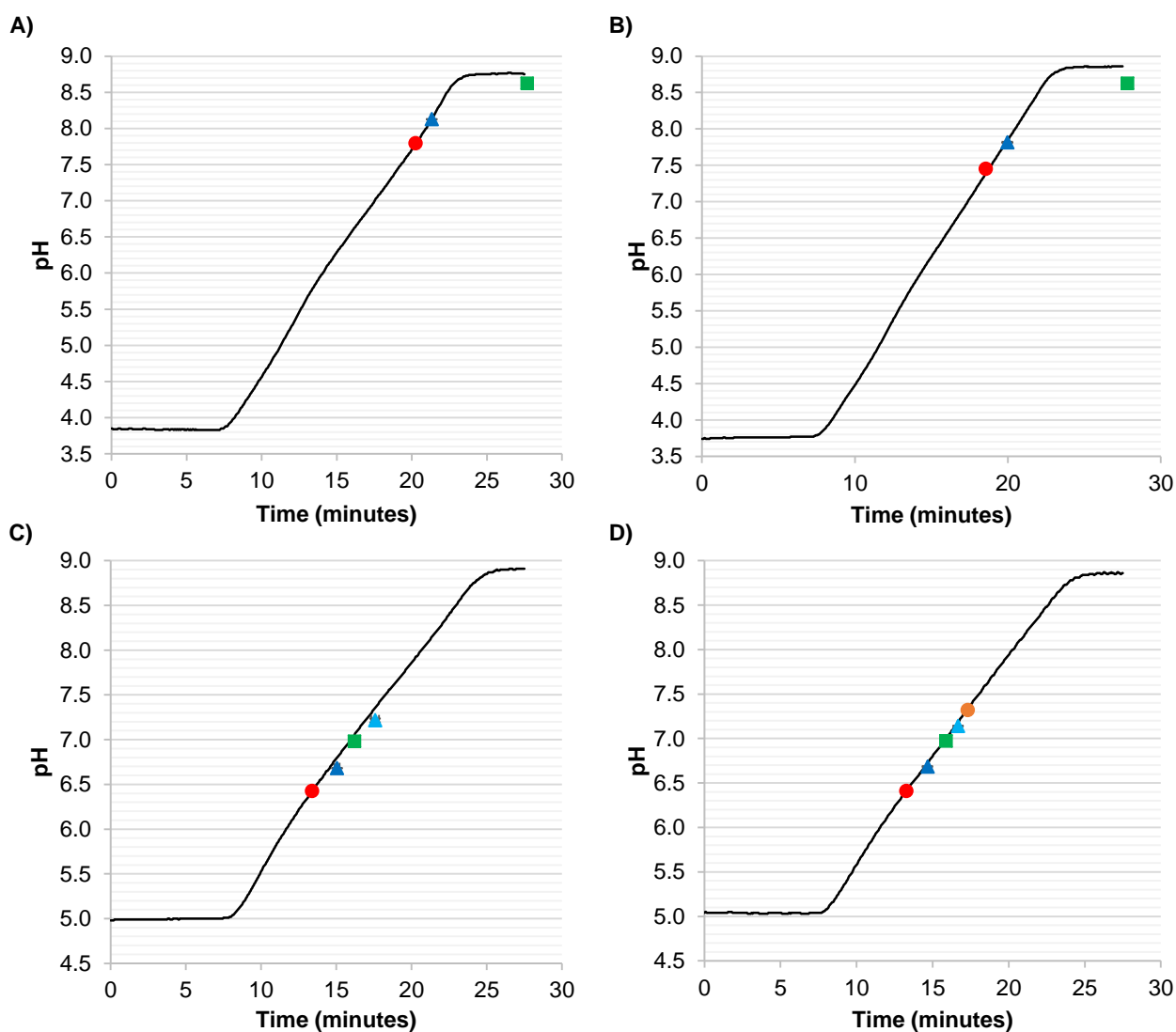


Figure IV.13 pH gradient curves obtained for the elution of acidic/neutral proteins from ProSep®-PB (A and B) and P6XL matrices (C and D). pH gradients were performed using two different buffer formulations – BAN1 (A and C) and BAN2 (B and D) - based on Kröner *et al.* (2013) [24]. Column regeneration was achieved using 1.5 M Tris-HCl, pH 8.5. 1 mg/mL of each acidic/neutral protein - amyloglucosidase (red and orange circles), cellulase (green square), pepsin (dark and light blue triangles) - were separately loaded in each column. The elution points represented, correspond to the maximum peak height obtained.

With the use of the P6XL resin all the proteins were eluted earlier within the pH gradient, *i.e.* at lower pH values, giving insights about the type and strength of the interactions established between ligand and proteins during the adsorption process (Figures IV.13C and IV.13D). For instance, the elution of all proteins being achieved at pH values ranging 6.4 to 7.3 could indicate that the adsorption process of these proteins towards the ligand was not predominantly achieved by *cis*-diol interactions. Indeed, such result was expected but only for the non-glycosylated pepsin. Additionally, partial elution of proteins namely within the pH gradient was observed using the P6XL resin (Figures IV.13C and IV.13D). The majority of cellulase was eluted during the pH gradient (60-75%) with the remaining protein being recovered at the regeneration step. Contrarily to what was observed with ProSep®-PB resin, cellulase was not retained to P6XL predominantly by *cis*-diol interactions. Otherwise, the presence of TAPS would led to a major if not total recovery of cellulase during the pH gradient (Figures IV.14C and IV.14D).

Herein, the interaction playing a major role in the desorption process is the electrostatic repulsion effect that occur between cellulase and the ligand. Pepsin, on the other hand, was recovered at two distinct timepoints of the pH gradient obtained using both buffer formulations (Figures IV.14C and IV.14D). The first timepoint may be related to the two major components of pepsin, which present pI values of 2.76 and 2.78, and the second timepoint to the two minor components that have pI values of 2.89 and 2.90 [37], demonstrating the PB ligands potential for the separation of isoforms. Nevertheless, the overall results obtained for pepsin are in accordance with the ones obtained for ProSep®-PB. Also, charge transfer interactions conducted the adsorptive process of pepsin and the electrostatic repulsion, the desorption process. Elution profiles of amyloglucosidase were the ones that presented major changes considering both resins and buffer formulations studied. Amyloglucosidase was majorly recovered at one timepoint of the pH gradient applied when using BAN1. In presence of TAPS, interestingly, a second elution point occurs during the pH gradient. The presence of two elution points can be related to the two isoenzymes of amyloglucosidase present in the commercial sample. Indeed, the relative molecular weight of amyloglucosidase is 97 kDa. However, the molecular weights of its isoforms are around 69.8 and 89.1 kDa [38]. Both isoenzymes are reported to be glycoproteins differing in their carbohydrate content which may explain the accomplishment of their separation only in presence of a Tris varied buffer. The promising results obtained for amyloglucosidase and pepsin show that PB ligands could also be used for the separation of isoforms that is commonly performed by ion exchange chromatography or isoelectric focusing.

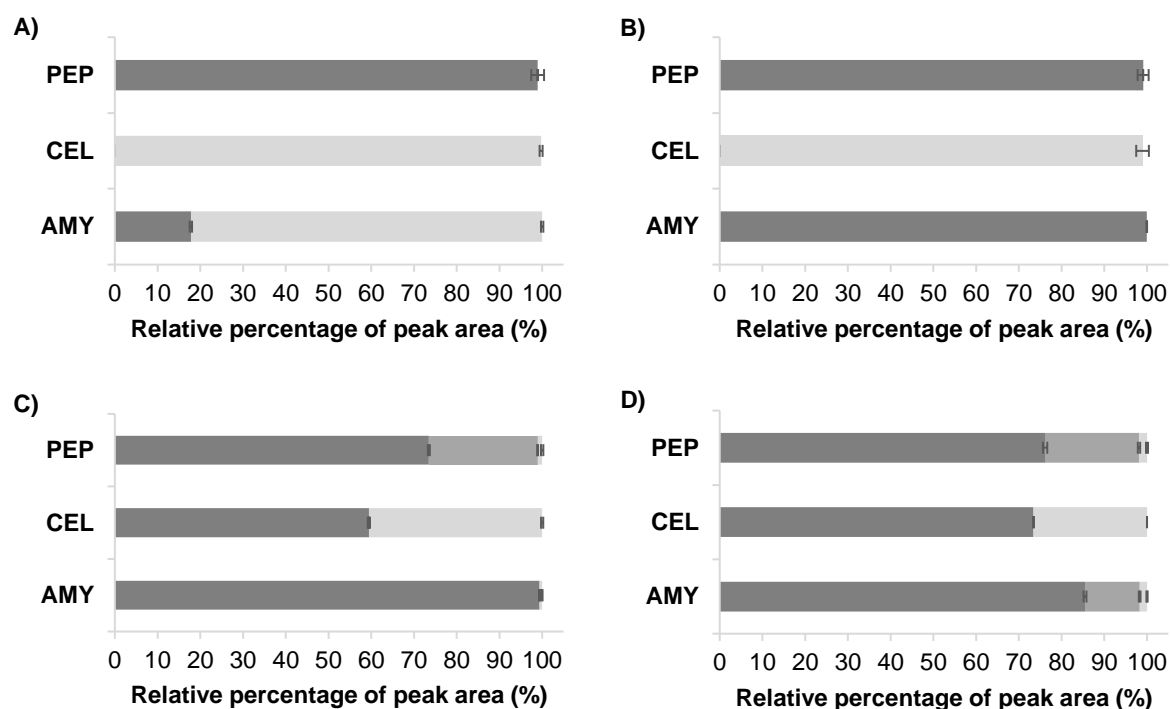


Figure IV.14 Percentage of each acidic/neutral protein recovered from ProSep®-PB (A and B) and P6XL matrices (C and D) during the employed elution pH gradient (■ and ▒) or at the regeneration step (□). pH gradients were performed using the buffer formulations BAN1 (A and C) and BAN2 (B and D), based on Kröner *et al.* (2013) work [24]. Column regeneration was achieved using 1.5 M Tris-HCl, pH 8.5. 1 mg/mL of each glycosylated protein - amyloglucosidase (AMY), cellulase (CEL) and pepsin (PEP) - were separately loaded in each column. Results correspond to the ratio between the areas of the peaks obtained during the elution peak gradient and regeneration step and the total peak area of the chromatogram. Results are displayed as average \pm STDV.

IV.4. Conclusions

The multimodal behaviour of phenylboronate ligands as *m*-aminophenylboronic acid (*m*-APBA), was investigated in order to develop effective elution strategies for glycoproteins comprising a broad range of isoelectric points and acidic/neutral proteins including glycosylated and non-glycosylated proteins. The elution strategies were designed considering the best suited adsorption conditions for each type of protein under study. Glycosylated proteins were adsorbed at alkaline conditions in order to promote their retention to the tetrahedral conformation of *m*-APBA ligand through *cis*-diol interactions. Acidic to neutral proteins adsorption was conducted at acidic conditions. In this case the driving forces for the retention of such proteins towards the trigonal conformation of *m*-APBA will be majorly related to the protein charge at the working pH. Therefore, elution strategies as the employment of displacers and pH gradients were explored.

The application of displacer gradients was the method that provided higher selectivity to the elution process either for glycosylated proteins or for acidic/neutral proteins. The use of Tris as displacer provided full protein recoveries as a selective elution of glycoproteins, contrarily to what was achieved with the commonly used displacers on PB chromatography - D-sorbitol and D-fructose. The use of these displacers led to recoveries of 100% however, did not confer any selectivity to the elution of glycoproteins. In the case of acidic/neutral proteins, only citrate was able to provide good elution selectivity as well as protein recover efficiencies of 100%, at acidic conditions. The results obtained are related to specific features that citrate presents. Citrate is able to interact with the trigonal form of the *m*-APBA ligand by charge transfer with one of its three carboxylate groups or by coordination interaction through the α -hydroxylate moiety. The charge transfer interactions will be responsible for the conversion of the trigonal form of the *m*-APBA ligand to the tetrahedral boronate anion configuration. In this condition, attractive or repulsive electrostatic interactions can now occur within the boron atom as with the two carboxylate groups present in the ligand structure. With the displacers chosen for each types of proteins under study, it was possible to optimize the separation of proteins applying gradients with different slopes. The best results were accomplished with rates of 0.6% tris/min (3 mM Tris/min) for glycoproteins and 0.75% citrate/min (3.75 mM citrate/min) for acidic/neutral proteins. Consequently, step gradients were developed, and protein separation improvements achieved.

Contrarily to what was accomplished by the use of displacer gradients, the full recovery of the majority of proteins was not reached by the application of pH gradients to the elution process. Due to the multimodal nature of the phenomena involved in the adsorption and desorption processes, a great part of the proteins under study were only partially eluted during the pH gradient with the remaining being recovered at the regeneration step with the use of 1.5 M Tris-HCl, pH 8.5. Furthermore, the differences in pH, at which the elution of proteins took place, were too short in order to get a reliable separation of proteins.

Regarding the two different resins analysed, the use of the silica-based resin ProSep®-PB provided better results than the agarose-based resin. ProSep®-PB presented higher protein adsorption yields as selectivity towards the elution of different glycoproteins and acidic/neutral proteins, especially when displacer gradients were applied. The agarose-based P6XL, for example, was not able to adsorb the

glycoprotein RNase B and did not promote selective elution of proteins when the displacer gradient strategy was applied. Also, P6XL led to the generation of two elution points during the pH gradients applied for the majority of the proteins analysed. Since the two resins share the same ligand – *m*-APBA – and no adsorption of proteins onto the core silica and agarose beads was observed in previous studies, the differences in resin performance are expected to be mainly due to different ligand densities and in particular, to the composition and extension of the spacer arms of each resin.

Overall, this work has demonstrate that as a multimodal ligand, *m*-APBA ligand, present unique features that make PB chromatography a useful tool for the capture and separation of a wide range of proteins and even to separate isoforms. Indeed, it was possible to observe that the PB ligand is able to adsorb and selectively elute glycoproteins differing in overall charge and acidic/neutral proteins (glycosylated or not) by the use of displacers as Tris and citrate, respectively. Accordingly, PB chromatography can be applied not only to protein separation by preparative chromatography but can be also considered for analytical purposes, envisaging the separation of protein isoforms, or even for proteomic studies.

IV.5. References

- [1] S.A. Barker, B.W. Hatt, P.J. Somers, R.R. Woodbury, Use of poly(4-vinylbenzeneboronic acid) resins in fractionation and interconversion of carbohydrates, *Carbohydr Res*, 26 (1973) 55-64.
- [2] M. Matsumoto, T. Shimizu, K. Kondo, Selective adsorption of glucose on novel chitosan gel modified by phenylboronate, *Sep Purif Technol*, 29 (2002) 229-233.
- [3] D. Zanette, A. Soffientini, C. Sottani, E. Sarubbi, Evaluation of phenylboronate agarose for industrial-scale purification of erythropoietin from mammalian cell cultures, *J Biotechnol*, 101 (2003) 275-287.
- [4] A.M. Azevedo, A.G. Gomes, L. Borlido, I.F. Santos, D.M. Prazeres, M.R. Aires-Barros, Capture of human monoclonal antibodies from a clarified cell culture supernatant by phenyl boronate chromatography, *J Mol Recognit*, 23 (2010) 569-576.
- [5] I. Uda, A. Sugai, K. Kon, S. Ando, Y.H. Itoh, T. Itoh, Isolation and characterization of novel neutral glycolipids from *Thermoplasma acidophilum*, *Biochim Biophys Acta*, 1439 (1999) 363-370.
- [6] N. Singh, R.C. Willson, Boronate affinity adsorption of RNA: possible role of conformational changes, *J Chromatogr A*, 840 (1999) 205-213.
- [7] A.G. Gomes, A.M. Azevedo, M.R. Aires-Barros, D.M.F. Prazeres, Studies on the adsorption of cell impurities from plasmid-containing lysates to phenyl boronic acid chromatographic beads, *J Chromatogr A*, 1218 (2011) 8629-8637.
- [8] I. Percin, N. Idil, A. Denizli, RNA purification from *Escherichia coli* cells using boronated nanoparticles, *Colloid Surface B*, 162 (2018) 146-153.
- [9] L. Borlido, A.M. Azevedo, A.C. Roque, M.R. Aires-Barros, Potential of boronic acid functionalized magnetic particles in the adsorption of human antibodies under mammalian cell culture conditions, *J Chromatogr A*, 1218 (2011) 7821-7827.
- [10] L. Ren, Z. Liu, M. Dong, M. Ye, H. Zou, Synthesis and characterization of a new boronate affinity monolithic capillary for specific capture of cis-diol-containing compounds, *J Chromatogr A*, 1216 (2009) 4768-4774.
- [11] L. Raiado-Pereira, A.P. Carapeto, A.M.B. do Rego, M. Mateus, Grafting hydrophobic and affinity interaction ligands on membrane adsorbers: A close-up "view" by X-ray photoelectron spectroscopy, *Sep Purif Technol*, 93 (2012) 75-82.
- [12] D.G. Hall, Structure, properties, and preparation of boronic acid derivatives. Overview of their reactions and applications, in: D.G. Hall (Ed.) *Boronic Acids*, Wiley, Weinheim, 2005, pp. 1-100.
- [13] B. Zhang, S. Mathewson, H. Chen, Two-dimensional liquid chromatographic methods to examine phenylboronate interactions with recombinant antibodies, *J Chromatogr A*, 1216 (2009) 5676-5686.
- [14] S.D. Bull, M.G. Davidson, J.M. van den Elsen, J.S. Fossey, A.T. Jenkins, Y.B. Jiang, Y. Kubo, F. Marken, K. Sakurai, J. Zhao, T.D. James, Exploiting the reversible covalent bonding of boronic acids: recognition, sensing, and assembly, *Accounts Chem Res*, 46 (2013) 312-326.
- [15] D.G. Hall, Structure, Properties, and Preparation Of Boronic Acid Derivatives. Overview of Their Reactions and Applications, 2nd ed., Wiley-VCH Verlag GmbH & Co. KGaA, Weinheim, Germany, 2011.

- [16] J. Yan, G. Springsteen, S. Deeter, B. Wang, The relationship among pKa, pH, and binding constants in the interactions between boronic acids and diols--it is not as simple as it appears, *Tetrahedron*, 60 (2004) 11205-11209.
- [17] M.A. Holstein, S. Parimal, S.A. McCallum, S.M. Cramer, Mobile phase modifier effects in multimodal cation exchange chromatography, *Biotechnol Bioeng*, 109 (2012) 176-186.
- [18] R.J. Carvalho, J. Woo, M.R. Aires-Barros, S.M. Cramer, A.M. Azevedo, Phenylboronate chromatography selectively separates glycoproteins through the manipulation of electrostatic, charge transfer, and cis-diol interactions, *Biotechnol J*, 9 (2014) 1250-1258.
- [19] S.A.S.L. Rosa, C.L. da Silva, M.R. Aires-Barros, A.C. Dias-Cabral, A.M. Azevedo, Thermodynamics of the adsorption of monoclonal antibodies in phenylboronate chromatography: Affinity versus multimodal interactions, *J Chromatogr A*, 1569 (2018) 118-127.
- [20] R. dos Santos, S.A.S.L. Rosa, M.R. Aires-Barros, A. Tover, A.M. Azevedo, Phenylboronic acid as a multi-modal ligand for the capture of monoclonal antibodies: development and optimization of a washing step, *J Chromatogr A*, 1355 (2014) 115-124.
- [21] B. Sprey, C. Lambert, Titration curves of cellulases from *Trichoderma reesei*: demonstration of a cellulase-xylanase- β -glucosidase-containing complex, *FEMS Microbiol Lett*, 18 (1983) 217-222.
- [22] B. Sprey, Complexity of cellulases from *Trichoderma reesei* with acidic isoelectric points: A two-dimensional gel electrophoretic study using immunoblotting, *FEMS Microbiol Lett*, 43 (1987) 25-32.
- [23] R.L. Moritz, R.J. Simpson, Liquid-based free-flow electrophoresis--reversed-phase HPLC: a proteomic tool, *Nat Methods*, 2 (2005) 863.
- [24] F. Kroner, J. Hubbuch, Systematic generation of buffer systems for pH gradient ion exchange chromatography and their application, *J Chromatogr A*, 1285 (2013) 78-87.
- [25] Y.C. Li, E.L. Larsson, H. Jungvid, I.Y. Galaev, B. Mattiasson, Shielding of protein-boronate interactions during boronate chromatography of neoglycoproteins, *J Chromatogr A*, 909 (2001) 137-145.
- [26] L. Borlido, A.M. Azevedo, A.G. Sousa, P.H. Oliveira, A.C. Roque, M.R. Aires-Barros, Fishing human monoclonal antibodies from a CHO cell supernatant with boronic acid magnetic particles, *J Chromatogr B*, 903 (2012) 163-170.
- [27] M.B. Smith, J. March, *March's Advanced Organic Chemistry - Reactions, Mechanisms, and Structure*, 6th ed., John Wiley & Sons, 2007.
- [28] L.I. Bosch, T.M. Fyles, T.D. James, Binary and ternary phenylboronic acid complexes with saccharides and Lewis bases, *Tetrahedron*, 60 (2004) 11175-11190.
- [29] J.H. Woo, D.M. Neville, Jr., Separation of bivalent anti-T cell immunotoxin from *Pichia pastoris* glycoproteins by borate anion exchange, *BioTechniques*, 35 (2003) 392-398.
- [30] G. Springsteen, B. Wang, A detailed examination of boronic acid-diol complexation, *Tetrahedron*, 58 (2002) 5291-5300.
- [31] X.C.S. Liu, W.H., Boronate Affinity Chromatography, in: D.S. Hage (Ed.) *Handbook of Affinity Chromatography*, CRC Press, 2005, pp. 215-229.
- [32] J.M. De Guzman, S.A. Soper, R.L. McCarley, Assessment of glycoprotein interactions with 4-[(2-aminoethyl)carbamoyl]phenylboronic acid surfaces using surface plasmon resonance spectroscopy, *Anal Chem*, 82 (2010) 8970-8977.
- [33] S. Gascon, J.O. Lampen, Purification of the internal invertase of yeast, *J Biol Chem*, 243 (1968) 1567-1572.
- [34] A. Seidel-Morgenstern, Preparative gradient chromatography, *Chem Eng Technol*, 28 (2005) 1265-1273.
- [35] C.R. Smith, R.B. DePrince, J. Dackor, D. Weigl, J. Griffith, M. Persmark, Separation of topological forms of plasmid DNA by anion-exchange HPLC: shifts in elution order of linear DNA, *J Chromatogr B*, 854 (2007) 121-127.
- [36] G. Carta, A. Jungbauer, Gradient elution chromatography, in: *Protein chromatography: process development and scale-up*, Wiley-VCH Verlag Gmb & Co KGaA, Germany, 2010, pp. 277-308.
- [37] P.G. Righetti, M. Chiari, S. Pranav K., E. Santaniello, Focusing of pepsin in strongly acidic immobilized pH gradients, *J Biochem Biophys Meth*, 16 (1988) 185-192.
- [38] N. Ramasesh, K.R. Sreekantiah, V.S. Murthy, Studies on the Two Forms of Amyloglucosidase of *Aspergillus niger* van Tieghem, *Starch - Stärke*, 34 (1982) 346-351.

IV.6. Supplementary Material

IV.S1 Characterization of the commercial proteins used by SDS-PAGE

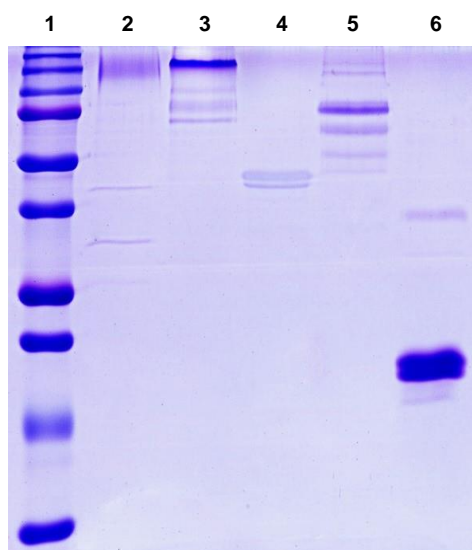


Figure IV.S1 Coomassie Blue stained SDS-PAGE of the commercial proteins constituents of the protein library under study. Lanes ID: 1: Precision Plus Protein™ Dual Color Standards (from top to bottom: 250, 200, 150, 100, 75, 50, 37, 25, 20 and 10 kDa); 2: Invertase (glycosylated and acidic protein), 3: Amyloglucosidase (glycosylated and acidic protein), 4: Pepsin (non-glycosylated and acidic protein), 5: Cellulase (glycosylated and acidic/neutral protein), 6: RNase B (glycosylated and basic protein). The mass of protein in lanes 2 to 6 is 5 µg.

IV.S2 Displacer studies for glycoproteins using a P6XL resin

In order to understand if the elution strategy developed could be implemented in a straightforward manner to the separation of glycoproteins using an agarose-based PB resin, a P6XL resin was tested. Unfortunately, the results obtained show that the separation efficacy is compromised when using the P6XL resin. The results from the evaluation of a linear gradient of Tris at a rate of 0.6% Tris/min demonstrate a low peak resolution, a very poor protein separation and consequently, low purity of the collected fractions (Figure IV.S2.1). The step gradient strategy revealed more resolved peaks however, the poor protein separation performance was maintained (Figure IV.S2.2). Moreover, it is also possible to observe that RNase B is not retained by P6XL resin. Although the ligand in question is the same and that P6XL is also an indicated resin for the capture of *cis*-diol containing compounds, the adsorption conditions applied (300 mM NaCl) failed to promote the adsorption of the glycoprotein RNase B onto this resin (Figures IV.S2.1 and IV.S2.2). Also, part of glycoproteins as amyloglucosidase, cellulase and invertase was lost in the flow-through fractions (Figures IV.S2.1 and IV.S2.2). The only feature that seems to be maintained is the fact that invertase is the protein which effective elution is only achieved with a higher concentration of Tris. Differences regarding the type of matrix under use (silica-based vs agarose), ligand density and *m*-APBA spacer arm composition and extension could dictate the achievement of such differences during the adsorptive and, consequently, in the desorption process of these molecules. In theory, it is possible that the silanol groups present in the silica backbone of ProSep®-PB could play a role in the adsorption and desorption processes of glycoproteins since at the

working pH, these groups are negatively charged (pKa 4.9 for isolated silanol groups). However, it was already reported that under similar adsorption conditions, glycoproteins such as monoclonal antibodies do not interact with silica-based nor agarose-based [19, 20].

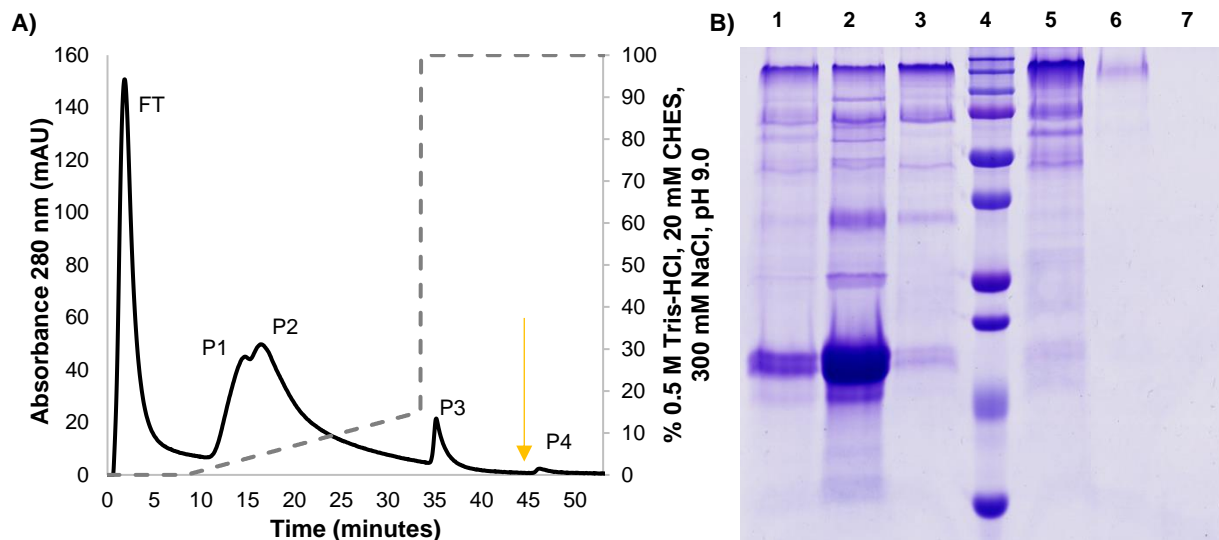


Figure IV.S2.1 (A) Chromatogram obtained using a P6XL resin for the separation of an artificial mixture containing 2.5 mg/mL of each glycoprotein under study, prepared in the adsorption buffer 20 mM CHES, 300 mM NaCl at pH 9.0. The elution process was performed using a linear gradient performed at a rate of 0.6% Tris/min. The elution buffer used was obtained by addition of 0.5 M Tris to the adsorption buffer. The chromatogram presents five peaks denominated as flow-through (FT), peak 1 (P1), peak 2 (P2), peak 3 (P3) and peak 4 (P4), from left to right. The time at which the system was imposed to start to pump 100% (v/v) of the regeneration buffer – 1.5 M Tris-HCl, pH 8.5 – is marked with a yellow arrow. (B) Coomassie Blue stained SDS-PAGE of the fractions collected during glycoproteins separation by PB chromatography using a P6XL resin and an elution gradient strategy accomplished by the use of 0.5 M Tris as displacer agent at a rate of 0.6% Tris/min. Lanes ID: 1: artificial mixture containing 5 μ g of each glycoprotein under study; 2: flow-through (FT) fraction; 3: P1; 4: Precision Plus Protein™ Dual Color Standards (from top to bottom: 250, 200, 150, 100, 75, 50, 37, 25, 20 and 10 kDa); 5: P2; 6: P3; 7: P4.

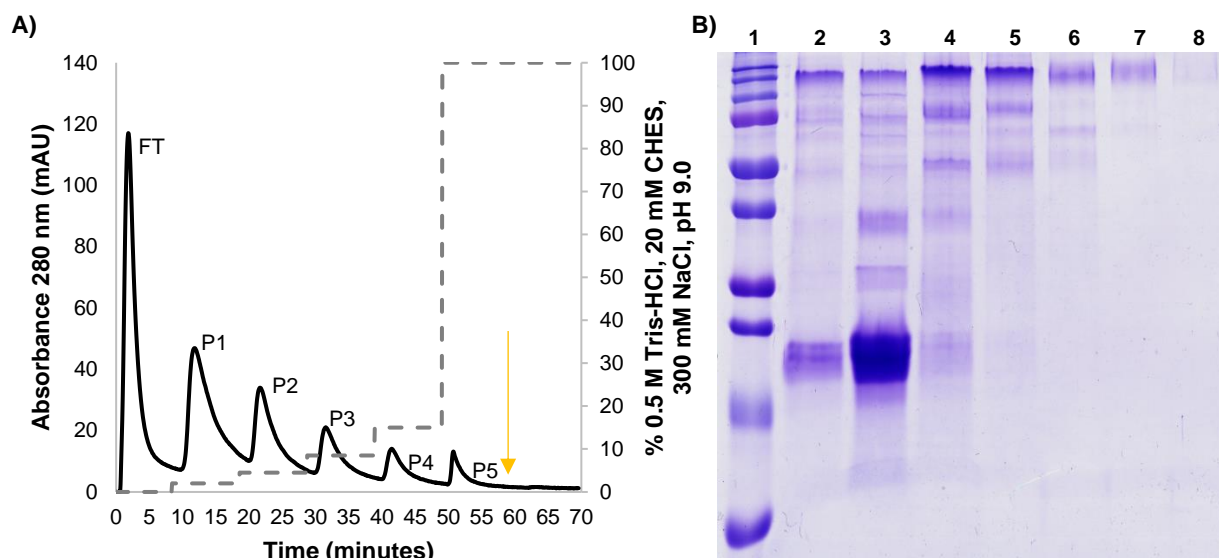


Figure IV.S2.2 (A) Chromatogram obtained using a P6XL resin for the separation of an artificial mixture containing 2.5 mg/mL of each glycoprotein under study, prepared in the adsorption buffer 20 mM CHES, 300 mM NaCl at pH 9.0. The elution process was performed using a series of step gradients – 2%, 4.5%, 8.5%, 15% and 100% (v/v). The elution buffer used was obtained by addition of 0.5 M Tris to the adsorption buffer. The chromatogram presents six peaks denominated as flow-through (FT), peak 1 (P1), peak 2 (P2), peak 3 (P3), peak 4 (P4) and peak 5 (P5) from left to right. The time at which the system was imposed to start to pump 100% (v/v) of the regeneration buffer – 1.5 M Tris-HCl, pH 8.5 – is marked with a yellow arrow. (B) Coomassie Blue stained SDS-PAGE of the fractions collected during glycoproteins separation by PB chromatography using a P6XL resin and an elution strategy accomplished by the use of a series of step gradients – 2%, 4.5%, 8.5%, 15% and 100% (v/v). Lanes ID: 1: Precision Plus Protein™ Dual Color Standards (from top to bottom: 250, 200, 150, 100, 75, 50, 37, 25, 20 and 10 kDa); 2: artificial mixture containing 5 µg of each glycoprotein under study; 3: flow-through (FT) fraction; 4: P1; 5: P2; 6: P3; 7: P4; 8: P5.

IV.S3 Displacer studies for acid/neutral proteins using a P6XL resin

To understand the impact of the chromatographic matrix in the desorption process of acidic/neutral proteins, the developed strategies were applied using an agarose-based PB resin – P6XL. The results obtained either by the application of a linear or a step gradient strategy showed no selectivity in the separation of the acidic/neutral proteins under study (Figures IV.S3.1 and IV.S3.2). Moreover, contrarily to what was observed using the ProSep®-PB resin, cellulase was not the last protein to be eluted. Instead, it is possible to detect part of cellulase in the flow-through fractions (Figures IV.S3.1B and IV.S3.2B). Phenomena that again, indicate different mechanisms of adsorption and desorption towards resins constituted by different matrices. In this particular case, the differences observed seem to be mostly due to the spacer arm structures composition of each matrices since they share the same ligand.

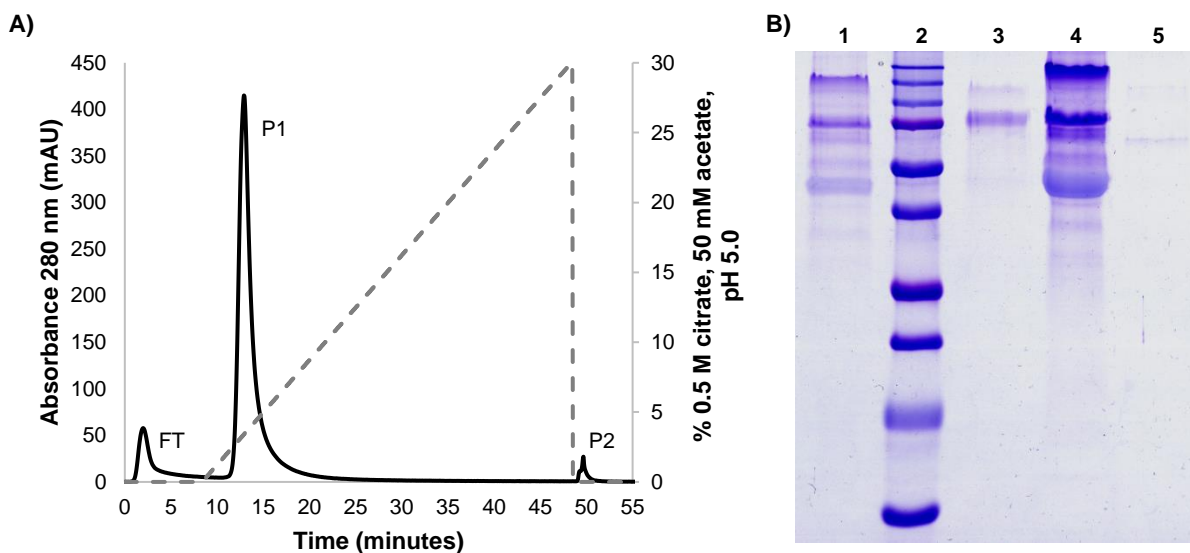


Figure IV.S3.1 (A) Chromatogram obtained using a P6XL resin for the separation of an artificial mixture containing 2.5 mg/mL of each acidic/neutral protein under study prepared in the adsorption buffer 50 mM citrate at pH 5.0. The elution process was performed using a linear gradient performed at a rate of 0.75% citrate/min. The elution buffer used was obtained by addition of 0.5 M citrate to the adsorption buffer. Immediately after the elution, column regeneration was conducted using 1.5 M Tris-HCl, pH 8.5. The chromatogram presents 3 peaks denominated as flow-through (FT), peak 1 (P1) and peak 2 (P2), from left to right. (B) Coomassie Blue stained SDS-PAGE of the fractions collected during acidic/neutral proteins separation by PB chromatography using a P6XL resin and an elution gradient strategy accomplished by the use of 0.5 M citrate as displacer agent at a rate of 0.75% citrate/min. Lanes ID: 1: artificial mixture containing 5 µg of each acidic/neutral protein under study); 2: Precision Plus Protein™ Dual Color Standards (from top to bottom: 250, 200, 150, 100, 75, 50, 37, 25, 20 and 10 kDa); 3: flow-through (FT) fraction; 4: P1; 5: P2.

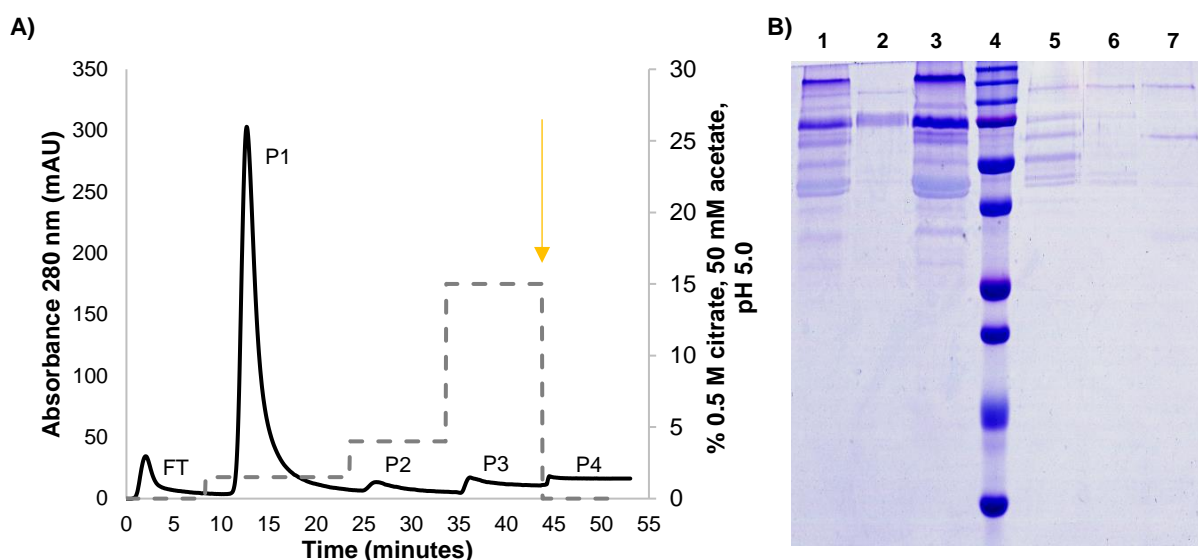


Figure IV.S3.2 (A) Chromatogram obtained using a P6XL resin for the separation of an artificial mixture containing 2.5 mg/mL of each acidic/neutral protein under study prepared in the adsorption buffer 50 mM citrate at pH 5.0. The elution process was performed using a series of step gradients – 1.5%, 4%, and 15% (v/v). The elution buffer used was obtained by addition of 0.5 M citrate to the adsorption buffer. The chromatogram presents five peaks denominated as flow-through (FT), peak 1 (P1), peak 2 (P2), peak 3 (P3), and peak 4 (P4), from left to right. The time at which the system was imposed to start to pump 100% (v/v) of the regeneration buffer – 1.5 M Tris-HCl, pH 8.5 – is marked with a yellow arrow. (B) Coomassie Blue stained SDS-PAGE of the fractions collected during acidic/neutral proteins separation by PB chromatography using a P6XL resin and an elution strategy accomplished by the use of a series of step gradients – 1.5%, 4%, and 15% (v/v). Lanes ID: 1: artificial mixture containing 5 μ g of each acidic/neutral protein under study; 2: flow-through (FT) fraction; 3: P1; 4: Precision Plus Protein™ Dual Color Standards (from top to bottom: 250, 200, 150, 100, 75, 50, 37, 25, 20 and 10 kDa); 5: P2; 6: P3; 7: P4.

Chapter V - General Conclusions and Future Perspectives

Therapeutic products based on monoclonal antibodies (mAbs) still represent the major class of biopharmaceutical products with worldwide sales expected to reach \$125 billion by 2020 [1]. This continuous trend has been related to major technology developments in the upstream processing [2-4]. The increasing knowledge of global authorities on the production process together with the effectiveness and safety of these therapeutic products have been the major driving forces for such success.

However, despite all efforts, a more generalized access to these biopharmaceuticals is still barred by high selling prices, with downstream processing (DSP) being considered the bottleneck in the manufacturing of mAbs. The established DSP relies on a platform-based approach that encompasses a protein A affinity chromatography capture step, which can represent up to 25% of the total manufacturing costs [5]. Therefore, the design of novel and more cost-effective operations and their implementation in the current industrial settings represents a major need. The alternatives range from non-chromatographic techniques, like aqueous two-phase separation, membrane filtration, precipitation or crystallization, to affinity chromatographic steps not based on protein A and emergent strategies like multimodal chromatography [6, 7].

This thesis focused the development of an effective alternative to protein A based on boronate chromatography. So far boronate chromatography has been described as affinity chromatography however and considering the results obtained, it was possible to conclude that boronate ligands, namely the *m*-APBA ligand, present a multimodal behaviour, which can be modulated by the experimental conditions as pH, conductivity and type of mobile phase modulator used.

The work developed in Chapter II, demonstrate the feasibility of using *on-line* Flow Microcalorimetry (FMC) to study the molecular interactions between *m*-APBA and an anti-IL8 mAb in boronate chromatography and to thermodynamically characterize the phenomena involved in the adsorption of mAbs. The reduction of ΔH_{ads} and shifts in the thermograms observed with the increase in the pH, in both absence and presence of different mobile phase modulators, show that FMC is able to indicate the influence that ligand conformational changes and formal charges have on anti-IL8 mAb adsorption. The combination of the FMC results with standard chromatographic assays allowed to conclude that the salt tolerance of the ligand can be improved using different mobile phase modulators.

The anti-IL8 mAb adsorption was characterized as enthalpically driven in all conditions tested, which was expected considering that the interaction between boronic acids or boronate ligands and molecules containing *cis*-diols relies on a reversible esterification. However, the decrease in ΔH_{ads} and the shifts in the thermograms, observed with the increase in pH, were indicative of the presence of electrostatic interactions between the protein and the ligand, which was also corroborated by salt tolerance studies. The use of salts, such as NaCl, NaF, MgCl₂ and (NH₄)₂SO₄, demonstrated ability to mitigate non-specific interactions with the agarose matrix and with the phenyl group present on the *m*-APBA ligand structure at pH \leq pKa, except in the presence of MgCl₂ at pH 8.5 and 9.0. Also at these conditions, the interaction between *m*-APBA and anti-IL8 mAb showed high salt tolerance with retentions between 97 and 100% being observed at pH values lower than the pKa of the ligand and salt concentrations up to 1 M NaCl.

However, when *m*-APBA is present in the tetrahedral conformation (pH > pKa), it can also behave as a cation exchanger and, consequently, a lower salt tolerance is observed. In the presence of the

mobile phase modulator NaCl, average adsorption yields of $67 \pm 4\%$ were obtained with 300 to 450 mM NaCl, against only $39 \pm 3\%$ in the presence of 600 mM to 1 M NaCl. The remaining anti-IL8 mAb was retained by the specific *cis*-diol interaction, which is still present, revealing the multimodal character of this ligand, especially at pH 9.0, contrarily to what has been reported in the last decades. The use of NaF, MgCl₂ and (NH₄)₂SO₄ as mobile phase modulators caused a decrease in the contribution of electrostatic interactions to the adsorption process of the anti-IL8 mAb and consequently, an increase in the ligand salt tolerance. The best results were achieved in the presence of NaF and (NH₄)₂SO₄.

To complement this work, it would be important to further determine the kinetic constants obtained from isotherms and the dynamic binding capacities from breakthrough curves, in order to conclude if the adsorption capacity of the ligand is increased by the use of the aforementioned mobile phase modulators. Also, it would be interesting to understand if the use of such mobile phase modulators can lead to the increase in ligand selectivity towards the anti-IL8 mAb, especially by *cis*-diol interactions with the glycans present in the Fc region of the mAb. For this purpose, the evaluation of the performance of the PBA ligand towards real cell culture supernatants or artificial mixtures, composed by the anti-IL8 mAb and other impurities, should be conducted at all the conditions tested.

Overall, the information retrieved through FMC provided a better understanding of the biomolecular phenomena involved in *m*-APBA – anti-IL8 mAb interaction revealing the thermodynamic parameters associated. Nevertheless, it is important to consider the combination of FMC with other analytical techniques to achieve an effective disclosure of all the mechanisms involved in the adsorption of biomolecules. For instance, surface plasmon resonance (SPR) could indicate the binding affinity in a high-throughput manner [8] while, small-angle X-ray scattering (SAXS) could give insights on the radius of the molecule and on the stoichiometry of the interaction mAb-ligand [9, 10]. Attenuated total reflection Fourier transform infrared (ATR-FTIR) spectroscopy and differential scanning calorimetry (DSC) could also be useful to understand if any conformational changes occur upon the adsorption process, namely in the mAb secondary structure [11-13]. The joint application of these methods towards the study of the adsorption process of mAbs onto *m*-APBA ligands/resins will promote a deeper knowledge about the underlying mechanisms of this adsorption process which could contribute towards the effective integration of boronate chromatography in the current mAb DSP platform. Moreover, the use of FMC in combination with other analytical methods can be foreseen with the aim of significantly shortening chromatography process development by designing and developing models that can be applied to better fit and predict the biomolecular phenomena.

In addition to the fundamental studies carried out in Chapter II, the viability of using PBA for the direct capture of mAbs from clarified cell culture supernatants was demonstrated in Chapter III, allowing high recovery yields as well as high impurity clearance. The optimization studies using ProSep®-PB chromatography media, performed using serum-containing cell culture supernatants, corroborate the results obtained in Chapter II with the most efficient pH condition being below PBA pKa, namely at pH 7.5. In Chapter III, the development and optimization of an additional washing step was essential to achieve high purities. The type of buffer, ionic strength, and pH of the wash buffer had to be well-defined in order to minimize IgG losses. The standard elution buffer, 1.5 M Tris-HCl, was successfully replaced

by an alternative competitor - 0.5 M D-sorbitol with 150 mM NaCl in 10 mM Tris-HCl. The later, besides being economically more favourable, also maintained the anti-IL8 biological activity at higher levels. The two-step elution process developed allowed to recover 99% of the anti-IL8 with a final protein purity of 81% using 0.1 M D-sorbitol in 10 mM Tris-HCl as washing buffer. The performance parameters achieved were identical to the ones obtained using protein A affinity chromatography – recovery yield of 99% and purities of around 87%.

PBA chromatography was also successfully used to purify the same anti-IL-8 mAb but from a serum-free culture media and a second mAb – an anti-HCV mAb - produced by a different CHO cell line. During the purification of the anti-HCV mAb was possible to observe that with the implementation of a washing step is possible to use PB chromatography for isoform separation.

Furthermore, the scalability of PBA chromatography was also successfully demonstrated in Chapter III with a 100-fold scale-up. Working superficial velocities of the different chromatographic steps were optimized to allow a reduction of the chromatographic run time of about 3 times without compromising the performance parameters. The 100-fold scale-up was successfully accomplished with recovery yields of about 97%, purities of 82% and removals of gDNA higher than 96% obtained at all the scales tested (0.4, 4, 16 and 40 cm³ columns). The DBC determined at 10% of breakthrough is lower than that of protein A chromatography (21.8 ± 3.8 mg IgG/cm³ resin vs > 50 mg IgG/cm³ resin, respectively). This low capacity could, however, be mitigated with further optimizations of the commercial ligand in terms of density and spacer arms structures [14-16]. Also, in order to overcome the low DBC of this resin, it can be considered the use of this standard capture step in a continuous mode since it would promote the use of the total static capacity of the resin and could bring other advantages to the process as reduction of production costs (in terms of resins, buffers, volume, and footprint) and increased productivity, largely because all equipment is in use at all times [17]. The column size used in the continuous approach is also smaller so, even if it was necessary to use more resin volume than with protein A, the associated costs would not be too high.

The lower costs, stability and selectivity of this synthetic ligand may lead to the implementation of PBA chromatography as a new platform in the DSP of mAbs, either as a protein A replacement or as a pre-chromatographic step for a longer life-time of the high costly protein A resin. Moreover, since boronic acids have the ability to recognize the 1,2-*cis*-diol compounds present in the glycan structure, it could be possible to purify antibody fragments lacking the Fc region proving that they are glycosylated in its Fv region, unlike protein A [18, 19].

PBA chromatography can therefore be described as a scalable, rapid, efficient and cost-effective multimodal process that has the potential to be used in an industrial setting.

In this thesis important developments were made considering the capture step of mAbs. However, it would be crucial to look at the whole process to understand how the current process could be reshaped in order to achieve a more efficient, sustainable and cost-effective platform. With the biopharmaceutical industry growing at an unparalleled rate, especially with regard to complex molecules as mAbs, it is imperative to incorporate innovative methodologies in DSP early on into the development process with novel strategies comprising the integration and intensification of the DSP of mAbs has been purposed.

It is known that the current downstream process train is unable to cope not only with high titres but also with the large cell densities, consequences from the major developments achieved upstream. Unit operations as chromatography are running into binding capacity limitations and the traditional solid-liquid technologies, like centrifugation and filtration, are achieving their capacity limits. Consequently, linear scale-up of traditional purification methods of cell harvest, concentration and primary recovery are incapable to meet the current product demand in terms of space requirements, cost, resources consumption and process time. Hence, technologies that offer process integration, *i.e.*, a reduction in the number of unit operations in the initial isolation and purification steps while maintaining high product recovery and purity, would not only increase process economy but also reduce process time [20, 21].

Techniques such as aqueous two-phase extraction (ATPE), expanded bed adsorption (EBA) chromatography and convective flow devices have shown to possess distinctive advantages that turns them viable candidates to meet and overcome the aforementioned challenges. Considering all the knowledge that the work developed during this thesis brought to the scientific community, three different strategies could be foreseen using the multimodal PBA chromatography. They rely on:

1) Cell harvest based on extraction using **aqueous two-phase systems** (ATPS) [22, 23], and further purification by packed-bed **multimodal chromatography** for mAbs capture directly from cell culture media and for mAbs polishing from intermediate streams [24-26];

2) Clarification based on extraction using **ATPS**, followed by mAbs purification by (i) packed-bed **multimodal chromatography** for mAbs capture and (ii) **convective flow adsorbers** (monoliths, membranes and fibres) for polishing purposes [27, 28];

3) Clarification and pre-capture of mAbs with **EBA chromatography** [29, 30] using PBA ligands followed by polishing steps ruled by **convective flow adsorbers** [31].

Altogether, these alternatives are expected to significantly shorten process development times, increase the production capacity currently available and, especially, to reduce the cost of mAbs that ultimately will foster the accessibility of these biomolecules to the general population. Nevertheless, innovation in all fields will be necessary to provide continuous-mode adaptations and combinations of these technologies in order to rush them into the market [21].

Finally, in Chapter IV, it was also possible to demonstrate that the *m*-APBA ligand can be usefully used for the capture and effective separation of a wide range of proteins from glycoproteins, comprising a broad range of isoelectric points, to acidic/neutral proteins (glycosylated or not), by the use of displacers as Tris and citrate, respectively. The elution strategies were designed firstly considering linear gradients which gave insights on the required concentrations of Tris or citrate needed to selectively elute proteins within the same group. The best results were accomplished with rates of 0.6% Tris/min (\approx 3 mM Tris/min) for glycoproteins and 0.75% citrate/min (\approx 3.75 mM citrate/min) for acidic/neutral proteins. Consequently, step gradients were developed, and protein separation improvements achieved.

The use of pH gradients was also evaluated however, the full recovery of the majority of proteins was not reached by the application of pH gradients to the elution process. Furthermore, the differences in pH, at which the elution of proteins took place, were too small to have a reliable separation of proteins. Nevertheless, optimizations regarding the buffers used to achieve the linear pH gradient as the rate at

which the gradient is conducted could turn the protein isoforms separation more effective in the case of the proteins as amyloglucosidase and pepsin.

Overall, this work has demonstrated that the *m*-APBA ligand, present unique features that make PB chromatography a useful tool for the capture and separation of a wide range of proteins and even to separate isoforms. Accordingly, PB chromatography can be applied not only to separate proteins on a preparative scale but can be also considered for analytical purposes, envisaging the separation of protein isoforms, or even for proteomic studies.

The development of effective ligands towards the glycan portion of glycoproteins and glycolipids are especially needed for pre-enrichment proteomics strategies [32]. As IMAC has been used for the enrichment of phosphopeptides due to their ability to interact with ion exchange beads and to participate in coordination interactions with immobilized metal ions [33], PB chromatography could be used to enrich mixtures in a specific glycoprotein considering differences in glycan structure and overall charge. These pre-enrichments steps combined with advanced MS/MS methods and computational data analysis have revealed to be crucial to identify, for instance, which post-translational modifications in proteins could be associated to the presence of a certain disease helping to understand its mechanism.

Nevertheless, more developments regarding the selectivity of the PB ligands should be explored in order to apply PB chromatography to proteomic studies. It would be essential to analyse the selectivity of a large variety of PB ligands, in addition to *m*-APBA, aiming to found different ligands with distinct specificities towards glycoproteins containing different glycan structure, for example. A ligand library should be constructed and evaluated against a large number of glycoproteins. This ligand library could be created using *de novo* design of the ligands based on Ugi scaffolds [32, 34]. Using this approach, the potential to identify ligands that exhibit high individual glycoprotein specificity could be increased due to the additional functional groups available for variation on the Ugi scaffold [32, 34].

V.1. References

- [1] D.M. Ecker, S.D. Jones, H.L. Levine, The therapeutic monoclonal antibody market, *mAbs*, 7 (2015) 9-14.
- [2] J. Zhu, Mammalian cell protein expression for biopharmaceutical production, *Biotechnol Adv*, 30 (2012) 1158-1170.
- [3] M. Butler, A. Meneses-Acosta, Recent advances in technology supporting biopharmaceutical production from mammalian cells, *Appl Microbiol Biot*, 96 (2012) 885-894.
- [4] F. Li, N. Vijayasankaran, A. Shen, R. Kiss, A. Amanullah, Cell culture processes for monoclonal antibody production, *mAbs*, 2 (2010) 466-477.
- [5] M.D. Costioli, C. Guillemot-Potelle, C. Mitchell-Logean, H. Broly, Cost of Goods Modeling and Quality by Design for Developing Cost-Effective Processes, *BioPharm Int*, 23 (2010).
- [6] P. Gagnon, Technology trends in antibody purification, *J Chromatogr A*, 1221 (2012) 57-70.
- [7] S.M. Cramer, M.A. Holstein, Downstream bioprocessing: recent advances and future promise, *Curr Opin Chem Eng*, 1 (2011) 27-37.
- [8] F. Cheng, M.Y. Li, H.Q. Wang, D.Q. Lin, J.P. Qu, Antibody-ligand interactions for hydrophobic charge-induction chromatography: a surface plasmon resonance study, *Langmuir*, 31 (2015) 3422-3430.
- [9] J. Plewka, G.L. Silva, R. Tscheliessnig, H. Rennhofer, C. Dias-Cabral, A.L. Jungbauer, H. C., Antibody adsorption in protein-A affinity chromatography-in-situ measurement of nanoscale structure by small-angle X-ray scattering, *J Sep Sci*, (2018).
- [10] G.L. Silva, J. Plewka, H. Lichtenegger, A.C. Dias-Cabral, A.T. Jungbauer, R., The pearl necklace model in Protein A chromatography - molecular mechanisms at the resin interface, *Biotechnol Bioeng*, 116 (2019) 76-86.

- [11] R. Ueberbacher, E. Haimer, R. Hahn, A. Jungbauer, Hydrophobic interaction chromatography of proteins: V. Quantitative assessment of conformational changes, *J Chromatogr A*, 1198-1199 (2008) 154-163.
- [12] B. Beyer, A. Jungbauer, Conformational changes of antibodies upon adsorption onto hydrophobic interaction chromatography surfaces, *J Chromatogr A*, 1552 (2018) 60-66.
- [13] M. Boulet-Audet, S.G. Kazarian, B. Byrne, In-column ATR-FTIR spectroscopy to monitor affinity chromatography purification of monoclonal antibodies, *Sci Rep-UK*, 6 (2016) 30526.
- [14] S. Hober, K. Nord, M. Linhult, Protein A chromatography for antibody purification, *J Chromatogr B*, 848 (2007) 40-47.
- [15] G. Zhao, X.Y. Dong, Y. Sun, Ligands for mixed-mode protein chromatography: Principles, characteristics and design, *J Biotechnol*, 144 (2009) 3-11.
- [16] W. Bicker, J. Wu, H. Yeman, K. Albert, W. Lindner, Retention and selectivity effects caused by bonding of a polar urea-type ligand to silica: a study on mixed-mode retention mechanisms and the pivotal role of solute-silanol interactions in the hydrophilic interaction chromatography elution mode, *J Chromatogr A*, 1218 (2011) 882-895.
- [17] A.L. Zydney, Continuous downstream processing for high value biological products: A Review, *Biotechnol Bioeng*, 113 (2016) 465-475.
- [18] L. Borlido, A.M. Azevedo, A.G. Sousa, P.H. Oliveira, A.C. Roque, M.R. Aires-Barros, Fishing human monoclonal antibodies from a CHO cell supernatant with boronic acid magnetic particles, *J Chromatogr B*, 903 (2012) 163-170.
- [19] A. Nascimento, I.F. Pinto, V. Chu, M.R. Aires-Barros, J.P. Conde, A.M. Azevedo, Studies on the purification of antibody fragments, *Sep Purif Technol*, 195 (2018) 388-397.
- [20] A.M. Azevedo, M.R. Aires-Barros, Novel strategies for the purification of monoclonal antibodies, in: R. Martins (Ed.) *Proceedings of 1st Portuguese Meeting in Bioengineering (ENBENG 2011)*, Oeiras, Portugal, 2011, pp. 72-75.
- [21] R.N. D'Souza, A.M. Azevedo, M.R. Aires Barros, N.L. Krajnc, P. Kramberger, M.L. Carbajal, M. Grasselli, R. Meyer, M. Fernandez Lahore, Emerging technologies for the integration and intensification of downstream bioprocesses, *Pharm Bioprocess*, 1 (2013) 423-440.
- [22] I. Campos-Pinto, E. Espitia-Saloma, S.A.S.L. Rosa, M. Rito-Palomares, O. Aguilar, M. Arévalo-Rodríguez, M.R. Aires-Barros, A.M. Azevedo, Integration of cell harvest with affinity-enhanced purification of monoclonal antibodies using aqueous two-phase systems with a dual tag ligand, *Sep Purif Technol*, 173 (2017) 129-134.
- [23] P.A. Rosa, A.M. Azevedo, S. Sommerfeld, M. Mutter, W. Backer, M.R. Aires-Barros, Continuous purification of antibodies from cell culture supernatant with aqueous two-phase systems: from concept to process, *Biotechnol J*, 8 (2013) 352-362.
- [24] S.A.S.L. Rosa, R. dos Santos, M.R. Aires-Barros, A.M. Azevedo, Phenylboronic acid chromatography provides a rapid, reproducible and easy scalable multimodal process for the capture of monoclonal antibodies, *Sep Purif Technol*, 160 (2016) 43-50.
- [25] R. dos Santos, S.A.S.L. Rosa, M.R. Aires-Barros, A. Tover, A.M. Azevedo, Phenylboronic acid as a multi-modal ligand for the capture of monoclonal antibodies: development and optimization of a washing step, *J Chromatogr A*, 1355 (2014) 115-124.
- [26] I.F. Pinto, R.R. Soares, S.A. Rosa, M.R. Aires-Barros, V. Chu, J.P. Conde, A.M. Azevedo, High-Throughput Nanoliter-Scale Analysis and Optimization of Multimodal Chromatography for the Capture of Monoclonal Antibodies, *Anal Chem*, 88 (2016) 7959-7967.
- [27] A. Nascimento, S.A.S.L. Rosa, M. Mateus, A.M. Azevedo, Polishing of monoclonal antibodies streams through convective flow devices, *Sep Purif Technol*, 132 (2014) 593-600.
- [28] I. Campos-Pinto, E.V. Capela, A.R. Silva-Santos, M.A. Rodríguez, P.R. Gavara, M. Fernandez-Lahore, M.R. Aires-Barros, A.M. Azevedo, LYTAG-driven purification strategies for monoclonal antibodies using quaternary amine ligands as affinity matrices, *J Chem Technol Biot*, 93 (2018) 1966–1974.
- [29] P.B. Kakarla, R.N. Dsouza, U. Toots, M. Fernández-Lahore, Interactions of Chinese Hamster Ovary (CHO) cell cultures with second generation expanded bed adsorbents, *Sep Purif Technol*, 144 (2015) 23-30.
- [30] R.N. D'Souza, P.B. Kakarla, V. Yelemane, R. Meyer, P. den Boer, M. Fernández-Lahore, Controlling cell adhesion in antibody purification by expanded bed adsorption chromatography, *Sep Purif Technol*, 183 (2017) 270-278.
- [31] P.R. Gavara, N.S. Bibi, M.L. Sanchez, M. Grasselli, M. Fernandez-Lahore, Chromatographic Characterization and Process Performance of Column-Packed Anion Exchange Fibrous Adsorbents for High Throughput and High Capacity Bioseparations, *Processes* 3 (2015) 204-221.

- [32] L. Rowe, G. El Khoury, C.R. Lowe, A benzoboroxole-based affinity ligand for glycoprotein purification at physiological pH, *J Mol Recognit*, 29 (2016) 232-238.
- [33] Y. Zhao, O.N. Jensen, Modification-specific proteomics: strategies for characterization of post-translational modifications using enrichment techniques, *Proteomics*, 9 (2009) 4632-4641.
- [34] C. Chen, G.E. Khoury, C.R. Lowe, Affinity ligands for glycoprotein purification based on the multi-component Ugi reaction, *J Chromatogr B*, , 969 (2014) 171-180.

